ABSTRACT

Title of Thesis: NUMERICAL SIMULATION STUDY OF VIBRATION MITIGATION EFFECTIVENESS OF TUNED MASS DAMPERS FOR TRAFFIC SIGNAL MAST ARM STRUCTURES

Yifan Zhu, Master of Science, 2016

Thesis Directed By: Professor Yunfeng Zhang
Research Professor Chung C. Fu
Department of Civil and Environmental Engineering

Fatigue damage in the connections of single mast arm signal support structures is one of the primary safety concerns because collapse could result from fatigue induced cracking. This type of cantilever signal support structures typically has very light damping and excessively large wind-induced vibration have been observed. Major changes related to fatigue design were made in the 2001 AASHTO LRFD Specification for Structural Supports for Highway Signs, Luminaries, and Traffic Signals, and supplemental damping devices have been shown to be promising in reducing the vibration response and thus fatigue load demand on mast arm signal support structures. Three prototype single mast arm signal support structures are selected for this numerical simulation. The primary objective of this study is to investigate the effectiveness and optimal use of one type of damping devices termed tuned mass damper (TMD) in vibration response mitigation.

NUMERICAL SIMULATION STUDY OF VIBRATION MITIGATION EFFECTIVENESS OF TUNED MASS DAMPERS FOR TRAFFIC SIGNAL MAST ARM STRUCTURES

by

Yifan Zhu

Thesis submitted to the Faculty of the Graduate School of the
University of Maryland, College Park, in partial fulfillment
of the requirements for the degree of
Master of Science
2016

Advisory Committee:
Professor Yunfeng Zhang, Chair
Research Professor Chung C. Fu, Co-Chair
Professor Amde M. Amde

Acknowledgements

I would like to express my gratefulness to Dr. Yunfeng Zhang and Dr. Chung C. Fu, who have been advising me and guiding me through the development of this thesis. Their insightfulness and encouragement are indispensable parts towards the completion of this thesis, and help me all the time when I was stuck in different challenges when doing researches and writing this thesis.

Special thank to my parents, Prof. Yanpeng Zhu and Dr. Xiuli Wang, who give all their love, guidance and supports to me and encourage me all through these years.

I am also deeply indebted to the group members, Heng Liu, Chaoran Xu, Yunchao Ye who helped me in learning the finite element program and doing the experiment.

I also thank Dr. Amde M. Amde for his valuable time serving on my thesis committee.

Table of Contents

List of Tables

List of Figures

List of Notations

E – Elastic modulus

I – Moment of inertia

m – mass of the structure

k – stiffness of the structure

ω – frequency of the structure, radian/sec.

ζ – viscous damping ratio

m_d – mass of the tuned mass damper

f_d – Natural frequency of the tuned mass damper

f_n– Fundamental frequency of the structure

f_F – Frequency of excitation force

$(\Delta F)_n$ - Nominal fatigue resistance

γ - Load factor per the fatigue I limit state

ϕ - Resistance factor (equal to 1.0)

ζ_j- Equavalenet viscous damping ratio

$\alpha = a_0$ – Coefficient in Rayleigh damping matrix associated with the mass matrix

$\beta = a_1$ - Coefficient in Rayleigh damping matrix associated with the stiffness matrix

Chapter 1:Introduction

1.1 Problem Statement and research motivation

Mast arm signal structure collapse in the US has been seen in the past several decades (Dexter and Ricker 2002 (NCHRP 469)). Some of the accidents happened on highway and the signal mast arm falling over fast moving vehicle poses high threat to drivers. After the accident in Michigan in 1990 (Culp et al 1990), AASHTO mandated the revision of the design code for traffic signal structures. In 2002, National Cooperative Highway Research Program (NCHRP) conducted a survey on the excessive vibration and detection of fatigue crack of sign, signal, or light support structures, and thirty states in US reported such problems (NCHRP Report 141, 2011). Hector (2007) reported that over 12 traffic signal mast arms failed or collapsed in the period of six years within the Missouri. Fatigue cracks typically start at highly stressed locations such as weld terminations of mast arm end connections.

The 1994 AASHTO Specifications included very limited vibration and fatigue design guidelines (i.e., only vortex shedding was included). Recommendations made as a result of the NCHRP Report 412 project led to the inclusion of an entire fatigue design chapter (Section 11) in the 2001 Specifications. The 2009, 2013 and 2015 interim AASHTO Specifications were further revised to account for the research with connection details and fatigue load design. The fatigue design loads allow the State Agencies some leeway in defining the design fatigue load categories and significantly impact the size of the structures and type of connection details. The MD SHA book of standards for Highway, Incidental Structures and Traffic Control Applications is designed per the 1994 AASHTO design criteria which doesn't account for fatigue design criteria. To control the maximum deflection of the mast arm and reduce the number of large stress range cycles for longer fatigue life, vibration mitigation device appear to provide a promising method that can be installed on both new and existing signal support structures and could potentially change the fatigue importance factors for extended fatigue life. This is especially appealing for existing designs of mast arm signal support structures that typically have a very light viscous damping ratio and are sensitive to wind-induced vibration.

In recent years, several vibration mitigation devices have been tested for signal support structure use. Cook et al. (2001) at the University of Florida studied tuned mass damper, tuned liquid damper, friction damper, etc., and Hamilton et al. (2000) at the University of Wyoming tested the strut, flat bar, strand, Alcoa Dumbbell damper, Hapco impact damper, and spring-mass impact damper for signal structure vibration control. Christenson et al. (2012) tested a new type of tuned mass damper termed Signal Head Vibration Absorber that integrates with the traffic signal fixture. All of the afore-mentioned dampers were tested in the lab or through field test. Based on an extensive literature review, the most effective vibration mitigation device for signal mast arm structures appears to be the tuned mass damper. However, the effectiveness and optimal use of tuned mass damper for vibration mitigation of typical Maryland signal support structures has not be studied and their impact on fatigue importance factor is unknown. Therefore, this study aims to investigate the vibration control effect of tuned mass damper for typical Maryland single mast arm signal pole structures and its optimal use for maximized stress range reduction at the connection.

1.2 Research Objective

The objective of this dissertation study is to investigate the optimal use of tuned mass damper (TMD) for vibration mitigation of typical Maryland single mast arm signal pole structures. In order to perform the parametric study, finite element models of three prototype single mast arm signal pole structures with or without TMD were built using a general FE analysis software - ANSYS (ANSYS Mechanical APDL, Version 15.0, ANSYS Inc.). Both linear time history analysis and frequency response analysis of the prototype structures with or without TMD were conducted. In this parametric study, the following parameters are varied and the trends of the analysis results are presented: mass, frequency, viscous damping ratio, and location of the TMD. Specifically, the following tasks are performed in this study,

- Determining the optimal use of TMD for typical Maryland single mast arm signal pole structures. In order to find the optimal parameters of the TMD, the definition of optimal value (in cost function) in this fatigue design context is to minimize the stress range or the total number of stress cycles exceeding a pre-specified threshold level. Trend of the cost function variation with changing TMD parameter values will be determined in the study.
- Investigating how sensitive is the vibration mitigation effect to the variation of TMD parameters (mass, frequency, and location). There might exist a range that TMD devices could still perform to some extent in reducing mast arm vibration. A quantitative relationship for this sensitivity curve will be presented.

1.3 Thesis organization

In Chapter 2, a literature review on standards, codes, and research reports related to the fatigue problem of mast arm signal pole and vibration mitigation devices are reported. The fatigue problems have been studied extensively in the past decade and relevant standards or codes have been updated and implemented recently. Then the vibration mitigation devices are discussed that potentially can reduce the collapse risk of the signal support structures. Chapter 3 describes the analytical results that are used to validate the finite element models based on static load analysis, modal analysis, and linear time history analysis, as well as frequency response analysis. Chapter 4 presents the results of the parametric study on typical Maryland single mast arm signal pole structures with or without TMD. The varying parameters of this parametric study are: mast arm length, TMD mass, TMD frequency, TMD viscous damping ratios, and the location of the TMD on the mast arm. Additionally, a set of free vibration test data is described in Chapter 5 that further validates the finite element model. Conclusions and potential future work are presented in Chapter 6.

Chapter 2: Literature Review

2. 1 Evaluation of Fatigue Importance Categories and Design Limit of Mast Arm Signal Support Structures

$$\gamma(\Delta f)_n \leq \phi(\Delta F)_n \qquad \textit{(Eq. 2-1)}$$

where:

$(\Delta f)_{\mathrm{n}}$ = the wind included nominal stress that shall be used when fatigue design of connection detail is carried out and shall be calculated at the site of potential fatigue cracking. Some details related to this study were provided in AASHTO specification 11.9.2 that:

'For potential penetration, groove-welded, mast arm-to-column pass-through connections, the nominal stress shall be calculated on the gross section of the column at the base of the connections.

For fillet-welded tube-to-transverse plate connections (socket connections), nominal stress shall be calculated on the gross section of the tube at the fillet-weld toe on the tube.'

$(\Delta F)_n$ = the nominal fatigue resistance as specified for the various detail classes identified, which depends on tube connection geometry and

$$\phi(\Delta F)_n = \phi\left(\frac{A}{N}\right)^{\frac{1}{3}} \qquad \textit{(Eq. 2-2)}$$

N = the number of wind load induced stress cycles expected during the life time of the structures

Finite Life Constant = $A \times 10^8$ Ksi^3,

γ = the load factor per the Fatigue I limit state, and

ϕ = the resistance factor equal to 1.0

Also an important relationship between the stress range ($(\Delta f)_n$) and the number of cycles (N) are shows in Figure 2-1.

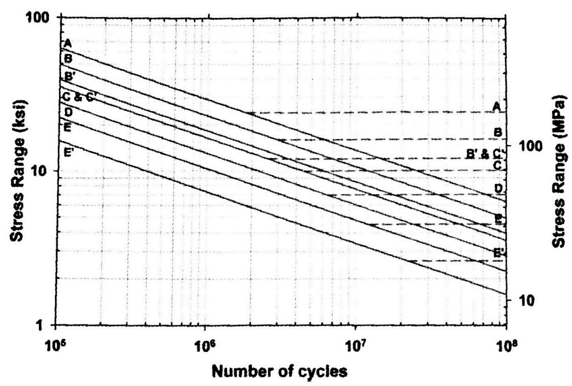

Figure 2-1 Stress Range Vs. Number of cycles (AASHTO Specification Figure C11.9.3-1)

Fatigue Importance Factors (IF), which are introduced by the AASHTO Specification to adjust the structure reliability of cantilevered and noncantilevered support structures and determined by the owner (AASHTO Specifications, C11.6, 2015). It is set by multiple conditions - the wind speed, traffic situation and the structure conditions. In this study, only one kind of signal support structure- single mast arm signal pole structure had been analyzed so only cantilever structures would be introduced as follows:

The AASHTO specification suggested (AASHTO Specifications, P 11-4 to P11-6, 2015) that 'all structures without effective mitigation device on roadways with a speed limit exceed 35 mph and average daily traffic (ADT) exceeding 10,000(one direction, regardless of number of lanes) or average daily truck traffic exceeding 1,000(one direction, regardless of number of lanes) should be classified as Category I structures. Also NCHRP report 718 suggests that cantilever structures that exceeding 50 ft. and without vibration mitigation device should be defined as Category I.' For traffic signal support structures exposed to the three wind load effects are present in Table 2-1.

Table 2-1 Fatigue Importance Factor (AASHTO specification Table 11.6-1)

Fatigue Category			Fatigue Importance Factor, I_F		
			Galloping	Natural Wind Gusts	Truck-Induced Gusts
Cantilever	I	Sign Traffic	1.0	1.0	1.0
		Signal	1.0	1.0	1.0
	II	Sign Traffic	0.70	0.85	0.90
		Signal	0.65	0.80	0.85
	III	Sign Traffic	0.40	0.70	0.80
		Signal	0.30	0.55	0.70

The deflection of the single mast arm sign and traffic signal support structures have not a specific limit in AASHTO Specification but describe as 'should not be excessive' in section 11.8. And NCHRP Report 412 recommends (NCHRP Report 412, AASHTO Specific C11.8) that the total deflection at the free end of single-arm sign supports and all traffic signal arms be limited to 8 in. vertically, when the equivalent static design wind, which was determined to estimate the stress range and introduced in NCHRP Project 10-38 by Lehigh University, effect from galloping and truck-induced gusts are applied to the structure.

2.2 Current Studies and Analysis of Traffic Signal Support Structures

Single mast arm traffic signal support structures are usually flexible and with properties of lightly damped, which are highly susceptible to wind-induced vibration, such as vortex shedding, galloping, natural wind gusts, and truck induced gusts as specified in the previous chapter. The cyclic large amplitude deflection in a high frequency and sustained for a long period caused by the vibration could easily cause a fatigue crack in a relative short period. NCHRP Report 141 had an observed data of 3% of signal support structures in Connecticut and over 30% in Wyoming. Such a poor fatigue performance will easily lead to brittle failure of structures and studies on the fatigue-reduced methods had done by many states and many vibration mitigation devices had been designed and test.

2.2.1 Fatigue design study in Mast Arm Structures

Lehigh University (NCHRP Project 10-70, 2006) had done the project by analytical and experimental evaluations. Then, they provided the result that the most critical details are the tube-to-transverse plate connections, which include the mast arm-to-transverse plate and pole-to-base plate damage. Then, the handholes, which is more focus on the fatigue stress concentration and may cause fatigue cracks, has been another issue that is relative minor but needs to be considered with all the design requirements. Also the mast arm-to-pole connection and mast arm-to pole pass-through connection should be considered as critical conditions. And some results had been used to revise the AASHTO Specification, 2006, like proposed for both finite and infinite lives in fatigue design, defined fatigue resistance as function of geometric parameters, and two-level specification, i.e. nominal stress-based design for most cases (AASHTO Specification 11.9), and local stress-based and experiment-based design for special cases (AASHTO Specification Chapter 11. Appendix D).

University of Minnesota (NCHRP REPORT 469: Fatigue-Resistant Design of Cantilevered Signal, Sign, and Light Support had found and summarized, 2002) did research on wind load, dynamic response, and fatigue of cantilever signal support structures. Some of their conclusions show the evidence that the effective vibration mitigation devices working on the signal support structures effectively would be able to change from the Fatigue Importance Category I to Fatigue Importance Category II so that the magnitude of designed wind load would be reduced but still cannot totally ignore the galloping load in this situation.

2.2.2 Technologies of Reducing Fatigue in signal support structures including Tuned Mass Damper

Many vibration mitigation tests showed that effective vibration mitigation devices would likely decrease galloping-induced stress by at least 35% (NCHRP REPORT 469). In recent decades, many vibration mitigation devices were used to verify the effectiveness by different states and universities. In these studies, the damper type that uses or includes the theory of Tuned Mass Damper (TMD) performs great on the mast arm vibration mitigation.

Tuned mass damper is a device that could reduce the dynamic response of the structure. This kind of devices is usually consisting of a spring, a mass, and a damper. The reason that called this device a ‘tuned mass damper’ is the frequency of the damper is tuned to, or match the same frequency of the structure wants to mitigate. When the force with this particular frequency is excited, the damper will resonate with the structural motion and the energy will be dissipated with the damper.

Because of the single mast arm signal support structures has a lightly damping ratio, an undamped structure with a damped TMD can be considered in the first step of analysis. Also if only take the mast arm into consideration, a simplified model using a beam with lumped mass model could be chosen. So the equation of motion (Jerome J. Connor, 2002) for only one lumped mass case is:

$$m_d \ddot{u}_d + c_d \dot{u}_d + k_d u_d + m_d \ddot{u} = -m_d a_g \qquad \textit{(Eq. 2-3)}$$

$$m\ddot{u} + ku - c_d \dot{u}_d - k_d u_d = -m a_g + p \qquad \textit{(Eq. 2-4)}$$

Where $c_d = 2\zeta_d \omega_d m_d$, $\omega_d = \sqrt{\frac{k_d}{m_d}}$.

Considering a periodic excitation

$$p = \hat{p} e^{-i\Omega t} \qquad \textit{(Eq. 2-5)}$$

$$a_g = \hat{a}_g e^{-i\Omega t} \qquad \textit{(Eq. 2-6)}$$

Expressing the response as

$$u = \hat{u} s e^{-i\Omega t} \qquad \textit{(Eq. 2-7)}$$

$$u_d = \hat{u}_d e^{-i\Omega t} \qquad \textit{(Eq. 2-8)}$$

And the solution of the governing equation is

$$\bar{u} = \frac{\hat{p}}{kD_2}[\beta^2 - \rho^2 + i2\zeta_d \rho\beta] - \frac{\hat{a}_g m}{kD_2}[(1+\bar{m})f^2 - \rho^2 + i2\zeta_d \rho\beta(1+\bar{m})] \qquad \textit{(Eq. 2-9)}$$

$$\bar{u}_d = \frac{\hat{p}\rho^2}{kD_2} - \frac{\hat{a}_g m}{kD_2} \qquad \textit{(Eq. 2-10)}$$

Where

$$\bar{m} = \frac{m_d}{m} \qquad \textit{(Eq. 2-11)}$$

$$D_2 = [1-\rho^2][\beta^2-\rho^2] - \bar{m}\beta^2\rho^2 + i2\zeta_d\rho\beta[1-\rho^2(1+\bar{m})] \qquad \textit{(Eq. 2-12)}$$

$$\beta = \frac{\omega_d}{\omega} \qquad \textit{(Eq. 2-13)}$$

$$\rho = \frac{\Omega}{\omega} = \frac{\Omega}{\sqrt{k/m}} \qquad \textit{(Eq. 2-14)}$$

Convert the solution into polar form,

$$\bar{u} = \frac{\hat{p}}{k} H_1 e^{-i\delta_1} - \frac{\hat{a}_g m}{k} H_2 e^{-i\delta_2} \qquad \textit{(Eq. 2-15)}$$

$$\bar{u}_d = \frac{\hat{p}}{k} H_3 e^{-i\delta_3} - \frac{\hat{a}_g m}{k} H_4 e^{-i\delta_3} \qquad \textit{(Eq. 2-16)}$$

The H and δ terms are:

$$H_1 = \frac{\sqrt{[\beta^2-\rho^2]^2 + [2\zeta_d\rho\beta]^2}}{|D_2|} \qquad \textit{(Eq. 2-17)}$$

$$H_2 = \frac{\sqrt{[(1+\bar{m})\beta^2-\rho^2]^2 + [2\zeta_d\rho\beta(1+\bar{m})]^2}}{|D_2|} \qquad \textit{(Eq. 2-18)}$$

$$H_3 = \frac{\rho^2}{|D_2|} \qquad \textit{(Eq. 2-19)}$$

$$H_4 = \frac{1}{|D_2|} \qquad \textit{(Eq. 2-20)}$$

$$|D_2| = \sqrt{([1-\rho^2][\beta^2-\rho^2] - \bar{m}\beta^2\rho^2 + 2\zeta_d\rho\beta[1-\rho^2(1+\bar{m})])^2} \quad \textit{(Eq. 2-21)}$$

$$\delta_1 = \alpha_1 - \delta_3 \qquad \textit{(Eq. 2-22)}$$

$$\delta_2 = \alpha_2 - \delta_3 \qquad \textit{(Eq. 2-23)}$$

$$tan\delta_3 = \frac{2\zeta_d\rho\beta[1-\rho^2(1+\bar{m})]}{[1-\rho^2][\beta^2-\rho^2]-\bar{m}\beta^2\rho^2} \qquad \textit{(Eq. 2-24)}$$

$$tan\alpha_1 = \frac{2\zeta_d\rho\beta}{[\beta^2-\rho^2]} \qquad \textit{(Eq. 2-25)}$$

$$tan\alpha_2 = \frac{2\zeta_d\rho\beta(1+\bar{m})}{[(1+\bar{m})\beta^2-\rho^2]} \qquad \textit{(Eq. 2-26)}$$

For most cases, the external loading amplification factor H_1 and ground motion amplification factor H_2 are essentially equal and the variation of H_2 with forcing frequency for specific values with damper mass ratio and frequency ratio are shown in Figure 2-2

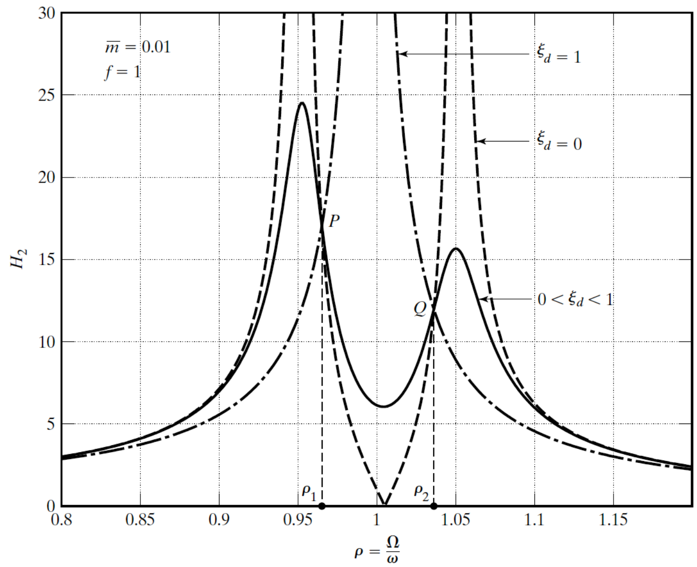

Figure 2-2 Plot of H_2 versus ρ (Figure 4.15, Plot of H_2 versus ρ Jerome J. Connor Introduction to Structural Motion Control, 2002, P251)

2.2.3 Lab and Field Test Results of Vibration Mitigation Devices

Many universities are designed and tested vibration mitigation devices in labs and fields. Gray et al. (1999), Hamilton et al. (2000) had done the field test and finite element analysis of the mast arm signal support structures and reported that failure occurs between the mast arm-to-pole connection and pole-to-base connections due to the fatigue crack. And that crack was resulted by the wind. Both the in-plane (galloping) and out-of-plane (gust) motions have a major contribution on that fatigue damage (Hetor, 2007). Researchers from University of Wyoming, University of Florida, and University of Connecticut had done a lot of works on the effectiveness on the current vibration mitigation devices and provide new types of devices that may get a better result. Some of the dampers with their performance are listed in **Table 2-2**. All data in Table 2-2 are from NCHRP Report 141, NCHRP Report 469, and originally from researches in Florida Department of Transportation (Cook, et al., 2001), University of Wyoming (Hamilton et al. 2000), and NCHRP Report 141.

Table 2-2 Comparison for current vibration mitigation devices on signal support structures

Type of Dampers	Variation	% Critical damping	Increase	Commons by Prior Research
Tuned Mass Damper	Traditional	8.71	32	Frequency sensitive
	Stockbridge	0.42	1.5	Ineffective
	Batten	1.82	6.7	Frequency sensitive
Liquid Damper	Horizontal	0.38	1.4	Ineffective
	U-tube	0.4	1.5	Ineffective
Friction Damper		6.49	23.9	Unattractive
Strut		2.4-6.0	16-40	Required Luminary extension
Alcoa Dumbbell		0.26	1.7	Ineffective
Impact	Vertical Spring-Mass Impact Damper	6.97	25	Lab free vibration
	Horizontal Spring-Mass Impact Damper	0.78	2.9	Ineffective
	Spring/mass liquid impact damper	6.12	22.5	Frequency sensitive and noisy
Signal Head Vibration Absorber (SHVA)		10.1	50.5	Lab test

2.3 Comparison on Traffic Signal Structures in Different States

In the State of Maryland, a standard named MDOT Standards for Highways and Incidental Structures are used for the signal support structures, which include structure type, dimensions, details, and attachment specifications. State of Pennsylvania, North Carolina, South Carolina, Virginia, and New York have no details on pipe size shows on the standard and designed in accordance with the AASHTO Specifications. No mitigation device is mandatory to be installed for all these states except Pennsylvania. Due to all the designs that were based on the previous version of standards or AASHTO Specifications, a vibration mitigation device is suggested be installed.

Chapter 3: Finite Element Modeling and Calibration of Single Mast Arm - Signal Pole Structures

3.1 Details of ANSYS finite element model for Signal Support Structures

3.1.1 Prototype Signal Support Structures

Single mast arm signal pole structure models were selected based on Maryland Department of Transportation State Highway Administration Standards for Highways and Incidental Structures (hereafter referred to as the Signal Pole Standards). Single mast arm signal pole structures are commonly used and can be typical structures in the analysis. In this study, a 70 ft. mast arm length signal support structure was selected and some basic information of the structure is as follows:

Material:

Structure Steel, ASTM A36

Elastic modulus (E): 29000 *Ksi,* Poison's Ratio: 0.3

Density: $490\ lb./ft^3$.

Mast arm-to-pole Condition: Connected using mast arm flange plate welding on the arm end with 4 bolts. (Details in Figure 3-2)

Mast pole-to-base plate: Connected using base plate welding on the pole end with bolts. (Details in Figure 3-1)

Arm Connections: overlap at least 1'-6" and a ¾" hole drilled to connect with 3/8" diameter A307 Galvanized thread stud. (Details in Figure 3-2)

Dimensions:

Pole :

Total height: 27 *ft*.

Height of Base to Arm-Pole connection: 18 *ft*.

Diameter of Pole Base: 15 *in.*

Taper Pole: 0.14 *in/ft*.

Thickness: 5/16 *in.*

Arm:

Arm Length: 70 *ft.*

Diameter Base: 12.5 *in.*

Segment lengths: 35 *ft.* from the flange plate, 25 *ft*.-9 *in.* for the first extension (with 1.75ft. overlap), and 10 *ft.*-6 *in.* for the second extension (with 1.5ft. overlap)

Thickness: 1/4 *in.* for the first 35 *ft.* section, and then 3/16 *in.*

All dimensions using in this study are as follows:

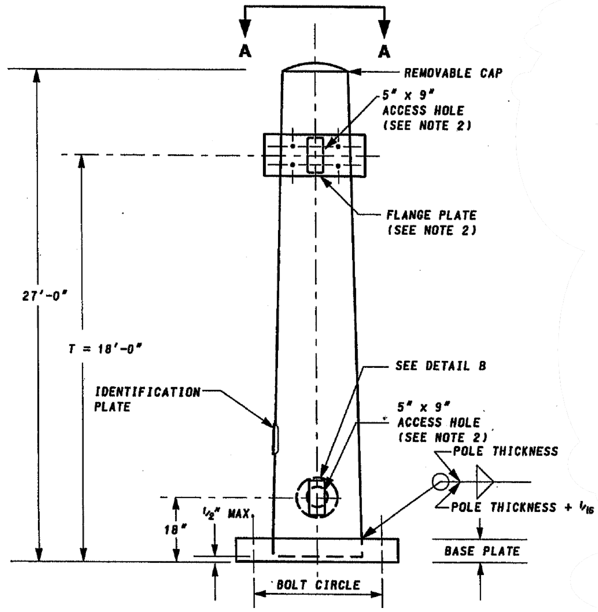

Figure 3-1 Standard Single Mast Pole (Signal Standard No. MD 818.06, 2007 Revised)

Table 3-1 Standard Single Mast Pole Dimensions (Signal Standard No. MD 818.06, 2007 Revised)

Pole Size (Wall thickness × O.D. at Base Plate × O.D. at Pole Top × Pole Height)	**Arm Size** (Flange Plate Shall Accept Any Mast Arm Listed With the Following inclusive Height)	**Anchor Bolts** (All Bolts Shall have a Class of fit rating of 2A/2B UNC.)	**Base Plate** (Side × Side × Plate Thickness)	**Bolt** Circle (Dia.)
3 GAUGE × 13” × 9.22” × 27’	50’	FOUR (4)-1 ¾” DIA. × 66” LENGTH FIVE (5) THREADS PER IN.	18 ½” × 18½” × 2”	18”
0 GAUGE × 15” × 11.22” × 27’	60’ & 70’	FOUR (4)-2” DIA. × 72” LENGTH 4 ½ THREADS PER IN.	23” × 23” × 2”	22”

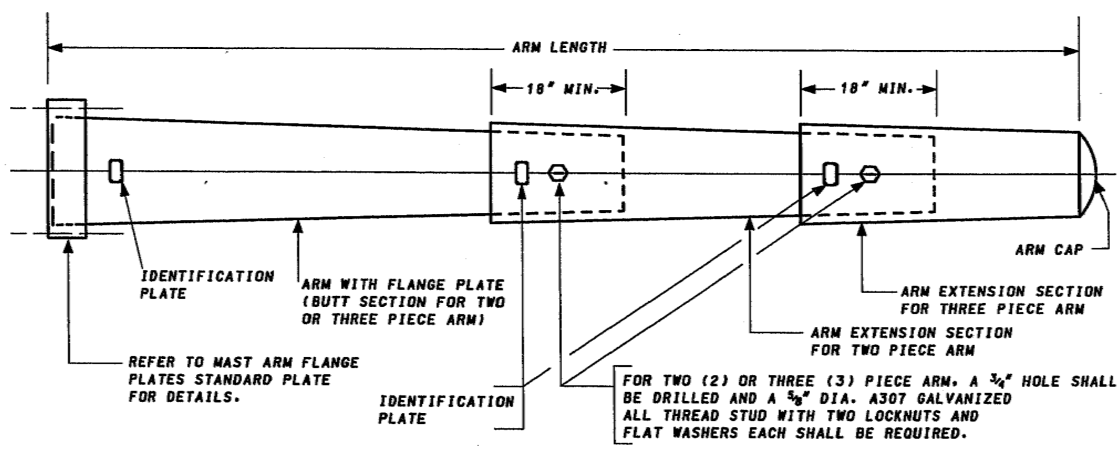

Figure 3-2 Standard Mast Arms (Signal Standard No. MD 818.13, 2007 Revised)

Table 3-2 Standard Single Mast Arm Dimensions (Signal Standard No. MD 818.13, 2007 Revised)

Arm Length	ARM LENGTH (Wall thickness × O.D. at Flange × O.D. at Arm End × Section Length)
50'-0"	(BUTT.) Three (3) GAUGE × 10" × 5.80" × 30'-0" (EXT. 1) Seven (7) GAUGE × 6.37" × 3.36" × 21'-6"
60'-0"	(BUTT.) Three (3) GAUGE × 12.5" × 7.60" × 35'-0" (EXT. 1) Seven (7) GAUGE × 8.24" × 4.50" × 26'-9"
70'-0"	(BUTT.) Three (3) GAUGE × 12.5" × 7.60" × 35'-0" (EXT. 1) Seven (7) GAUGE × 8.24" × 4.50" × 26'-9" (EXT. 2) Seven (7) GAUGE × 5.11" × 3.50" × 11'-6"

3.1.2 Details of ANSYS model

Before building the model, there are some basic assumptions that applied. All the connections (include the connection of the arm sections, mast arm-to-pole connection, pole-to-base connection) are considered to be in fixed conditions and without base plate and overlap. Also the signal is considered only as a mass on the mast arm, and also ignores the instruction plate on the arm due to changeable sizes, weight and locations. Then the handhole on the mast pole is ignored due to it has little influence on the stiffness of the structure and won't be able to be the primary reason that cause the structure collapse (NCHRP Project 10-70). The deflection due to gravity would also be ignored since this study is to compare the difference and effectiveness of mast arm signal structures with TMD.

In these models, Beam188 element was selected to build the main structure. Mass21 element was used as the traffic signal. Consider that the material of the structure is always in a linear condition and use material model of linear-isotropic with the density of 490 $lb./ft.^3$ =0.2836 $lb./in.^3$. Also open small displacement in static and dynamic analysis. Due to the ANSYS program is unitless, and need to define the unit by user, this model chooses inch for length, *lbf* for force, and mass that is based on the Newton Second Law: $m = \frac{F}{a} = \frac{lbf.}{g} = {1\ lbf}/{386.4\ (in./sec^2)}$. Four models with different mesh sizes and section properties were built in the beginning to keep the balance between the calculation time and the accuracy (Table 3-3). When ignoring the overlap of two sections, two parts are divided in each overlap and by using the section of the adjacent arm section for the cylinder model, and use tapered section for the entire arm segment (i.e. 34.125 *ft.* for the butt. section, 26.625 *ft.* for the first extension and 9.25 *ft.* for the second extension.)

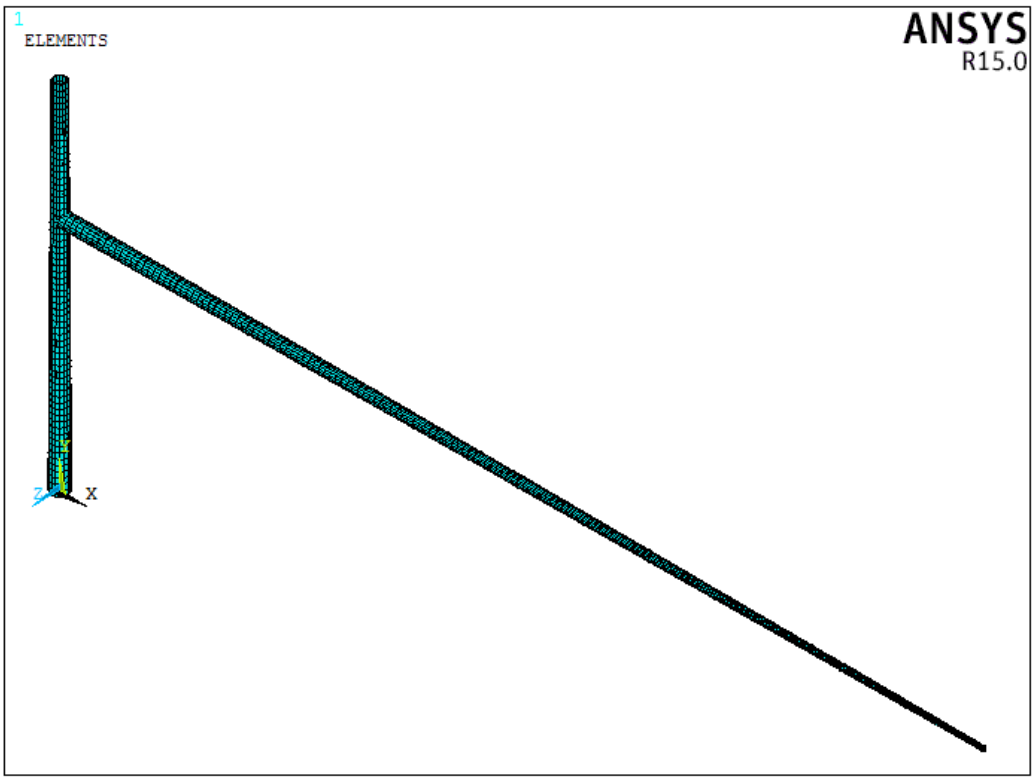

Figure 3-3 Finite Element Model built in ANSYS for 70 ft. mast arm signal pole structure

The first two models use both pole and arm as tapered section. Model 1 uses the mesh size of 0.125 inch in length and section mesh of 512 segments while the second model chooses the mesh size of 1 in. and 72 parts per section. Models 3 and 4 are using cylinder section in each segment. For model 3, the mesh of the pole is 3 *ft.*/

segment; the mesh of the arm is 5 *ft./* segment in the regular part, 0.875 *ft./* segment in the first connection and 0.75 *ft./* segment mesh in the second connection. In model 4, method of bisection mesh of model 3 was selected, that is, use 1.5 *ft./* segment mesh in signal pole, 2.5 *ft./* segment in mast arm regular part, 0.4375 *ft./* segment mesh in the first connection and 0.375 *ft./* segment in the second connection. Details are listed in Table 3-3:

Table 3-3 Details of model mesh size

Model number	Section Type	Section mesh segments	Signal Pole mesh size	Mast arm mesh size	Arm connections mesh size
Model 1	Tapered	512	0.125 in.	0.125 in.	0.125 in.
Model 2	Tapered	72	1 in.	1 in.	1 in.
Model 3	Cylinder	32	3 ft.	5 ft.	0.875 in. & 0.75 in.
Model 4	Cylinder	32	1.5 ft.	2.5 ft.	0.4375 in. & 0.375 in.

To choose the best model, static analyses and modal analyses were done. In the static analysis, add 10 lb. force on the tip of the arm, output the tip displacement to see the difference (the gravity will be ignored). In the modal analysis, output the first 10 modal frequencies in vertical direction, i.e. Y direction in this situation. The result listed in Table 3-4.

Table 3-4 Difference comparing with all four models in ANSYS static and modal analysis

Model number	Computation Speed	Tip deflection (in.)	Difference (Compared with Model 1, %)	First mode frequency in Y direction (Hz)	Difference (Compared with Model 1, %)
Model 1	Very slow	1.27	0	0.75	0
Model 2	Slow	1.27	0	0.75	0
Model 3	Fast	1.27	0.11	0.75	0.391
Model 4	Fast	1.27	0.01	0.75	0.133

Based on the result of static and modal analysis of these four models, model 4 with cylinder section was selected to do the rest of analyses.

When doing the numerical integration in dynamic analysis, Newmark Beta methods was selected using gamma equal to 0.5 and beta equal to 0.25, as well as constant acceleration. Based on the result of modal analysis of the structure, the time interval equal to 0.004 second was selected and the time duration is 40s for free vibration and 60s for force vibration. Use Rayleigh damping to damp out high mode vibration, for the damping of the main structure (without TMD), use Rayleigh damping so that first modal damping ratio is 0.2% and 2nd modal damping ratio is 0.4%.

$$\frac{1}{2}\begin{pmatrix} 1/\omega_i & \omega_i \\ 1/\omega_j & \omega_j \end{pmatrix}\begin{pmatrix} a_0 \\ a_1 \end{pmatrix} = \begin{pmatrix} \zeta_i \\ \zeta_j \end{pmatrix} \qquad \textit{(Eq. 3-1)}$$

3.2 Response Simulation of ANSYS model and calibration with analytical result

3.2.1 Analytical model

In order to get a trustable result from ANSYS, using MATLAB to build a simplified model using as an analytical result and comparing with each other. For the first step of building the model, regard only the mast arm fixed at the arm-to-pole connection. Calculate the static response and then consider the rotation due interaction between mast arm and signal pole. For both models, delete density and use three lumped masses for simplified the whole calculation when doing the verification with the MATLAB code. And at the same time, do an analysis by ANSYS using the same model. The entire calibration is based on the procedures shown below:

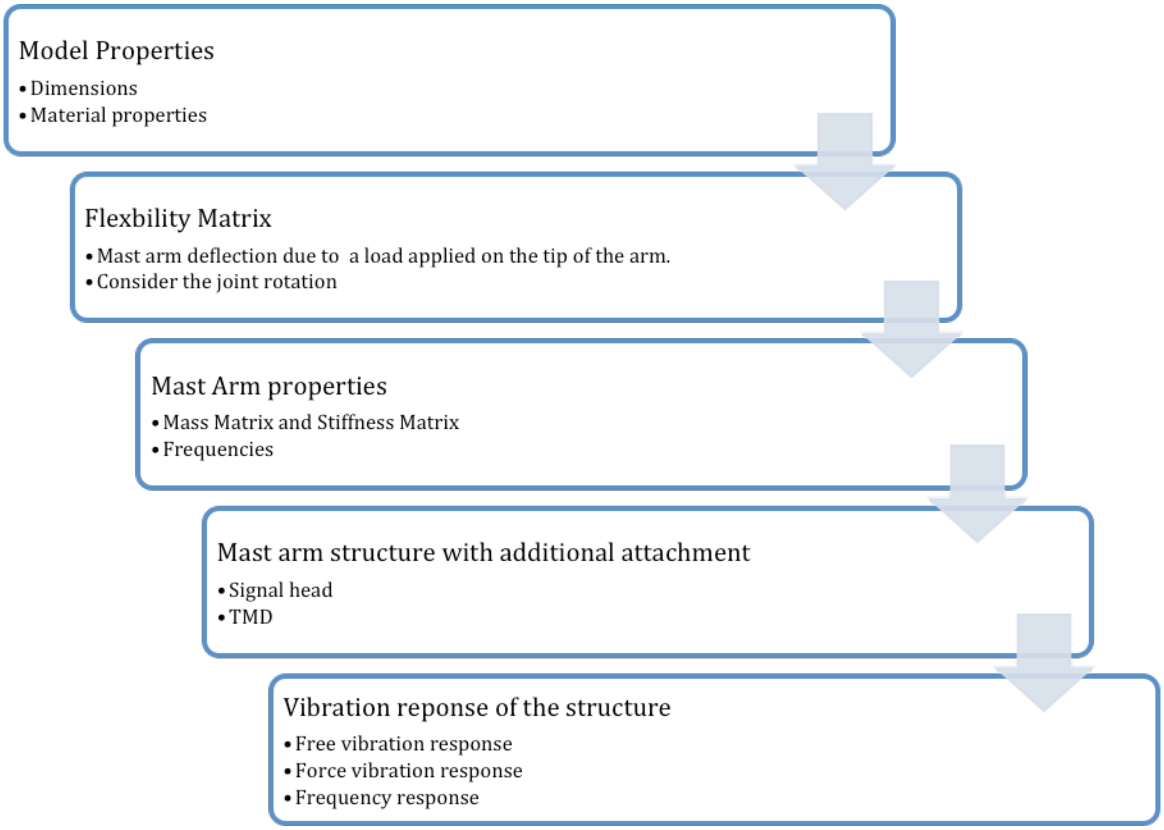

Figure 3-4 Flowchart of the procedures of Analysis

3.2.1.1 Equation of Motion

Based on the theory of structure dynamics (Anil K. Chopra, 2012, DYNAMICS OF STRUCTURES Theory and Application to Earthquake Engineering, 4th edition), for the multi DOF system, the general equation of motion is

$$m\ddot{u} + c\dot{u} + ku = p(t) \qquad \textit{(Eq. 3-2)}$$

Where k is the stiffness matrix and c is the damping matrix for the structure, as well as m for the mass matrix and u for the displacement vector, $\dot{u}$ for the velocity vector, and $\ddot{u}$ for the acceleration vector.

In the beginning, a calculation for the deflection of the mast arm under a certain load is done using the cantilever deflection equation:

$$\delta = \frac{Fl^3}{3EI} \qquad \textit{(Eq. 3-3)}$$

Due to the structure is assumed a three DOFs, the tip deflection would be the accumulate of all three node deflection caused by load and equivalent moment, and the rotation angle times the length from the section tip to the tip of the entire mast arm. The deflection of each node could be calculated and assembly to the flexibility matrix δ. By determine the flexibility matrix δ, the stiffness matrix could be calculated

$$k = \delta^{-1} \qquad \textit{(Eq. 3-4)}$$

Frequencies and mode shapes could also be calculate by:

$$det(\boldsymbol{k} - \boldsymbol{\omega}^2\boldsymbol{m}) = 0 \qquad \textit{(Eq. 3-5)}$$

$$(\boldsymbol{k} - \omega_i{}^2\boldsymbol{m})\boldsymbol{\phi_i} = 0 \qquad \textit{(Eq. 3-6)}$$

where $\boldsymbol{\omega}$ refers to the frequencies vector

$$\boldsymbol{\omega} = \begin{pmatrix} \omega_1 \\ \vdots \\ \omega_n \end{pmatrix} \qquad \textit{(Eq. 3-7)}$$

where ω_i is the $i^{th.}$ modal frequency with the unit *rad/s*

and ϕ_i refers to the normalized corresponding $i^{th.}$ mode shape

$$\boldsymbol{\Phi} = (\phi_1 \quad \cdots \quad \phi_n) \qquad \textit{(Eq. 3-8)}$$

By doing these preparations, the structure's free vibration response, force vibration response and modal analysis could be done by solving the equation of motions.

3.2.1.2 Model Details

In this verification, a simplified analytical model has been built. The model is assumed as a cantilever beam, that is, fixed at the mast arm end and free at the other end. Use tapered section for three segments and lumped the mass of 699.8 *lb*., 251.1 *lb*., and 67.1 *lb*. in 3 nodes, i.e. 35 *ft*., 60 *ft.* and 70 *ft.* Assume the material is isotropic with Elastic modules $E=29000ksi$ and other properties and parameters as in ANSYS model. Mass of three signal heads had been lumped to each node.

3.2.2 Finite Element Model

The first step is to use finite element model built in ANSYS is using Model 2 in mesh size, fixed the arm end, and lumped the mass into three nodes, which is used to match with analytical model, to run the same cases as analytical analysis. Also, a distribute mass model with accurate location of signal heads is used for comparing the result. Ignore the gravitation for both analytical and finite element model. Use Rayleigh damping to damp out high mode vibration, and the damping ratio of the arm is 0.2% for the first mode and 0.4% for the second mode damping ratio based on the field test and lab test results from University of Florida (Ronald A. Cook et al, 2000). Because the mast arm model in MATLAB is considered the rotation of the mast arm-to-pole connection after the first validation procedure, all results below shows the equivalent result for the whole signal support structure.

3.2.3 Validation of Finite Element model using analytical results

As the flowchart described above, do the static analysis by adding 10lbf at the free tip and got the deflection of the mast arm:

Table 3-5 Static analysis result comparison between analytical and finite element models

Model type	Tip deflection (in.)	Difference (Compared with Analytical Model, %)
Analytical model	1.23	0
FE model using lumped mass	1.27	3.057
FE model using density and mass	1.27	3.057

Then calculate the frequencies and mode shape:

Table 3-6 Modal analysis result comparison between analytical and finite element models

Model type	First modal Frequencies in vertical direction (Hz.)	Difference (Compared with Analytical Model, %)
Analytical model	0.57	0
FE model using lumped mass	0.54	-5.41
FE model using density and mass of signal heads	0.64	12.73

The third step is to validate the free vibration response by applying an excitation sinusoidal load with frequency of the first mode on the structure free the end, and after reaching the steady state, delete the load and let the mast arm do the free vibration and record the result:

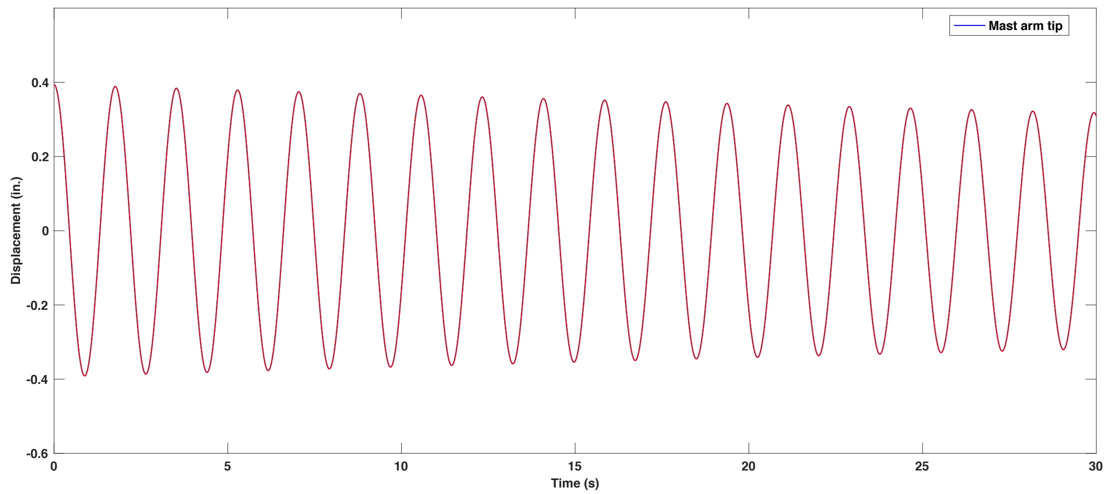

Figure 3-5 Free vibration displacement response using analytical model

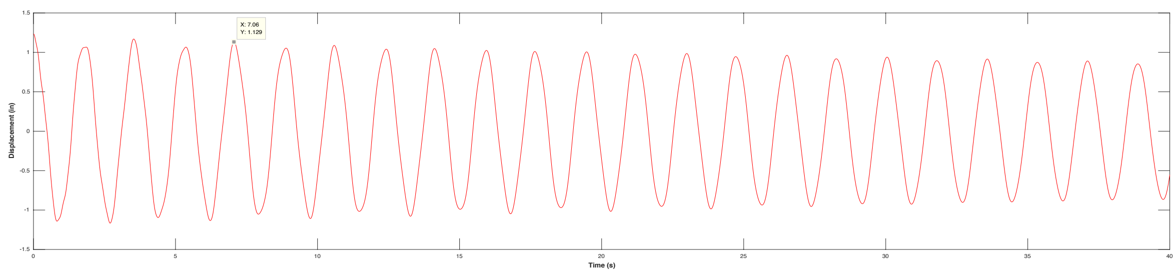

Figure 3-6 Free vibration displacement response using ANSYS model with lumped mass

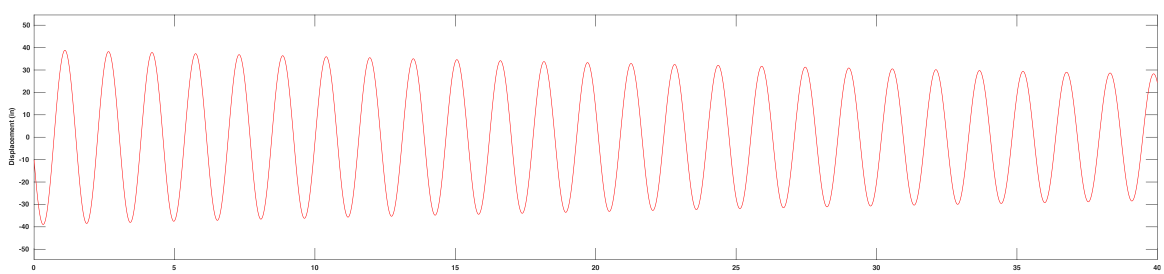

Figure 3-7 Free vibration displacement response using ANSYS model with distributed mass and mass of signal heads

Then the equivalent viscous damping ratio could be calculated by using the logarithmic decay formula:

$$\zeta = \frac{ln\left(\frac{u_i}{u_j}\right)}{2\times\pi\times(j-i)} \qquad \textit{(Eq. 3-9)}$$

Using this formula by choosing the third and fifth of the peak value from the result and calculate the equivalent viscous damping ratio shows in Table 3-7:

Table 3-7 Result comparison between analytical and finite element model

Model type	The third maximum peak value from the output figure u_3*(in)*	The fifteenth maximum peak value from the output figure u_{15}*(in)*	*Calculated equivalent damping ratio* ζ	Difference (Compared with Analytical Model, %)
Analytical model	0.39	0.33	0.2%	0
FE model using lumped mass	1.011	0.86	0.22%	10
FE model using density and mass of signal heads	37.81	32.48	0.2%	0

And the different between the first and the second model is unchanged (the value used the same as the third model) alpha and beta values in Rayleigh damping.

Finally, the harmonic analysis for the frequency response under the amplitude of 5-lbf cyclic excitation load had been plotted for comparison in Figure 3-11 and Figure 3-12.

3.3 Tuned Mass Damper Model

The typical Florida damper (Figure 3-8) and Alcoa damper (Figure 3-9) are used to analysis in this study, and choose the Florida damper as the calibration model due to sufficient data from previous researches and effectiveness of the devise's performance on vibration mitigation.

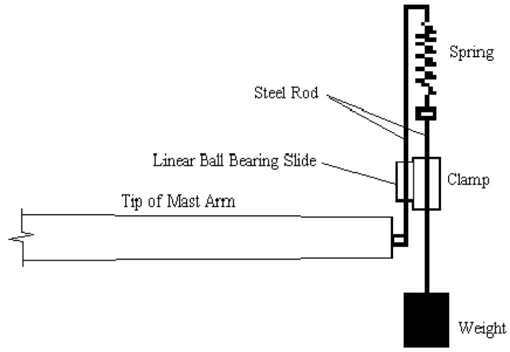

Figure 3-8 Florida damper (Ronald A. Cook et. al, NCHRP report 141, page 27 Figure 3.19)

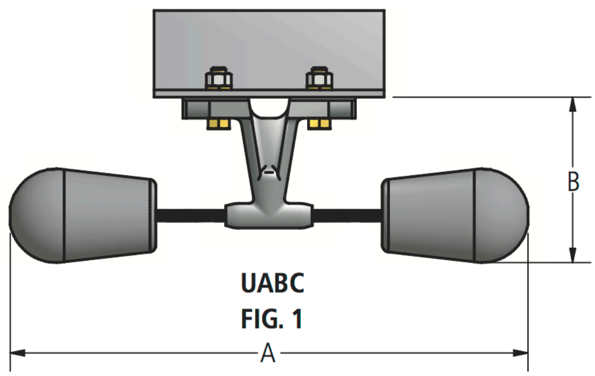

Figure 3-9 Alcoa damper. (From AFL Substation Bus Dampers catalog)

3.3.1 Prototype TMD – Alcoa damper and Florida damper

Luminary manufactures recommend (NCHRP Report 469) some damping devices that show a good behavior on vibration mitigation. Dogbone dampers, which are also called Stockbridge dampers, are similar with Alcoa dampers where they consist of two weights at end of a flexible shaft. Alcoa and Florida dampers are two of most commonly used vibration mitigation devices in signal support structures. The Alcoa damper is consisting of two masses linked with a steel cable. And the Florida damper could be regarded as the basic TMD model, i.e. a spring, a dashpot, and a mass.

3.3.2 Model description (in ANSYS)

In this study, combin14 element and mass21 element has been used to simulate the vibration mitigation device. Two nodes will be created at the same location and using the combin14 element to link these two nodes without mesh, inputting the real constant stiffness (k) and damping coefficient (c) values. The output option 2 is set as only moving in vertical (Y) direction. Add the mass element on the free node and connect the other node to the main structure.

3.3.3 Calibration of Viscous Damping ratio

Viscous Damping ratio usually needed to be calibrated by experiment; each structure and damper has its own viscous damping ratio.

Based on the FLDOT report, the spring-mass damper for 15lb mass model has an approximate 6% damping ratio by doing logarithmic decay of the free vibration tip deflection time-history curve. In this study, the stiffness and damping coefficient could be calculated as:

$$k = (2\pi f)^2 \times m \qquad \textit{(Eq. 3-10)}$$

$$c = \zeta \times (2\sqrt{km}) \qquad \textit{(Eq. 3-11)}$$

3.4 Combined TMD with mast arm structures

After calibrating of the parameters of TMD, the final case that combined TMD with the single mast arm signal support structure was build (Figure 3-10). In this case, just choose the analytical model and finite element model using distributed mass and mass of signal heads. Also, change the tapered section into cylinder section since this finite element model is the one that used for the rest of the analysis.

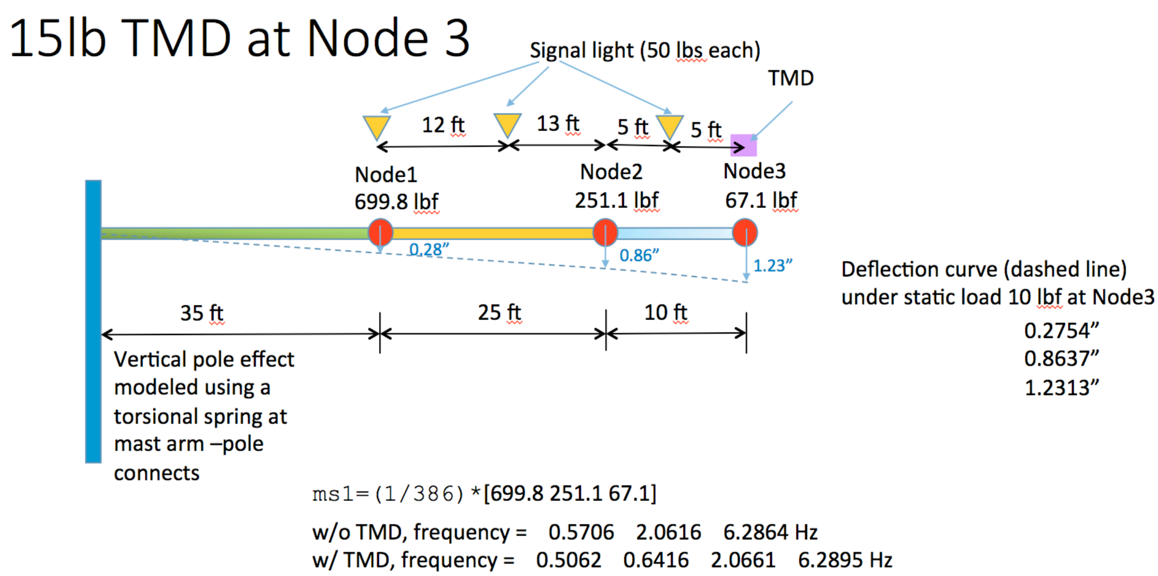

Figure 3-10 Model and static summary of MATLAB model for the TMD with the mast arm

The result for the static analysis remains the same as before because the stiffness of the structure has not change. For the frequencies of the structure, results are shown in Table 3-8, and frequency response is shown in Figure 3-11 and Figure 3-12.

Table 3-8 Frequencies comparison for models with TMD

Model type	First modal Frequencies in vertical direction (Hz.)	Second modal Frequencies in vertical direction (Hz.)
Analytical model	0.5062	0.6416
Finite Element model	0.56304	0.73499

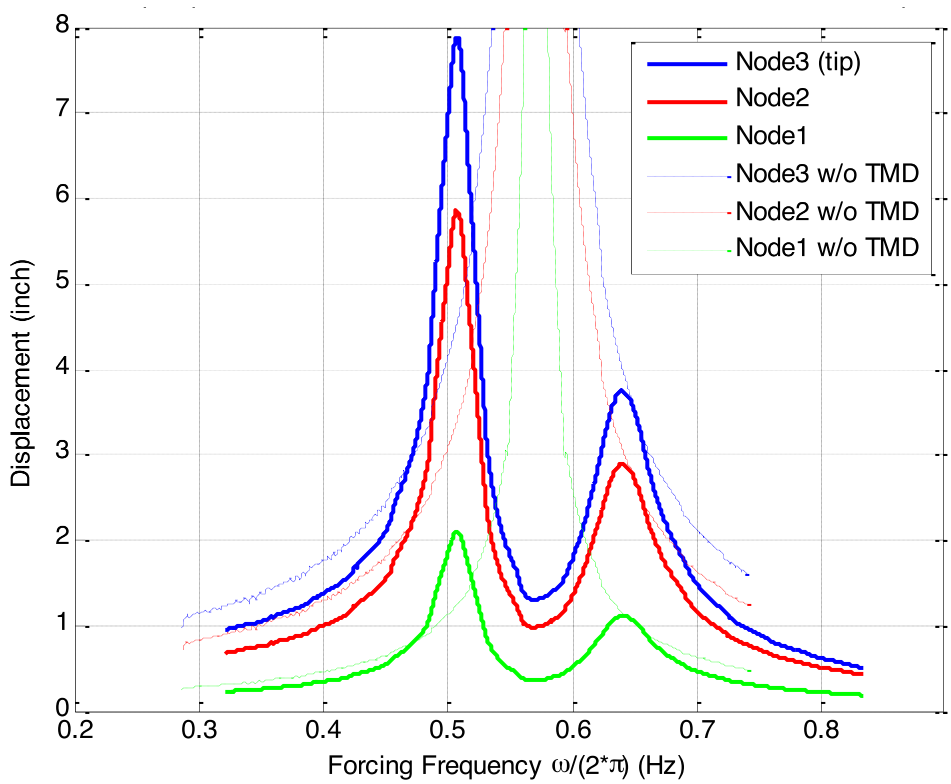

Figure 3-11 Harmonic Analysis for the Analytical model using 15lb. mass TMD

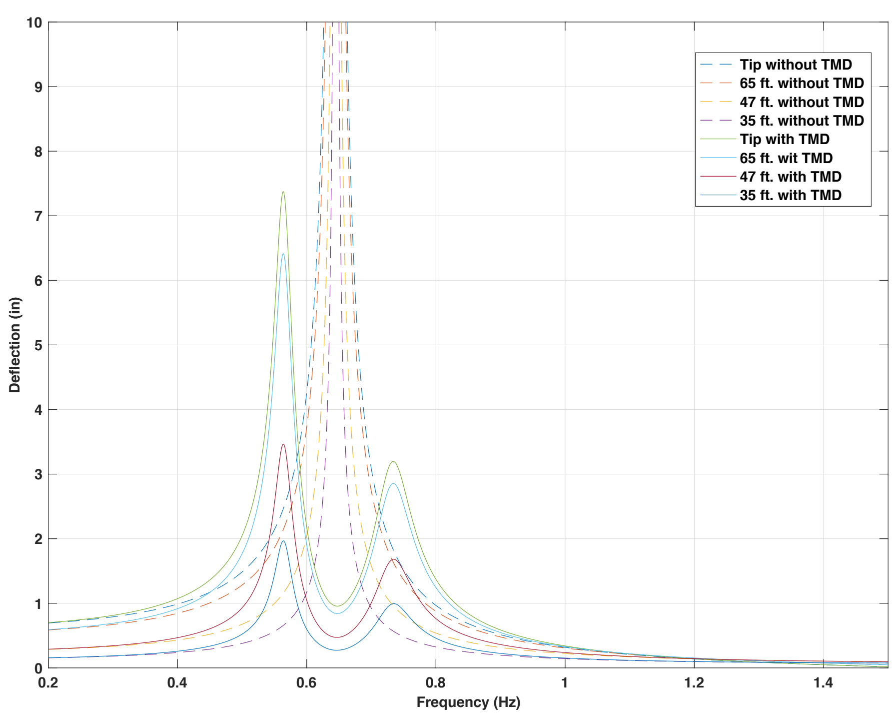

Figure 3-12 Harmonic Analysis for the finite element model using 15lb. mass TMD

3.5 Conclusion for the verification

Form the result comparisons in section 3.1 to section 3.4, outputs for the same analysis are in an acceptable range comparing the finite element model and the analytical model. This finite element model is verified that the method to build finite element model and the result of the analysis for the parametric study is acceptable.

Chapter 4: Parametric Study of Vibration Mitigation Effectiveness of TMD on Single Mast Arm- Signal Pole Structures

4.1 Overview of Parametric Study - Variation in parameters

In this study, three types of single mast arm signal support structures were selected. The differences between these models are mainly the different arm lengths and dimensions based on the Signal Pole Standard. Section 4.1 will use 70 feet arm length single mast arm signal pole model, while section 4.2 will use 60 feet arm length model, and the 50 feet arm length model will be analysis in section 4.3. These three types of mast arm are the most commonly used in the State of Maryland. In each model, various types of analysis will be done for obtaining the response properties of the structure. All models are summarized in Table 4-1.

In the first case of these three models, applied TMD with different mass but with the same damping ratio. For the structure total mass, which has calculated before, varied between approximate 1500 lb. to 2600 lb., while a TMD mass is usually less than about 5% of the whole system (Jerome J. Connor, 2002). Also the Florida damper were used in the mass of 15lb. and the Alcoa damper is used in 20 lb. to 30 lb., so that the 15 lb. and 25 lb. damper masses were selected.

Because of the TMD efficiency is frequency-depended, several of TMD frequencies was selected to analyze in case 2 of each model. For all three models, choose the frequencies equal to 125%, 75%, 50% and 150% of the structure frequency and compared with the natural frequency model to determine the effectiveness of the TMD.

Table 4-1 Summary of the cases in the parametric study

Arm length	Model	TMD			
		Damping Ratio	Mass	Frequency	Location
50 ft.	Without TMD	N/A	N/A	N/A	N/A
	With TMD	6%	15 lb.	Fundamental Frequency (f_n))	Tip
		6%	25 lb.	Fundamental Frequency (f_n)	Tip
		6%	15 lb.	$1.1f_n$	Tip
		6%	15 lb.	$0.9f_n$	Tip
		6%	15 lb.	$1.25f_n$	Tip
		6%	15 lb.	$0.75f_n$	Tip
		6%	15 lb.	$1.5f_n$	Tip
		6%	15 lb.	$0.5f_n$	Tip
		1%	25 lb.	Fundamental Frequency (f_n)	Tip
		6%	15 lb.	Fundamental Frequency (f_n)	2.5ft. From Tip
		6%	15 lb.	Fundamental Frequency (f_n)	5ft. From Tip
		6%	15 lb.	Fundamental Frequency (f_n)	10ft. From Tip
60 ft.	Without TMD	N/A	N/A	N/A	N/A
	With TMD	6%	15 lb.	Fundamental Frequency (f_n)	Tip
		6%	25 lb.	Fundamental Frequency (f_n)	Tip
		6%	15 lb.	$1.1f_n$	Tip
		6%	15 lb.	$0.9f_n$	Tip
		6%	15 lb.	$1.25f_n$	Tip
		6%	15 lb.	$0.75f_n$	Tip
		6%	15 lb.	$1.5f_n$	Tip
		6%	15 lb.	$0.5f_n$	Tip
		1%	25 lb.	Fundamental Frequency (f_n)	Tip
		6%	15 lb.	Fundamental Frequency (f_n)	2.5ft. From Tip
		6%	15 lb.	Fundamental Frequency (f_n)	5ft. From Tip
		6%	15 lb.	Fundamental Frequency (f_n)	10ft. From Tip
70 ft.	Without TMD	N/A	N/A	N/A	N/A
	With TMD	6%	15 lb.	Fundamental Frequency (f_n)	Tip

		6%	25 lb.	Fundamental Frequency (f_n)	Tip
		6%	15 lb.	$1.1f_n$	Tip
		6%	15 lb.	$0.9f_n$	Tip
		6%	15 lb.	$1.25f_n$	Tip

Continue Table 4-1 Summary of the cases in the parametric study

In the third case, use dampers with different damping ratios in the same model to compare the difference. Based on the reviews and calibration in previous chapter, two kinds of TMDs that can be regarded as simplified model - Alcoa damper (using approximate 1% damping ratio) and Florida damper (using approximate 6% damping ratio).

The location of TMD will also influence the effectiveness of TMD by changing the frequency of the whole structure, etc. The fourth case is therefore to put the same TMD in different location on mast arm of the structure models and make comparisons. Then, calibrate with Harmonic Analysis result in ANSYS to get the reasonable suggested location of TMD.

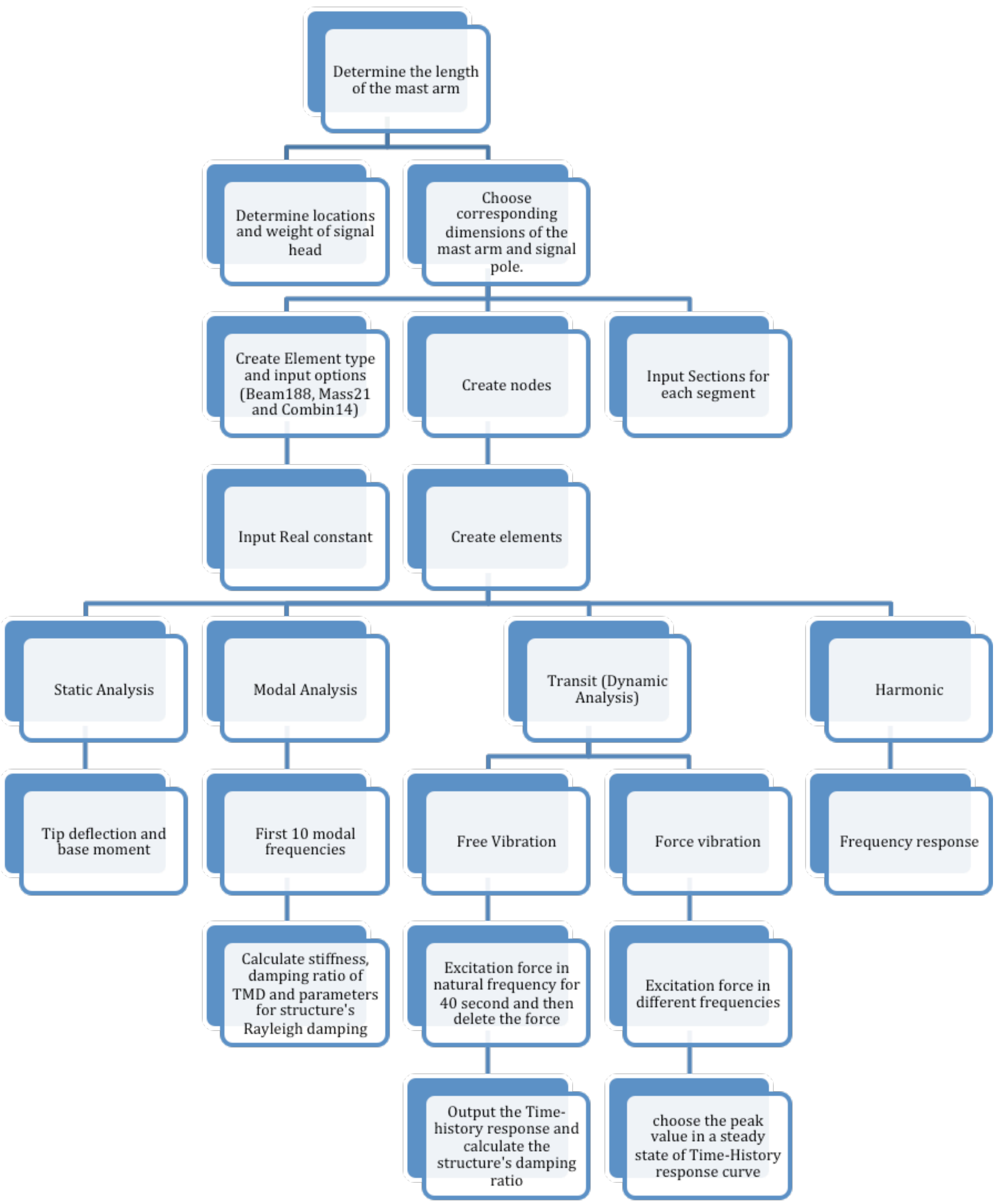

Figure 4-1 Procedures for doing the entire analysis

4.2 Signal Support Structure with 70 ft. Arm Length

4.2.1 Finite Element Model description

For the 70 ft. arm length structure, beam188 element was selected to build the main structure. Mass21 element was used as the traffic signal and mass of the TMD. And combin14 element is used for simulates the TMD's spring stiffness and damping ratio. The locations of signals could vary. In this model, use three signals at 35 *ft*. 47 *ft*. and 65 *ft*. from the arm-pole joint. For the arm-pole joint and base, simply regard it as in fixed condition. The gravitation is ignored in the dynamic analysis. Input real constant of mass21 and combin14: use 50 *lb.* / signal to be conservative for traffic signal and 15 *lb.* or 25 *lb.* mass of the TMD; ignore the initial deflection of the structure due to self-weight and probable raise angle of the mast arm and assumed the TMD is rigidly connected to the mast arm. The mesh size is using 1.5 *ft./*segment for signal pole, and 2.5-*ft./* segment for mast arm primary part. And for the connections between arm segments, use 0.4375-*ft*. per segment for the connection of base arm and the first extension, and 0.375-*ft.* per segment for the first and second extension connection.

The dimensions of the pole and mast arm are shown in Table 3-1 and Table 3-2.

For the Model without TMD, use Model 4 in chapter 3 with density and put three traffic signals in 35ft., 47ft., and 65ft. from the mast arm-to-pole connection. All the traffic signal heads are assumed rigidly connected to the mast arm. Run the modal analysis first to get the first 10 modes of frequencies. The TMD will be on the tip of the mast arm unless specified.

4.2.2 Mast arm signal support structure model without TMD and its outputs

After plotting each mode of frequencies, choose the first mode frequency and the second mode frequency in Y direction, in this case 0.645Hz and 2.29 Hz, to calculate the alpha and beta values in Rayleigh damping matrix. Choose 0.2% in the first mode and 0.4% for the second mode, and the value would be:

$$\frac{1}{2}\begin{pmatrix} 1/\omega_1 & \omega_1 \\ 1/\omega_2 & \omega_2 \end{pmatrix}\begin{pmatrix} a_0 \\ a_1 \end{pmatrix} = \begin{pmatrix} \zeta_1 \\ \zeta_2 \end{pmatrix} \qquad \textit{(Eq. 4-1)}$$

Where, $\zeta_1 = 0.2\%$, $\zeta_2 = 0.4\%$

$\omega_1 = 2\pi f_1 = 2\times\pi\times0.64484 = 4.05165\ rad/s$

$\omega_2 = 2\pi f_2 = 2\times\pi\times2.2865 = 14.3665\ rad/s$

Solve the Equation 4-1, then,

$$\begin{pmatrix} a_0 \\ a_1 \end{pmatrix} = \begin{pmatrix} \alpha \\ \beta \end{pmatrix} = \begin{pmatrix} 0.00765812 \\ 0.0005166 \end{pmatrix}$$

Put these values back in Rayleigh damping matrix for Newmark beta method and do the dynamic analysis for free vibration and force vibration. For the free vibration, use harmonic excitation force with the frequency of first mode frequency at the tip of the arm for 40 seconds, then delete all forces to let the whole structure to do the free vibration for another 40 seconds. Then output the time-history result of 4 nodes (Tip of the arm, 3 signals locations, i.e., 35 *ft.* 47 *ft.* and 65 *ft.* from the mast arm-to-pole connection) deflections, accelerations, and maximum moment at the arm-pole joint (shows in Figure 4-2). Then using the equation

$$\varepsilon = \frac{M\times R_0}{EI} \qquad \textit{(Eq. 4-2)}$$

where R_0 equals to the outer diameter of the arm section in the arm-to-pole connection.

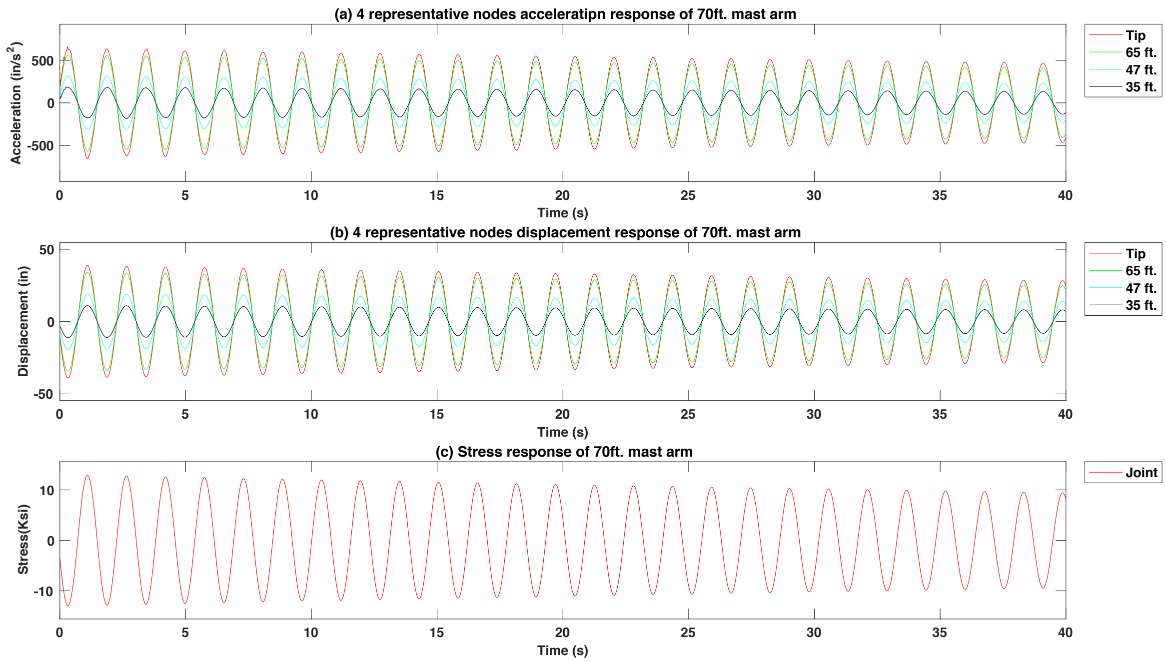

Figure 4-2 Free vibration response of the 70 ft. arm signal support structure model without TMD

Then calculate the mast arm equivalent viscous damping ratio using logarithmic decay formula based on the free vibration response. Choose the third maximum peak value and the fifteenth maximum peak value and use Equation 3-9.

$$\zeta = \frac{ln\left(\frac{u_3}{u_{15}}\right)}{2\times\pi\times(15-3)} = \frac{ln\left(\frac{37.79}{32.48}\right)}{2\times\pi\times 12} = 0.2\%$$

The results above can verify that the finite element result and the calibration assumption are using the same damping ratio, which means that the initial model is performing correctly and can be used for the rest of the analysis.

After doing the free vibration response analysis and verified the model, add different harmonic excitation force on the free tip of the mast arm in Y direction. And also plot the acceleration, displacement, and strain of the representative nodes.

For the frequency of excitation force equal to the natural frequency and amplitude of 5 lb., that is

$$F = 5 \times sin\ (2\pi f \times t)$$

where F refers to the excitation force of the structure.

The result (Figure 4-3) shows a trend that all output tend to increase in a long period, and may not have the maximum value if the structure has no damping ratio. However, the mast arm signal pole, even has a very small damping ratio of 0.2% that due to material damping and interaction with structure and the air, can reach to a maximum value of 140 in. and keep the amplitude if continue to excite the tip using the same excitation force. Acceleration and strain show the same trend as displacement.

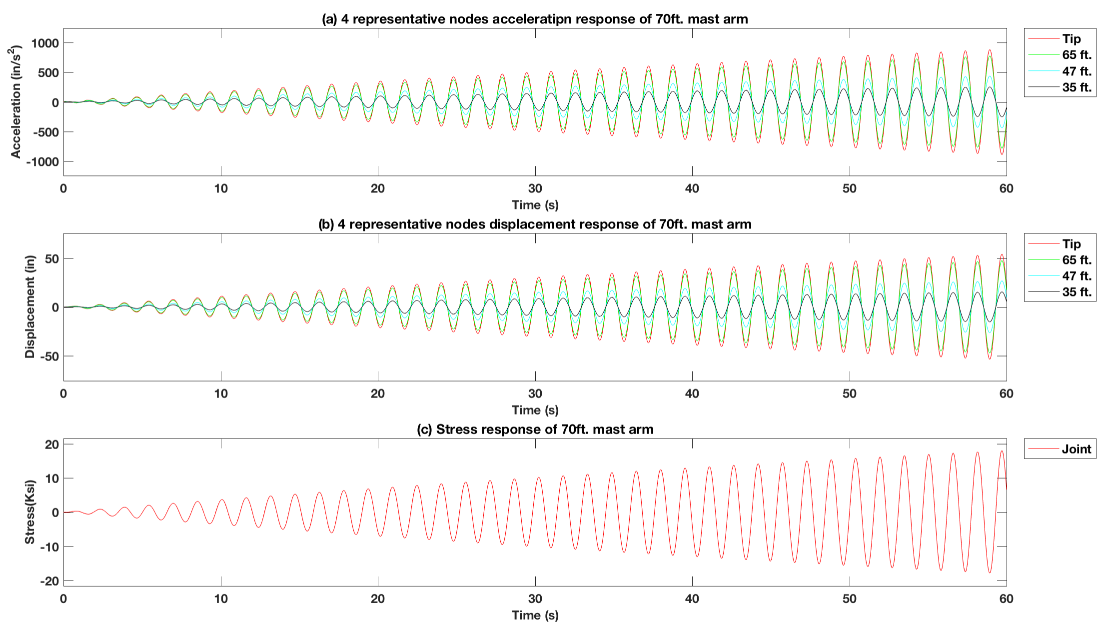

Figure 4-3 Force vibration response of excitation force at tip in natural frequency of the 70 ft. mast arm signal pole structure model without TMD

Then, the responses using the same model as previous but different excitation force frequency from *0.6f* to *1.4f*, which applied on the tip of the mast arm, are computed and plotted. Due to very large amount of data and figures, just some representative figures would be shown.

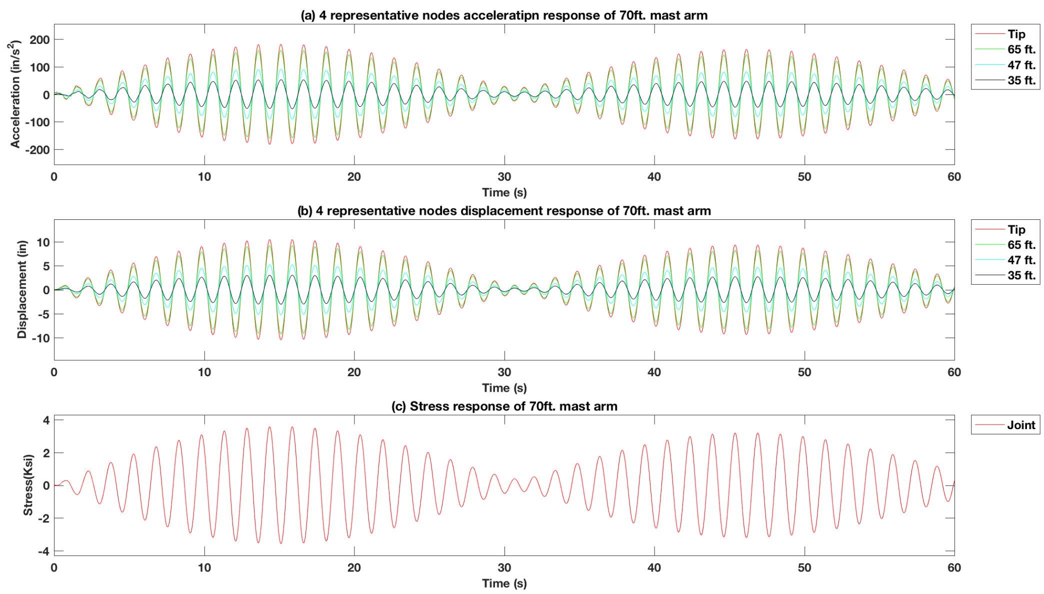

Figure 4-4 Force vibration response of excitation force at tip in $f_2 = 1.05\times\text{Natural frequency}$ of the 70 ft. arm signal support structure model without TMD

When finishing all the force vibration analysis case, run a harmonic case using the applied load equal to 5 *lbf* at the free tip for the real part and 0 for the imagine part. Set load step equal to 5000, stepped load, frequency from 0.2 Hz to 1.5 Hz. Then, plot the frequency response curve.

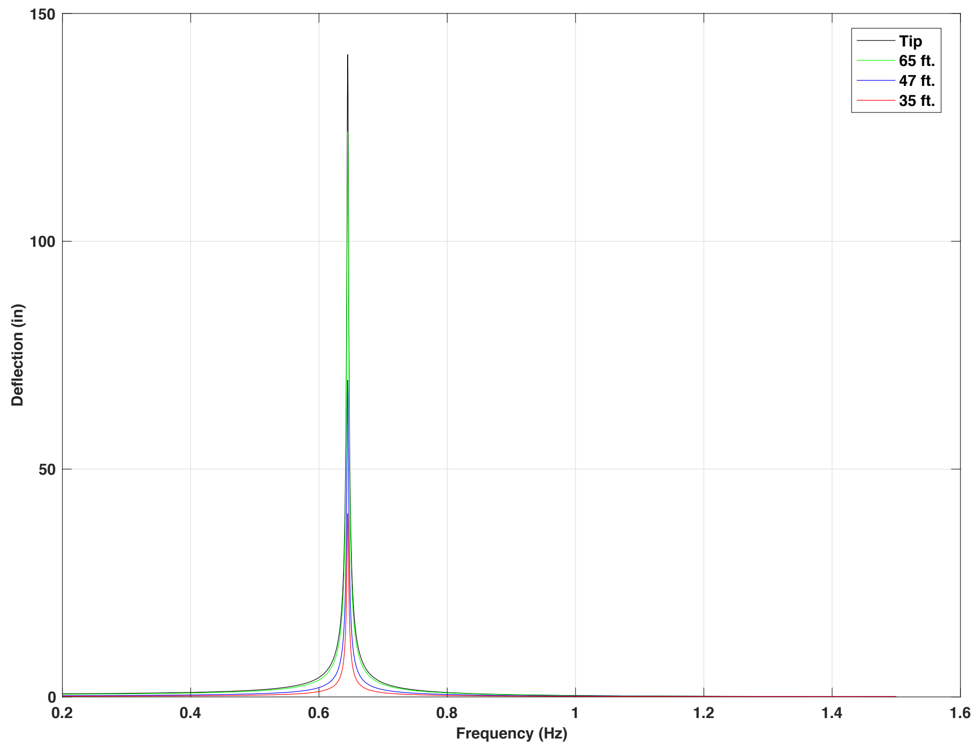

Figure 4-5 Harmonic response for excitation force on the mast arm tip of the 70 ft. arm signal support structure model without TMD

The peak value would be the case when the excitation force has a frequency in the natural frequency of the entire structure.

Also using the half-power bandwidth of the frequency response, which use the amplitude $u_0 = 1/\sqrt{2}\,u_{peak}$, check corresponding frequency ω, and calculate the damping ratio using:

$$\frac{f_b - f_a}{f_n} = 2\zeta \qquad \textit{(Eq. 4-3)}$$

Then applied excitation force frequency $f = f_0 \sim f_{10}$ at different locations, use the same model and excitation force frequency from $0.5f_{TL}$ to $1.5f_{TL}$ applied on the location of three signal heads, compute for the displacements, accelerations, stress at the mast arm-to-pole connection, as well as the Harmonic analysis of frequency response curve. Due to very large amount of data and figures, just some representative figures would be shown.

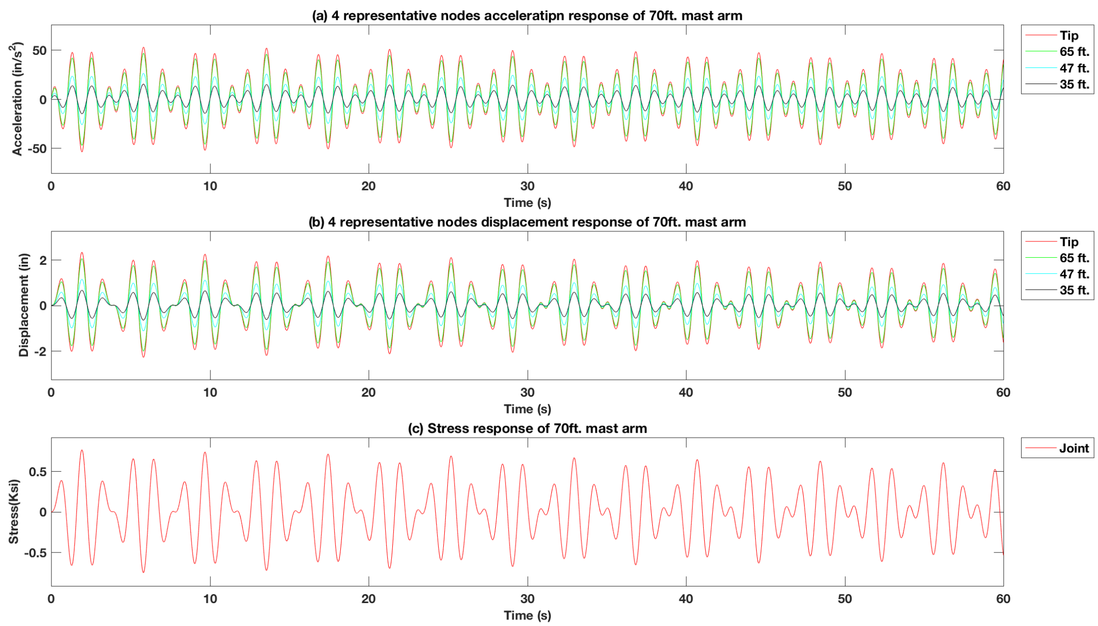

Figure 4-6 Force vibration response of excitation force at mast arm signal heads locations in $f_2 = 1.5 \times \text{Natural frequency}$ of the 70 ft. arm signal support structure model without TMD

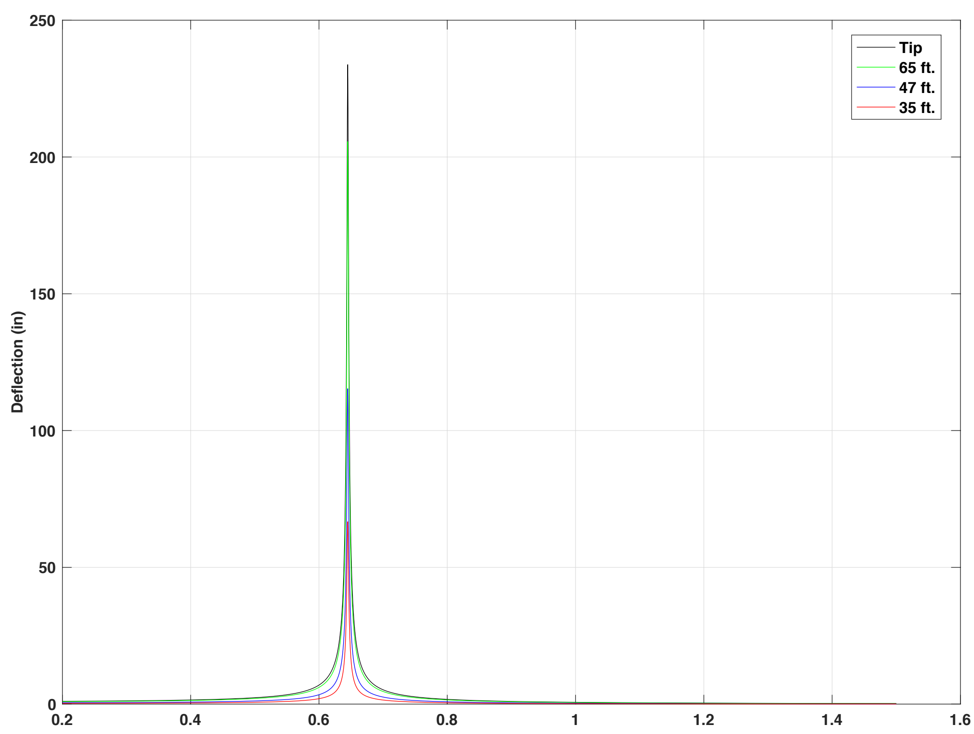

Figure 4-7 Harmonic response for excitation force on the mast arm signal heads locations of the 70 ft. arm signal support structure model without TMD

Calculate the corresponding damping ratio using half-power band width methods and the equivalent damping ratio is:

$$\frac{0.6462 - 0.6436}{2\times 0.6449} = 2\%$$

4.2.3 TMD Mass

In this comparison, TMD masses of 15 lb. and 25 lb. were chosen. Based on the initial model, the first mode frequency in Y direction is 0.64484 Hz, and the second mode frequency in Y direction is 2.2856 Hz. So the properties of the TMD will be calculated using

$$k = (2\pi f)^2 \times m \qquad \textit{(Eq. 4-4)}$$

$$c = \zeta \times (2\sqrt{km}) \qquad \textit{(Eq. 4-5)}$$

Where: $\zeta = 6\%$ for both these two TMD. Also the impact by the mass and the tube will be ignored.

For the frequency of the damper, use the approximate optimal damper frequency, where

$$f_d = f = 0.645\ Hz \qquad \textit{(Eq. 4-6)}$$

After input parameters of the TMD, run modal analysis for the first three modal frequencies, choose the one of the first or second frequency, and third frequency in Y direction to recalculate alpha and beta values in the Rayleigh damping matrix for the structure damping. All the calculated parameters are list in Table 4-2.

Table 4-2 Preliminary model analysis for 70 ft. arm with 15lb. and 25lb. TMD

TMD mass	f_1 (Hz)	f_2 (Hz)	f_3 (Hz)	k	c	α	β
15 lb.	0.56	0.73	2.29	0.64	0.019	0.007	5.35E-04
25 lb.	0.54	0.76	2.30	1.06	0.031	0.007	5.19E-04

Since both the first and second mode shapes are shown as the first mode shape (ignore the position of TMD) for the signal support structures, and shows less contribution in deflection of the mast arm for the first mode when got same TMD deflection, the second mode frequency is usually chosen for the free vibration excitation force frequency and initial frequency for force vibration excitation force.

Then do the free vibration response as initial model, that is, excitation force use the harmonic force with the frequency of f_2 for 40 seconds and remove the force to let that node to be free, then plot the result of displacements' response curve and accelerations' response curve of the same four representative node (mast arm tip and 3 signals' location), and moment of the mast arm-to-pole joint, then calculate for the stress by the equation

$$\sigma = \frac{M \times R_0}{I} \qquad \text{(Eq. 4-7)}$$

For free vibration response, the curve shows not an excellent smooth curve because of the excitation force. Even though using the second modal natural frequency as the excitation force, there are still interactions between the mast arm and mast pole, as well as the mast arm and TMD.

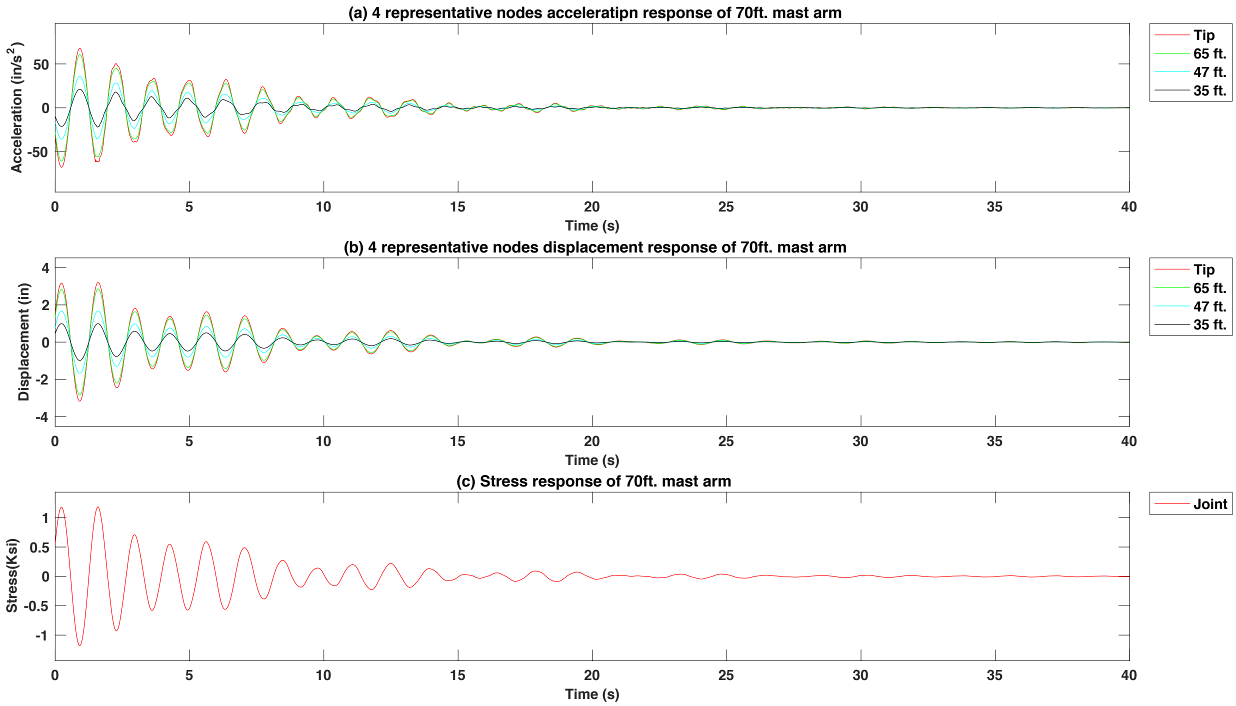

Figure 4-8 Free vibration response of the 70 ft. arm signal support structure model with 15 lb. TMD in the same frequency of the structure

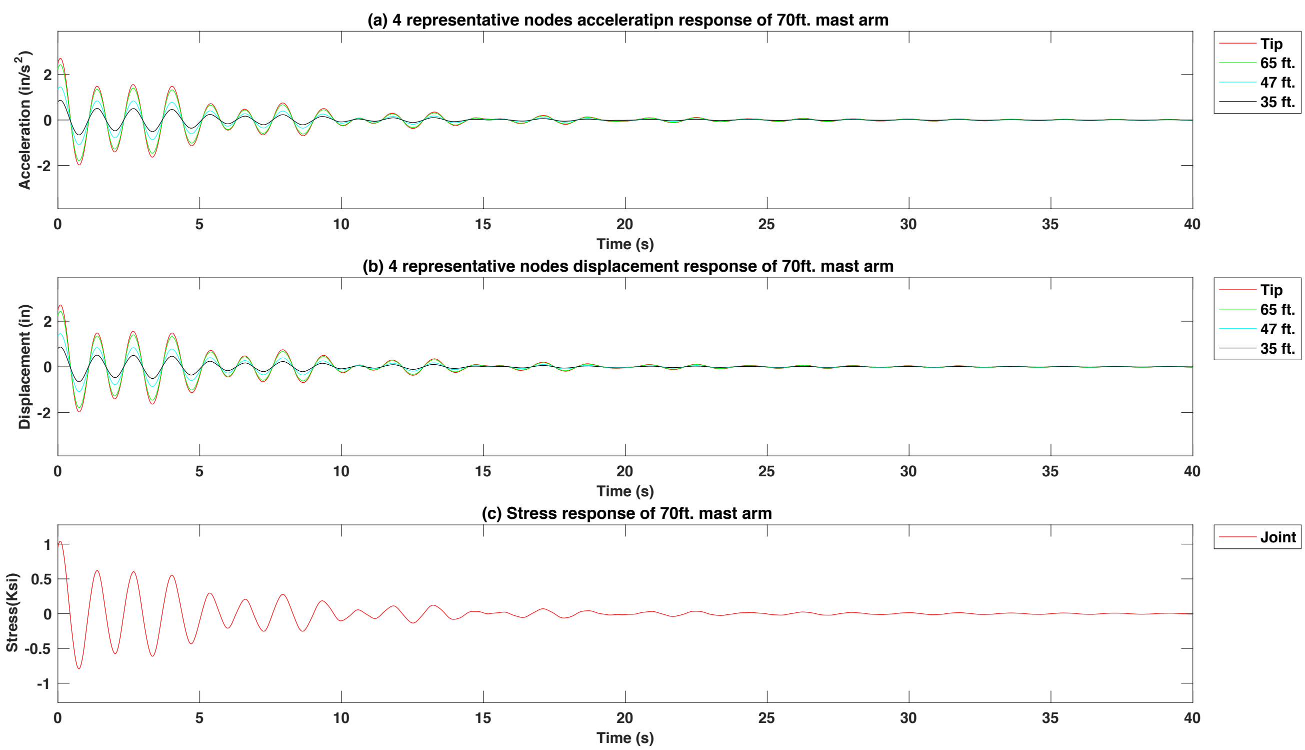

Figure 4-9 Free vibration response of the 70 ft. arm signal support structure model with 25 lb. TMD in the same frequency of the structure

After get the result of free vibration, the equivalent viscous damping ratio of the whole signal support structure could be calculated using logarithmic decay formula (Eq. 3-1):

For 15 *lb.* mass TMD,

$$\boldsymbol{\zeta = \frac{\ln\left(\frac{u_3}{u_{15}}\right)}{2\times\pi\times(15-3)} = \frac{\ln\left(\frac{1.81}{0.2105}\right)}{2\times\pi\times12} = 3.14\%}$$

For 25 *lb.* mass TMD,

$$\boldsymbol{\zeta = \frac{ln\left(\frac{u_3}{u_{15}}\right)}{2\times\pi\times(15-3)} = \frac{ln\left(\frac{1.561}{0.135}\right)}{2\times\pi\times12} = 3.25\%}$$

The result shows the damping ratio increased ${}^{3.14\%}/_{0.2\%} = 15.71$ times from the initial model to the model with 15 lb. TMD, and ${}^{3.25\%}/_{0.2\%} = 16.25$ times from the initial model to the model with 25 lb. TMD.

After doing the free vibration response analysis, run the rest of force vibration analysis cases. The difference of these cases is the frequency of excitation force and the different excitation location.

The first set of cases are using the $1.0f$, $0.95f$, $1.05f$, $0.9f$, $1.1f$, $0.8f$, $1.2f$, $0.7f$, $1.3f$, $0.6f$, and $1.4f$ to be the frequencies of the sinusoidal excitation force at the tip of the mast arm, where f= natural frequency (f_2 in this case) of the structure, and for the excitation force, use sinusoidal force with amplitude of 5 lbf., as well as the force frequency of structural natural frequency (f_2 in this model). Using the excitation force equation

$$F = 5 \times sin\,(2\pi f_i \times t) \qquad \textit{(Eq. 4-8)}$$

where f_i= the i^{th}. case of excitation force's frequency and the representative excitation force curve is shown below:

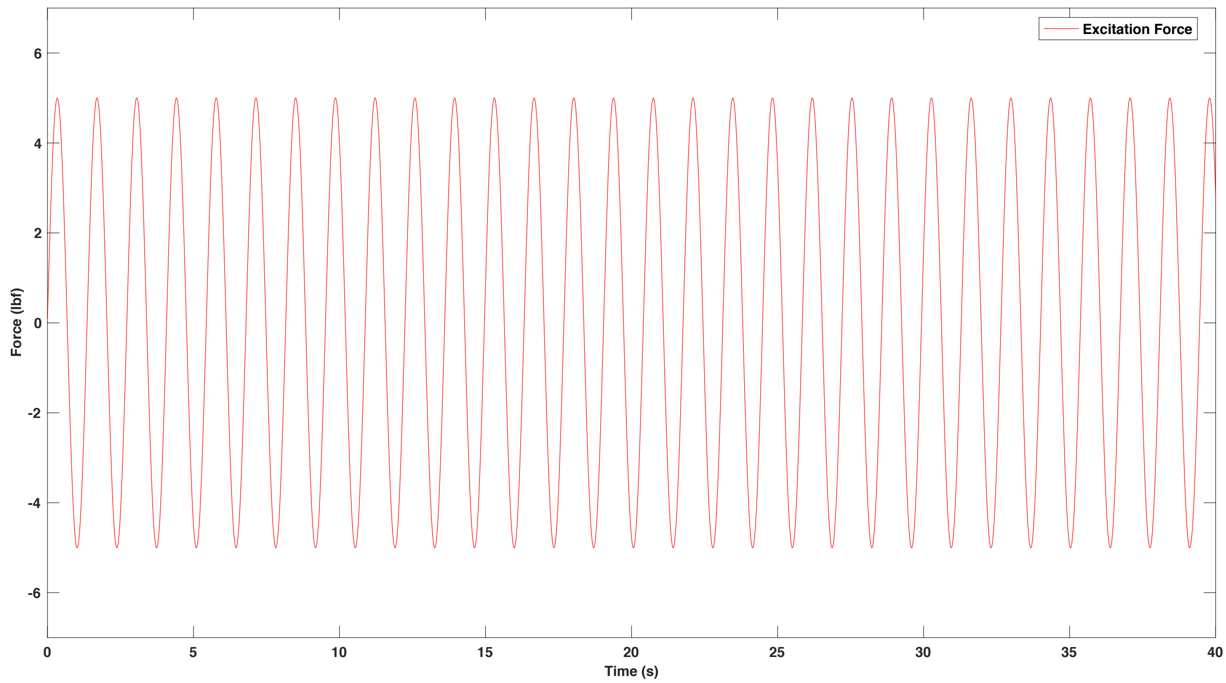

Figure 4-10 Representative of excitation force curve ($f_i = f_{12}$)

The output contains the deflections and accelerations of the tip, 3 signal locations, and the moment of the mast arm-to-pole connection. And use Equation 4-1 to calculate for the joint maximum stress and plot the response.

Some of the representative respond curve are plotted:

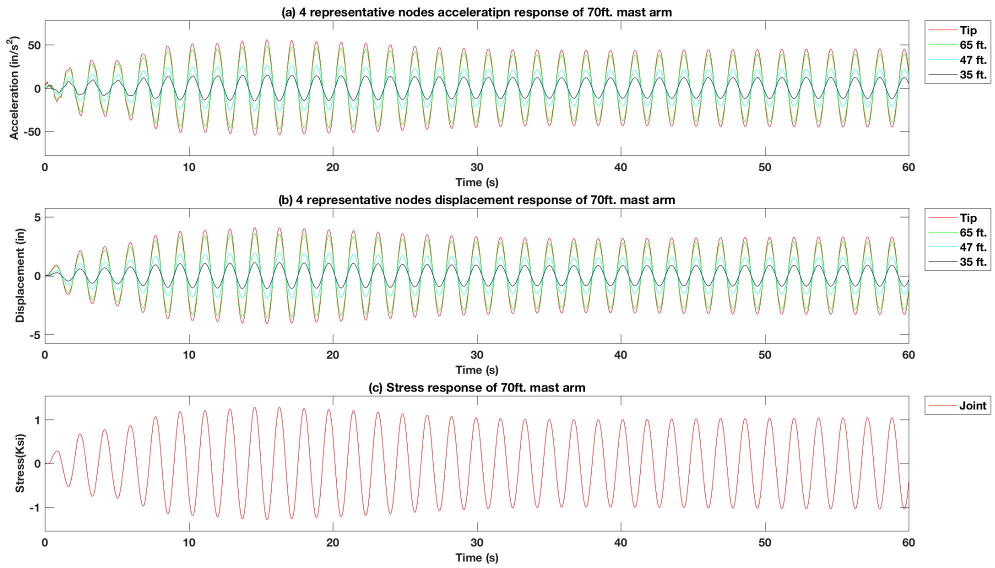

Figure 4-11 Force vibration response of excitation force at tip of the 70 ft. mast arm signal pole structure model with 15 lb. mass TMD using the $f_f = 0.8f_n$

By picking the peak value of tip displacement when the curve shows a steady state (almost the same cyclic waves with the same amplitude and frequency) in each case, a response curve with 11 nodes will be plotted.

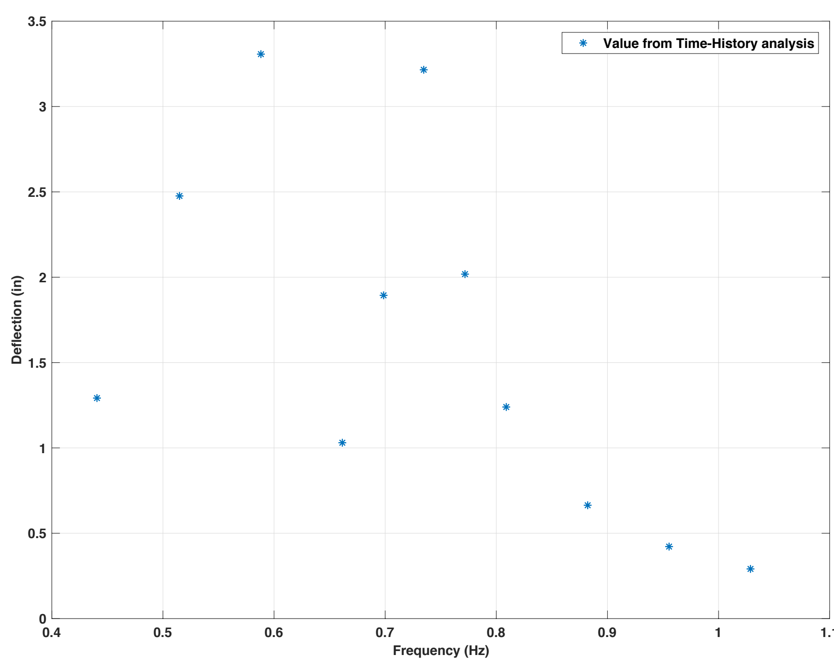

Figure 4-12 Peak value in steady state for different excitation force frequencies, 70ft. mast arm with 15lb mass TMD

Also doing Harmonic analysis in ANSYS to plot the frequency response (Figure 4-13) curve:

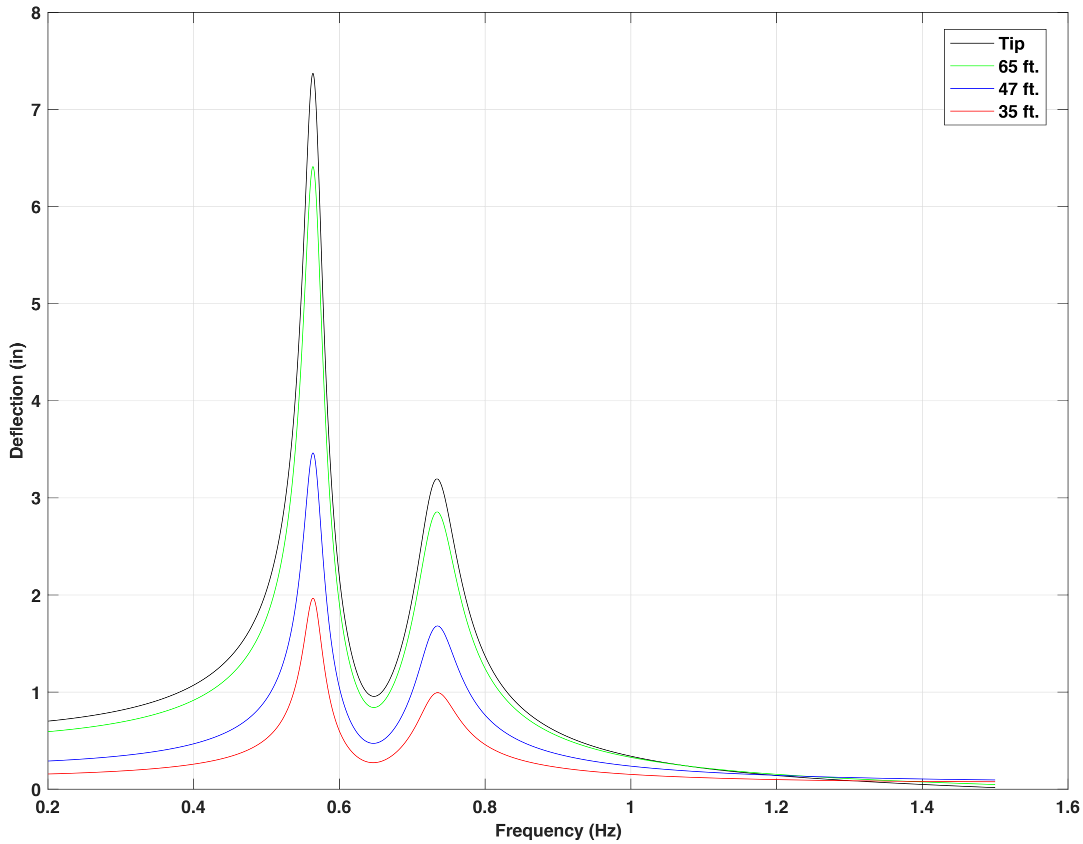

Figure 4-13 Frequency response for 70*ft*. mast arm with 15lb mass TMD, force on the tip

In order to verifying the result of these analyses, put those peak value points above and the frequency response for at tip in the same figure (Figure 4-14) to see the difference.

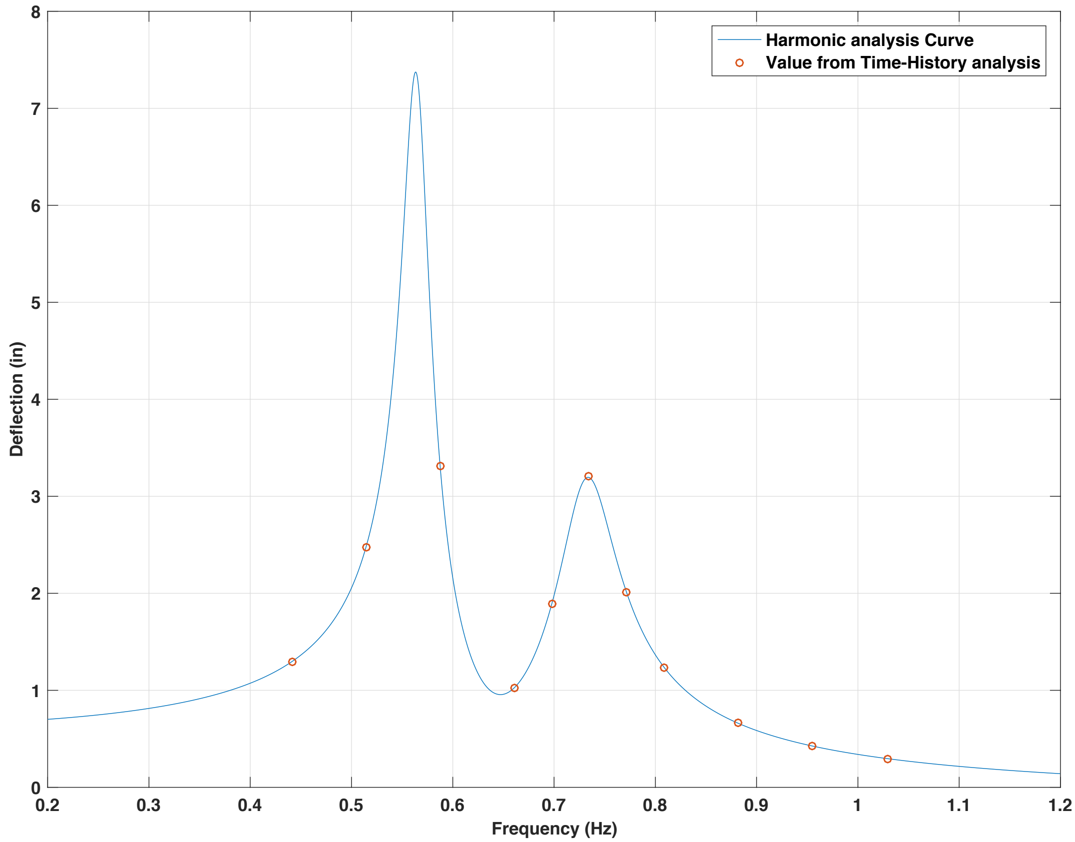

Figure 4-14 Verification of results from force vibration response and harmonic analysis

Which shows the result match perfectly that the harmonic response could be used in the rest of analysis.

For the 25 lb. TMD, plot the representative force vibration response and harmonic response:

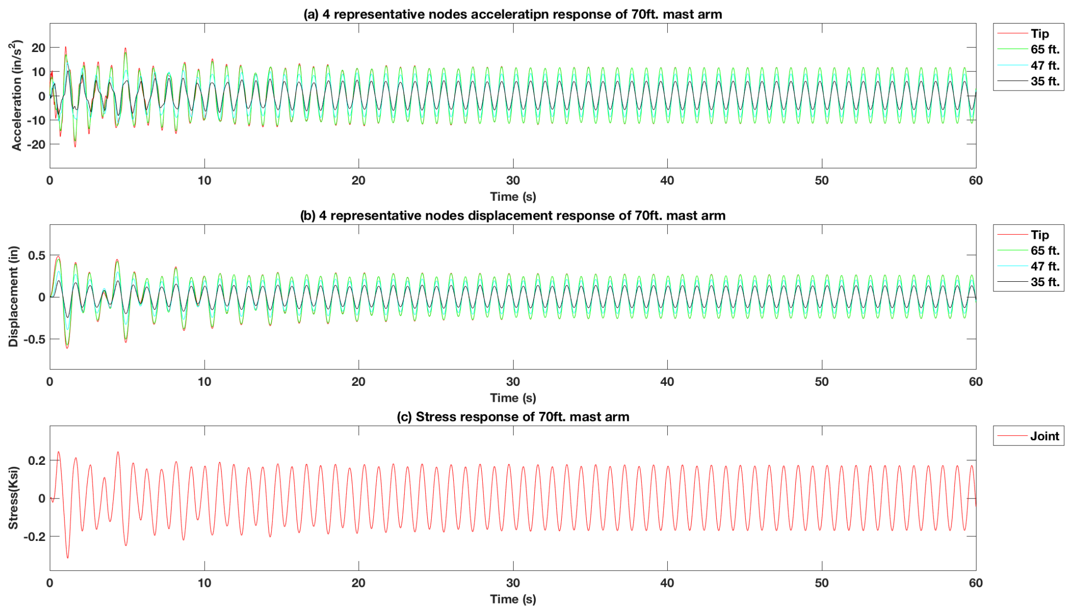

Figure 4-15 Force vibration response of excitation force at tip of the 70 ft. mast arm signal pole structure model with 25 lb. mass TMD using the $f_r = 0.6f_n$

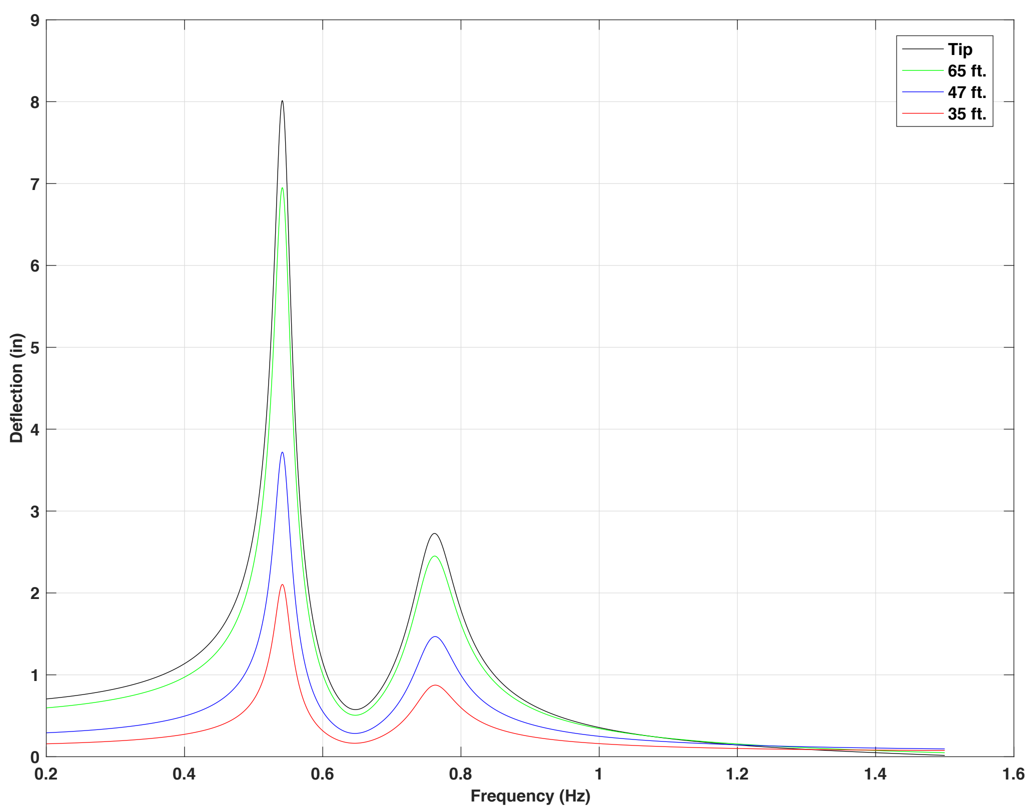

Figure 4-16 Frequency response for 70ft. mast arm with 25lb mass TMD, force on the tip

The second set of cases is using the frequencies above but applied the excitation force at signal head locations (37 *ft*, 42 *ft*, and 65 *ft*. from the arm-to-pole connection). And plot all of these results. Some representative results are plotted below:

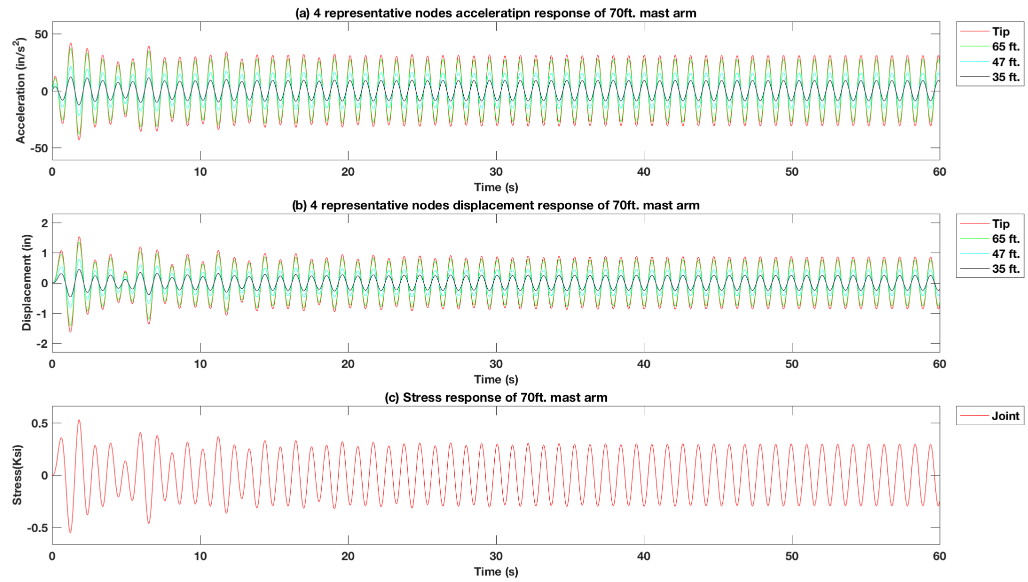

Figure 4-17 Force vibration response of excitation force at signal heads' location of the 70 ft. mast arm signal pole structure model with 15 lb. mass TMD using the $f_r = 1.3 f_n$

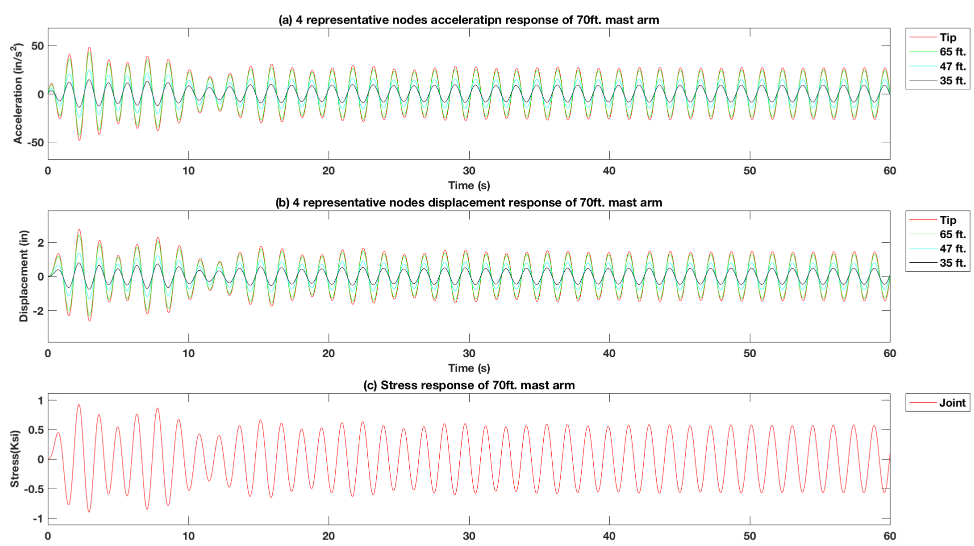

Figure 4-18 Force vibration response of excitation force at signal heads' location of the 70 ft. mast arm signal pole structure model with 25 lb. mass TMD using the $f_r = 1.1 f_n$

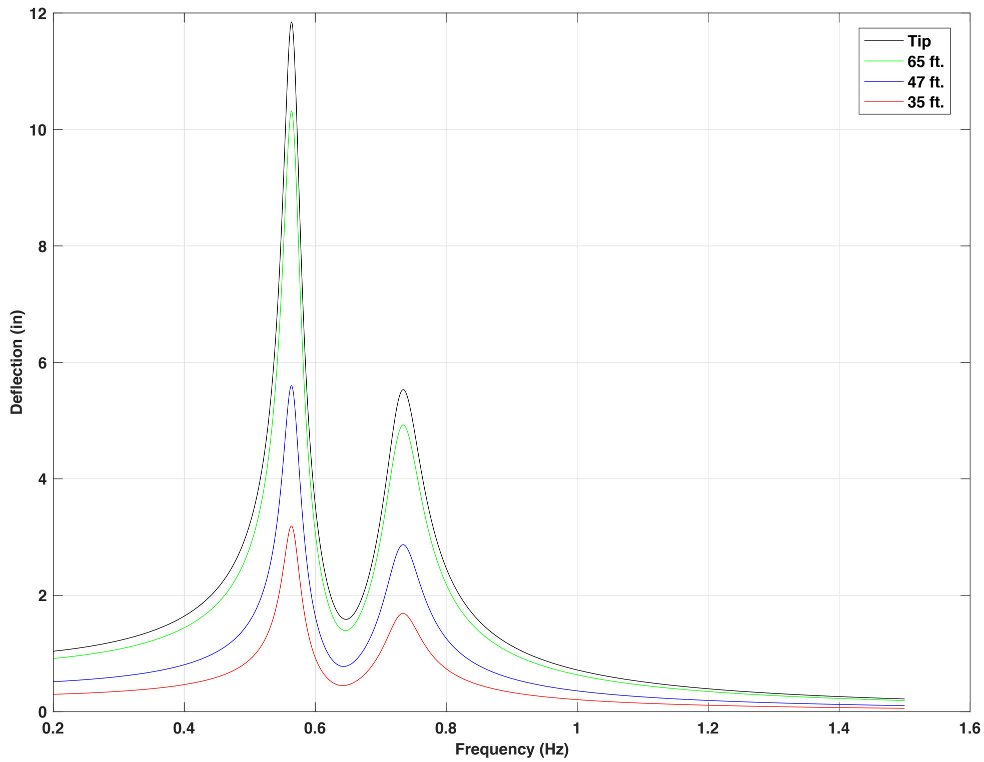

Figure 4-19 Frequency response for 70ft. mast arm with 15lb mass TMD, force on signal heads' location

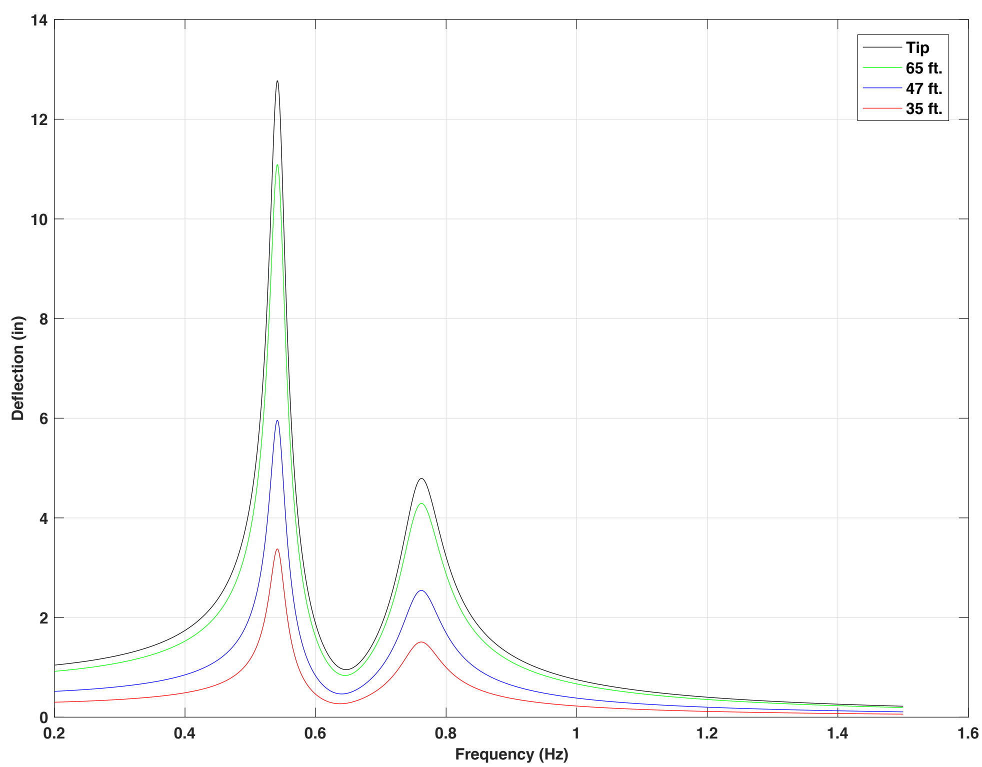

Figure 4-20 Frequency response for 70ft. mast arm with 25lb mass TMD, force on signal heads' location

4.2.4 TMD Frequencies

Due to the sensitiveness of the TMD/ structure frequencies ratio, selecting the damper frequencies of 1.1 f_n, 0.9 f_n, 1.25 f_n, 0.75 f_n, 1.5 f_n, and 0.5 f_n, build the finite element model then do the modal analysis to get mode shapes and frequencies, and calculate corresponding stiffness and damping coefficient of the TMD, then corresponding Rayleigh damping matrix would be computed for the analysis input that listed in Table 4-3

Table 4-3Preliminary model analysis for 70-ft. arm with varied TMD frequencies

TMD Frequency	f_1 (Hz)	f_2 (Hz)	f_3 (Hz)	k	c	α	β
1.1 f_n	0.58	0.78	2.30	0.77	0.021	0.008	5.17E-04
0.9 f_n	0.53	0.70	2.29	0.52	0.017	0.008	5.19E-04
1.25 f_n	0.60	0.86	2.30	1.00	0.024	0.008	5.16E-04
0.75 f_n	0.46	0.67	2.29	0.36	0.014	0.008	5.19E-04
1.5 f_n	0.61	0.10	2.31	1.43	0.028	0.008	5.15E-04
0.5 f_n	0.32	0.65	2.29	0.16	0.009	0.008	5.19E-04

Then do the same analysis as before, i.e. free vibration response, force vibration response and harmonic analysis. The representative result for each case are shown below:

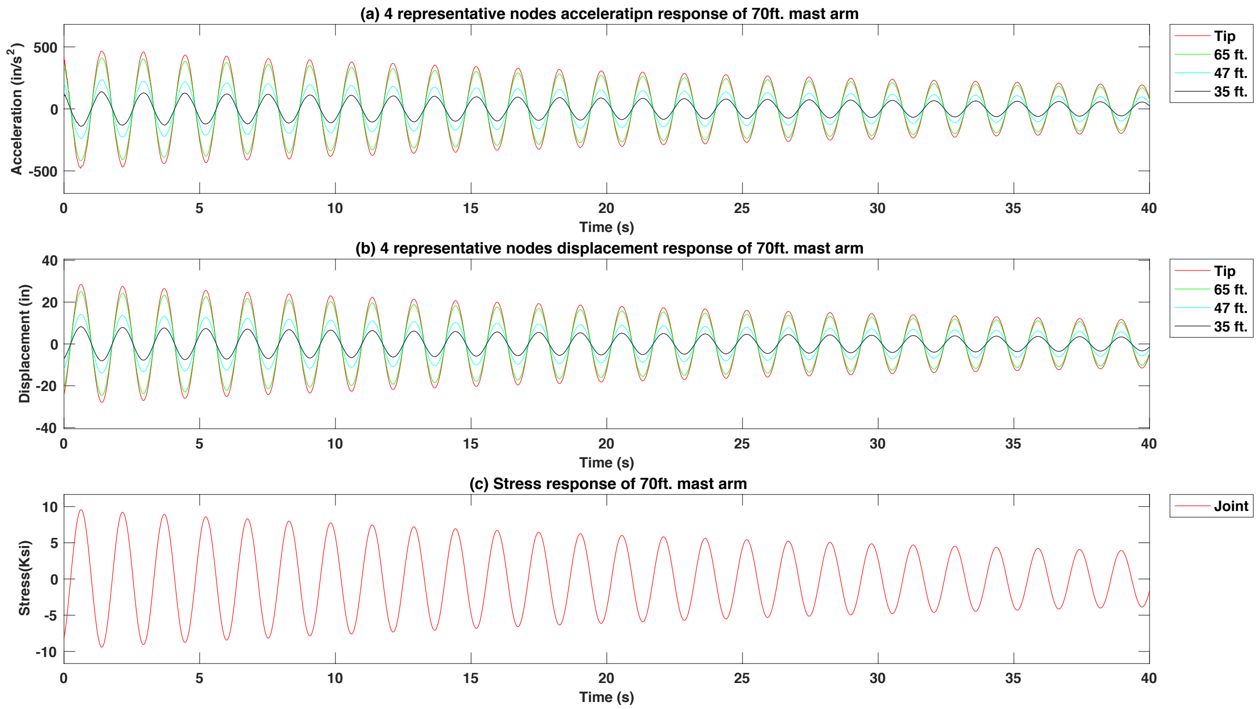

Figure 4-21 Free vibration response of excitation force at tip in the first mode frequency of the 70ft. mast arm signal pole structure model with 15 lb. mass TMD using the $f_d = 0.5f_n$

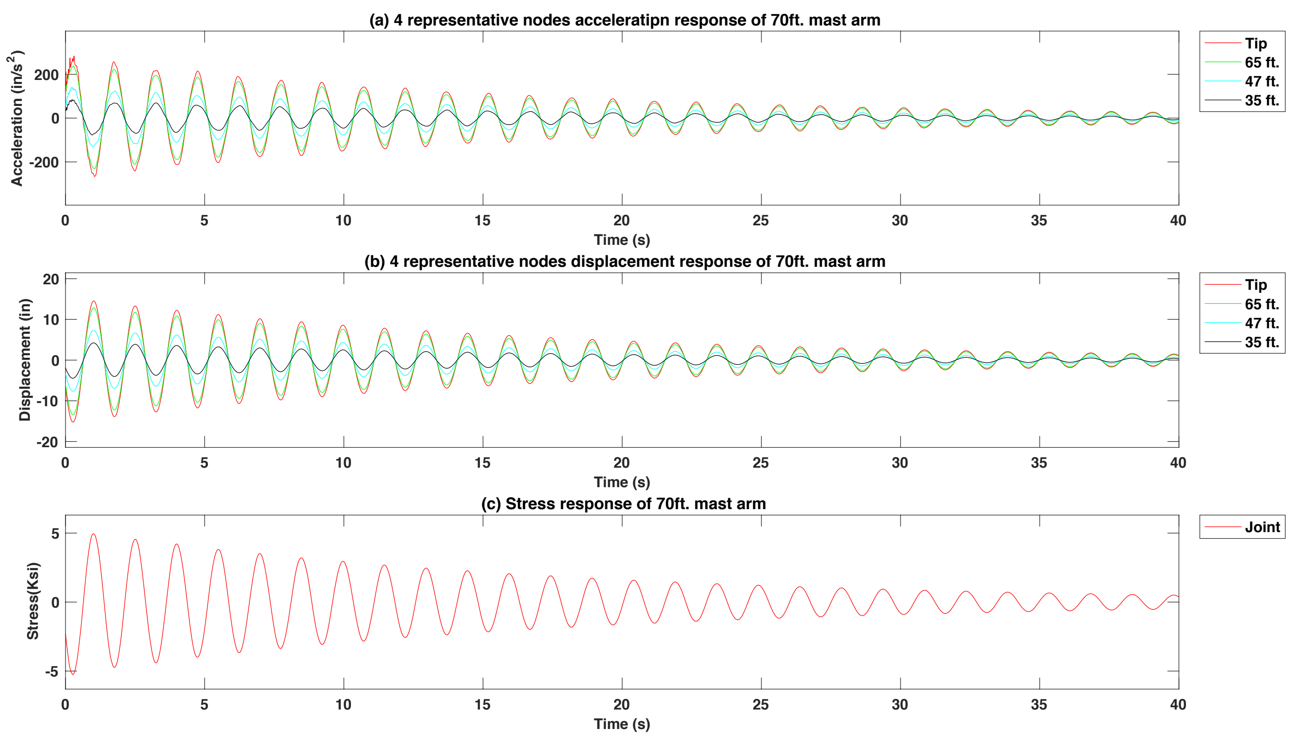

Figure 4-22 Free vibration response of excitation force at tip in natural frequency of the 70 ft. mast arm signal pole structure model with 15 lb. mass TMD using the $f_d = 0.75f_n$

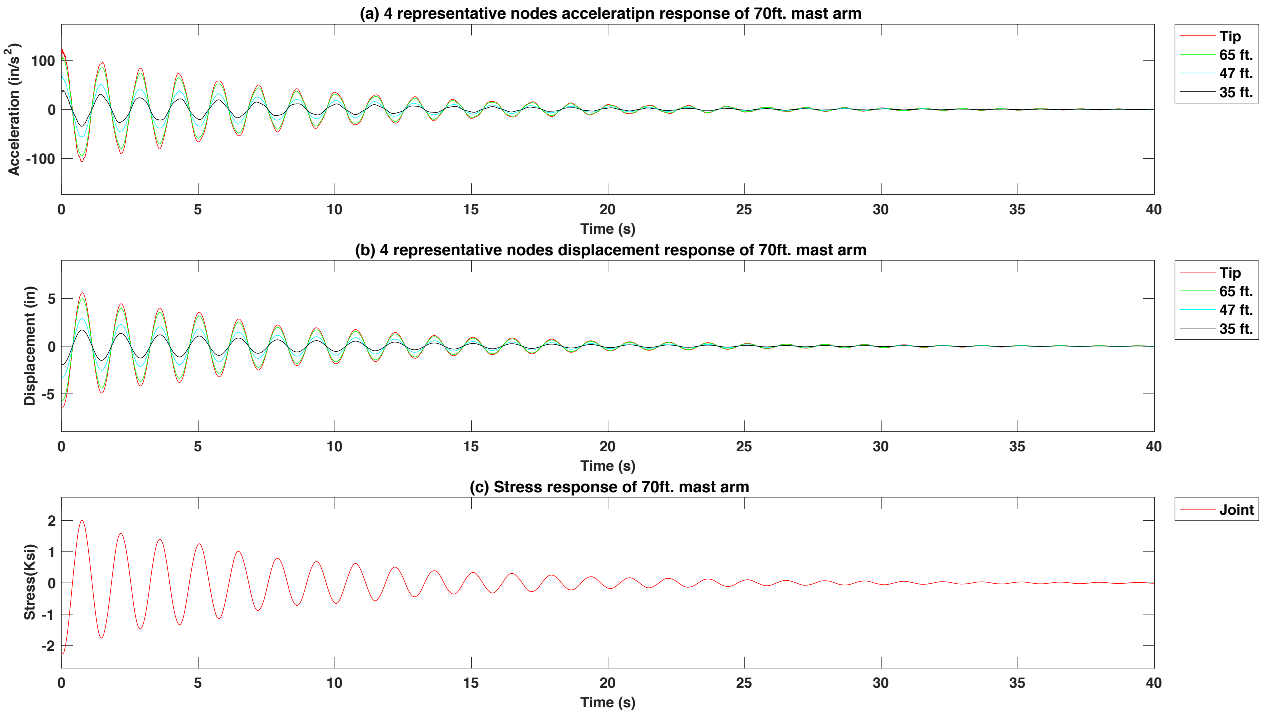

Figure 4-23 Free vibration response of excitation force at tip in natural frequency of the 70 ft. mast arm signal pole structure model with 15 lb. mass TMD using the $f_d = 0.9 f_n$

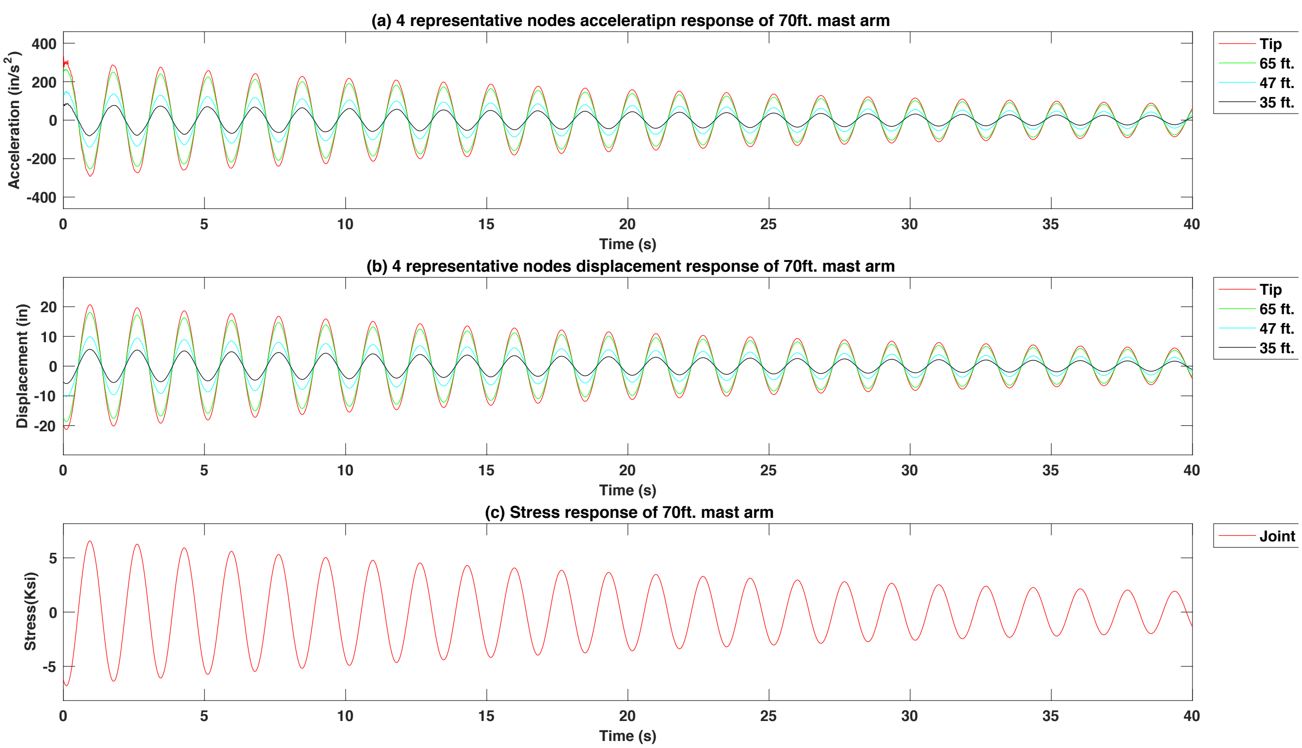

Figure 4-24 Free vibration response of excitation force at tip in the second mode frequency of the 70 ft. mast arm signal pole structure model with 15 lb. mass TMD using the $f_d = 1.25 f_n$

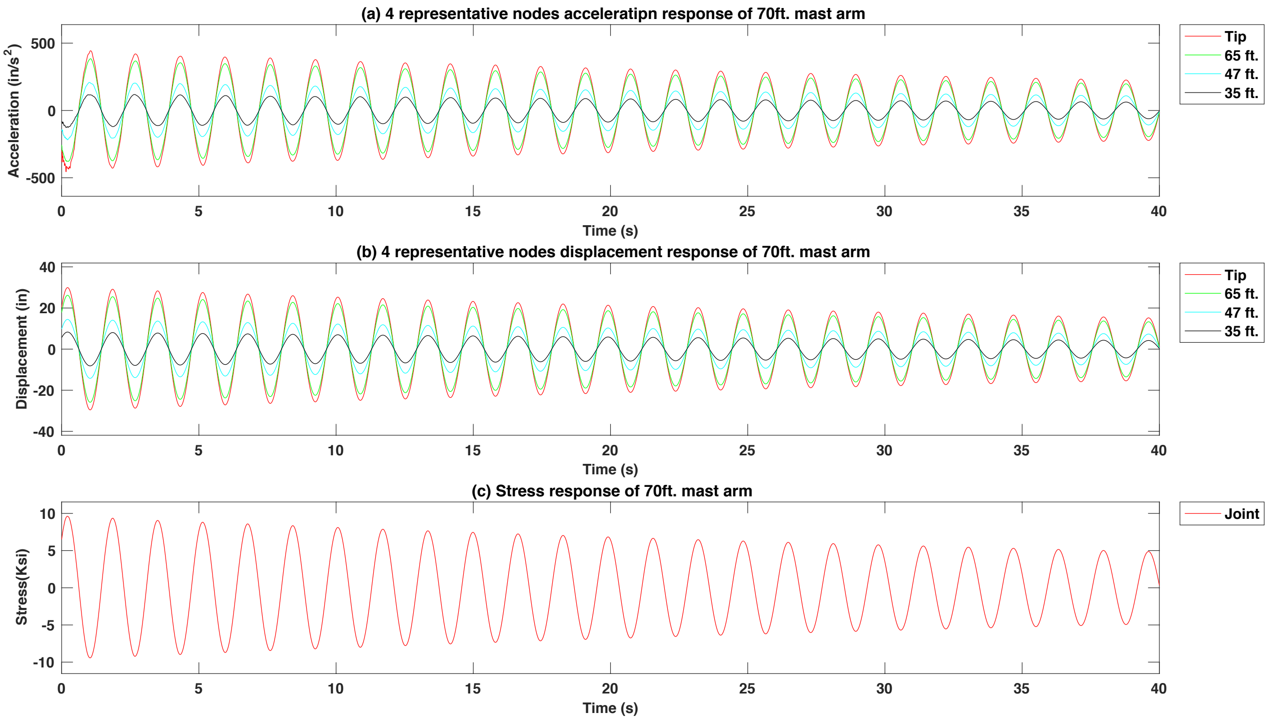

Figure 4-25 Free vibration response of excitation force at tip in the second mode frequency of the 70 ft. mast arm signal pole structure model with 15 lb. mass TMD using the $f_d = 1.5 f_n$

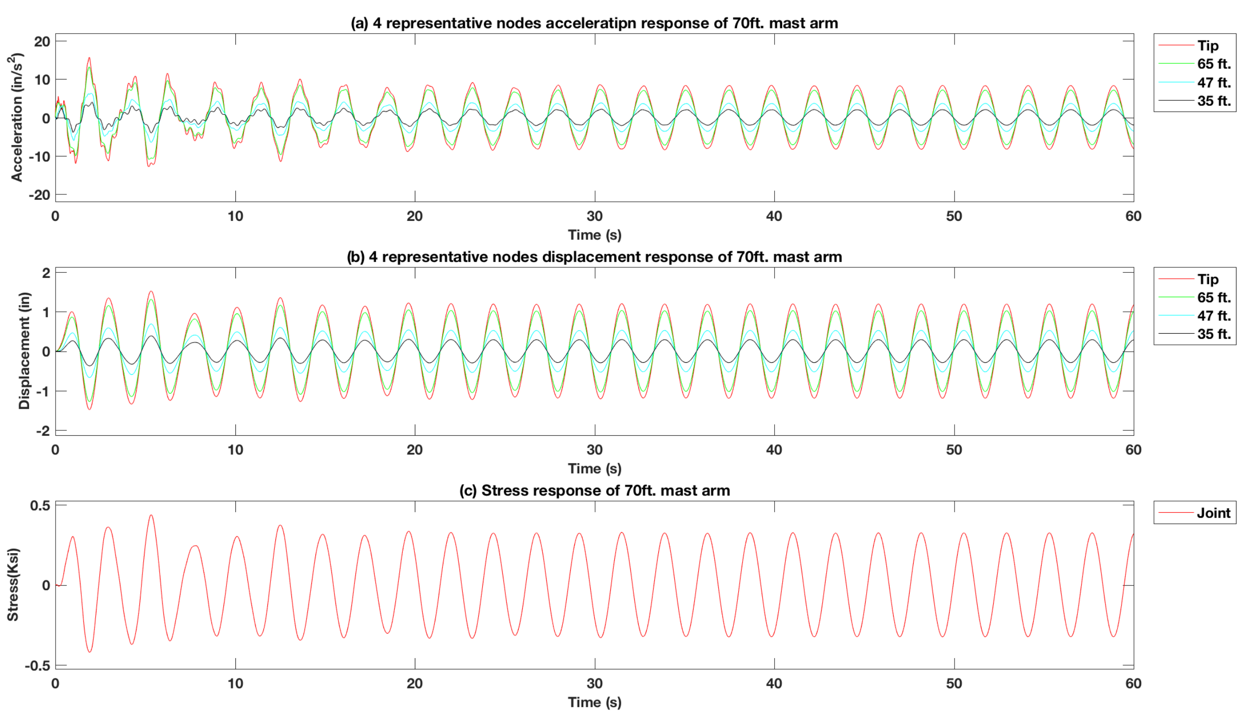

Figure 4-26 Force vibration response of excitation force at tip of the 70 ft. mast arm signal pole structure model with 15 lb. mass TMD using the $f_d = 0.9 f_n$, $f_r = 0.6 f_n$

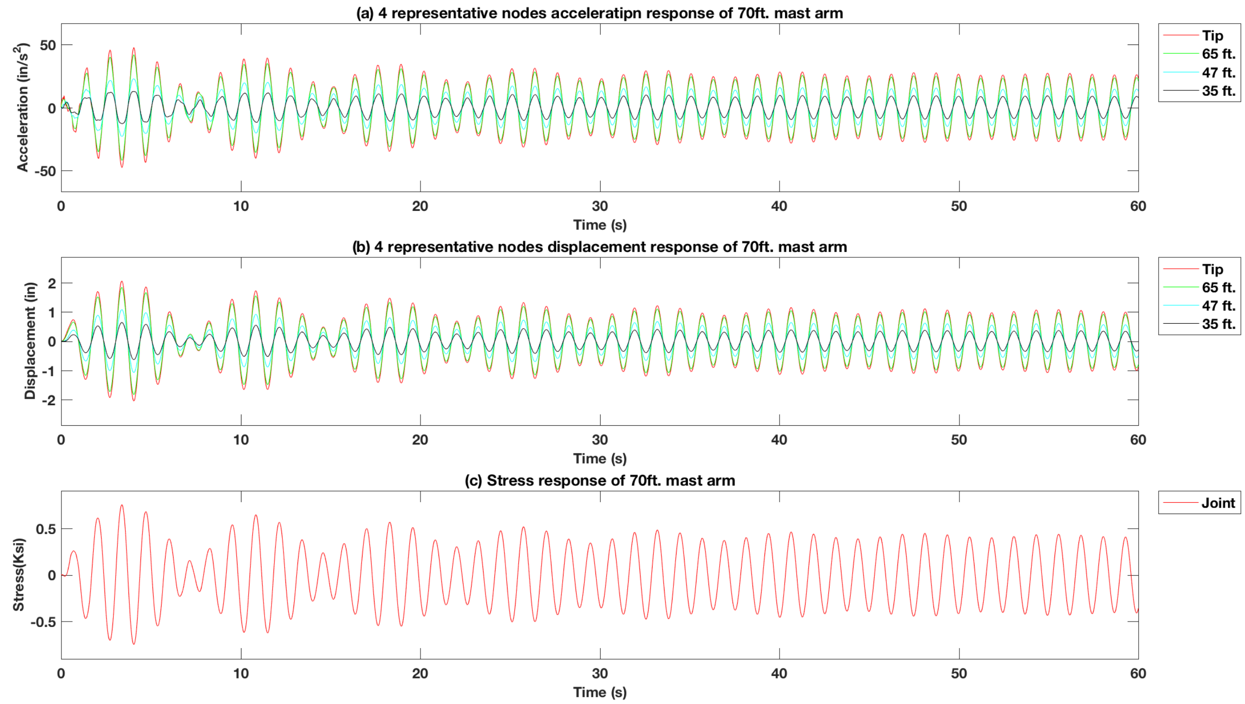

Figure 4-27 Force vibration response of excitation force at tip of the 70 ft. mast arm signal pole structure model with 15 lb. mass TMD using the $f_d = 0.75\, f_n, f_s = 1.2 f_n$

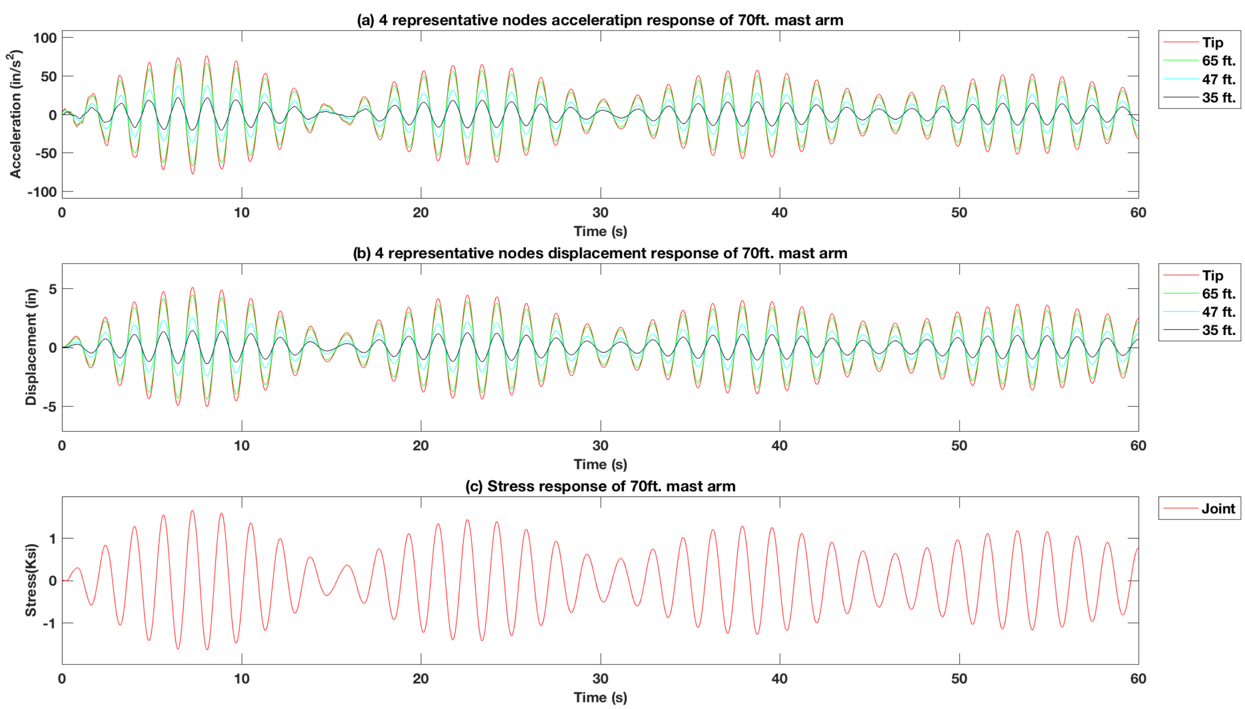

Figure 4-28 Force vibration response of excitation force at tip of the 70 ft. mast arm signal pole structure model with 15 lb. mass TMD using the $f_d = 0.5\, f_n, f_s = 1.1 f_n$

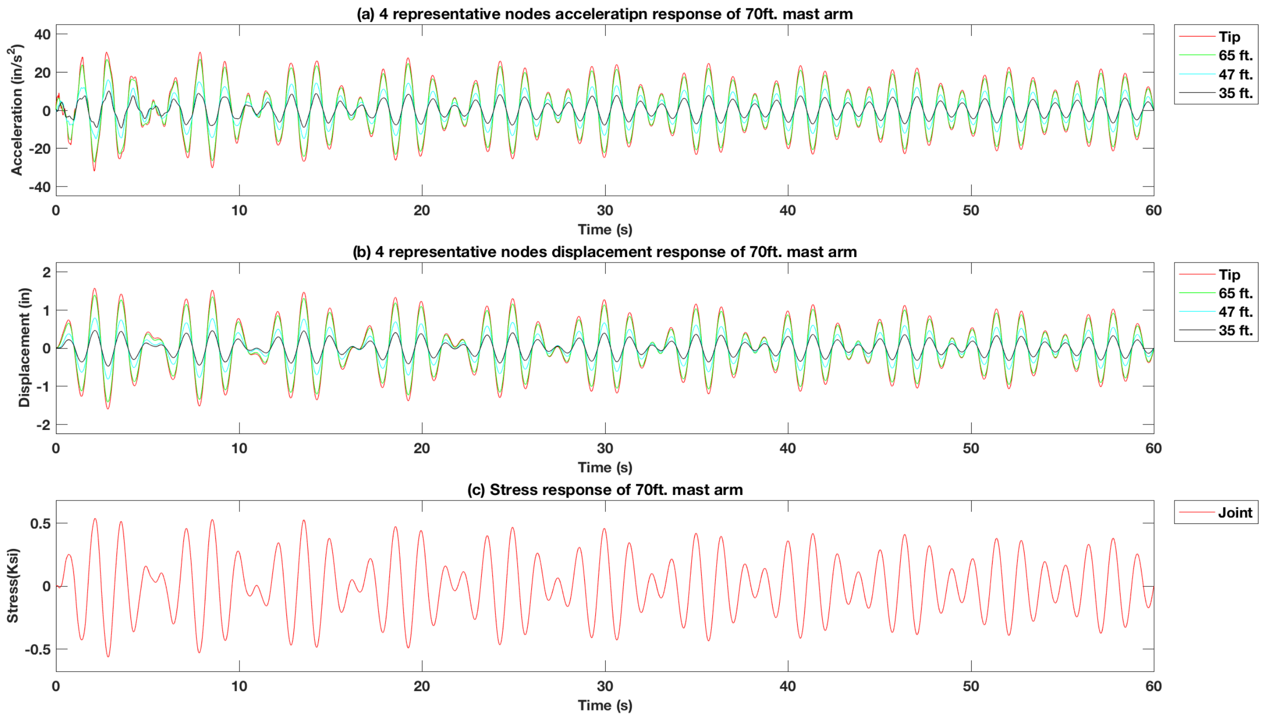

Figure 4-29 Force vibration response of excitation force at tip of the 70 ft. mast arm signal pole structure model with 15 lb. mass TMD using the $f_d = 1.5 f_n$, $f_r = 1.3 f_n$

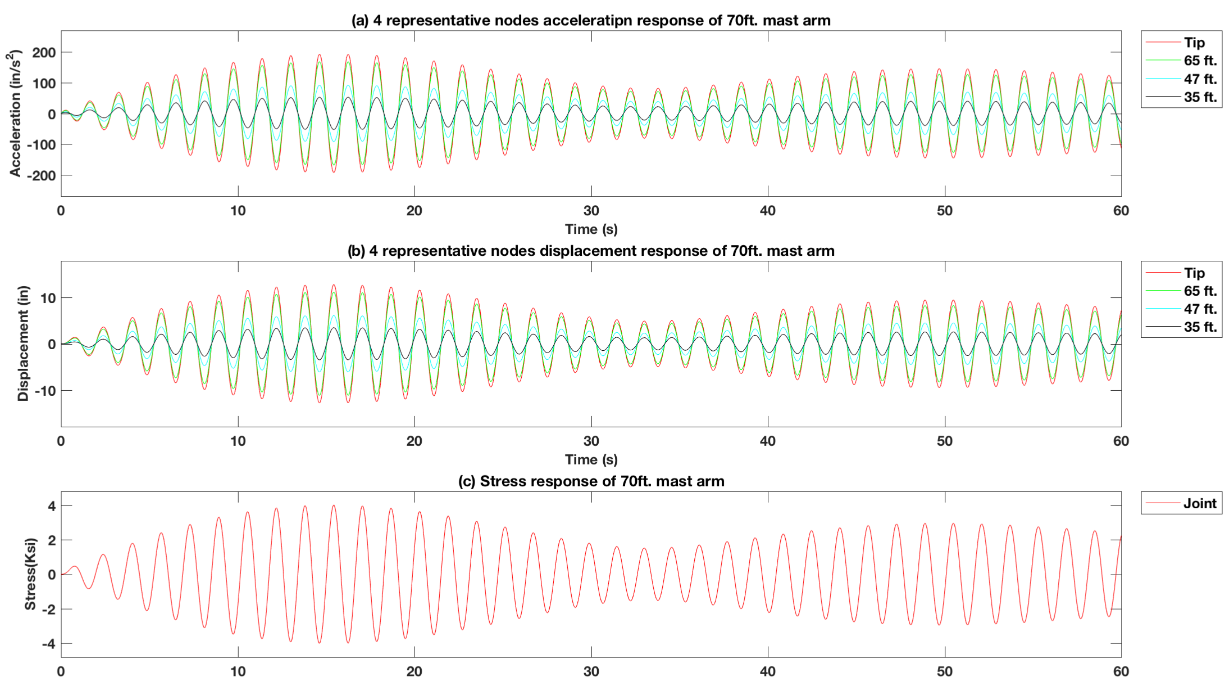

Figure 4-30 Force vibration response of excitation force at 3 signal heads position on the 70 ft. mast arm signal pole structure model with 15 lb. mass TMD using the $f_d = 1.25 f_n$, $f_r = 1.05 f_n$

For harmonic analysis, plot all frequency response curves:

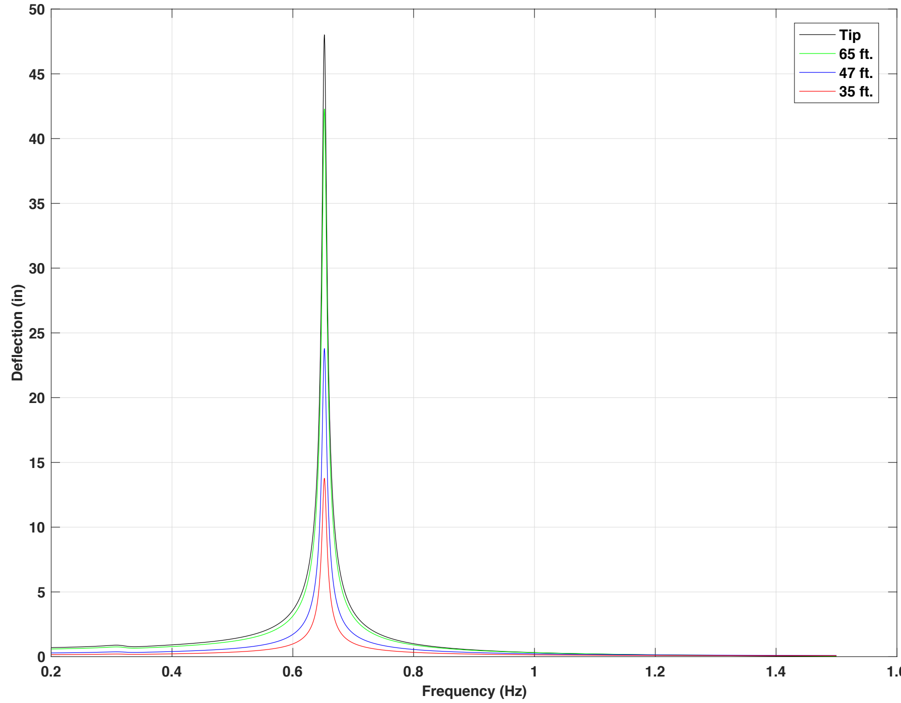

Figure 4-31 Frequency response for 70ft. mast arm with 15lb mass TMD, 5 lbf force on tip, $f_d = 0.5 f_n$

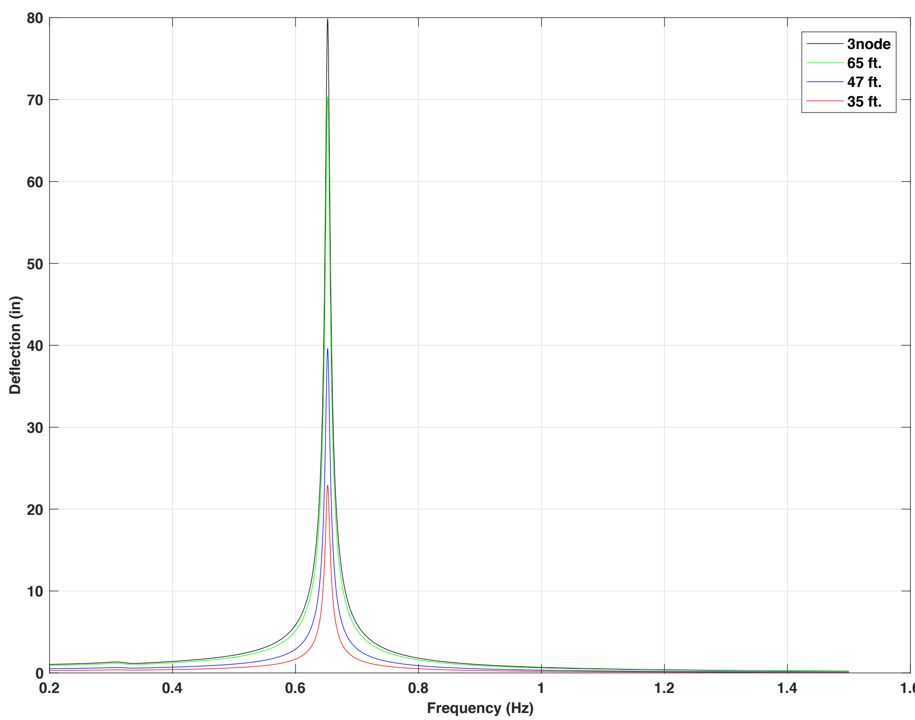

Figure 4-32 Frequency response for 70ft. mast arm with 15lb mass TMD, *5 lbf* force on 3 signal heads location, $f_d = 0.5 f_n$(notation 3node means tip deflection under this situation)

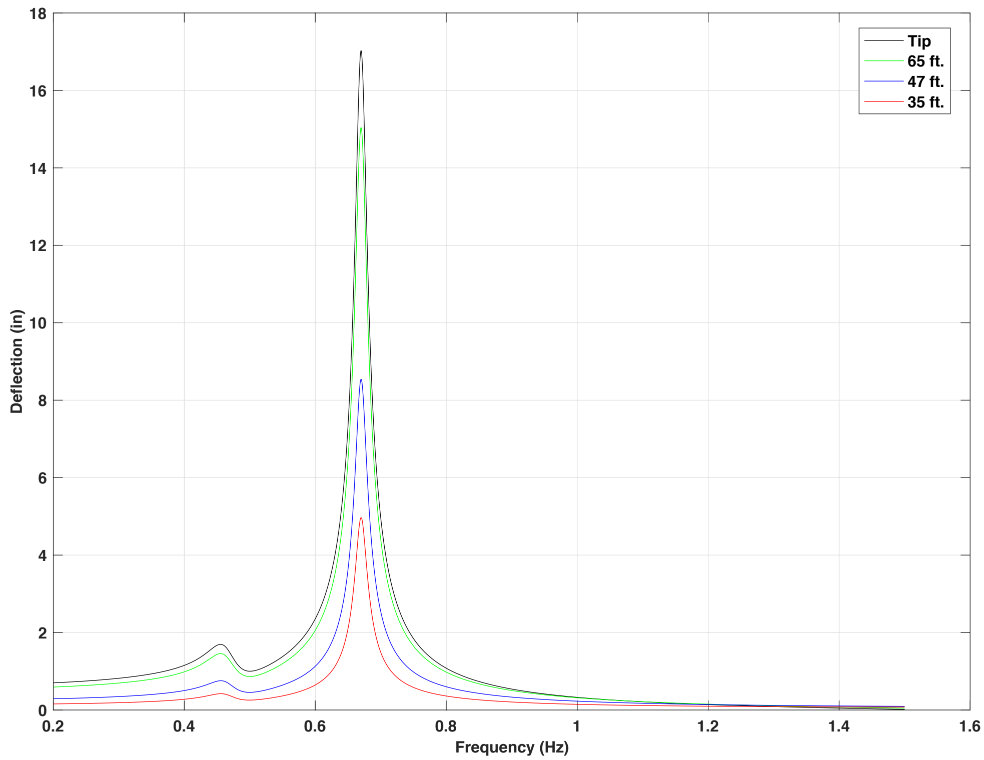

Figure 4-33 Frequency response for 70ft. mast arm with 15lb mass TMD, 5 lbf force on tip, $f_d = 0.75 f_n$

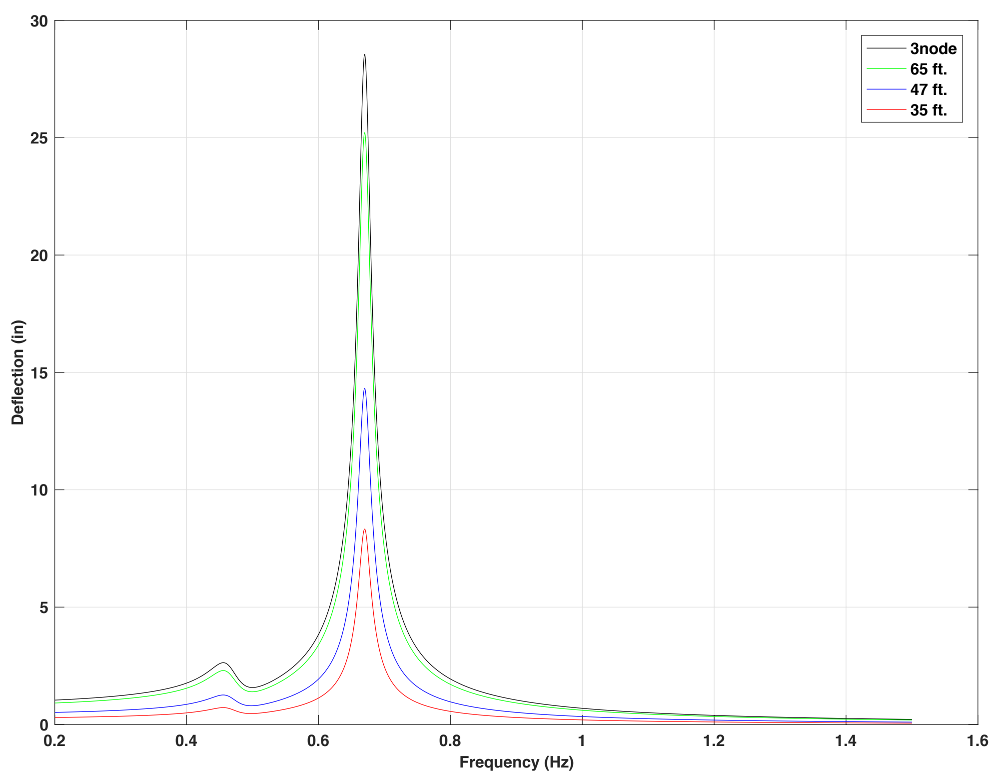

Figure 4-34 Frequency response for 70ft. mast arm with 15lb mass TMD, 5 lbf force on 3 signal heads location, $f_d = 0.75 f_n$, (notation 3node means tip deflection under this situation)

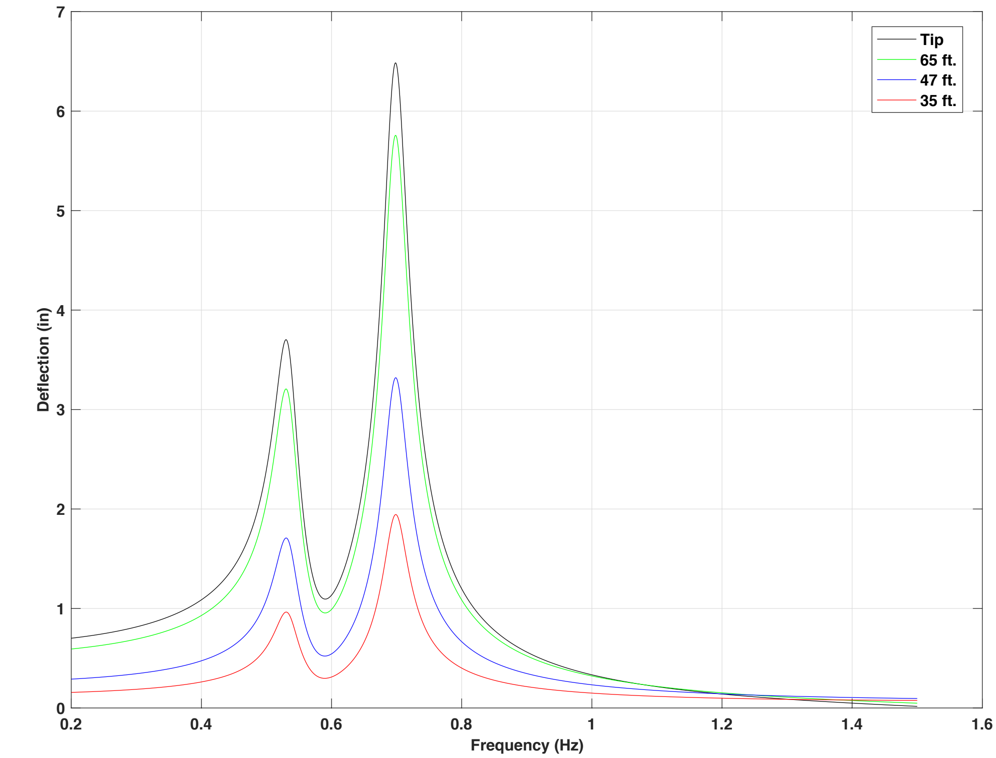

Figure 4-35 Frequency response for 70ft. mast arm with 15lb mass TMD, 5 lbf force on tip, $f_d = 0.9 f_n$

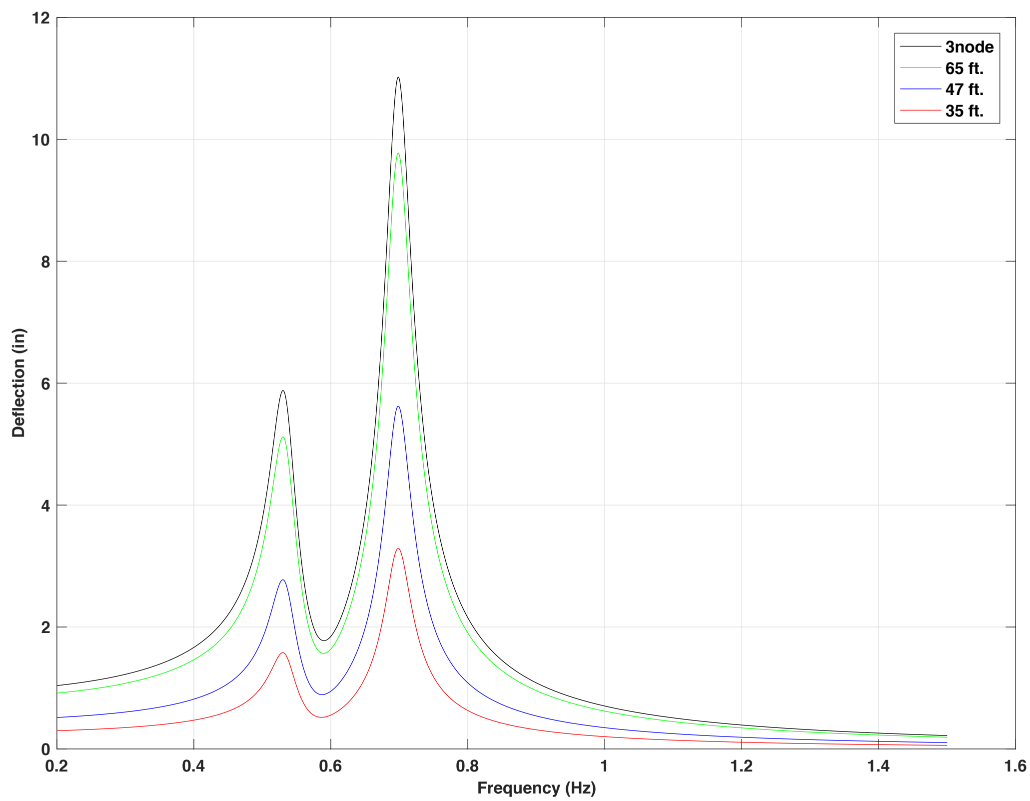

Figure 4-36 Frequency response for 70ft. mast arm with 15lb mass TMD, 5 lbf force on 3 signal heads location, $f_d = 0.9 f_n$(notation 3node means tip deflection under this situation)

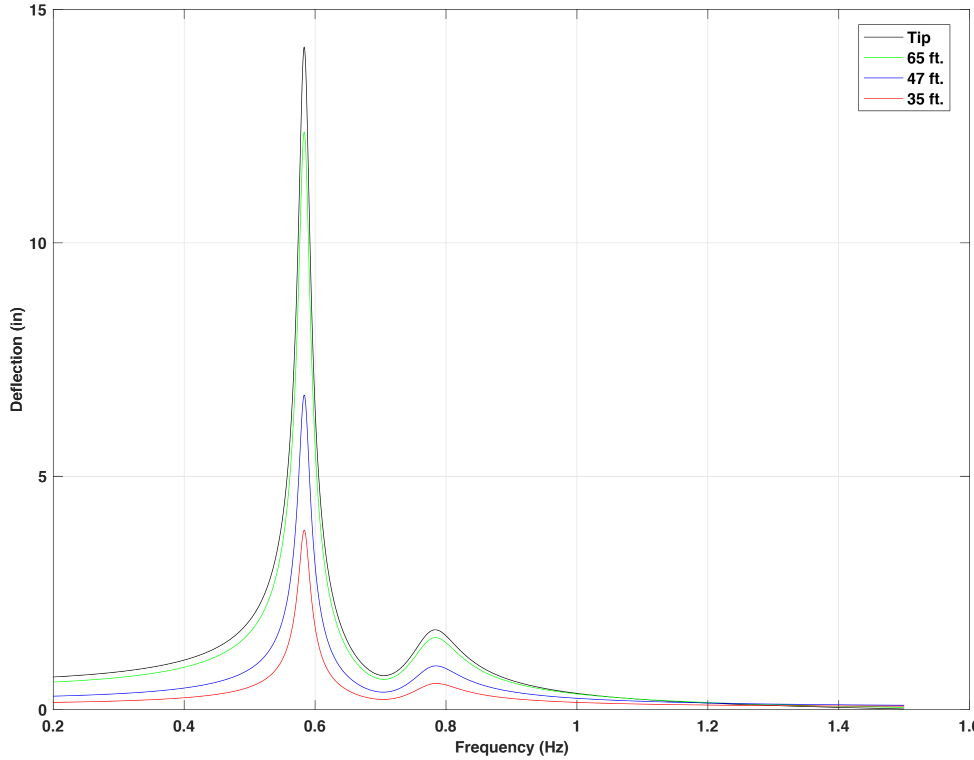

Figure 4-37 Frequency response for 70ft. mast arm with 15lb mass TMD, 5 lbf force on tip, $f_d = 1.1 f_n$

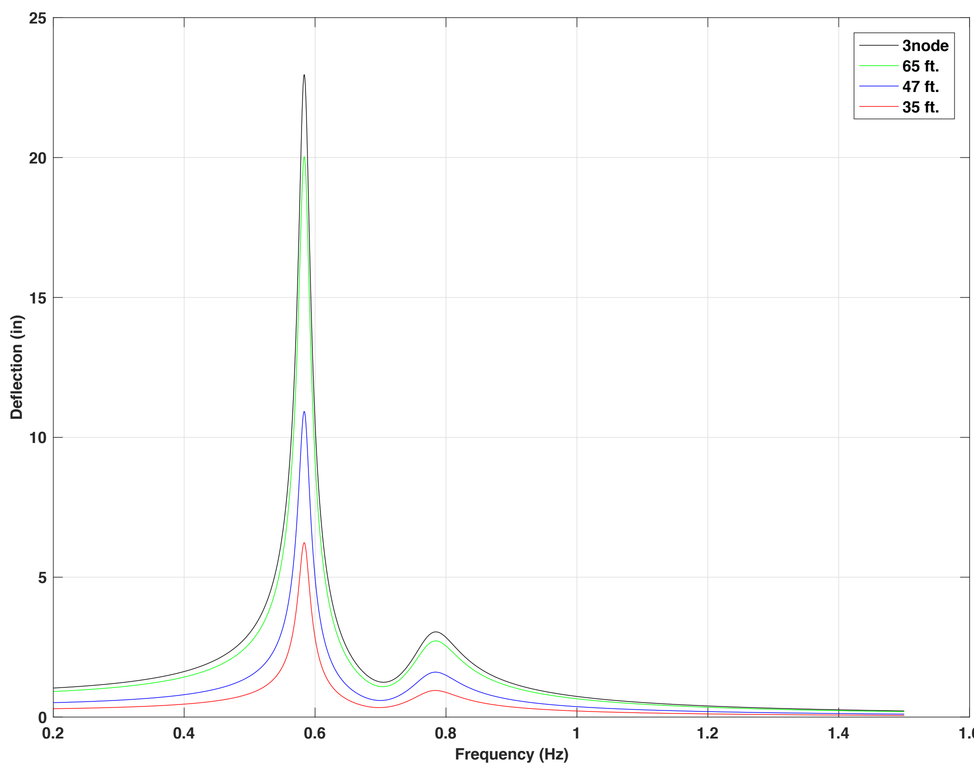

Figure 4-38 Frequency response for 70ft. mast arm with 15lb mass TMD, 5 lbf force on 3 signal heads location, $f_d = 1.1 f_n$ (notation 3node means tip deflection under this situation)

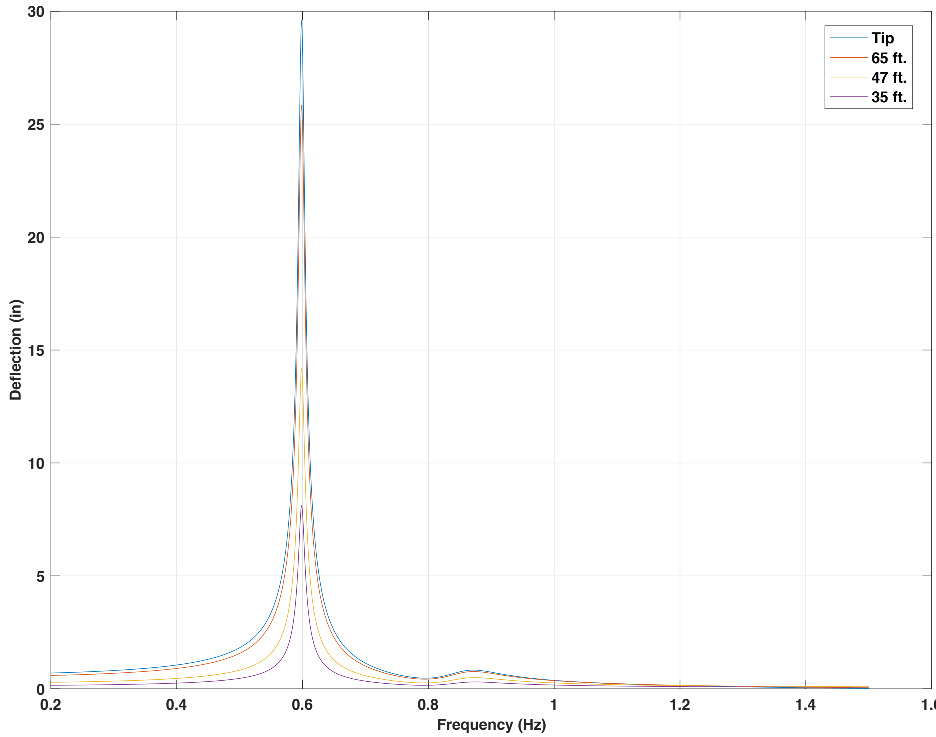

Figure 4-39 Frequency response for 70ft. mast arm with 15lb mass TMD, 5 lbf force on tip, $f_d = 1.25 f_n$

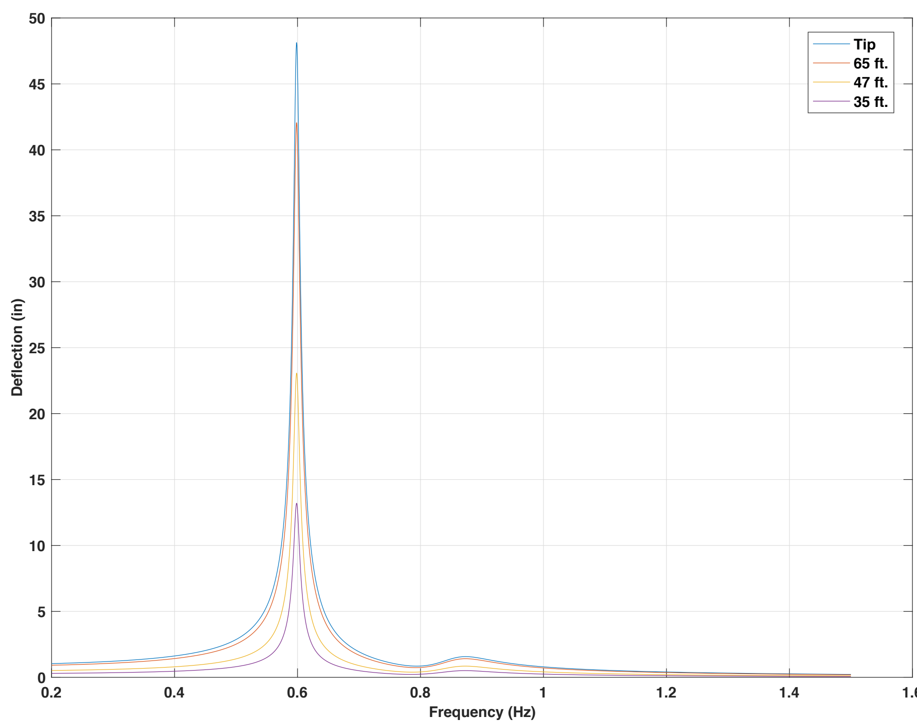

Figure 4-40 Frequency response for 70ft. mast arm with 15lb mass TMD, 5 lbf force on 3 signal heads location, $f_d = 1.25 f_n$

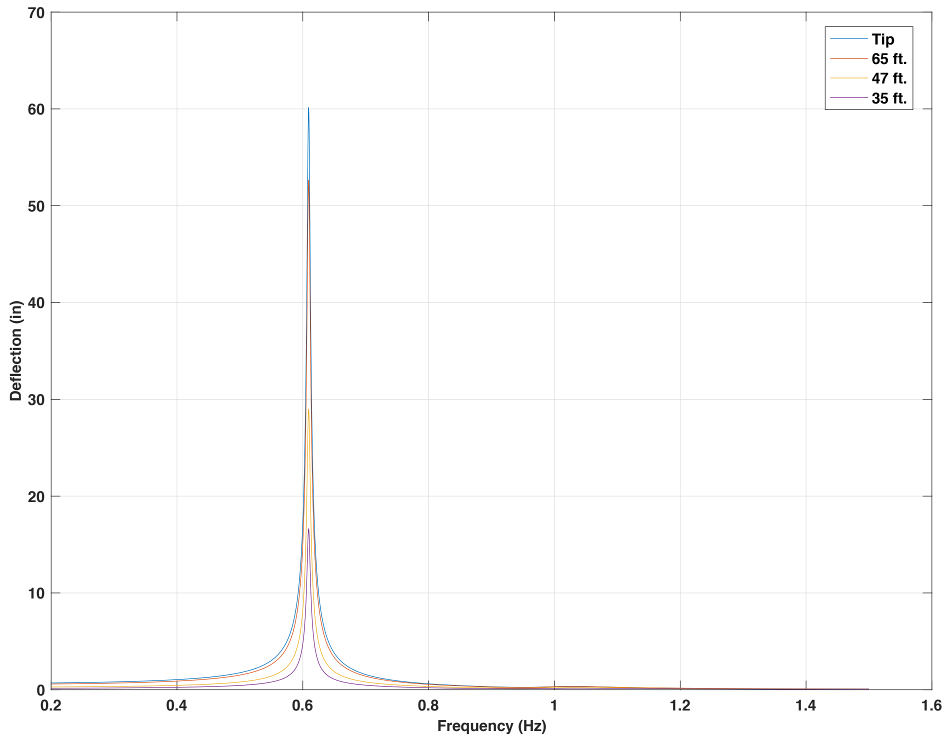

Figure 4-41 Frequency response for 70ft. mast arm with 15lb mass TMD, 5 lbf force on tip, $f_d = 1.5 f_n$

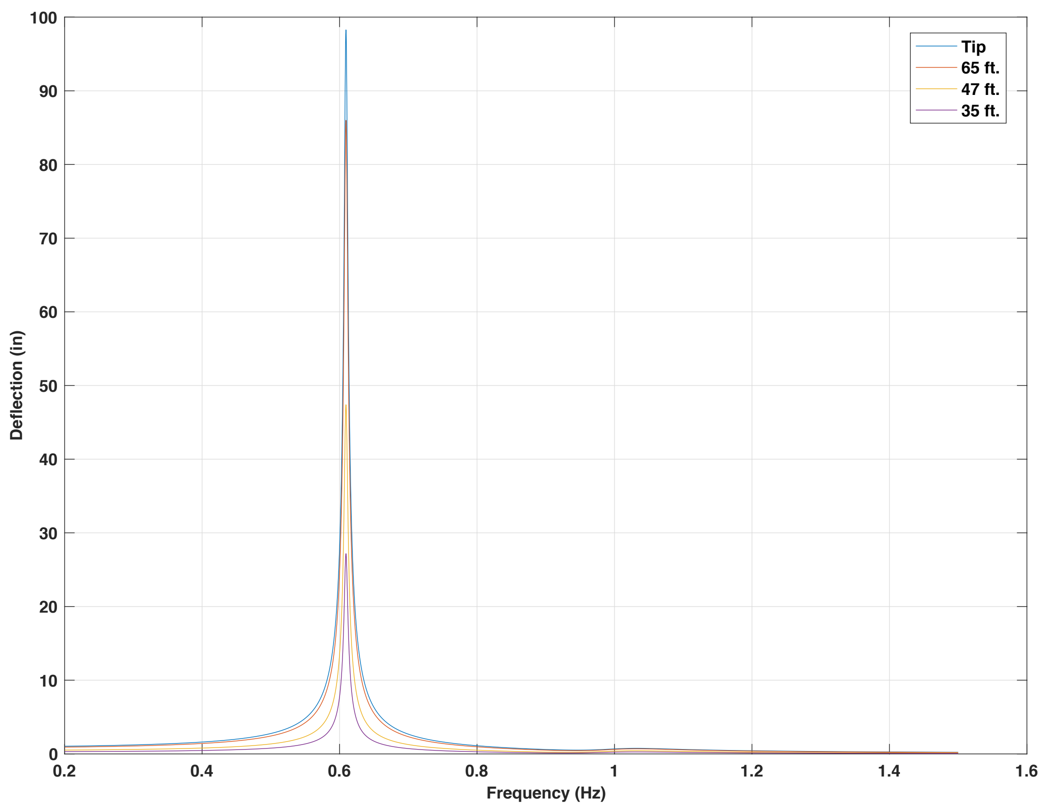

Figure 4-42 Frequency response for 70ft. mast arm with 15lb mass TMD, 5 lbf force on 3 signal heads location, $f_d = 1.5 f_n$

4.2.5 TMD Damping Ratio

In this case study, two types of dampers are more concerned- Alcoa damper and Florida damper. Alcoa damper, which has much less damping ratio as previous researches, need to be simulated by assume to use different damping ratio and do the same analysis. Since the type of Alcoa damper on signals uses heavier mass, in this case, 1% of damping ratio with 25 lb. mass was selected and will be compared with 6% damping ratio with 25 lb. mass TMD, which had been calculated before. The pre-analysis calculation for the damper:

TMD damping ratio	f_1 (Hz)	f_2 (Hz)	f_3 (Hz)	k	c	α	β
1%	0.5411	0.76	2.3	1.06	0.00525	0.00726	5.19E-04

Table 4-4 pre-calculation on model analysis for 70 ft. arm with TMD in 1% damping ratio

And the representative plots of all the results are:

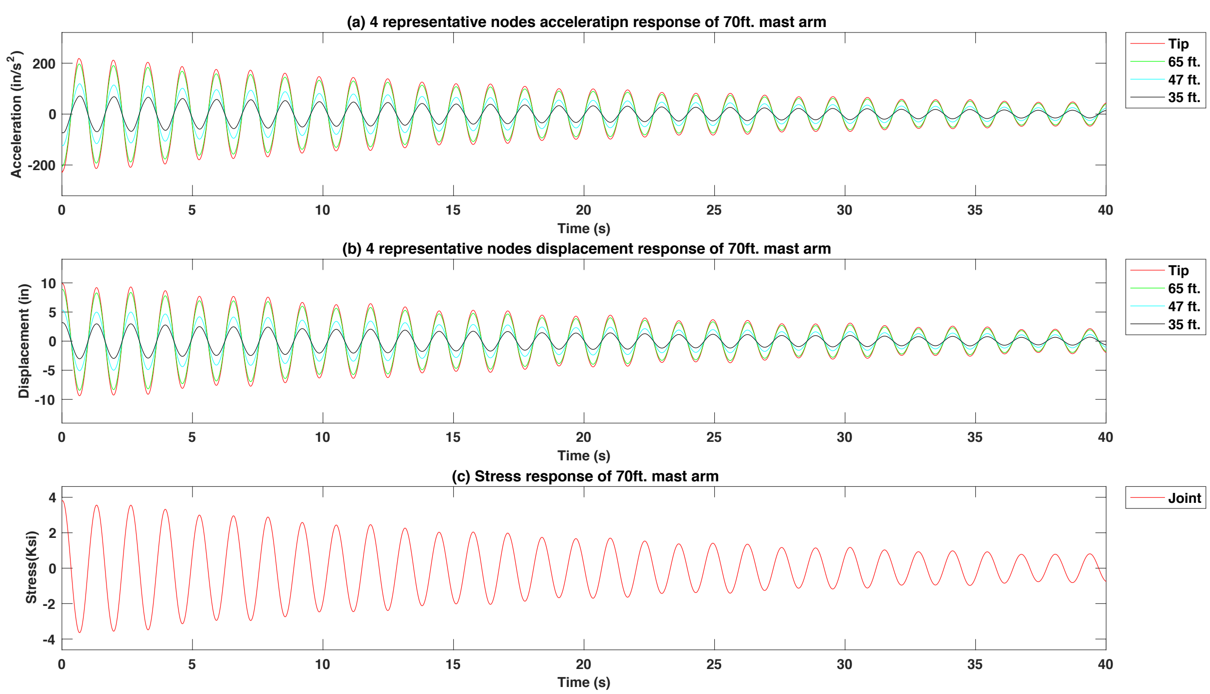

Figure 4-43 Free vibration response of excitation force at tip on the 70 ft. mast arm signal pole structure model with 25 lb. mass TMD using the ζ = 1%

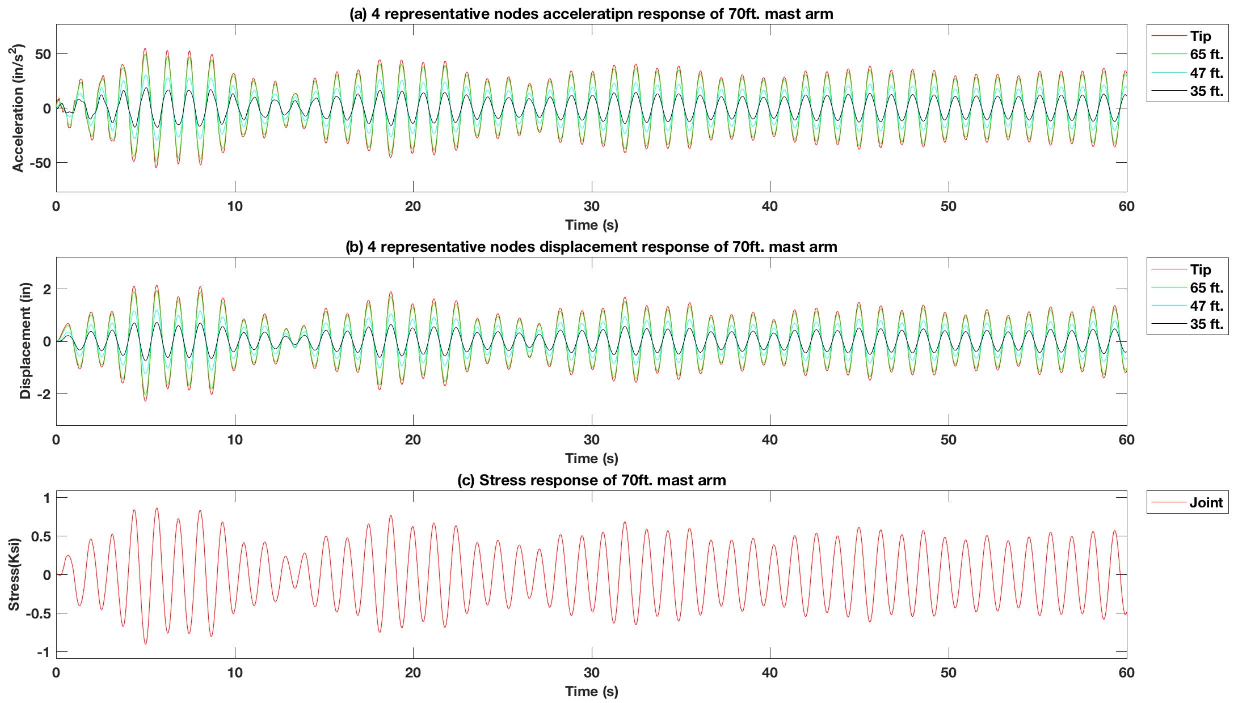

Figure 4-44 Force vibration response of excitation force at tip on the 70 ft. mast arm signal pole structure model with 25 lb. mass TMD using the $\xi = 1\%, f_r = 1.1 f_n$

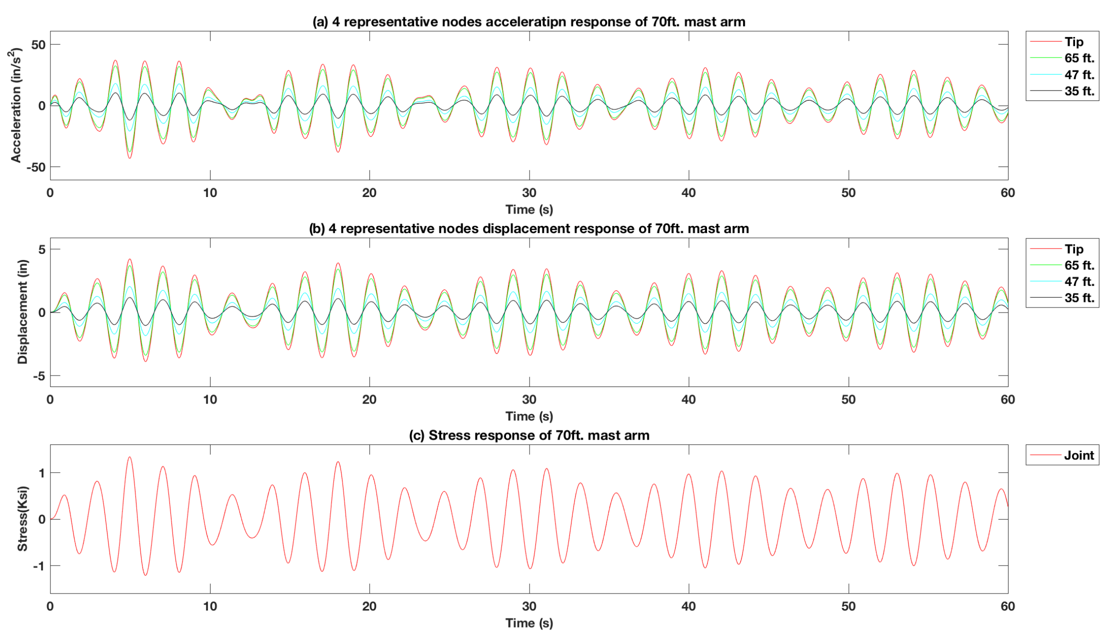

Figure 4-45 Force vibration response of excitation force at 3 signal heads position on the 70 ft. mast arm signal pole structure model with 25 lb. mass TMD using the $\xi = 1\%, f_r = 0.6 f_n$

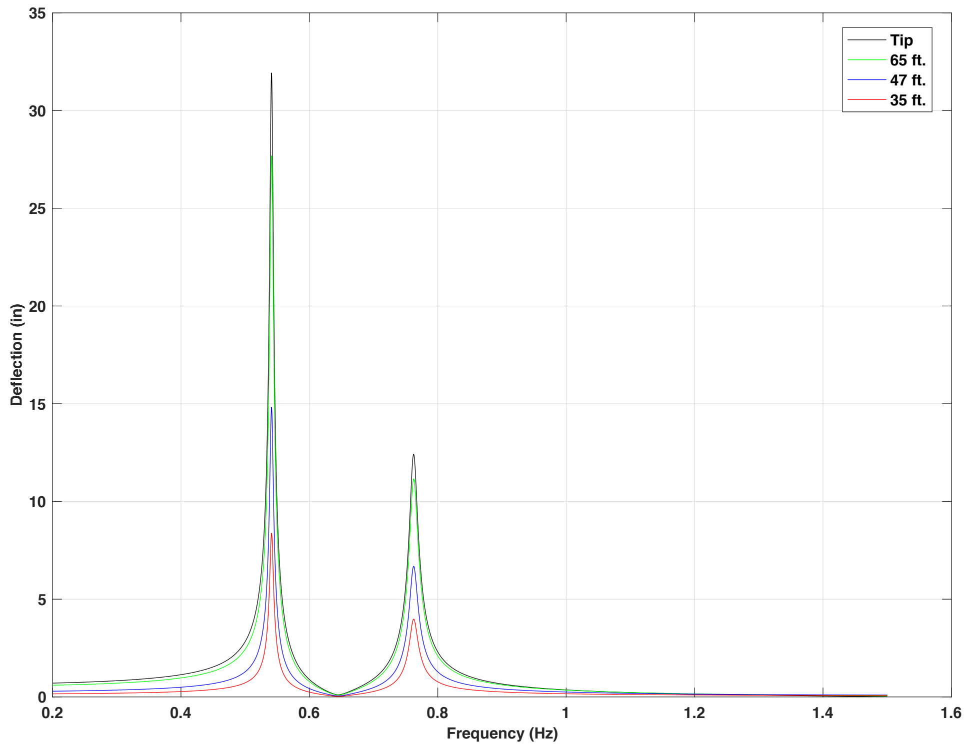

Figure 4-46 Frequency response for 70ft. mast arm with 25 lb. mass TMD using the $\zeta = 1\%$, 5 lbf force on tip of mast arm, $f_d = 1.0 f_n$

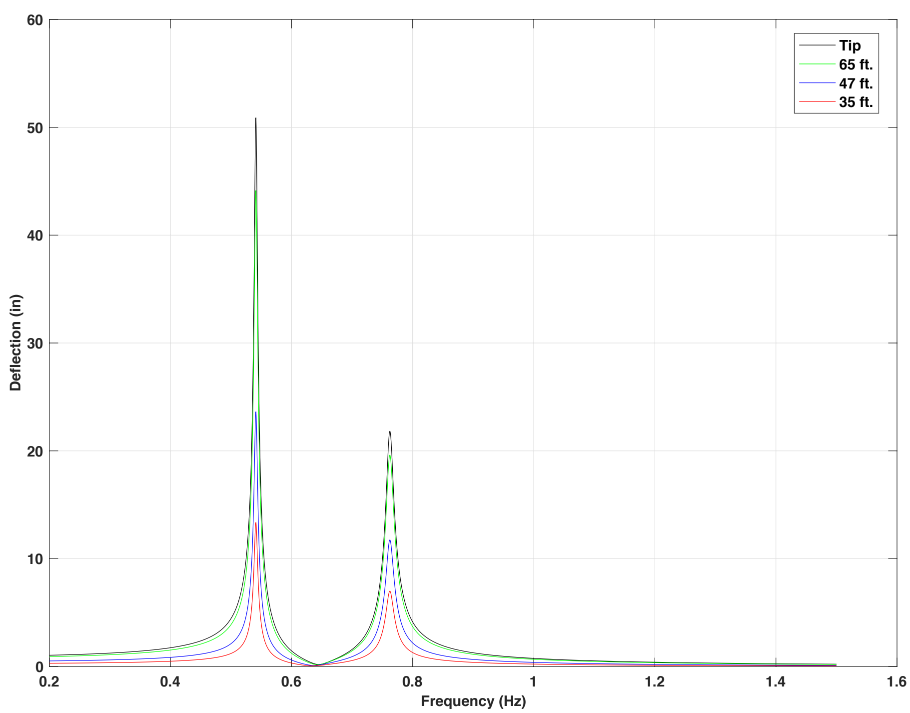

Figure 4-47 Frequency response for 70ft. mast arm with 25 lb. mass TMD using the $\zeta = 1\%$, 5 lbf force on 3 signal head location

4.2.6 TMD Locations

Because the location of TMD could influence the structure's frequencies by changing the whole structure's stiffness matrix, location changes of TMD using 2.5ft., 5ft. and 10ft. from mast arm tip with the same damper is applied.

The initial of the TMD location is on the mast tip, and with 15 lb. mass and 6% damping ratio, which had already been calculated before.

The pre-analysis calculation is:

TMD Location (ft.)	f_1 (Hz)	f_2 (Hz)	f_3 (Hz)	k	c	α	β
2.5	0.57	0.73	2.29	0.64	0.019	0.007	5.20E-04
5	0.57	0.72	2.29	0.64	0.019	0.007	5.20E-04
10	0.58	0.71	2.29	0.64	0.019	0.007	5.20E-04

Table 4-5 pre-calculation on model analysis for 70 ft. arm with TMD in different location

And the representative plots of these results are:

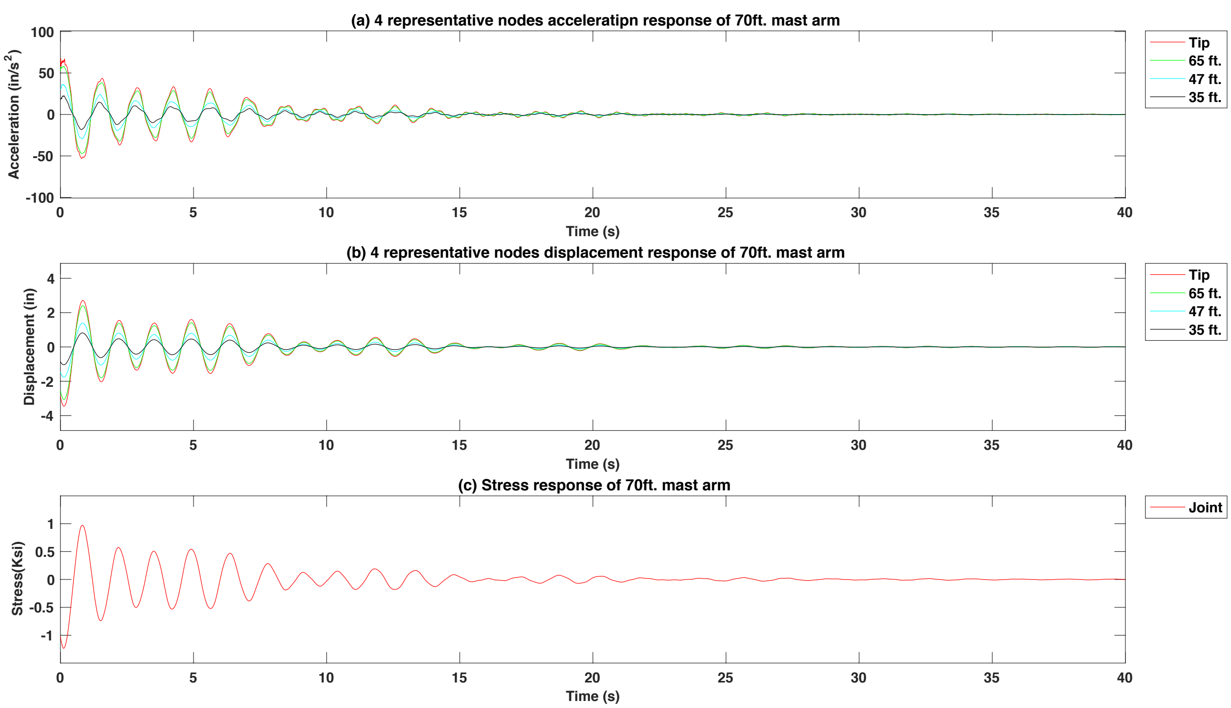

Figure 4-48 Free vibration response of excitation force at tip on the 70 ft. mast arm signal pole structure model with 15 lb. mass TMD at 5 ft from the tip

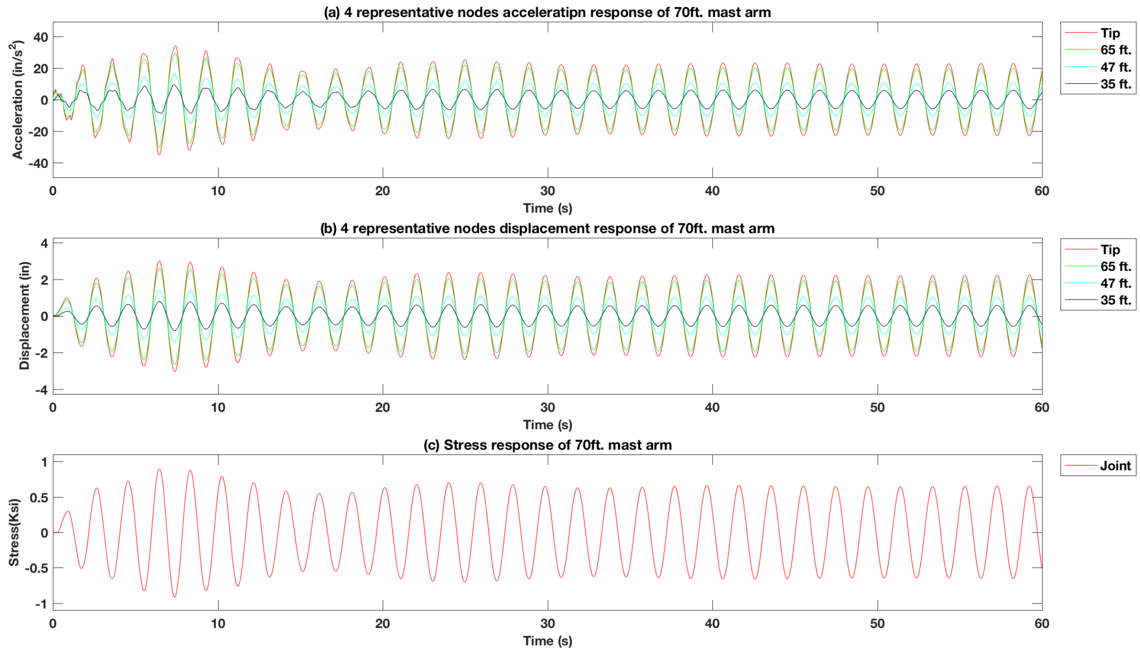

Figure 4-49 Force vibration response of excitation force at tip on the 70 ft. mast arm signal pole structure model TMD at 2.5 ft from the tip $f_e = 0.7f_n$

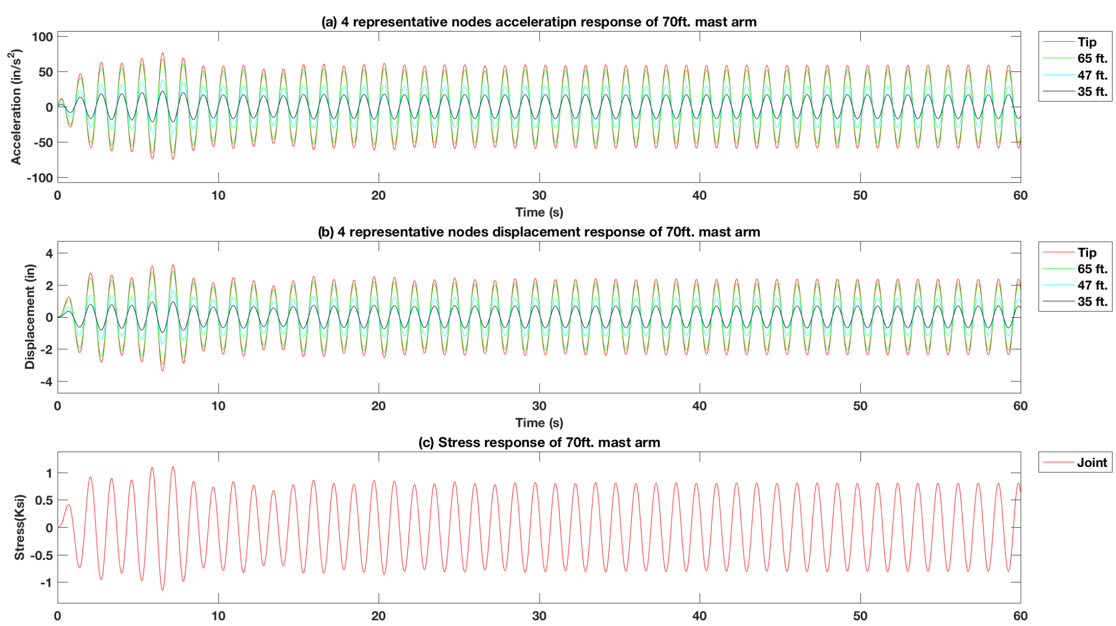

Figure 4-50 Force vibration response of excitation force at 3 signal heads position on the 70 ft. mast arm signal pole structure model TMD at 5 ft from the tip $f_e = 1.1f_n$

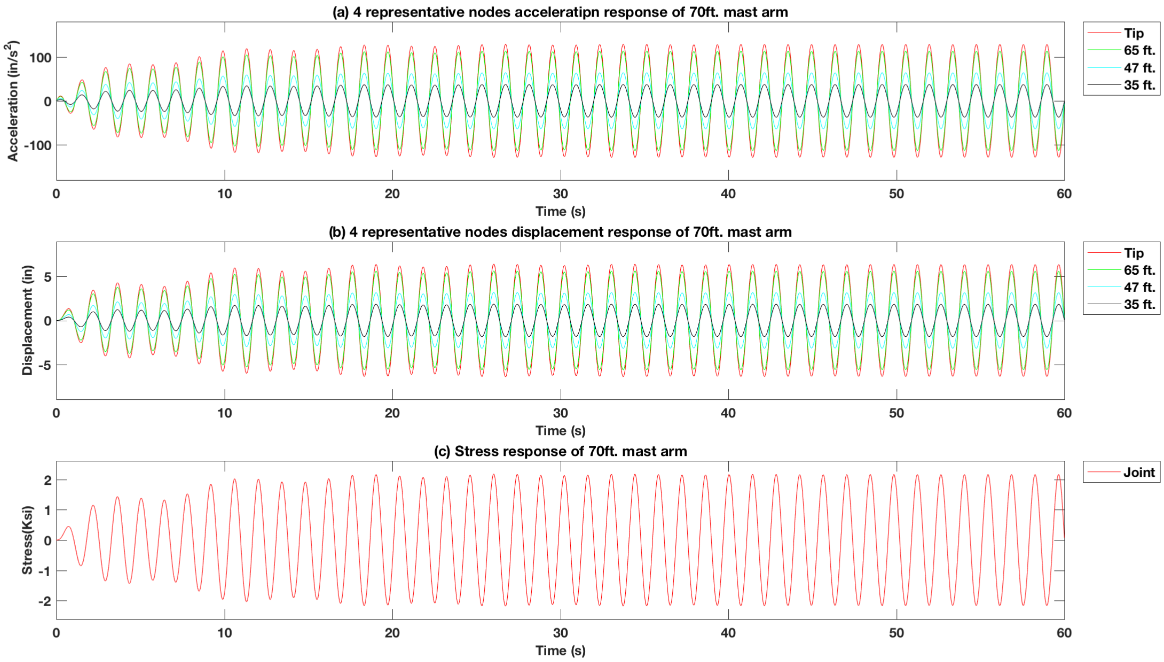

Figure 4-51 Force vibration response of excitation force at 3 signal heads position on 70 ft. mast arm signal pole structure model TMD at 10 ft from the tip $f_t = 1.0 f_n$

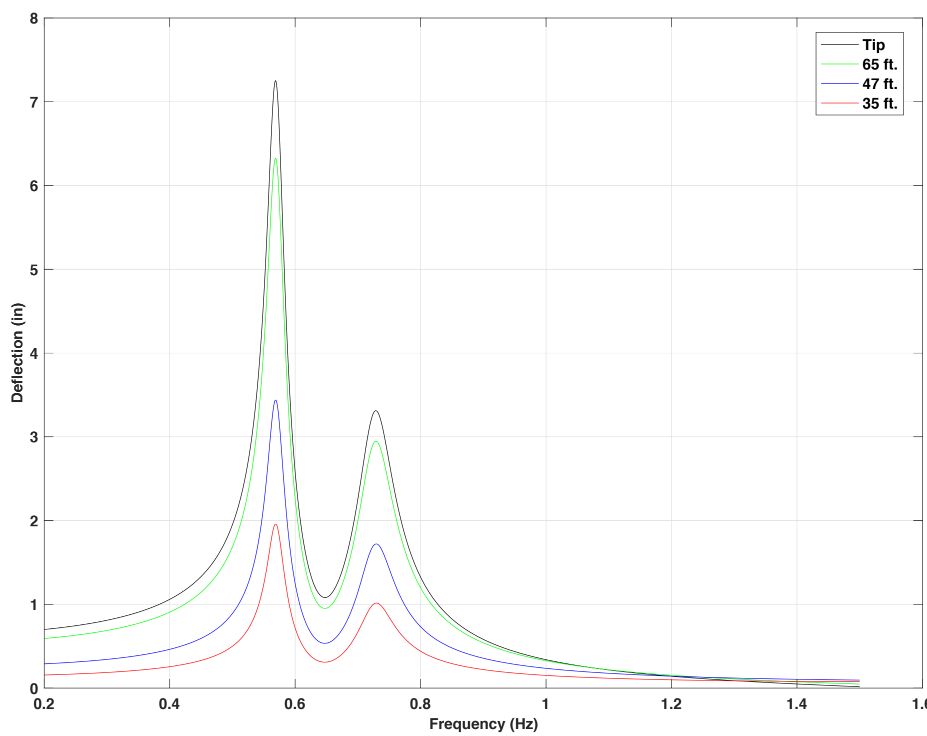

Figure 4-52 Frequency response for 70ft. mast arm with 15 lb. mass TMD at 2.5 ft from the tip $f_d = 1.0 f_n$. 5 lbf force on tip of mast arm

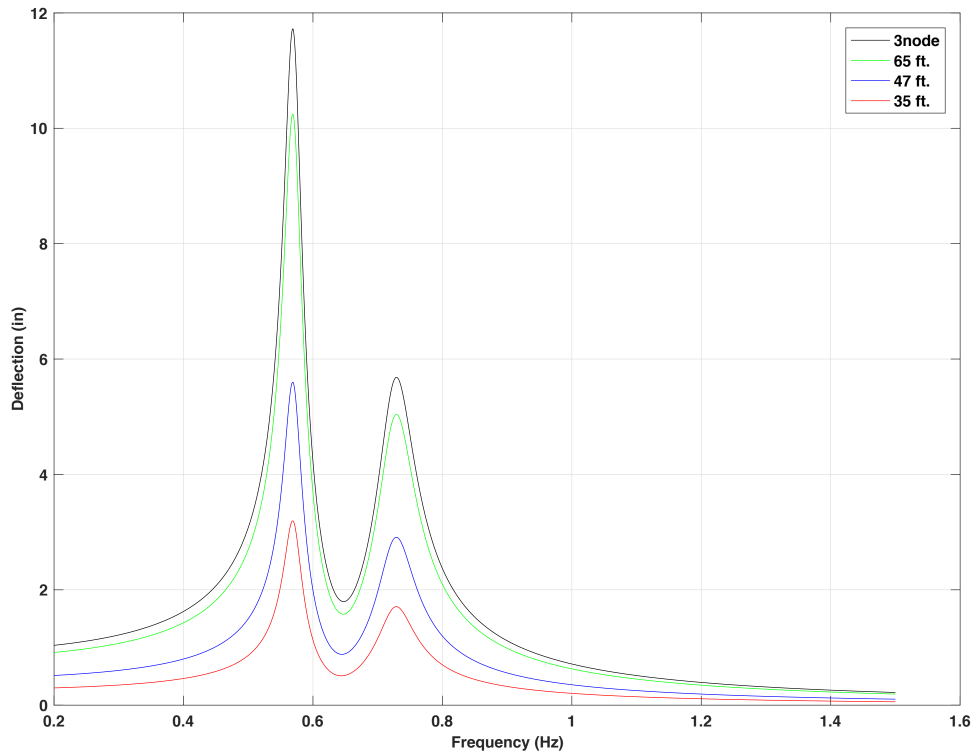

Figure 4-53 Frequency response for 70ft. mast arm with 15 lb. mass TMD at 2.5 ft from the tip, $f_d = 1.0 f_n$, 5 lbf force on 3 signal head location (notation 3node means tip deflection under this situation)

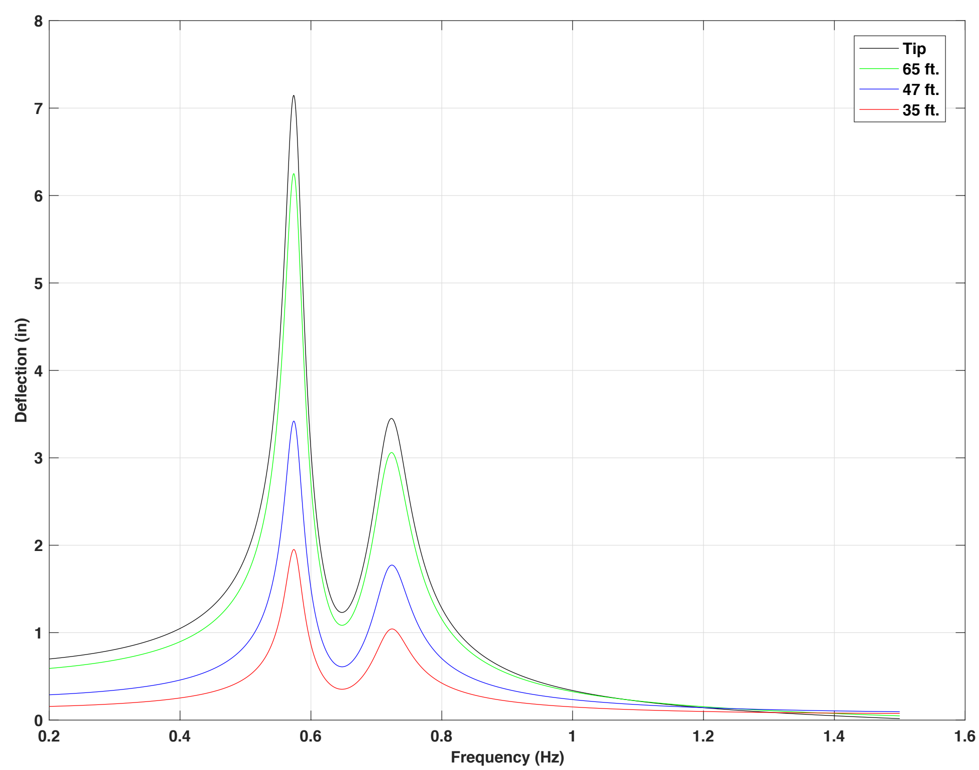

Figure 4-54 Frequency response for 70ft. mast arm with 15 lb. mass TMD at 5 ft from the tip $f_d = 1.0 f_n$, 5 lbf force on tip of mast arm

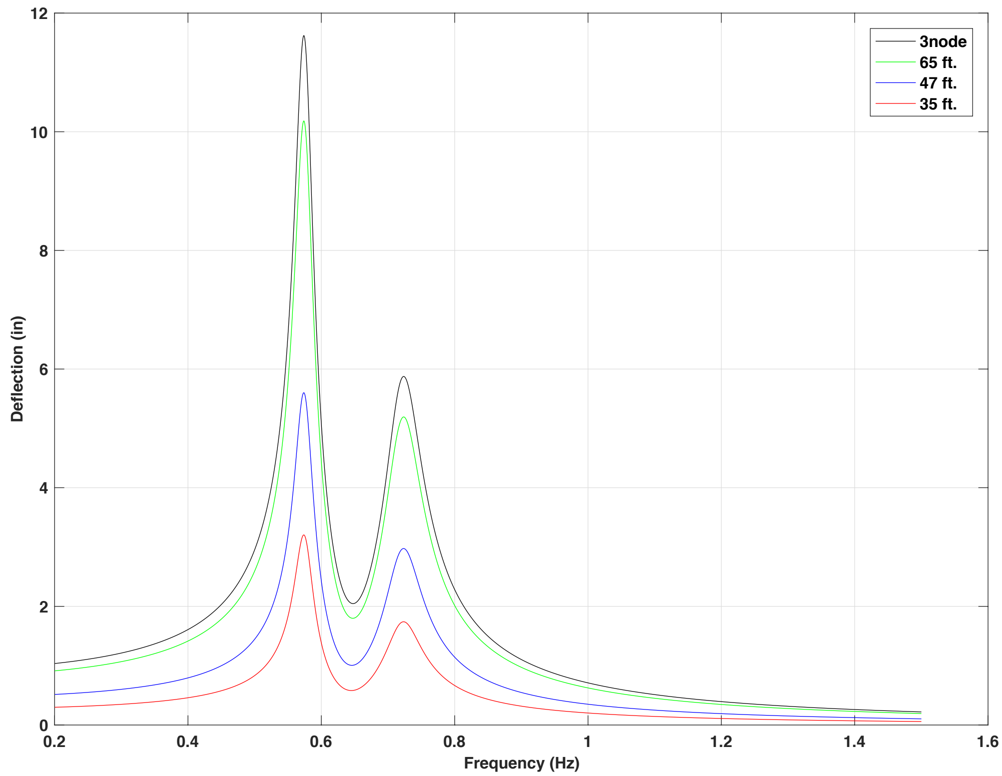

Figure 4-55 Frequency response for 70ft. mast arm with 15 lb. mass TMD at 5 ft from the tip, $f_d = 1.0 f_n$, 5 lbf force on 3 signal head location

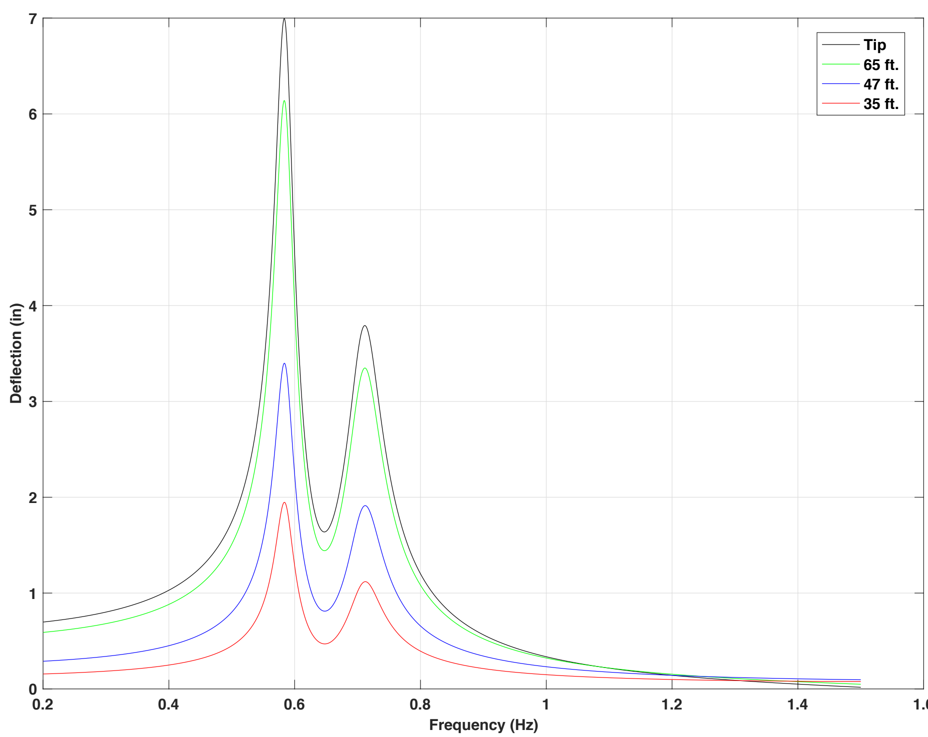

Figure 4-56 Frequency response for 70ft. mast arm with 15 lb. mass TMD at 2.5 ft from the tip $f_d = 1.0 f_n$, 5 lbf force on tip of mast arm

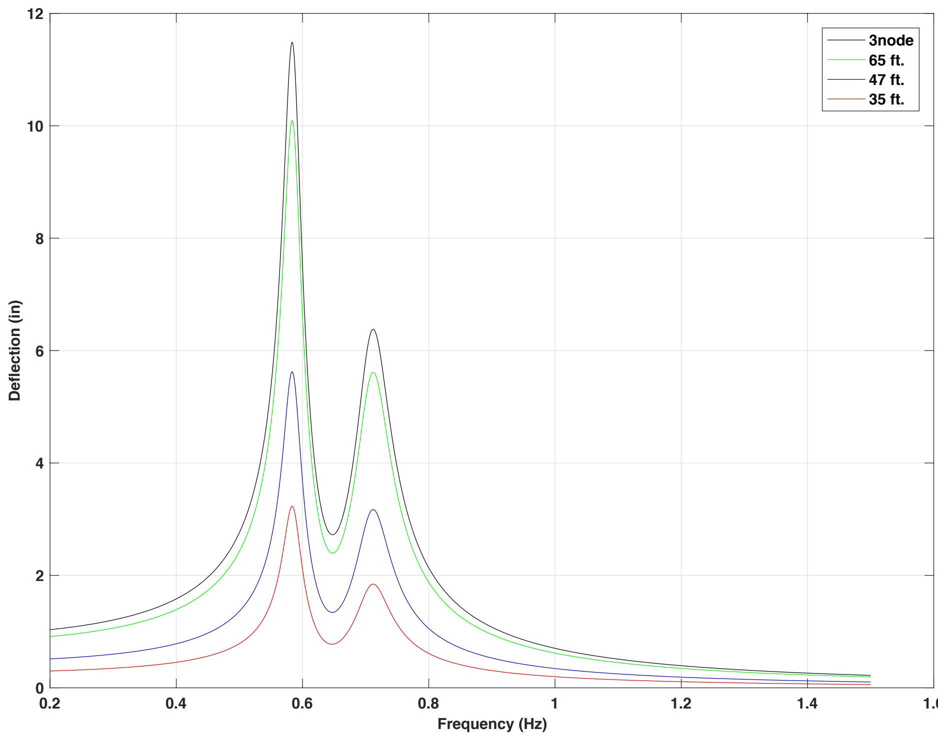

Figure 4-57 Frequency response for 70ft. mast arm with 15 lb. mass TMD at 2.5 ft from the tip, $f_d = 1.0 f_n$, 5 lbf force on 3 signal head location

4.3 Signal Support Structure with 60 ft. Arm Length

4.3.1 Finite Element Model description

For the 60 ft. arm length structure, beam188 element is selected to build the main structure. Mass21 element was used as the traffic signal and mass of the TMD. And combin14 element is used for simulates the TMD's spring stiffness and damping ratio. The locations of signals could vary. In this model, use three signals at 25*ft*. 37.5*ft*. and 52.5*ft*. from the arm-pole joint. For the arm-pole joint and base, simply regard it as fixed condition. The gravitation is ignored in the dynamic analysis. Input real constant of mass21 and combin14: use 50 *lb*. per signal head to be conservative for traffic signal and 15 *lb*. or 25 *lb*. mass of the TMD; ignore the initial deflection of the structure due to self-weight and probable raise angle of the mast arm and assumed the TMD is rigid connected to the mast arm. The mesh size is using 1.5 *ft./*segment for signal pole, and 2.5-*ft./* segment for mast arm primary part. And for the connections between arm segments, use 0.4375-*ft*. per segment for the connection of base arm and the first extension, and 0.375-*ft.* per segment for the first and second extension connection.

The dimensions of the pole and mast arm are shown in Table 3-1 and Table 3-2.

From the Signal Pole Standards, the 60 ft. mast arm signal pole model is using the same pole and first two segment of mast arm in 70 ft. arm in dimensions. All the traffic signals head are assumed rigidly connected to the mast arm. Run the modal analysis first to get first 10 modes of frequencies.

4.3.2 Mast arm signal support structure model without TMD and its outputs

After plot each mode of frequencies, choose the first mode frequency in Y direction and the second mode frequency in Y direction, in this case 0.848Hz and 3.153Hz, to calculate the alpha and beta values in Rayleigh damping matrix. Choose 0.2% in the first mode and 0.4% for the second mode, and the value would be:

$$\begin{pmatrix} a_0 \\ a_1 \end{pmatrix} = \begin{pmatrix} \alpha \\ \beta \end{pmatrix} = \begin{pmatrix} 0.010643 \\ 0.000377 \end{pmatrix}$$

Put these values back in Rayleigh damping matrix for Newmark beta method and do the dynamic analysis for free vibration and force vibration using the same methods in analysis of 70 ft. mast arm, section 4.2. Some of the representative results are plotted:

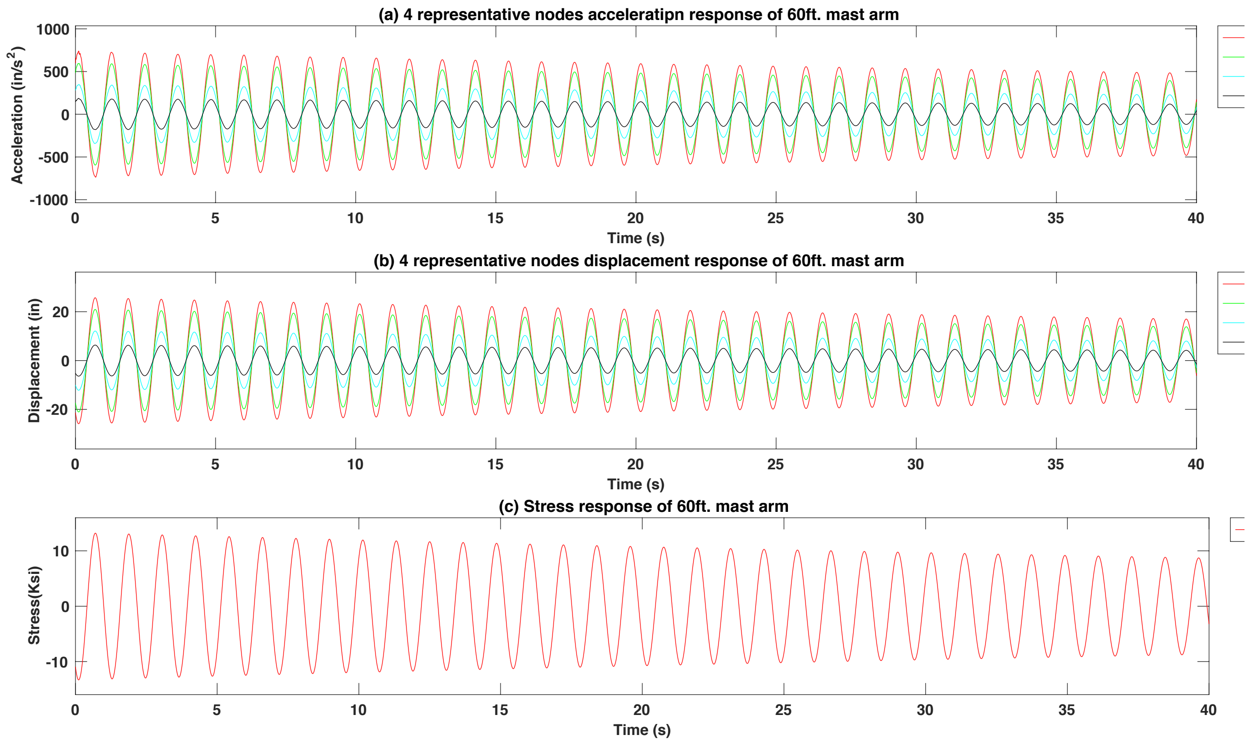

Figure 4-58 Free vibration response of the 60 ft. arm signal support structure model without TMD

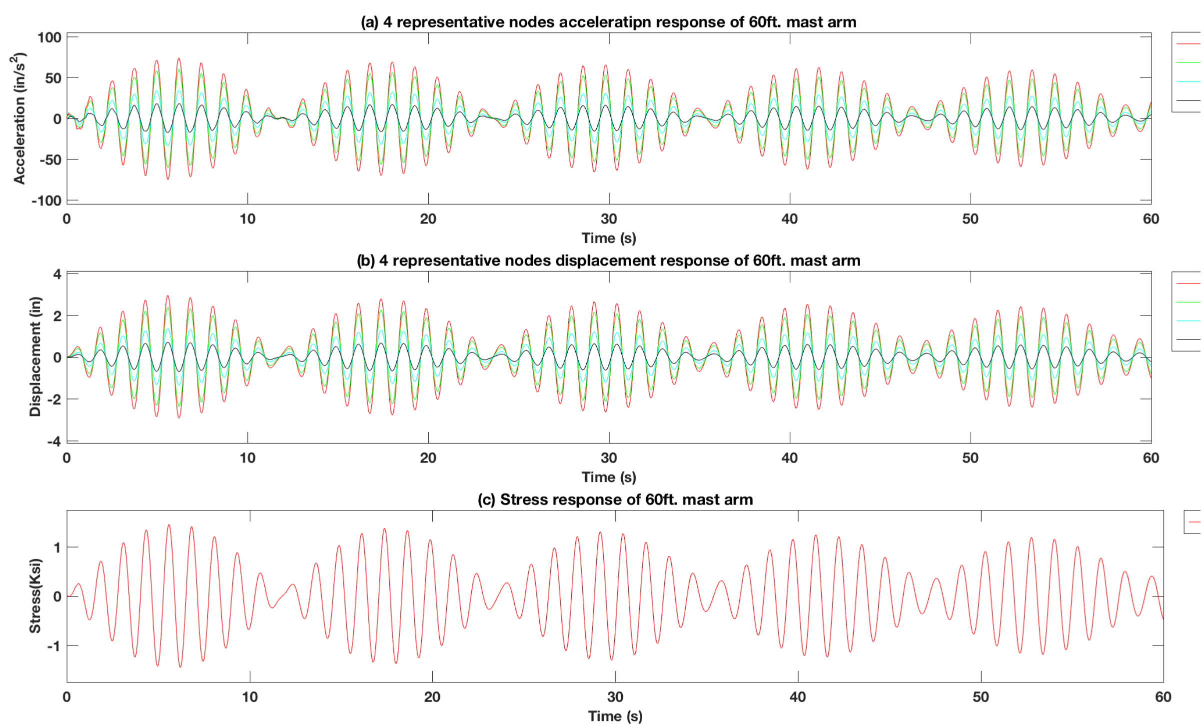

Figure 4-59 Force vibration response of excitation force at tip in $f_x = 0.9\times f$ of the 60 ft. mast arm signal pole structure model without TMD

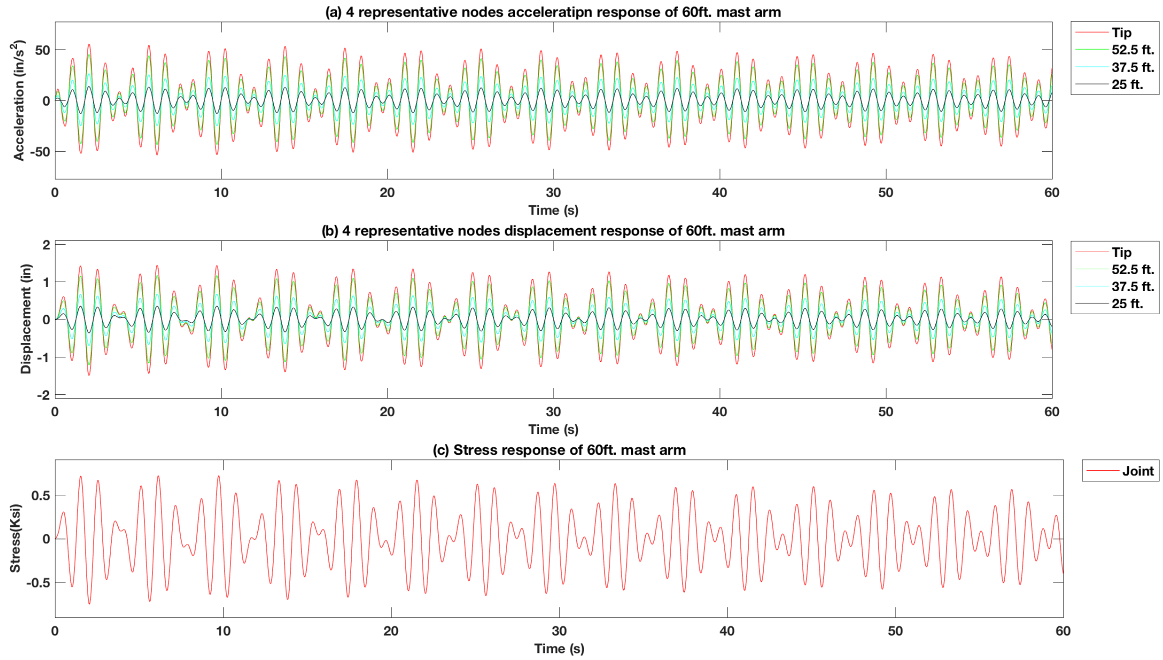

Figure 4-60 Force vibration response of excitation force at tip in $f_e = 1.3\times f$ of the 60 ft. arm signal support structure model without TMD

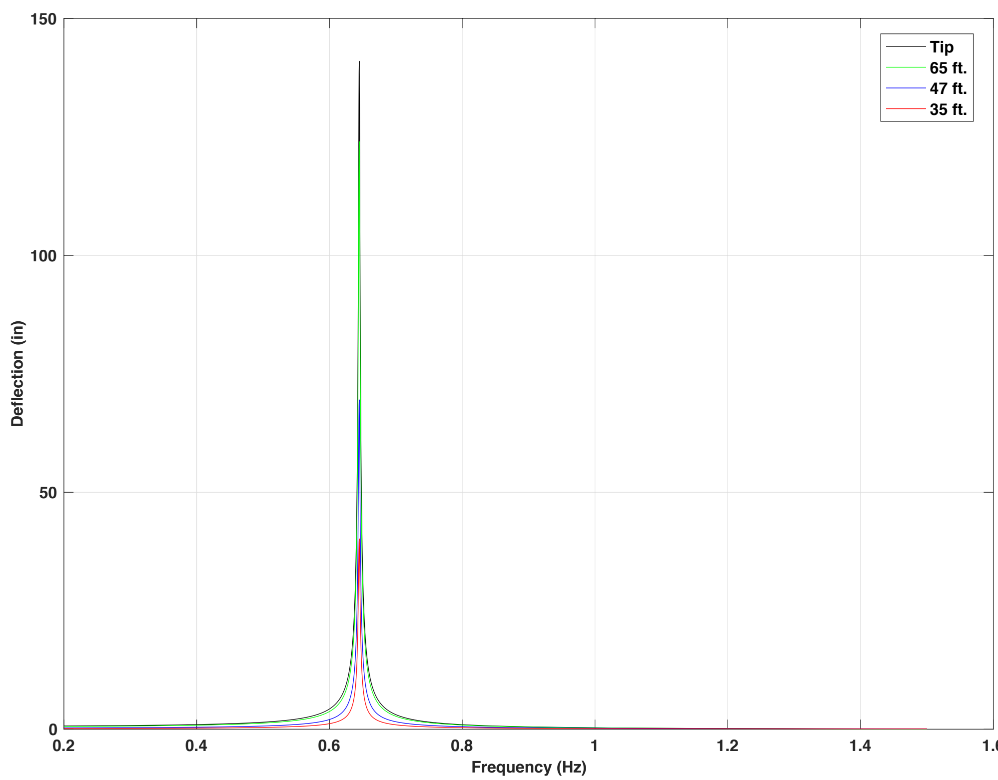

Figure 4-61 Harmonic response for excitation force on the mast arm tip of the 60 ft. arm signal support structure model without TMD

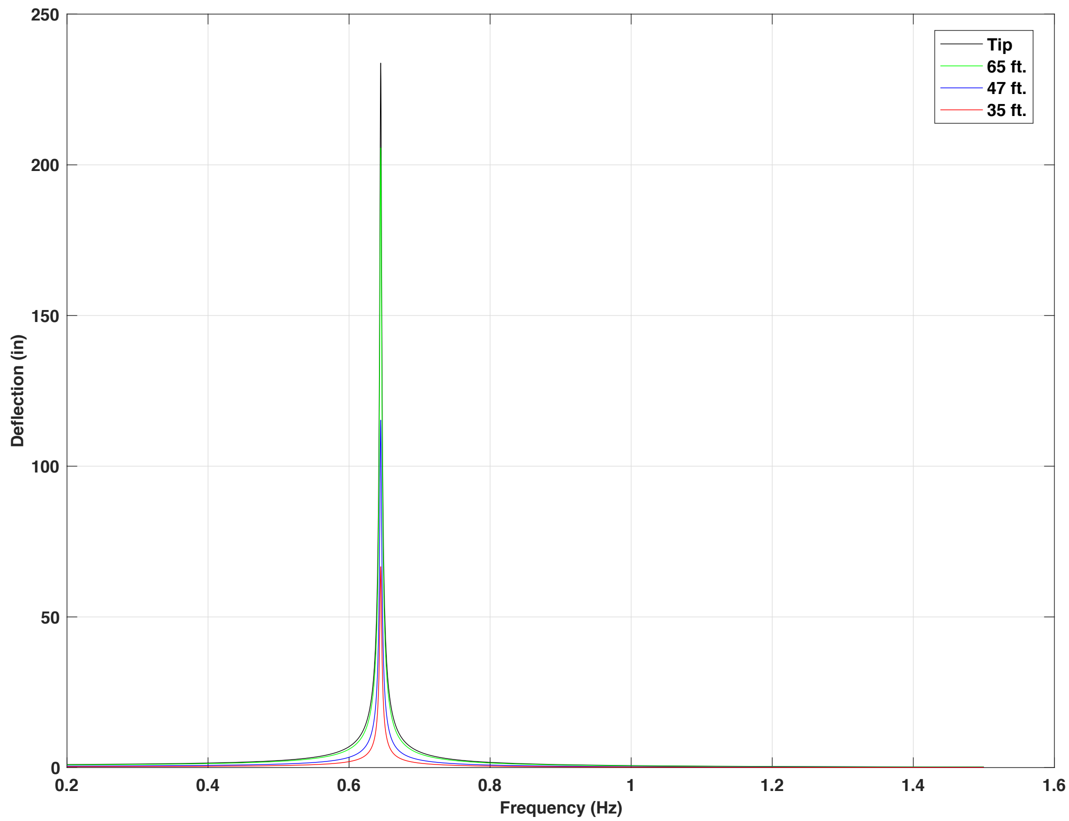

Figure 4-62 Harmonic response for excitation force on the mast arm signal heads locations of the 60 ft. arm signal support structure model without TMD

4.3.3 TMD Mass

In this comparison, also choose TMD masses of 15 *lb*. and 25 *lb.* Based on the initial model, calculate parameters for analyses:

TMD mass	f_1 (Hz)	f_2 (Hz)	f_3 (Hz)	k	c	α	β
15 lb.	0.74	0.96	3.16	1.10	0.025	0.010	3.76E-04
25 lb.	0.72	1.00	3.17	1.83	0.041	0.010	3.76E-04

Table 4-6 pre-calculation on model analysis for 60 ft. arm with 15lb. and 25lb. TMD

Although both the first and second mode shapes are shown as the first mode shape (ignore the position of TMD) for the signal support structures, and the contribution in deflection cannot determine the structure's peak value in harmonic analysis or force excitation, the frequency could be chosen between the first and second mode frequency. In this study choose the second mode frequency as the free vibration excitation force frequency and initial frequency for force vibration excitation force.

Some of the representative results are shows below:

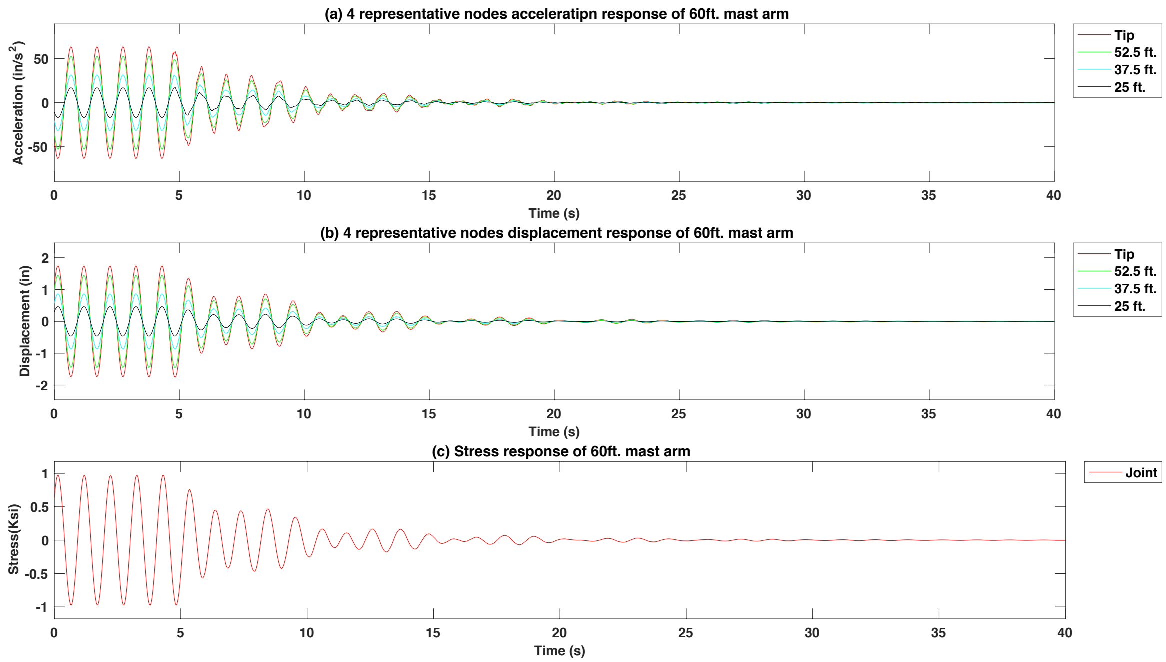

Figure 4-63 Free vibration response of the 60 ft. arm signal support structure model with 15lb. TMD in the same frequency of the structure

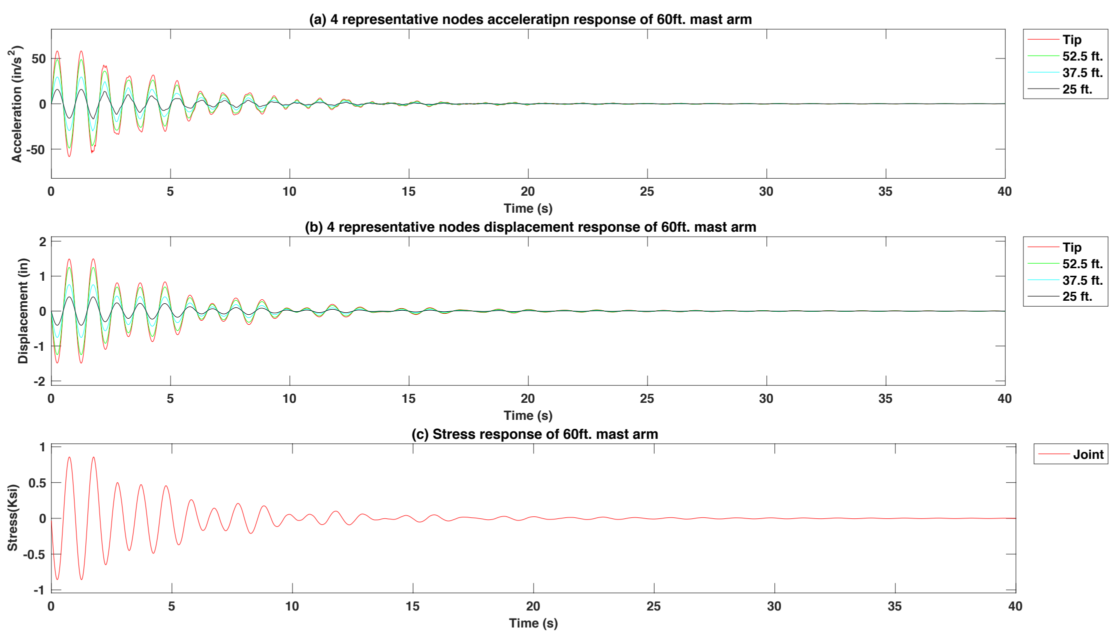

Figure 4-64 Free vibration response of the 60 ft. arm signal support structure model with 25lb. TMD in the same frequency of the structure

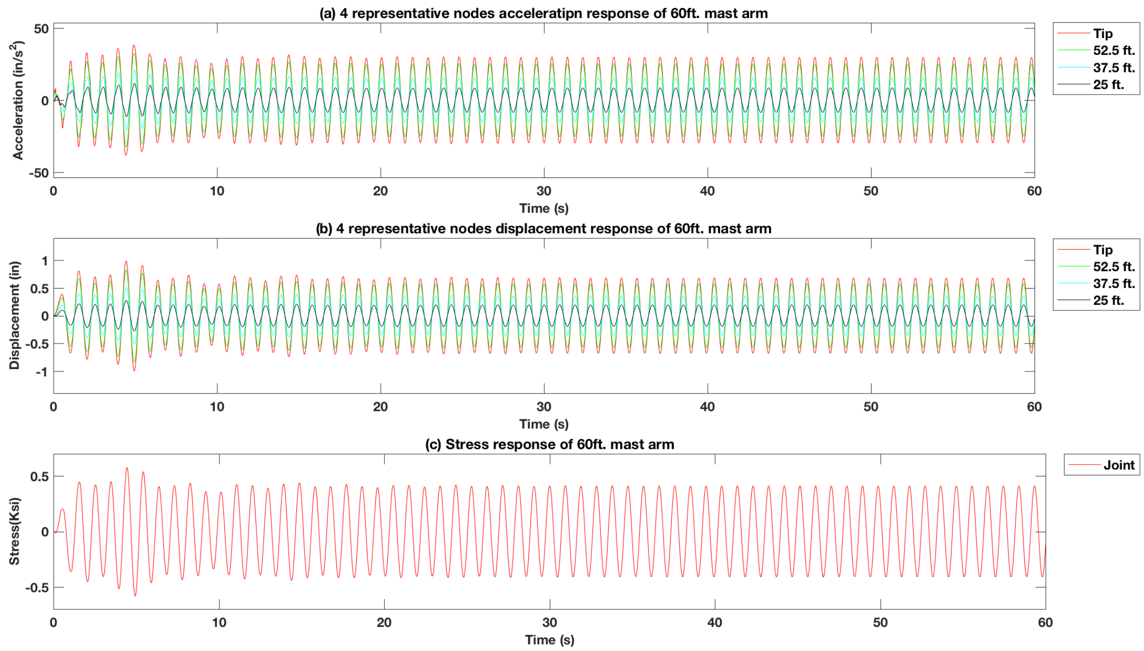

Figure 4-65 Force vibration response of excitation force at tip of the 60 ft. mast arm signal pole structure model with 15 lb. mass TMD using the $f_r = 1.1f_n$

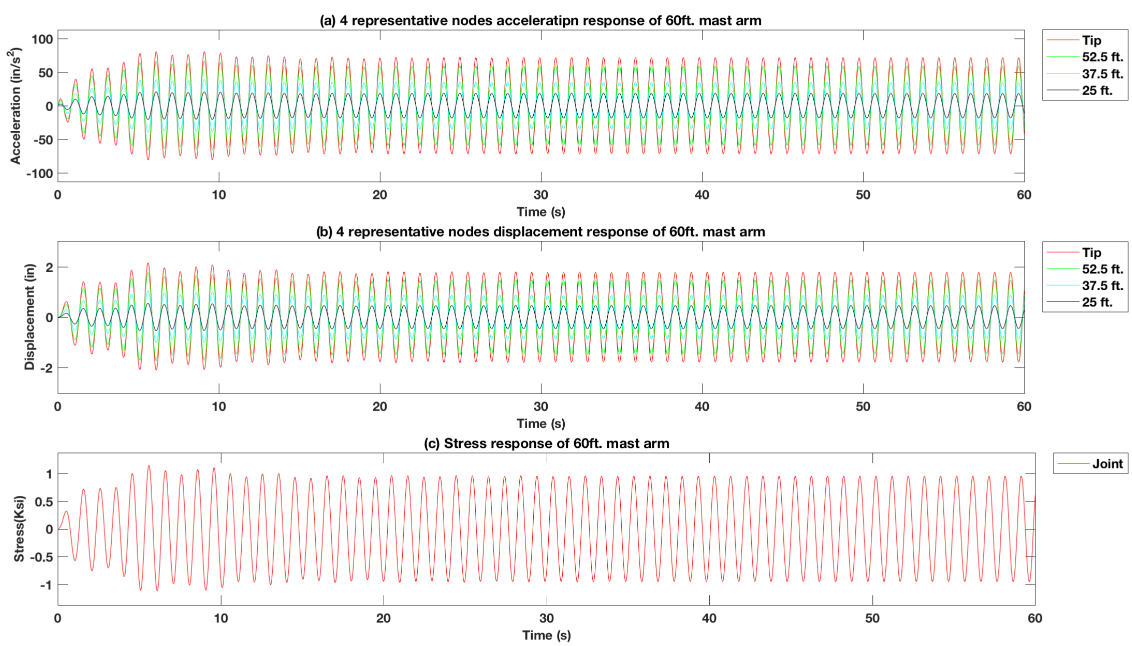

Figure 4-66 Force vibration response of excitation force at 3 signal heads location of the 60 ft. mast arm signal pole structure model with 15 lb. mass TMD using the $f_r = 1.05f_n$

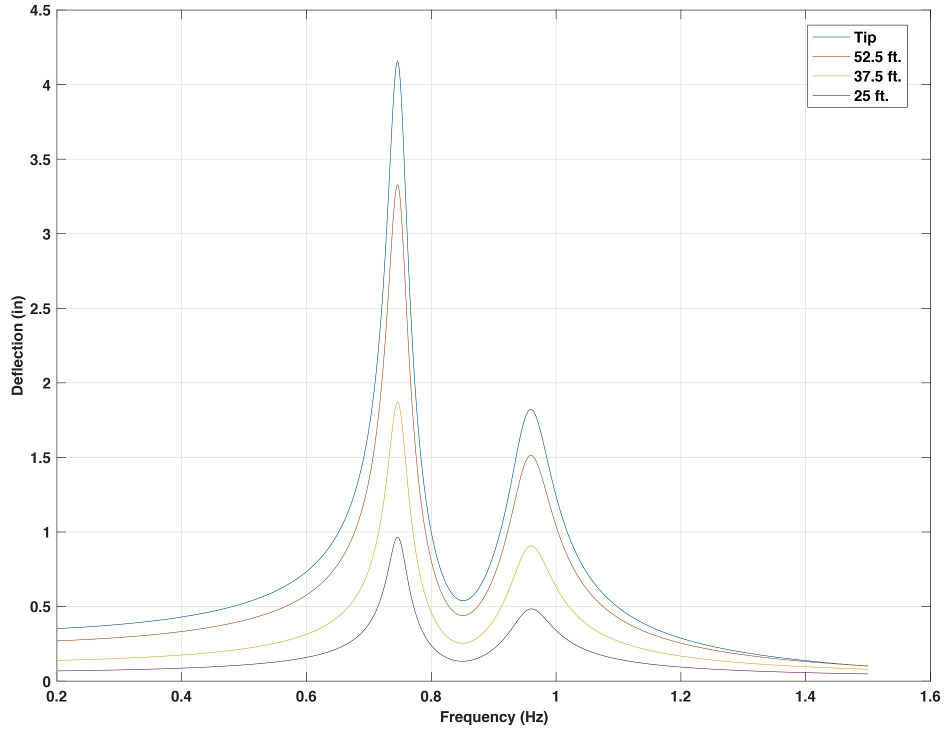

Figure 4-67 Frequency response for 60ft. mast arm with 15lb mass TMD, force on the tip

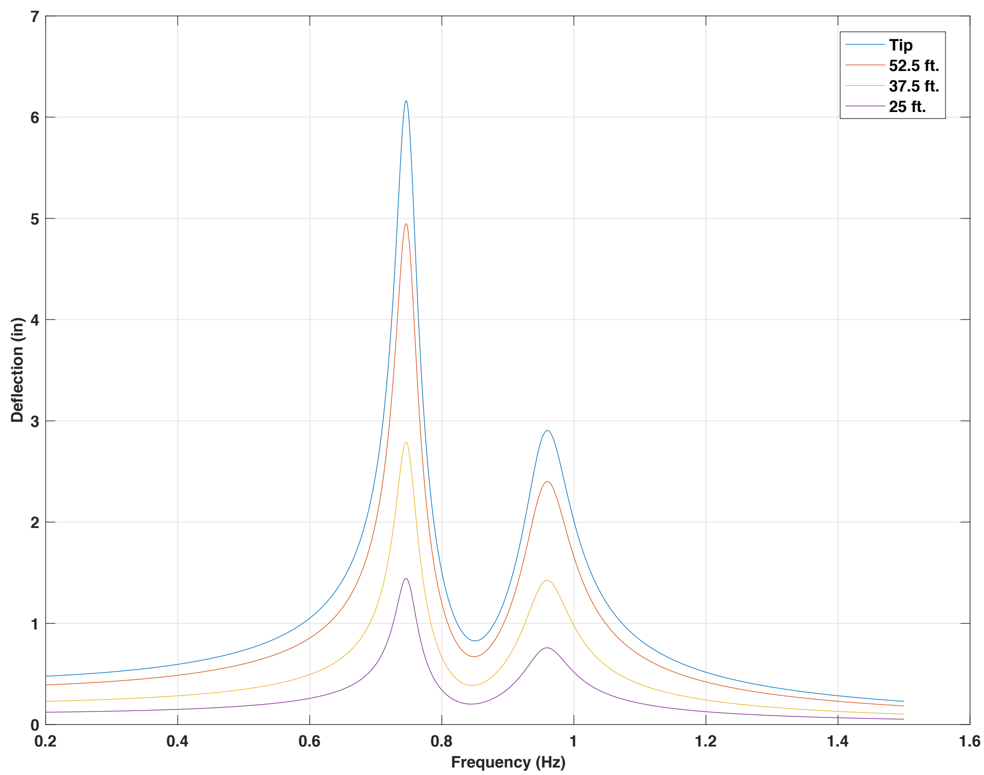

Figure 4-68 Frequency response for 60ft. mast arm with 15lb mass TMD, force on signal heads' location

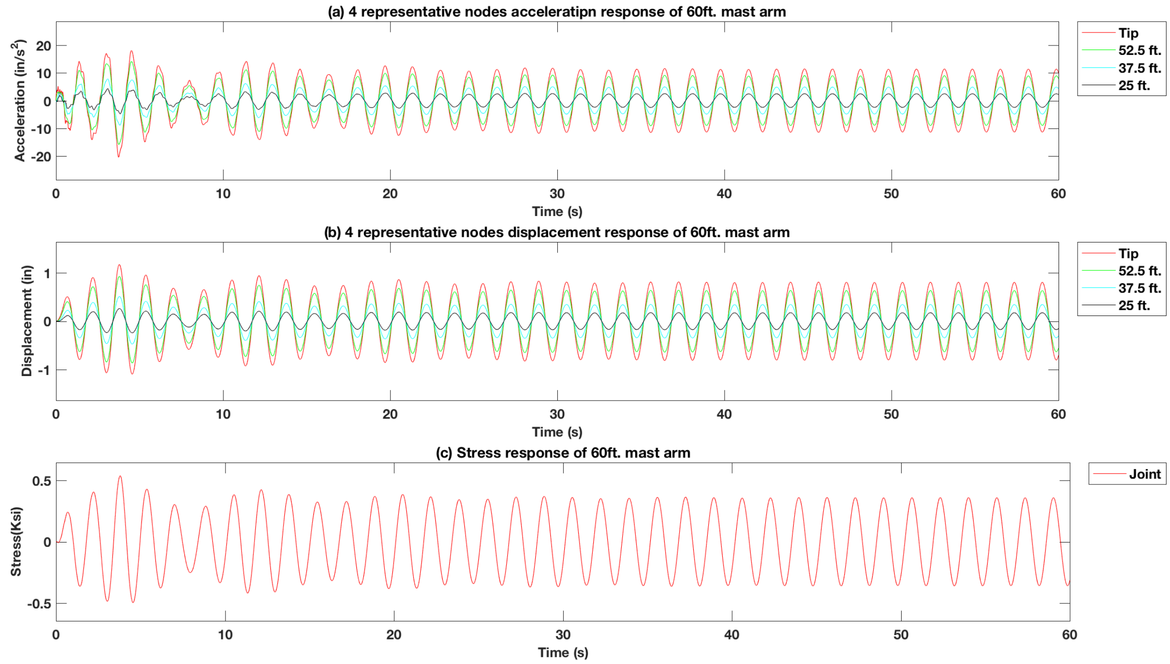

Figure 4-69 Force vibration response of excitation force at tip of the 60 ft. mast arm signal pole structure model with 25 lb. mass TMD using the $f_r = 0.6f_n$

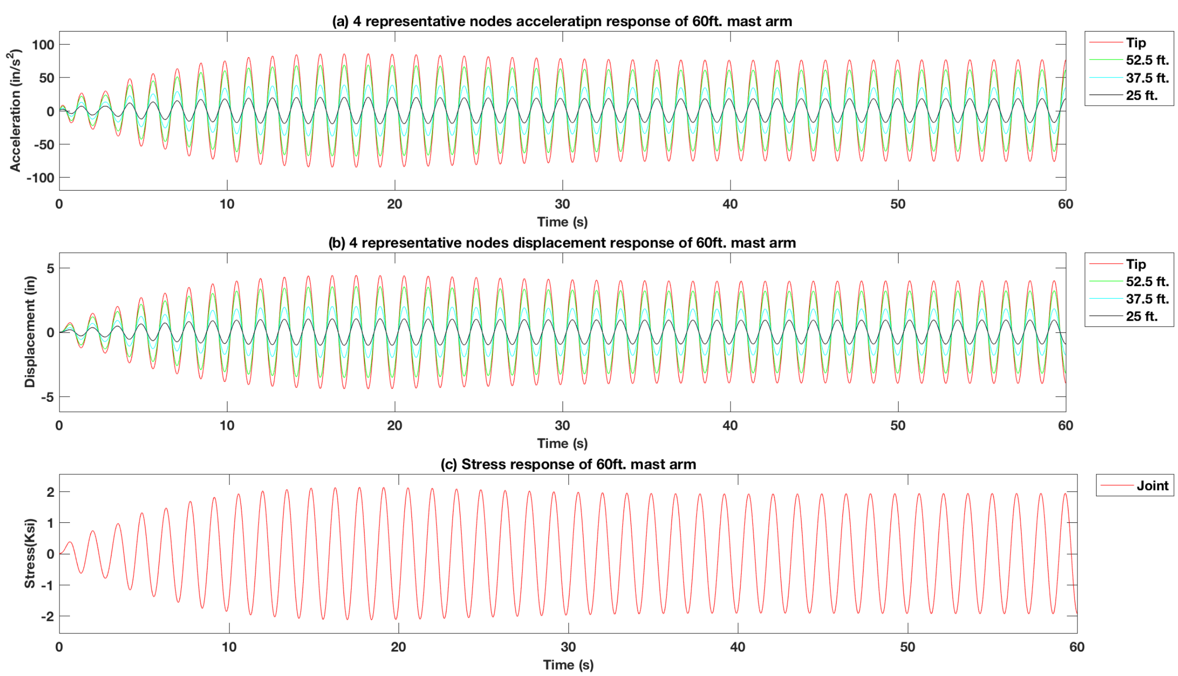

Figure 4-70 Force vibration response of excitation force at 3 signal head of the 60 ft. mast arm signal pole structure model with 25 lb. mass TMD using the $f_r = 0.7f_n$

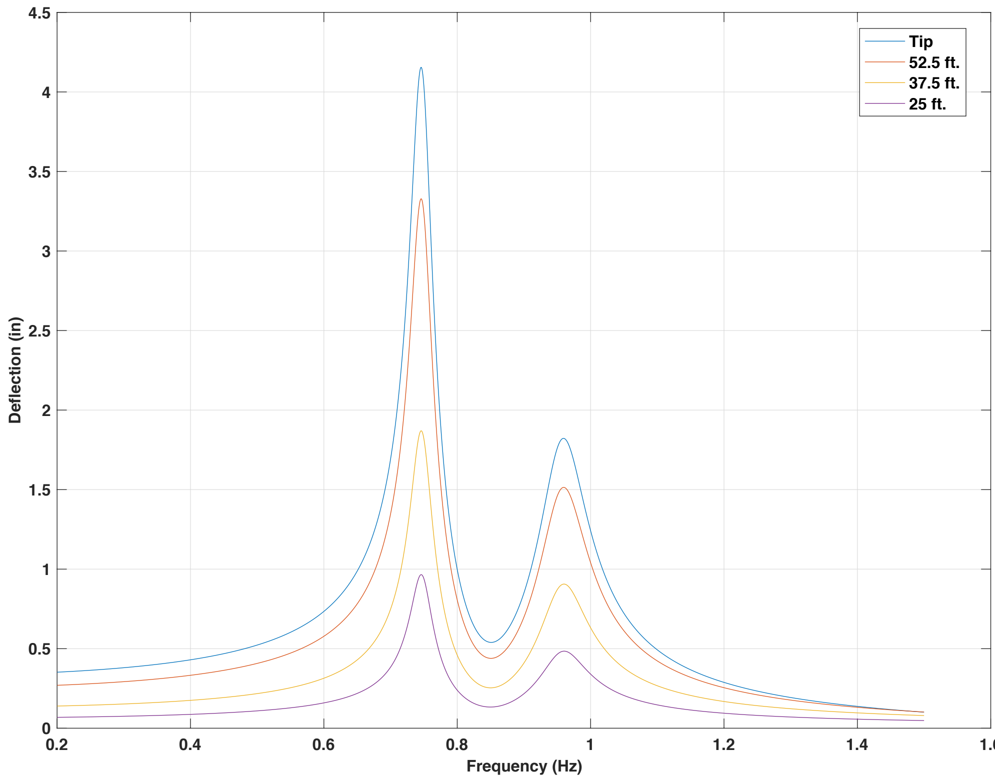

Figure 4-71 Frequency response for 60ft. mast arm with 25lb mass TMD, force on the tip

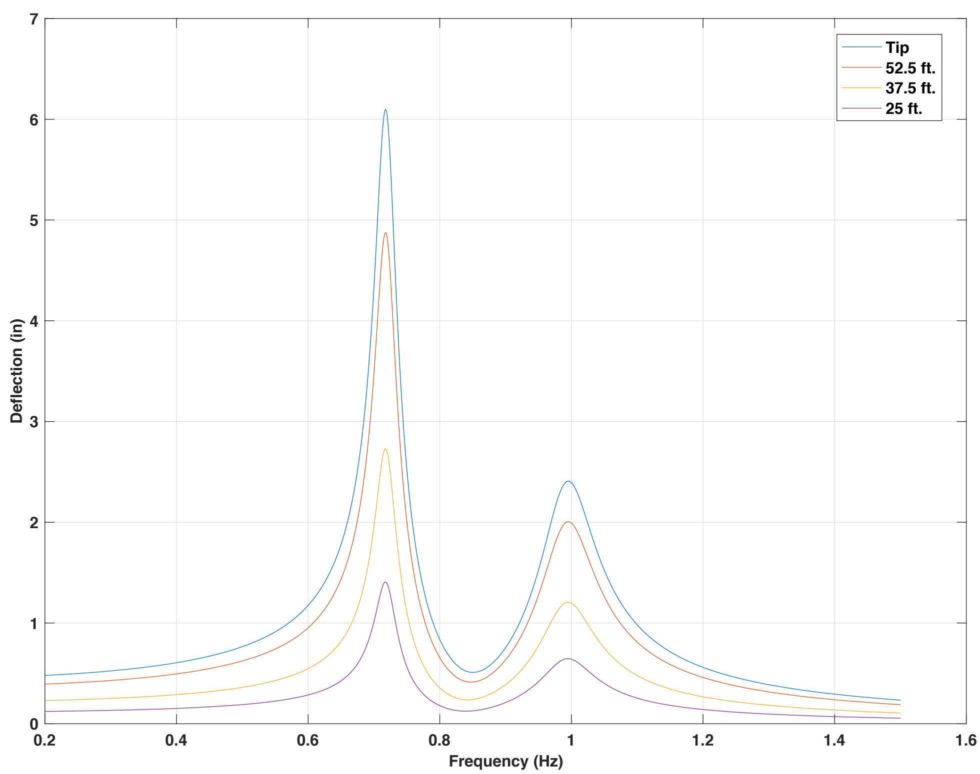

Figure 4-72 Frequency response for 60ft. mast arm with 25lb mass TMD, force on signal heads' location

4.3.4 TMD Frequencies

As analyzed for the previous model, i.e. 70 feet mast arm model, before, selecting the damper frequencies of 1.1 f, 0.9 f, 1.25 f, 0.75 f, 1.5 f, and 0.5 f, build the finite element model then do the modal analysis to get mode shapes and frequencies, and calculate corresponding stiffness and damping coefficient of the TMD, then corresponding Rayleigh damping matrix would be computed for the analysis input.

TMD Frequency	f_1 (Hz)	f_2 (Hz)	f_3 (Hz)	k	c	α	β
1.1 f_{12}	0.77	1.02	3.16	1.33	0.029	0.011	3.758E-4
0.9 f_{12}	0.70	0.92	3.16	0.89	0.223	0.011	3.762E-4
1.25 f_{12}	0.79	1.13	3.17	1.72	0.031	0.011	3.753E-4
0.75 f_{12}	0.61	0.88	3.16	0.62	0.019	0.011	3.763E-4
1.5 f_{12}	0.80	1.33	3.17	2.48	0.037	0.011	3.747E-4
0.5 f_{12}	0.42	0.86	3.15	0.28	0.012	0.011	3.765E-4

Table 4-7 pre-calculation on model analysis for 60 ft. arm with 15lb. and 25lb. TMD

Then do the same analysis as before, i.e. free vibration response, force vibration response and harmonic analysis. The representative result for each case are shown below:

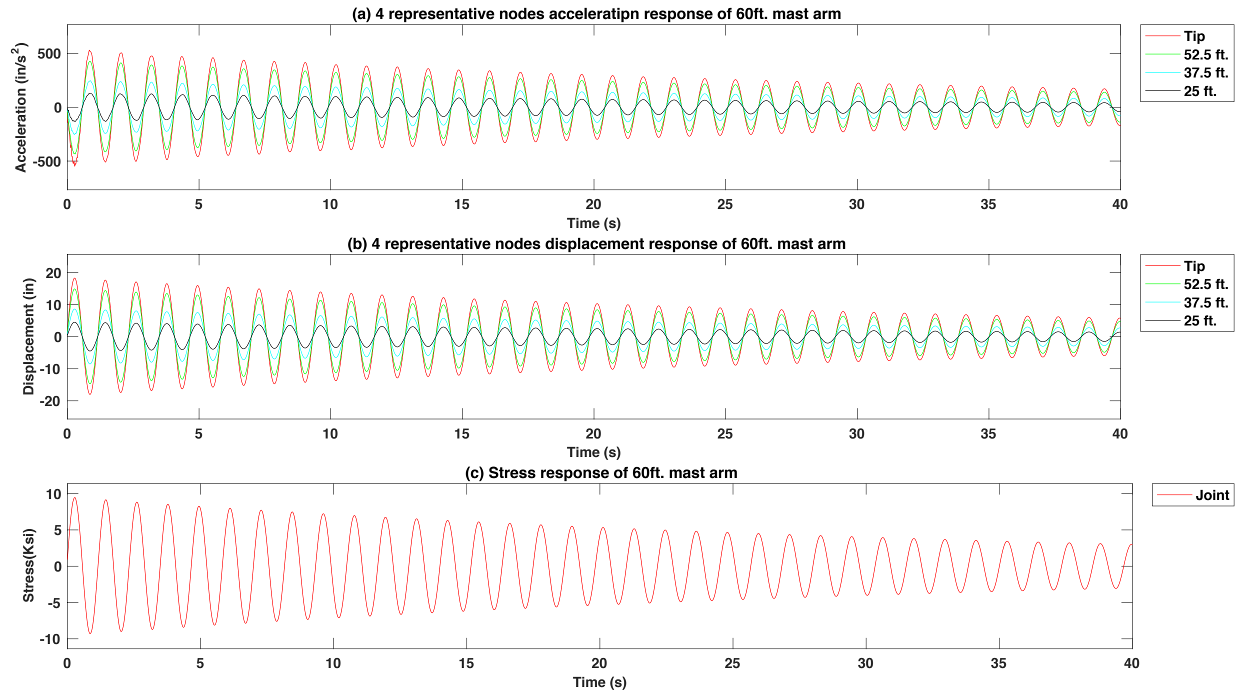

Figure 4-73 Free vibration response of excitation force at tip of the 60 ft. mast arm signal pole structure model with 15 lb. mass TMD using the $f_d = 0.5 f_n$

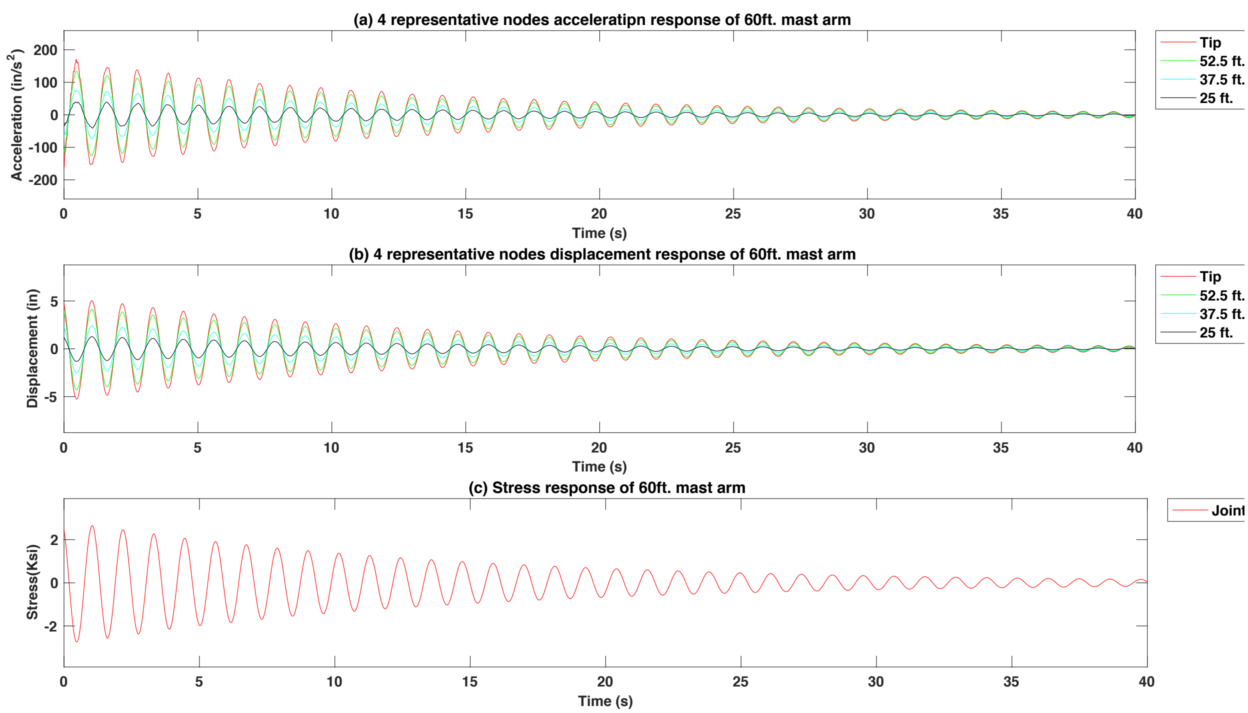

Figure 4-74 Free vibration response of excitation force at tip in natural frequency of the 60 ft. mast arm signal pole structure model with 15 lb. mass TMD using the $f_d = 0.75 f_n$

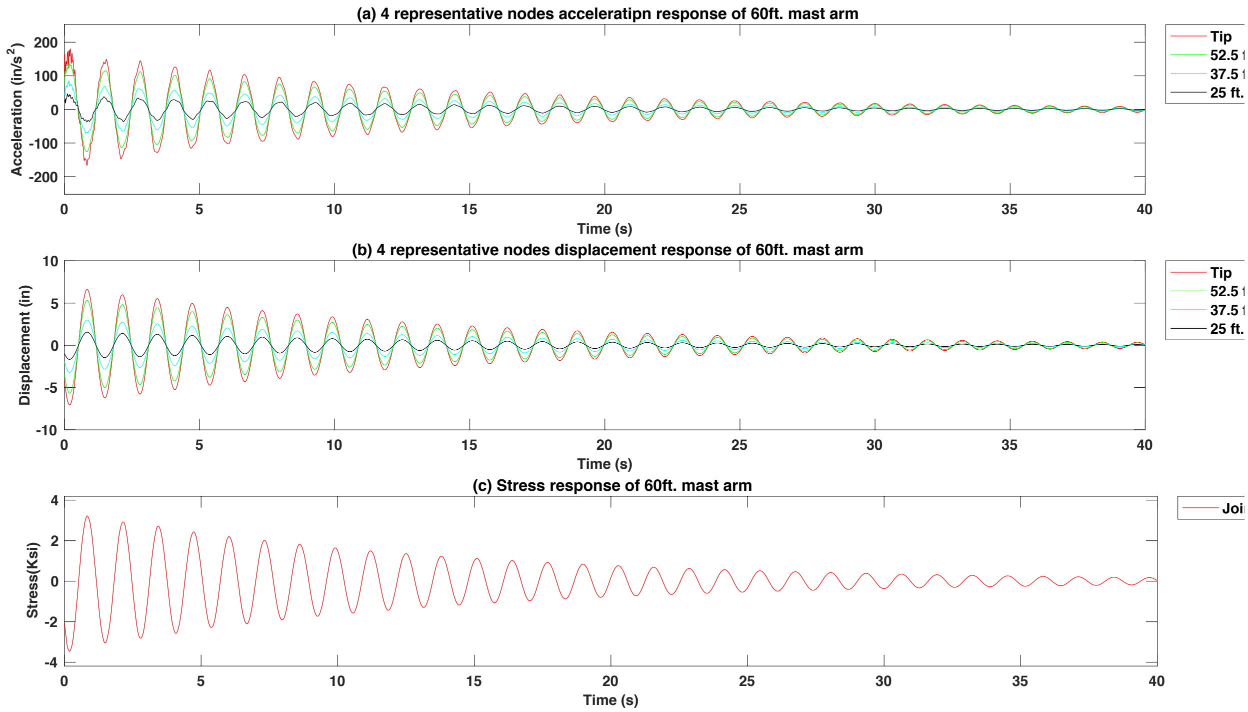

Figure 4-75 Free vibration response of excitation force at tip of the 60 ft. mast arm signal pole structure model with 15 lb. mass TMD using the $f_d = 1.1 f_n$

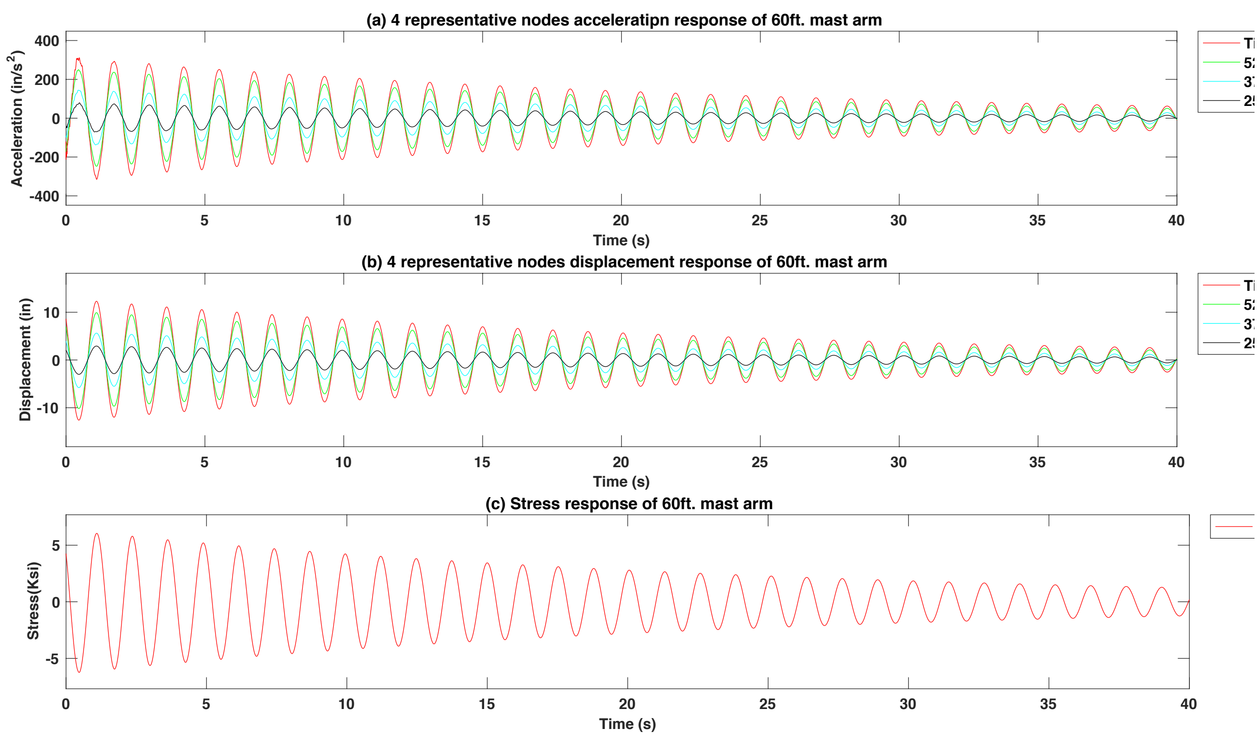

Figure 4-76 Free vibration response of excitation force at tip of the 60 ft. mast arm signal pole structure model with 15 lb. mass TMD using the $f_d = 1.25 f_n$

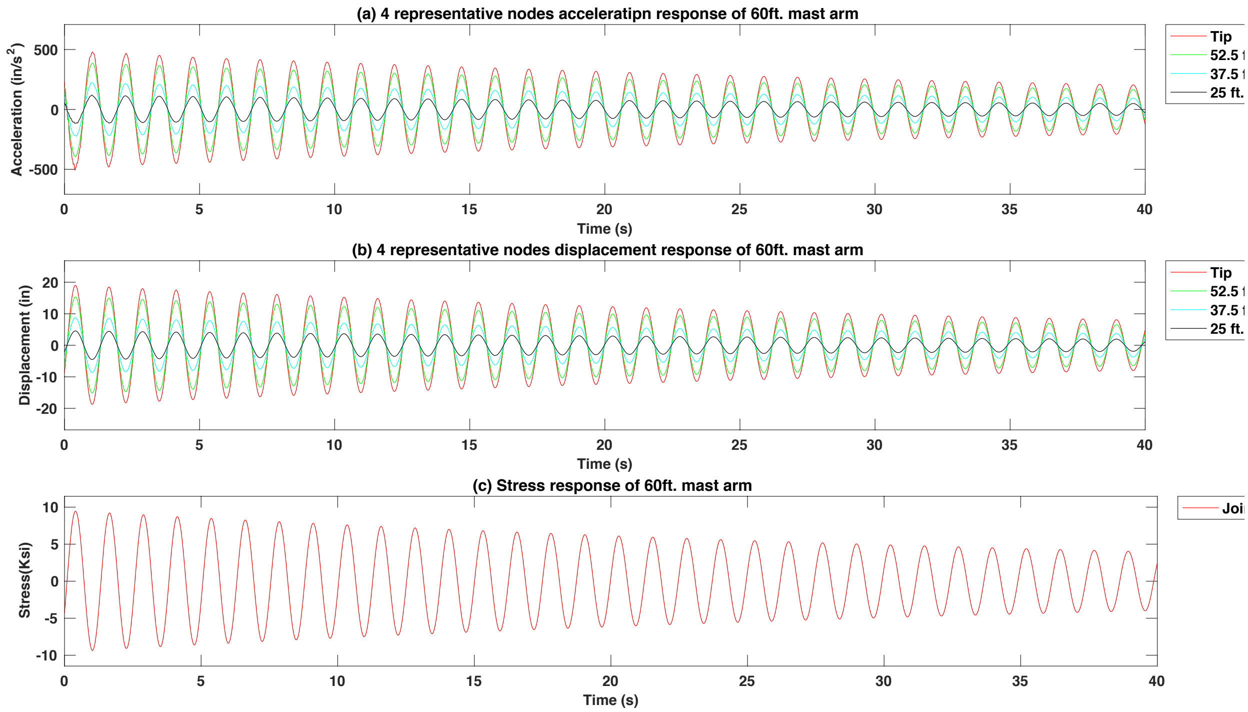

Figure 4-77 Free vibration response of excitation force at tip of the 60 ft. mast arm signal pole structure model with 15 lb. mass TMD using the $f_d = 1.5 f_n$

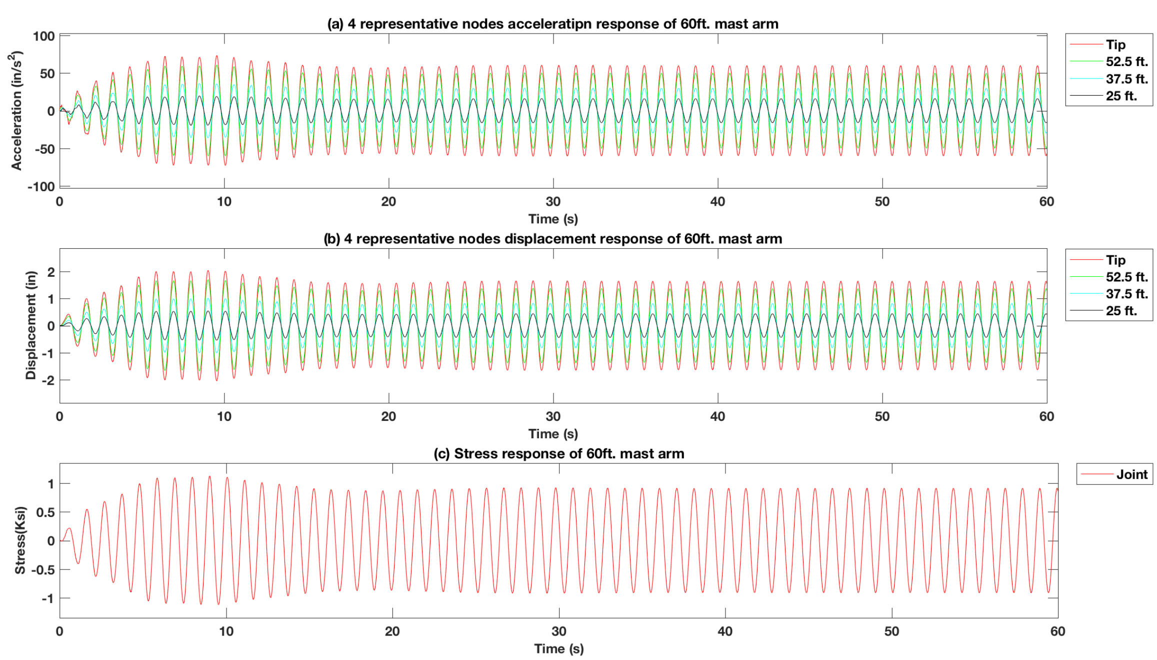

Figure 4-78 Force vibration response of excitation force at tip of the 60 ft. mast arm signal pole structure model with 15 lb. mass TMD using the $f_d = 0.9 f_n$, $f_s = 1.05 f_n$

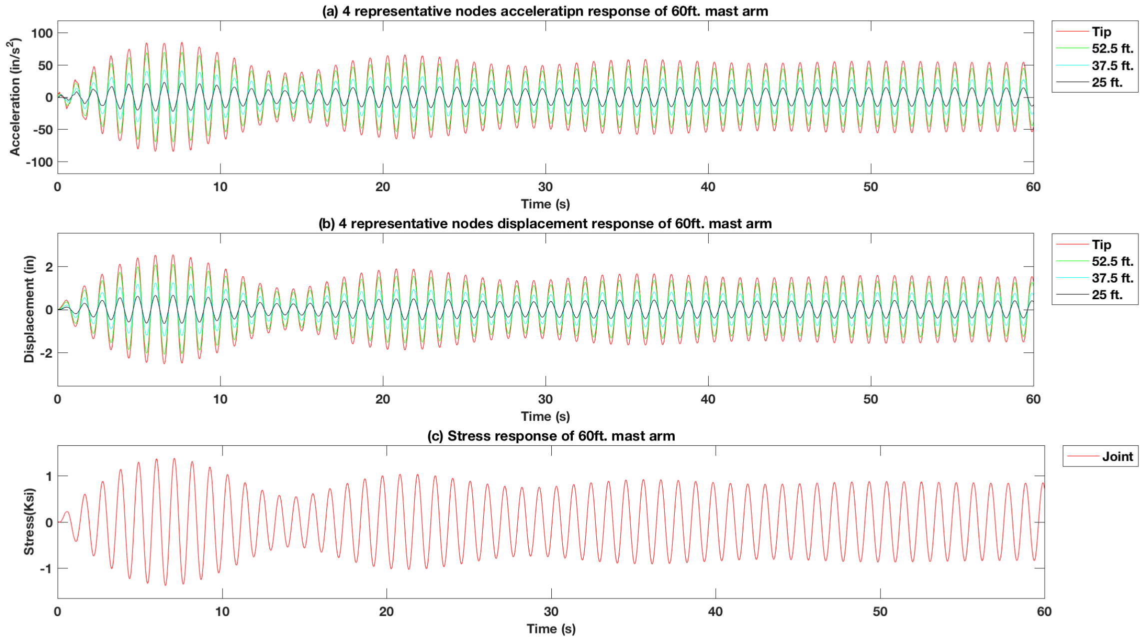

Figure 4-79 Force vibration response of excitation force at tip of the 60 ft. mast arm signal pole structure model with 15 lb. mass TMD using the $f_d = 0.75\, f_n, f_s = 1.1 f_n$

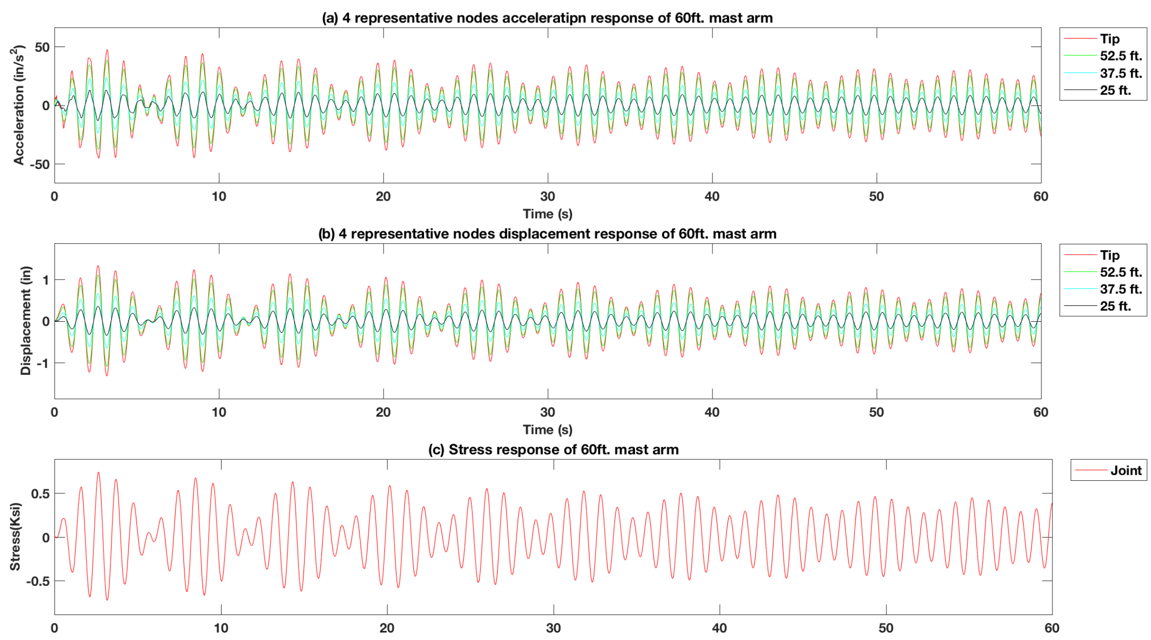

Figure 4-80 Force vibration response of excitation force at tip of the 60 ft. mast arm signal pole structure model with 15 *lb.* mass TMD using the $f_d = 0.5\, f_n, f_s = 1.2 f_n$

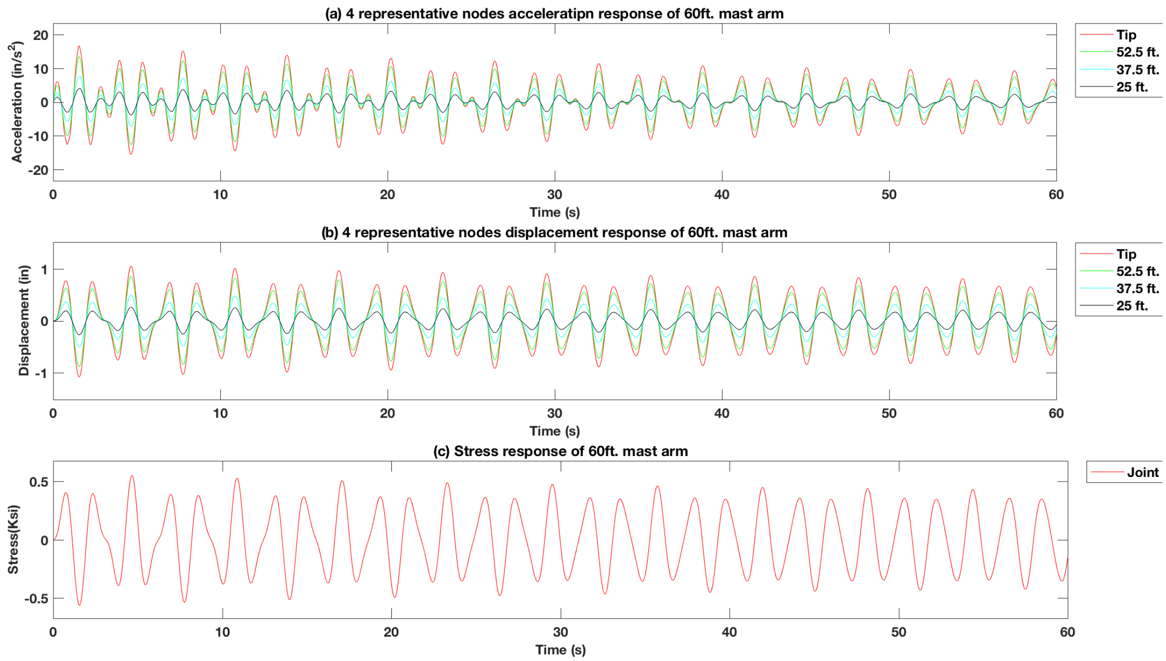

Figure 4-81 Force vibration response of excitation force at 3 signal heads location of the 60 ft. mast arm signal pole structure model with 15 lb. mass TMD using the $f_d = 1.5 f_n, f_s = 0.6 f_n$

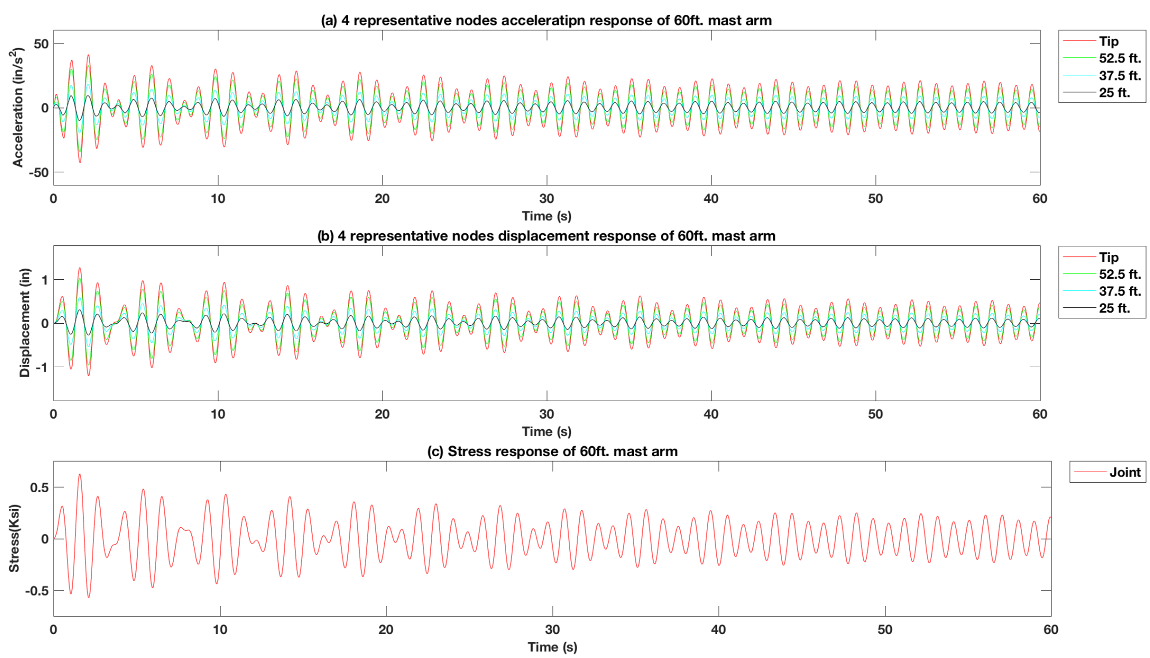

Figure 4-82 Force vibration response of excitation force at 3 signal heads location of the 60 ft. mast arm signal pole structure model with 15 lb. mass TMD using the $f_d = 1.25 f_n, f_s = 1.3 f_n$

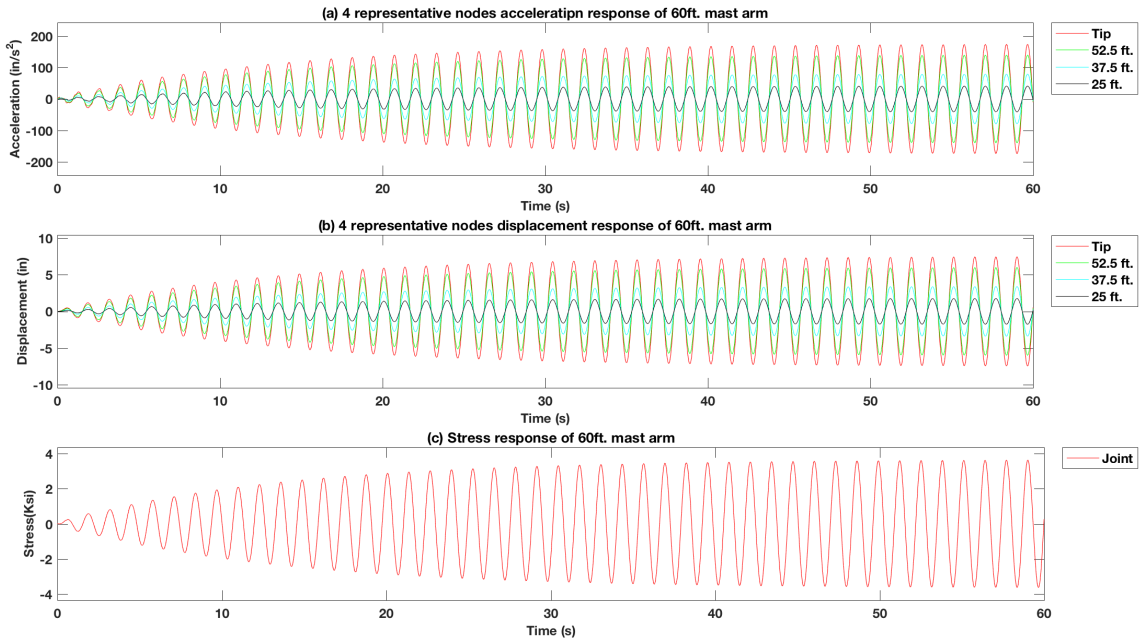

Figure 4-83 Force vibration response of excitation force at tip of the 60 ft. mast arm signal pole structure model with 15 lb. mass TMD using the $f_d = 1.1 f_n$, $f_r = 1.0 f_n$

For harmonic analysis, plot all frequency response curves:

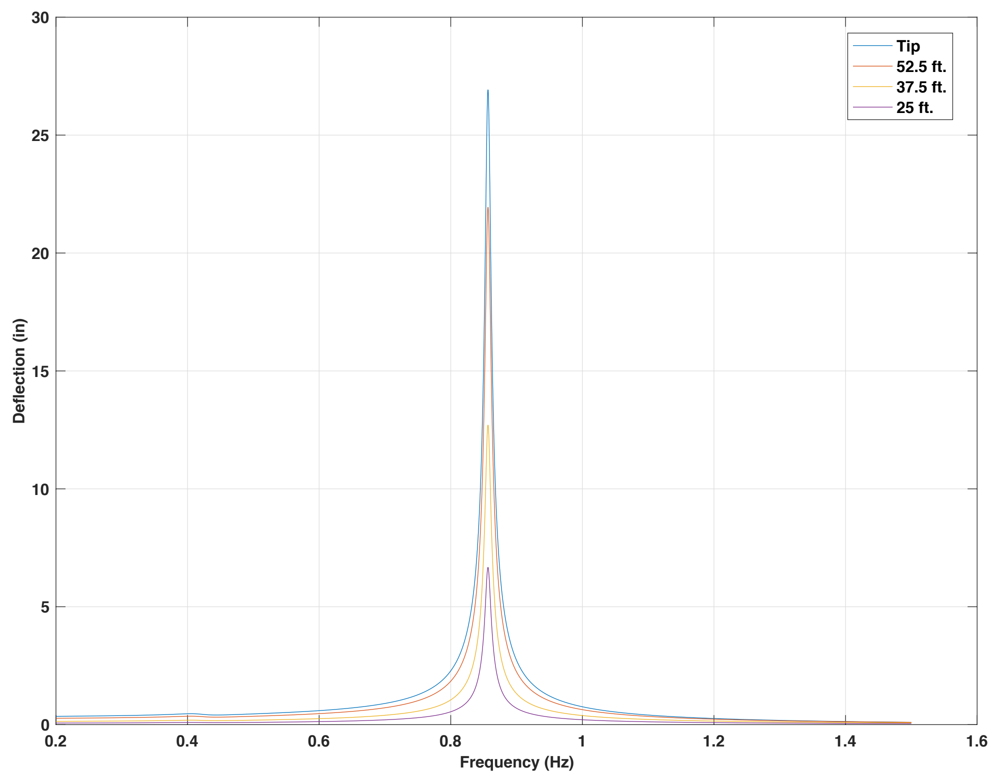

Figure 4-84 Frequency response for 60ft. mast arm with15lb mass TMD, 5 lbf force on tip, $f_d = 0.5 f_n$

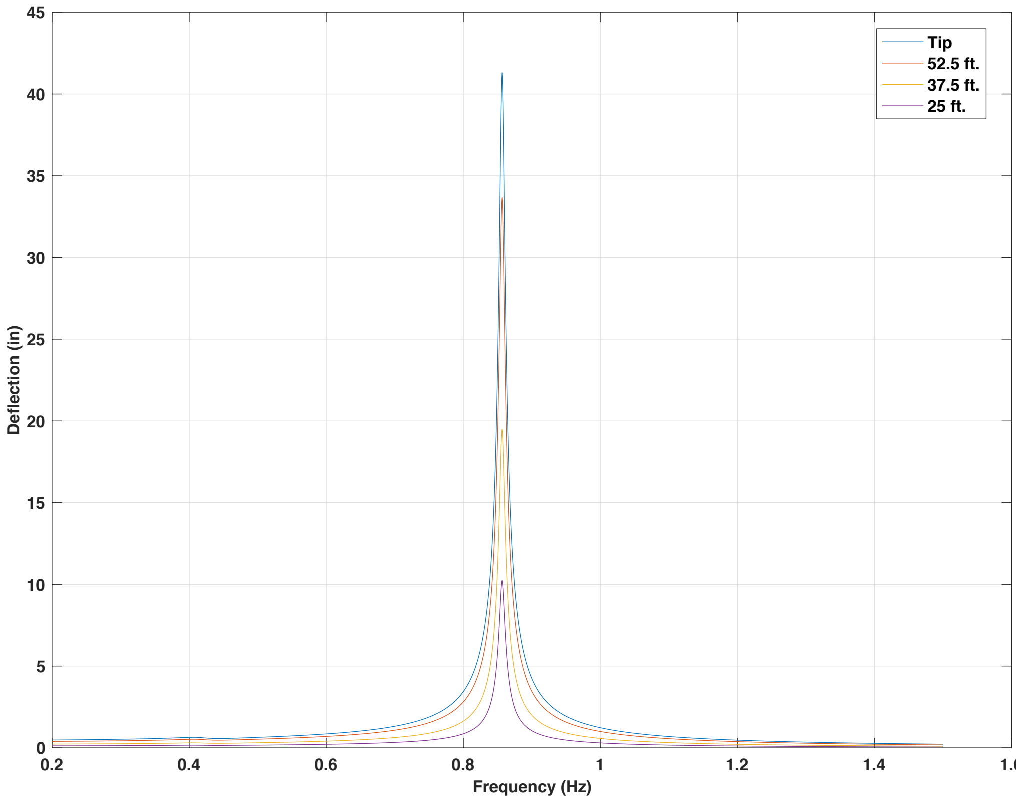

Figure 4-85 Frequency response for 60ft. mast arm with 15lb mass TMD, 5 lbf force on 3 signal heads location, $f_d = 0.5\, f_n$

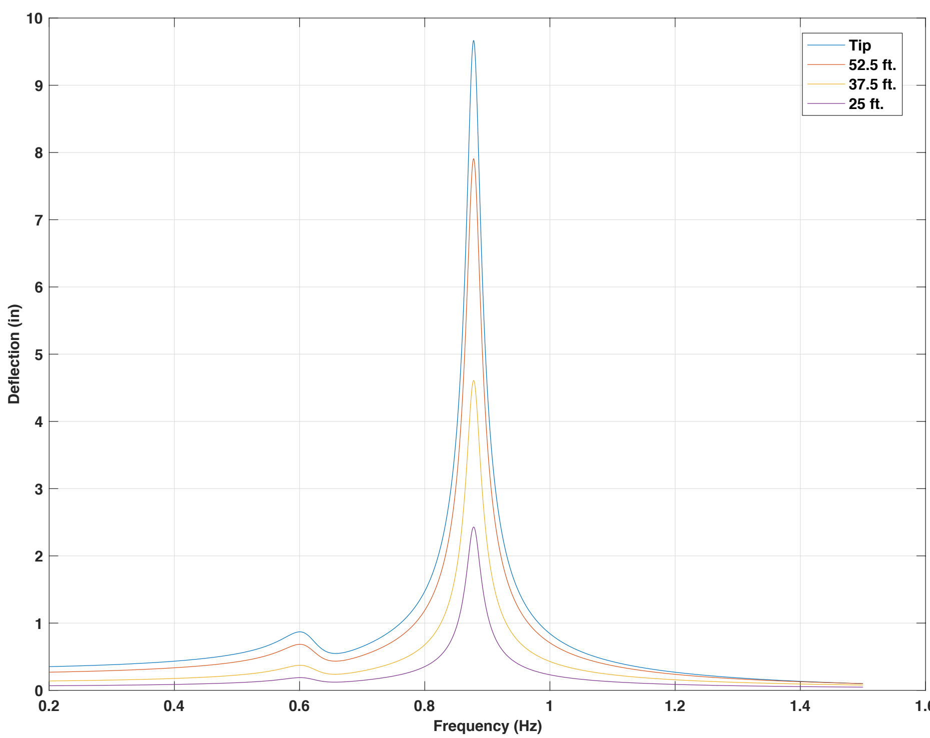

Figure 4-86 Frequency response for 60ft. mast arm with 15lb mass TMD, 5 lbf force on tip, $f_d = 0.75\, f_n$

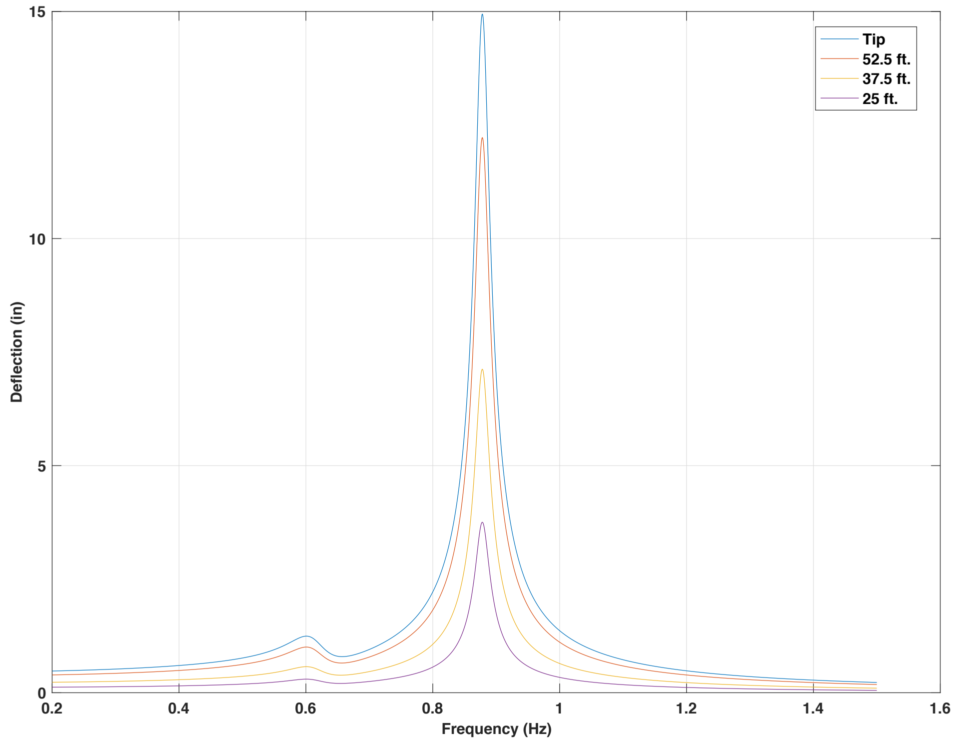

Figure 4-87 Frequency response for 60ft. mast arm with 15lb mass TMD, 5 lbf force on 3 signal heads location, $f_d = 0.75\ f_n$

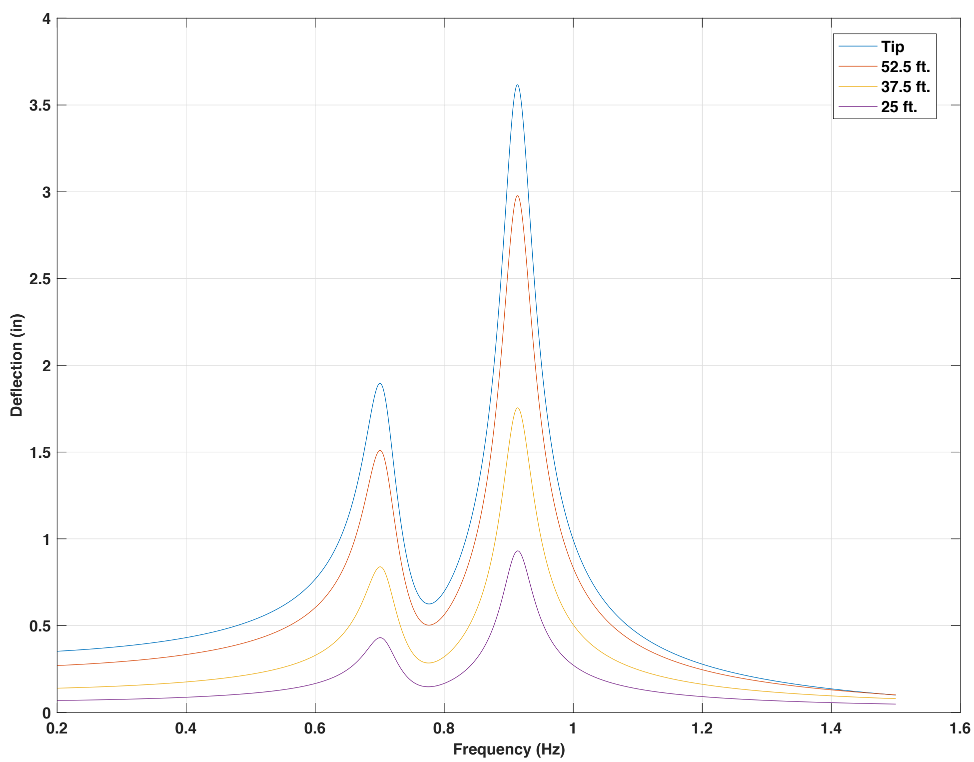

Figure 4-88 Frequency response for 60ft. mast arm with 15lb mass TMD, 5 lbf force on tip, $f_d = 0.9 f_n$

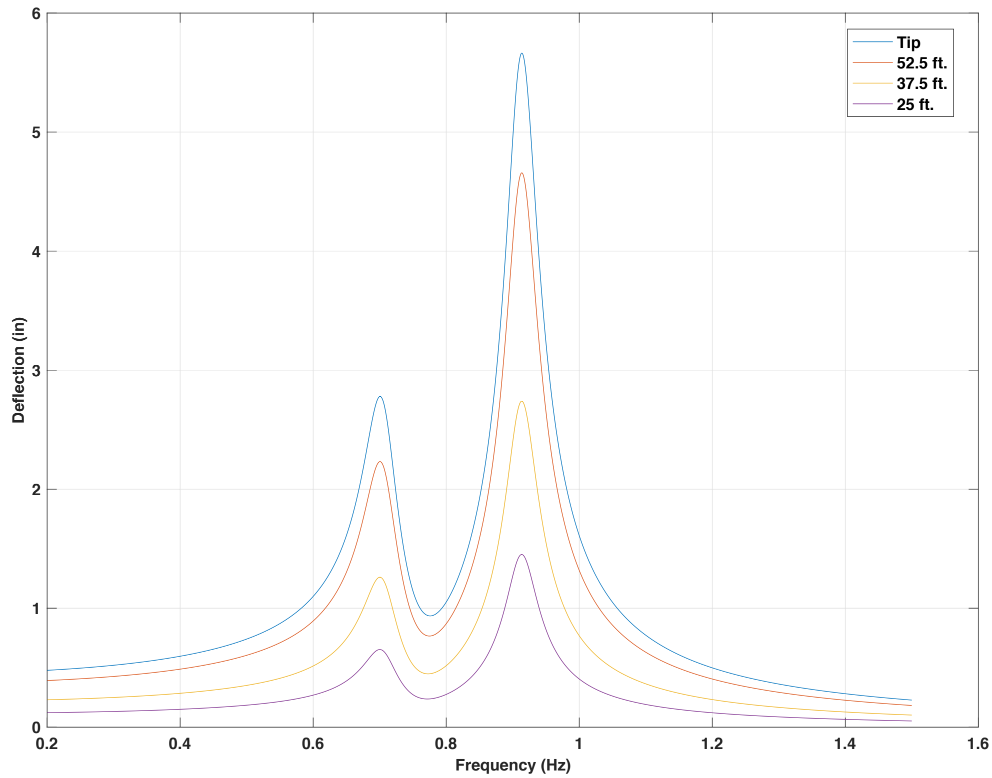

Figure 4-89 Frequency response for 60ft. mast arm with 15lb mass TMD, 5 lbf force on 3 signal heads location, $f_d = 0.9 f_n$

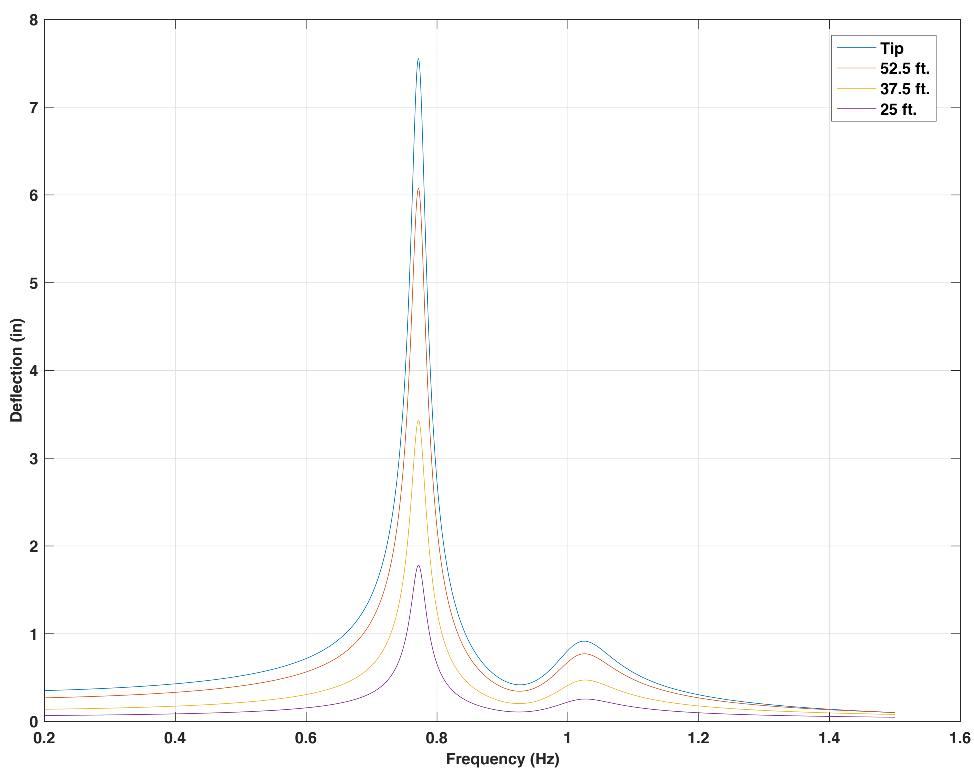

Figure 4-90 Frequency response for 60ft. mast arm with 15lb mass TMD, 5 lbf force on tip, $f_d = 1.1 f_n$

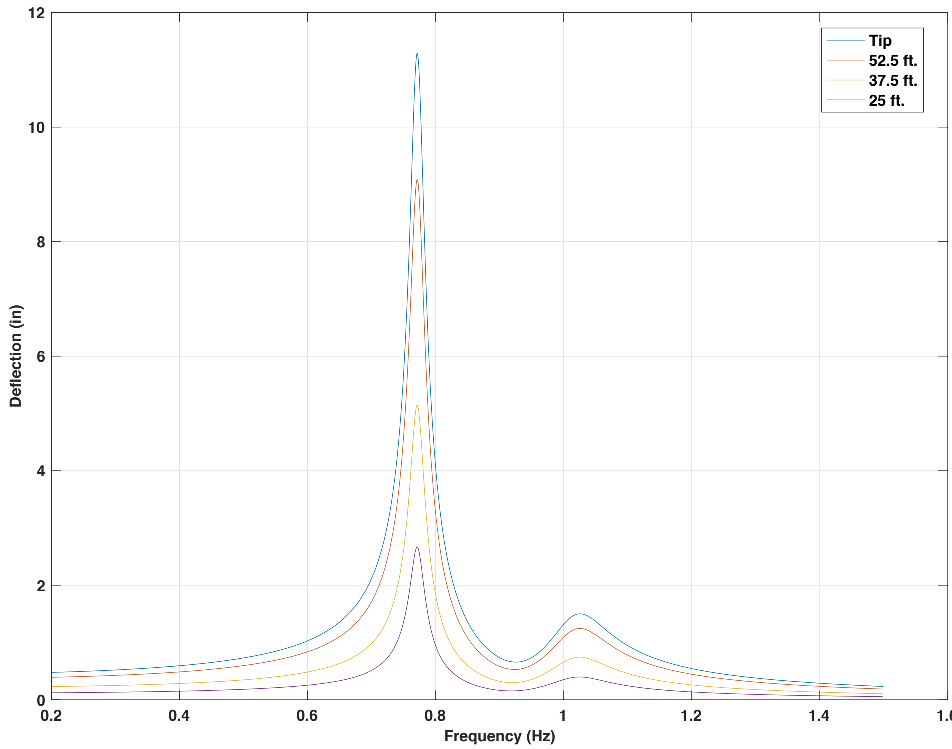

Figure 4-91 Frequency response for 60ft. mast arm with 15lb mass TMD, 5 lbf force on 3 signal heads location, $f_d = 1.1 f_n$

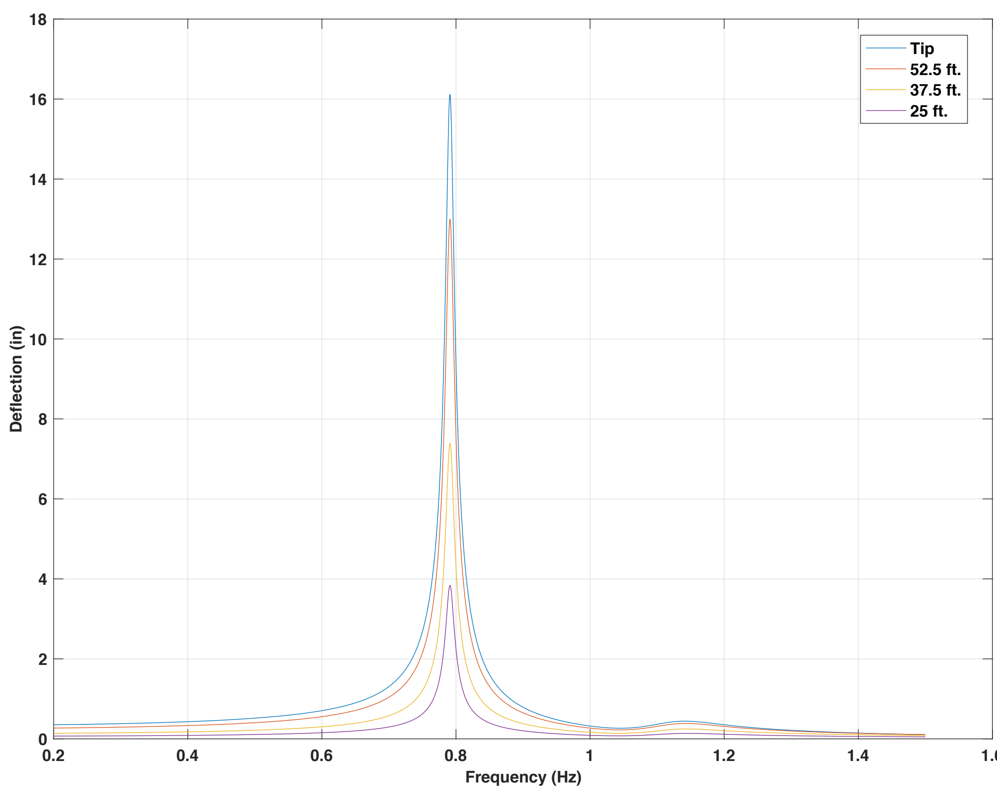

Figure 4-92 Frequency response for 60ft. mast arm with 15lb mass TMD, 5 lbf force on tip, $f_d = 1.25 f_n$

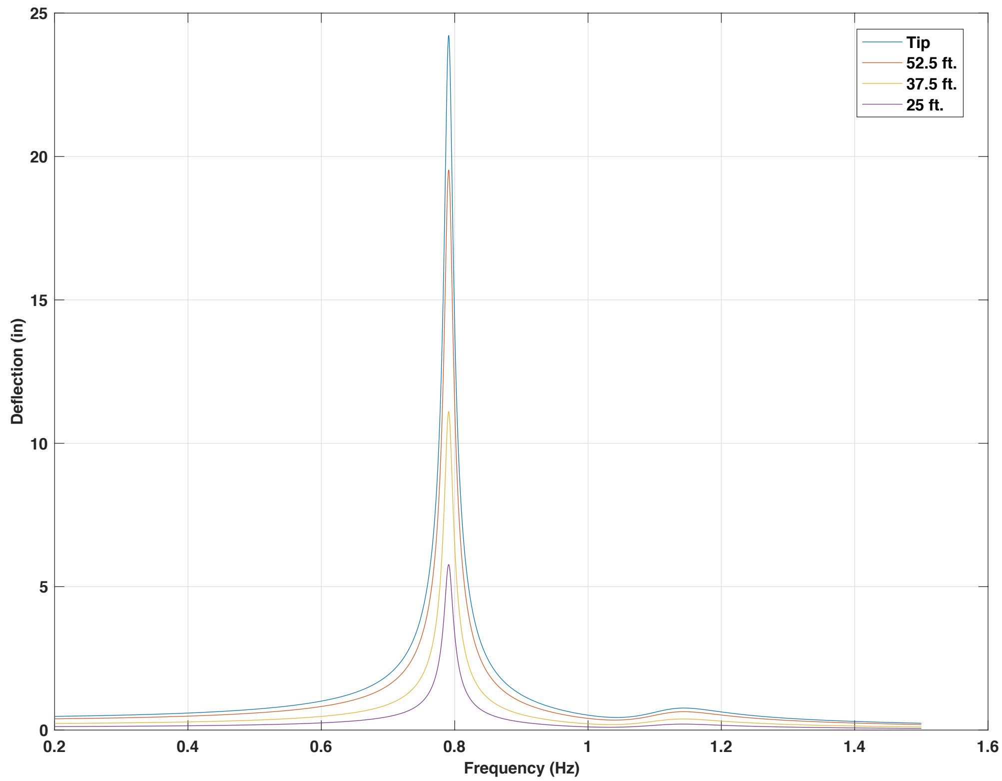

Figure 4-93 Frequency response for 60ft. mast arm with 15lb mass TMD, 5 lbf force on 3 signal heads location, $f_d = 1.25\,f_n$

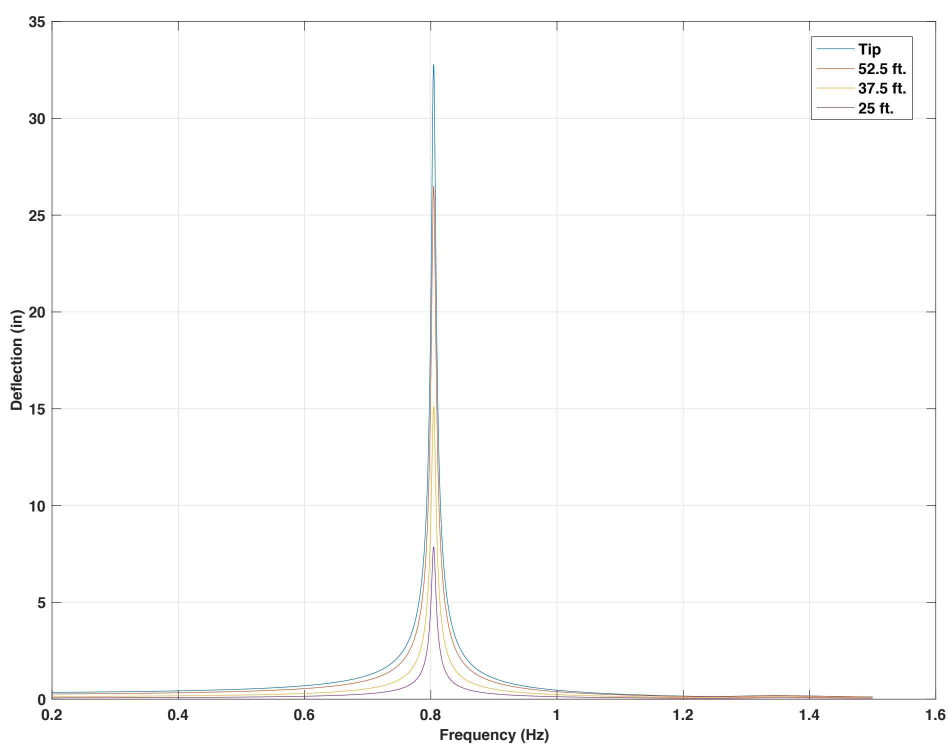

Figure 4-94 Frequency response for 60ft. mast arm with 15lb mass TMD, 5 lbf force on tip, $f_d = 1.5\,f_n$

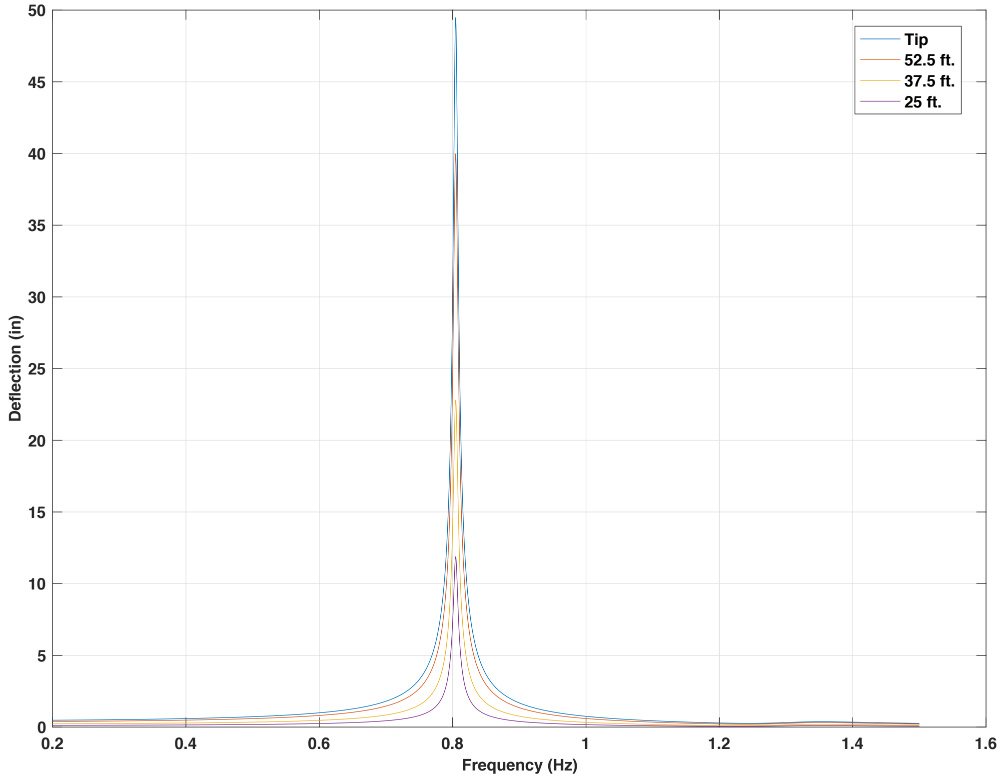

Figure 4-95 Frequency response for 60ft. mast arm with 15lb mass TMD, 5 lbf force on 3 signal heads location, $f_d = 1.5 f_n$

4.3.5 TMD Damping Ratio

As mentioned in previous section, this case will also use a TMD in 1% of damping ratio with 25 *lb*. mass to be compared with the 6% damping ratio with 25 *lb*. mass TMD, to simulate an Alcoa damper. The TMD will be at the tip of the mast arm unless specified. The pre-analysis calculation for the damper:

TMD damping ratio	f_1 (Hz)	f_2 (Hz)	f_3 (Hz)	k	c	α	β
1%	0.72	1.00	3.17	1.84	0.007	0.010	3.60E-04

Table 4-8 pre-calculation on model analysis for 60 ft. arm with TMD in 1% damping ratio

And the representative plots of all the results are:

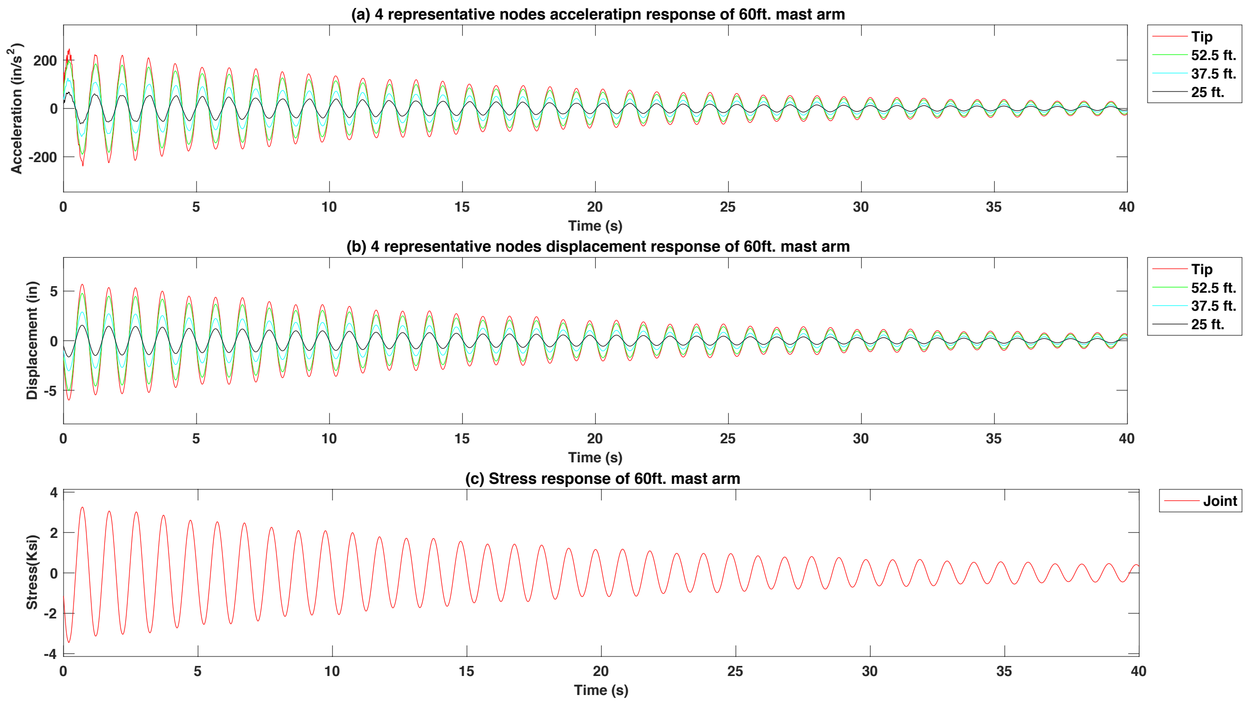

Figure 4-96 Free vibration response of excitation force at tip of the 60 ft. mast arm signal pole structure model with 25 lb. mass TMD using the $\zeta = 1\%$

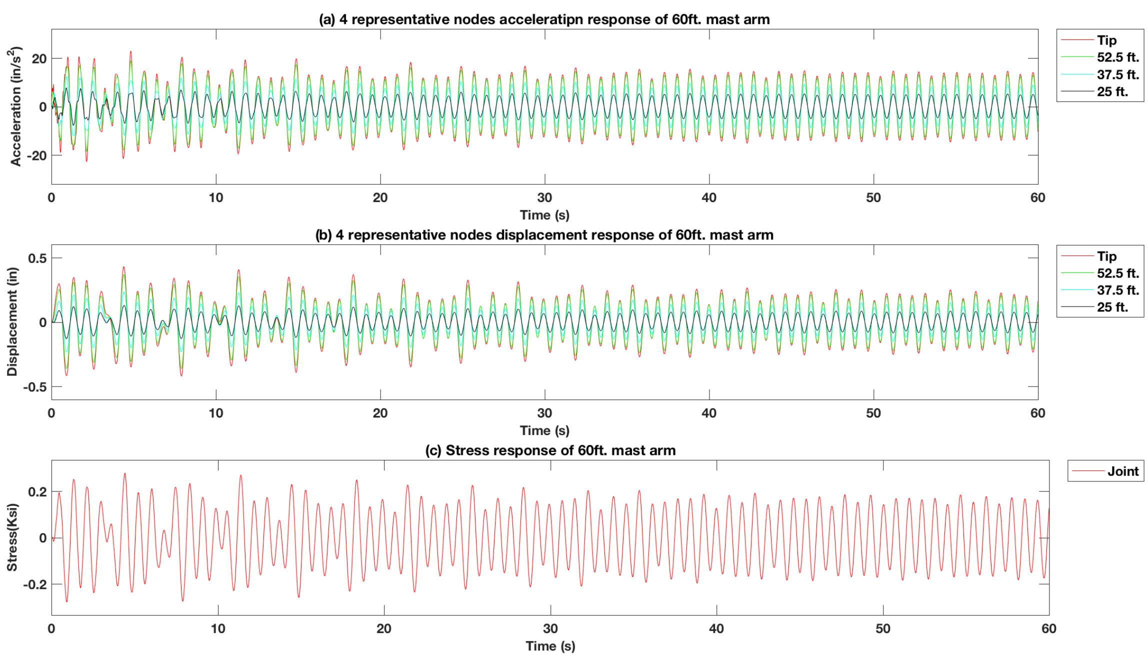

Figure 4-97 Force vibration response of excitation force at tip of the 60 ft. mast arm signal pole structure model with 25 lb. mass TMD using the $\zeta = 1\%$, $f_s = 1.3f_n$

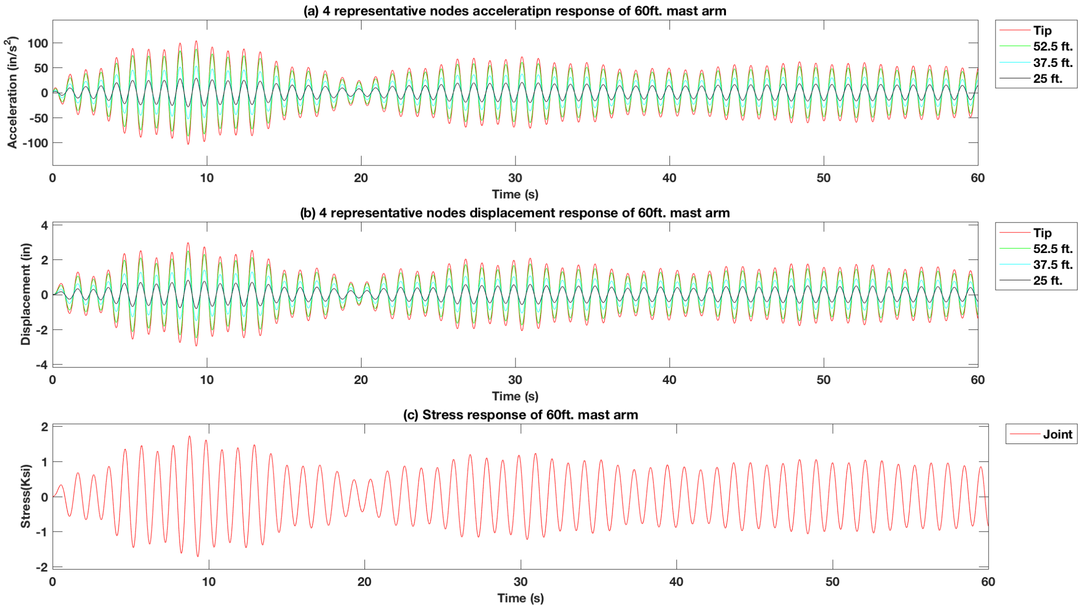

Figure 4-98 Force vibration response of excitation force at 3 signal heads position of the 60 ft. mast arm signal pole structure model with 25 lb. mass TMD using the $\zeta = 1\%$, $f_d = 0.95 f_n$

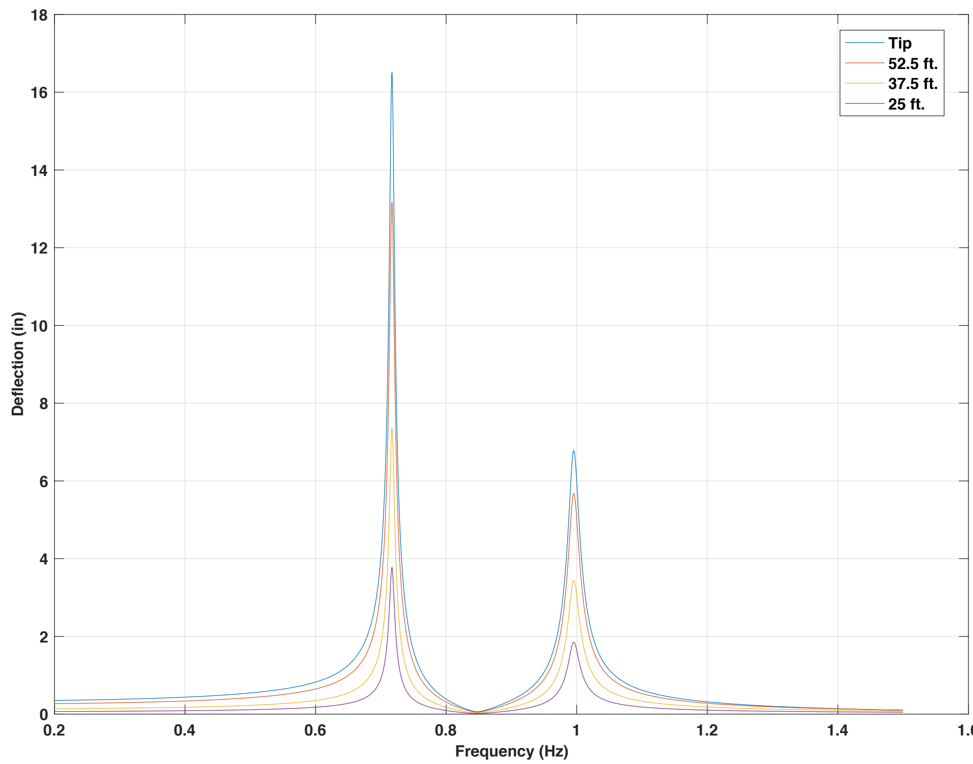

Figure 4-99 Frequency response for 60ft. mast arm with 25 lb. mass TMD using the $\zeta = 1\%$, 5 lbf force on tip of mast arm

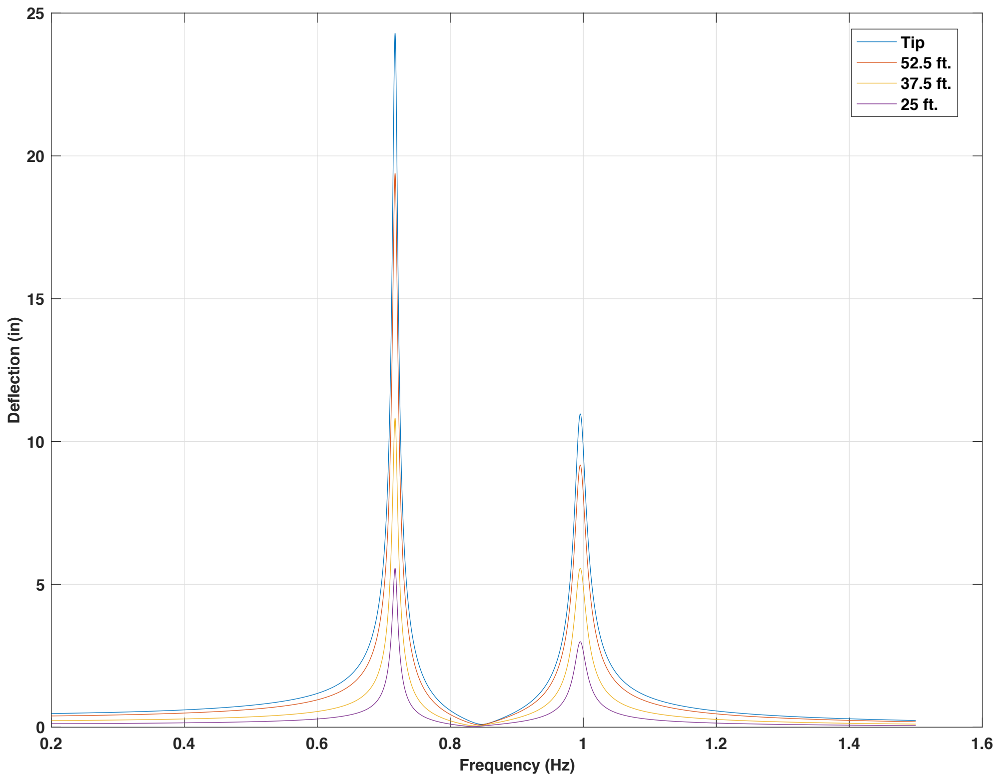

Figure 4-100 Frequency response for 60ft. mast arm with 25 lb. mass TMD using the $\xi = 1\%$, 5 lbf force on 3 signal head location

4.3.6 TMD Locations

Because the location of TMD could influence the structure's frequencies by changing the whole structure's stiffness matrix, location changes of TMD using 1.5 *ft*., 5 *ft.* and 10 *ft*. from mast arm tip with the same damper are applied in this case.

The pre-analysis calculation is:

Table 4-9 Preliminary model analysis for 60 ft. arm with TMD in different location

TMD Location (*ft*.)	f_1 (Hz)	f_2 (Hz)	f_3 (Hz)	k	c	α	β
1.5	0.75	0.96	3.16	1.10	0.025	0.010	3.765E-4
5	0.76	0.95	3.16	1.10	0.025	0.010	3.768E-4
10	0.77	0.93	3.15	1.10	0.025	0.010	3.77E-4

And the representative plots of the results are:

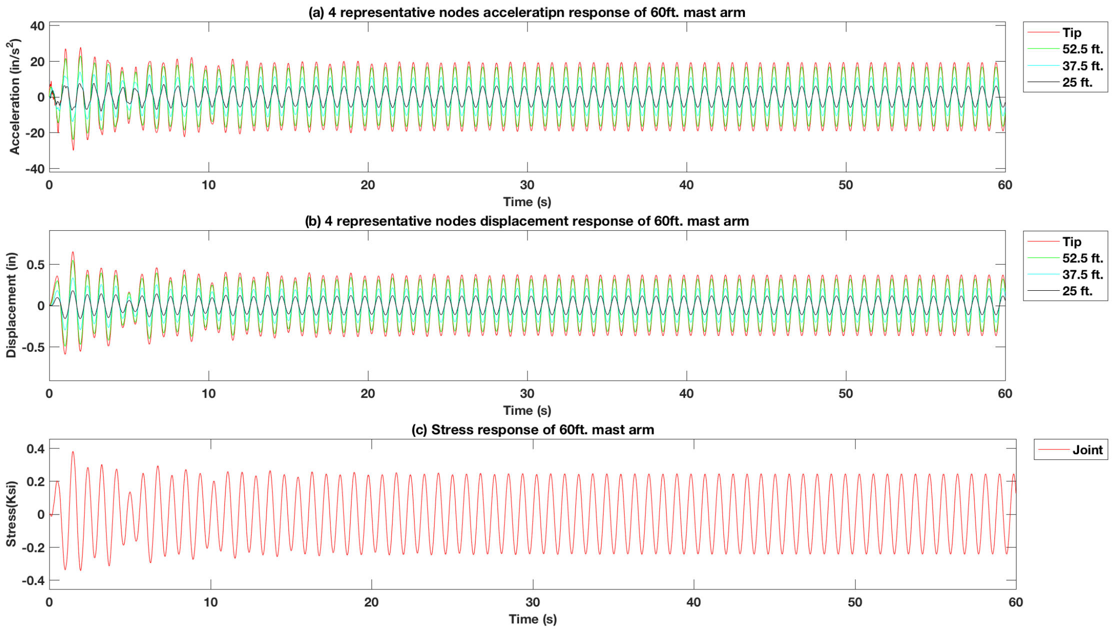

Figure 4-101 Force vibration response of excitation force at tip in the second mode frequency of the 60 ft. mast arm signal pole structure model TMD at 1.5 ft from the tip $f_r = 1.2 f_n$

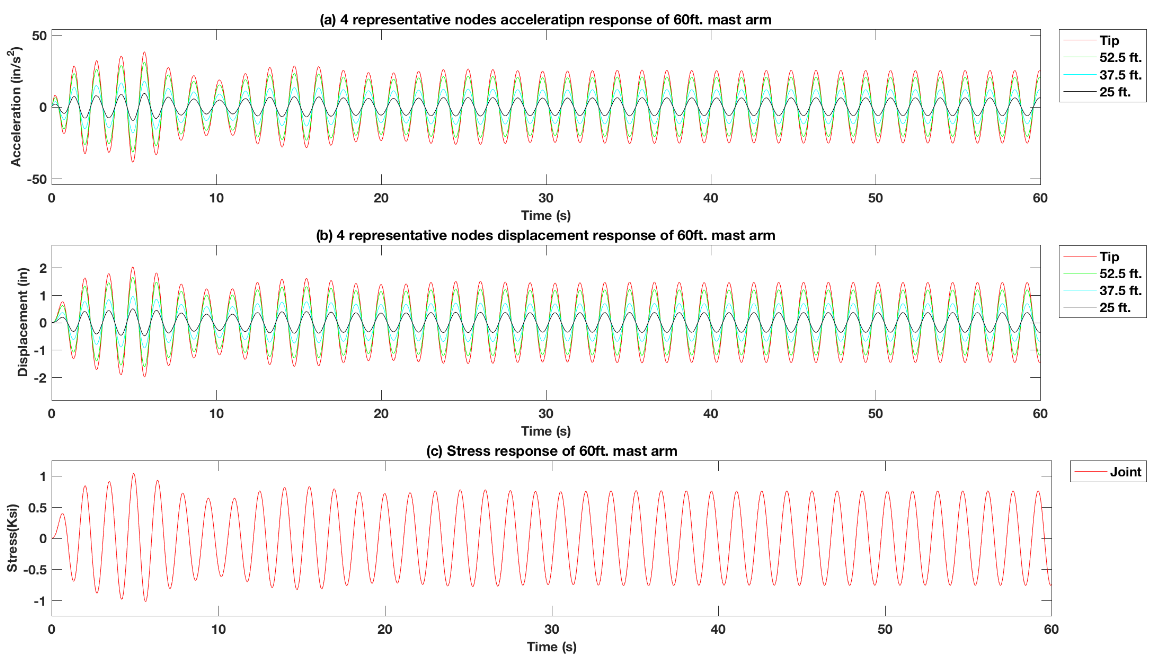

Figure 4-102 Force vibration response of excitation force at 3 signal heads position of the 60 ft. mast arm signal pole structure model TMD at 5 ft from the tip $f_r = 0.7 f_n$

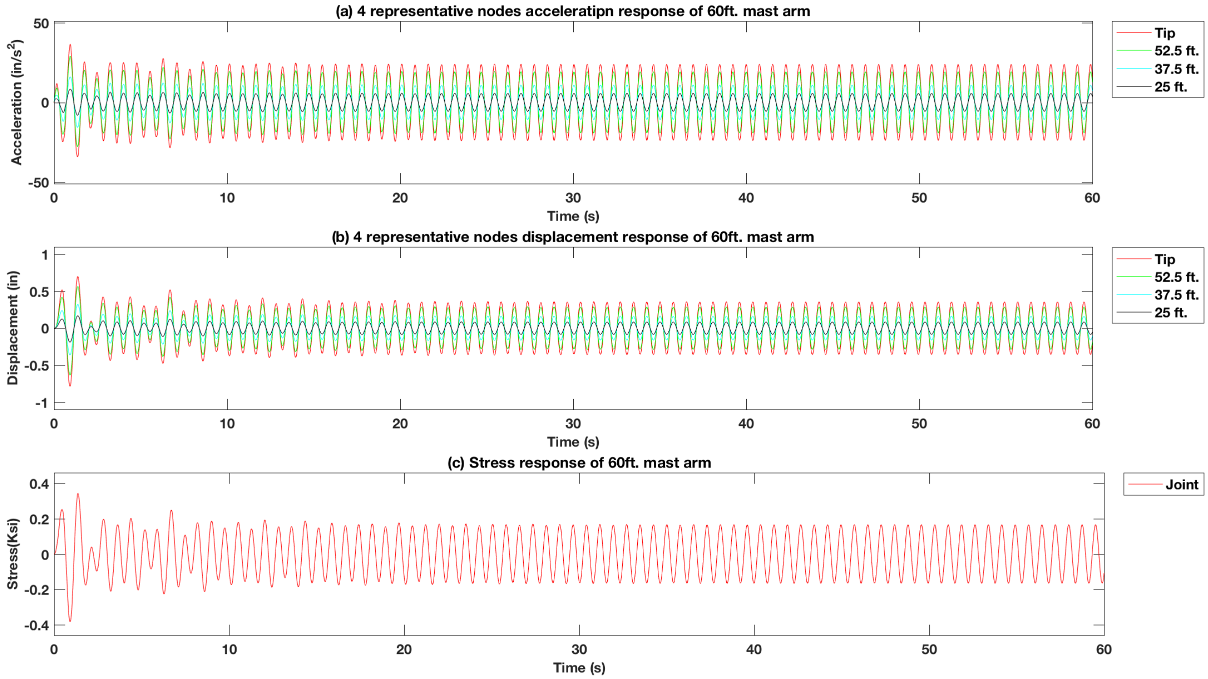

Figure 4-103 Force vibration response of excitation force at 3 signal heads position of the 60 ft. mast arm signal pole structure model TMD at 10 ft from the tip $f_r = 1.4f_n$

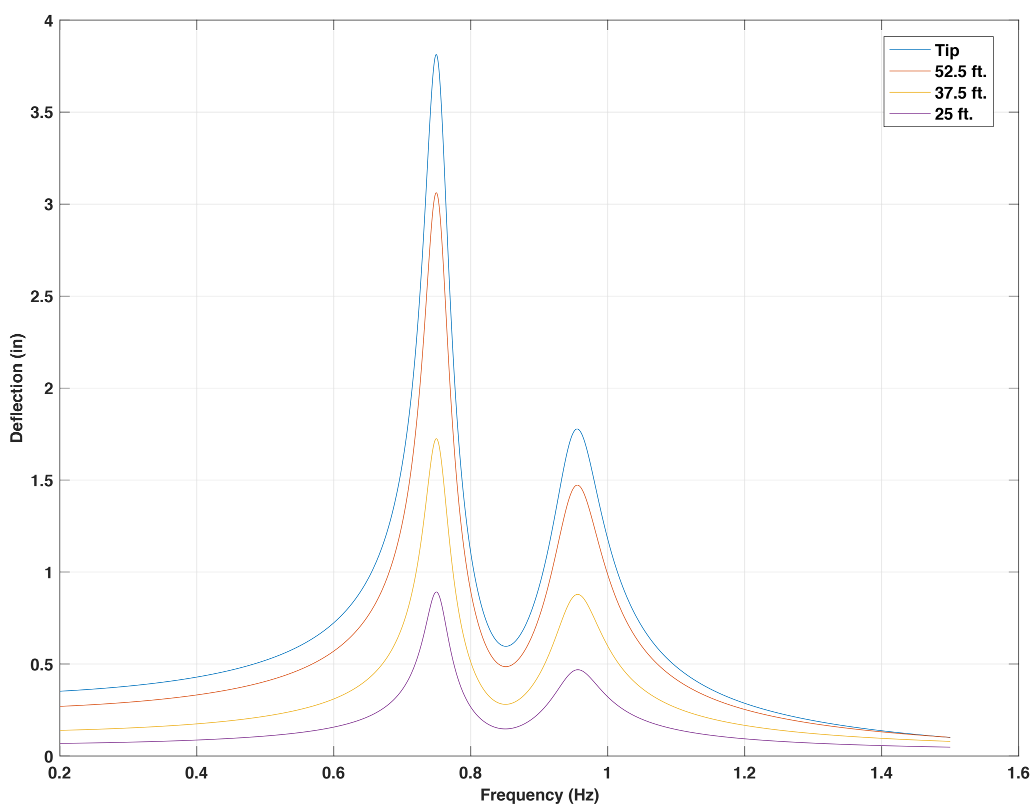

Figure 4-104 Frequency response for 60ft. mast arm with 15 lb. mass TMD at 1.5 ft from the tip, 5 lbf force on tip of mast arm, $f_d = 1.0 f_n$

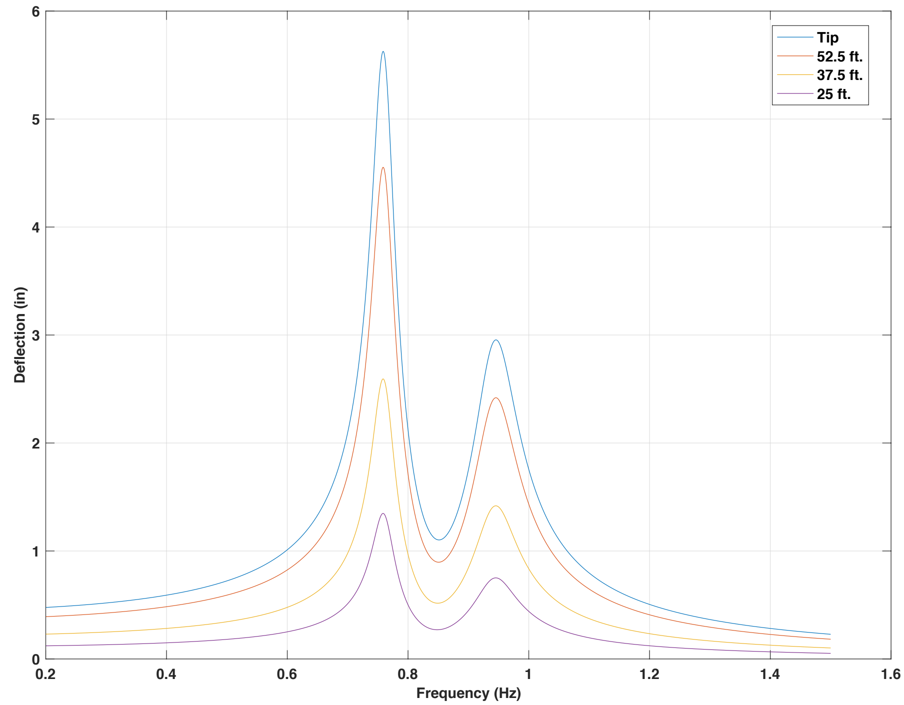

Figure 4-105 Frequency response for 60ft. mast arm with 15 lb. mass TMD at 2.5 ft from the tip, 5 lbf force on 3 signal head location, $f_d = 1.0 f_n$

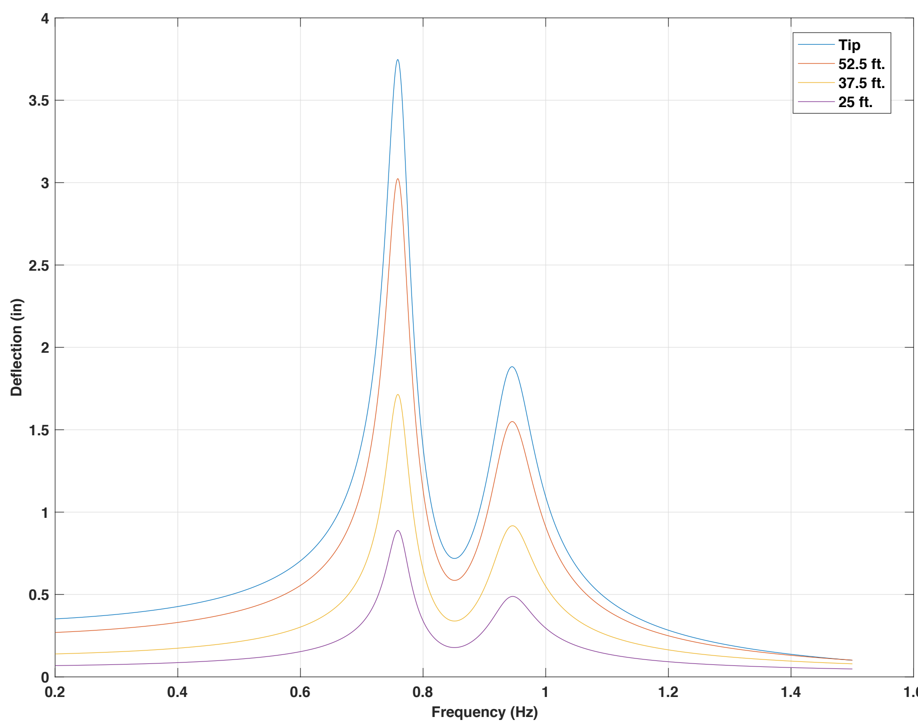

Figure 4-106 Frequency response for 60ft. mast arm with 15 lb. mass TMD at 5 ft from the tip $f_d = 1.0 f_n$, 5 lbf force on tip of mast arm

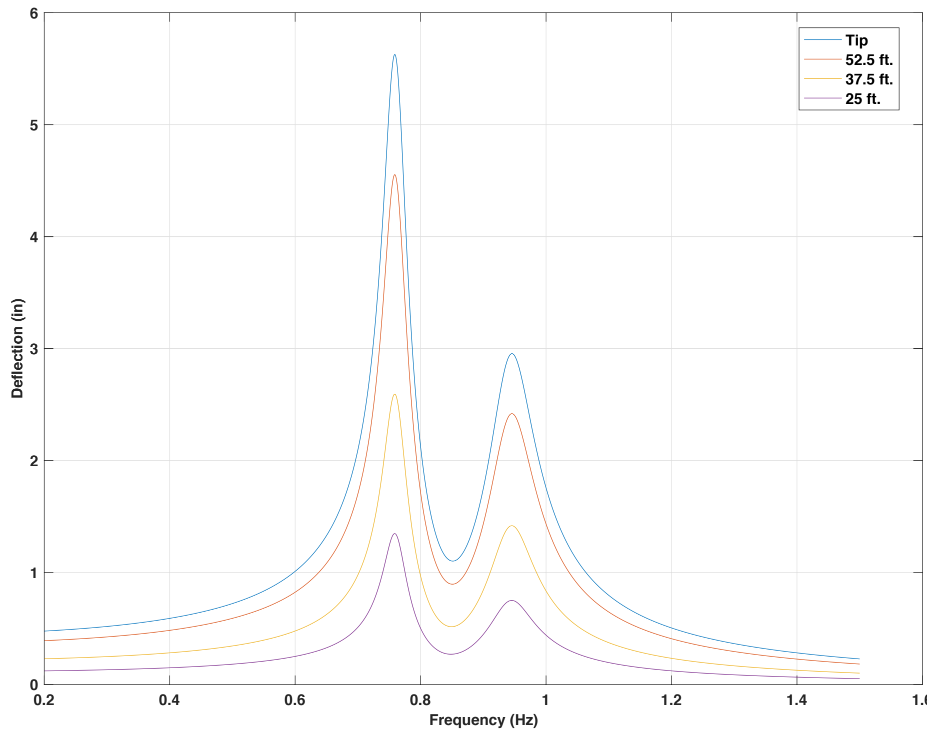

Figure 4-107 Frequency response for 60ft. mast arm with 15 lb. mass TMD at 5 ft from the tip, $f_d = 1.0 f_n$, 5 lbf force on 3 signal head location

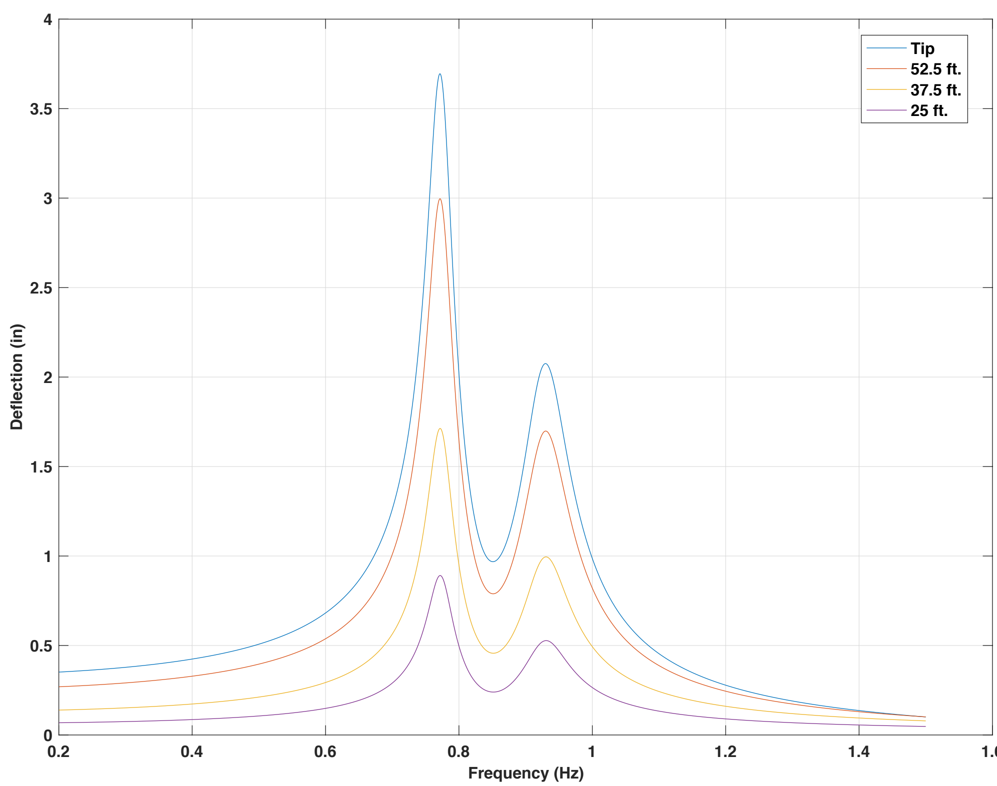

Figure 4-108 Frequency response for 60ft. mast arm with 15 lb. mass TMD at 2.5 ft from the tip $f_d = 1.0 f_n$, 5 lbf force on tip of mast arm

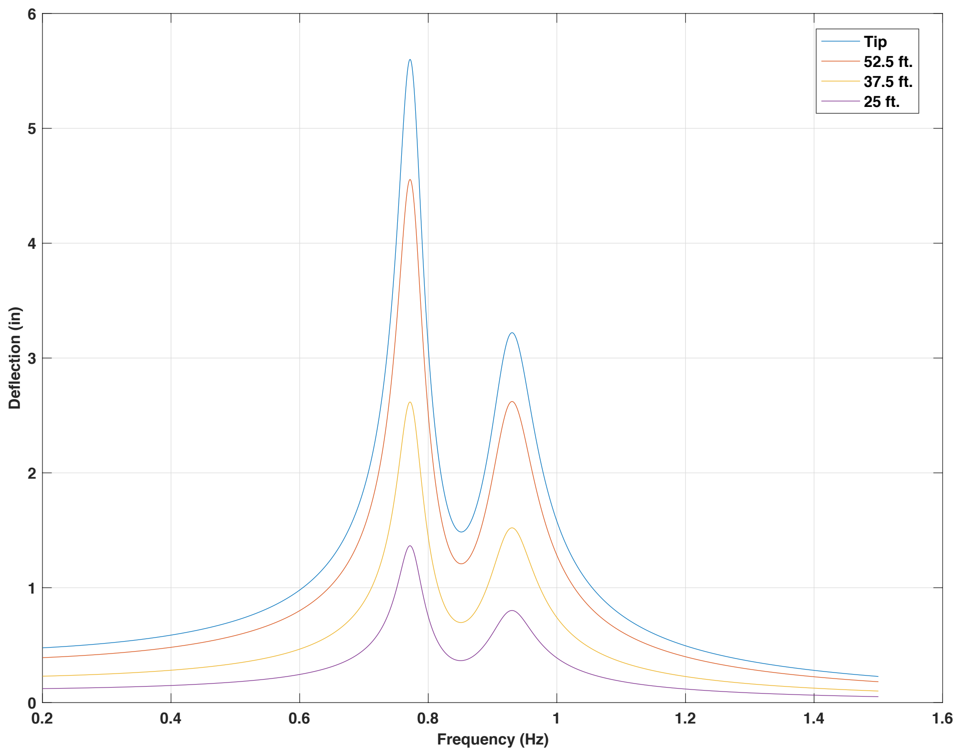

Figure 4-109 Frequency response for 60ft. mast arm with 15 lb. mass TMD at 2.5 ft from the tip, $f_d = 1.0f_n$, 5 lbf force on 3 signal head location

4.4 Signal Support Structure with 50 ft. Arm Length

4.4.1 Finite Element Model description

For the 50 ft. arm length structure, beam188 element was selected to build the main structure. Mass21 element was used as the traffic signal and mass of the TMD. And combin14 element is used for simulates the TMD's spring stiffness and damping ratio. The locations of signals could vary. In this model, use three signals at 17.5-*ft*. 30.125-*ft*. and 42.5-*ft.* from the arm-pole joint. For the arm-pole joint and base, simply regard it as a fixed condition. The gravitation is ignored in the dynamic analysis. Input real constant of mass21 and combin14: use 50 *lb*. per signal head to be conservative for traffic signal and 15 *lb*. or 25 *lb*. mass of the TMD; ignore the initial deflection of the structure due to self-weight and probable raise angle of the mast arm and assumed the TMD is rigidly connected to the mast arm. The mesh size is using

1.5 ft./segment for signal pole and 2.5 ft./ segment for mast arm primary part and 0.375 ft./ segment for the connection of base arm and the extension and the first and second extension connection.

The dimensions of the pole and mast arm are shown in Table 3-1 and Table 3-2.

4.4.2 Mast arm signal support structure model without TMD and its outputs

After plotting each mode of frequencies, choose the first mode frequency in Y direction and the second mode frequency in Y direction, in this case 0.9225Hz and 3.2286 Hz, to calculate the alpha and beta values in Rayleigh damping matrix. Choose 0.2% in the first mode and 0.4% for the second mode, and the value would be:

$$\begin{pmatrix} a_0 \\ a_1 \end{pmatrix} = \begin{pmatrix} \alpha \\ \beta \end{pmatrix} = \begin{pmatrix} 0.01082 \\ 0.000368 \end{pmatrix}$$

Put these values back in Rayleigh damping matrix for Newmark beta method and do the dynamic analysis for free vibration and force vibration using the same methods as previous analyses. Some of the representative results are plotted:

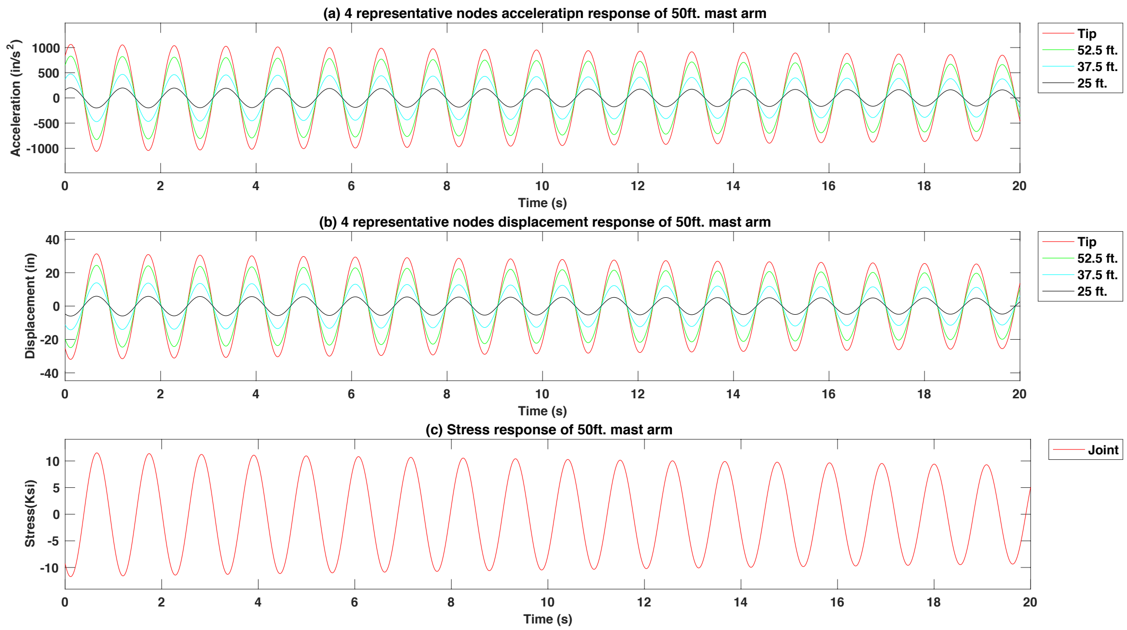

Figure 4-110 Free vibration response of the 50 ft. arm signal support structure model without TMD

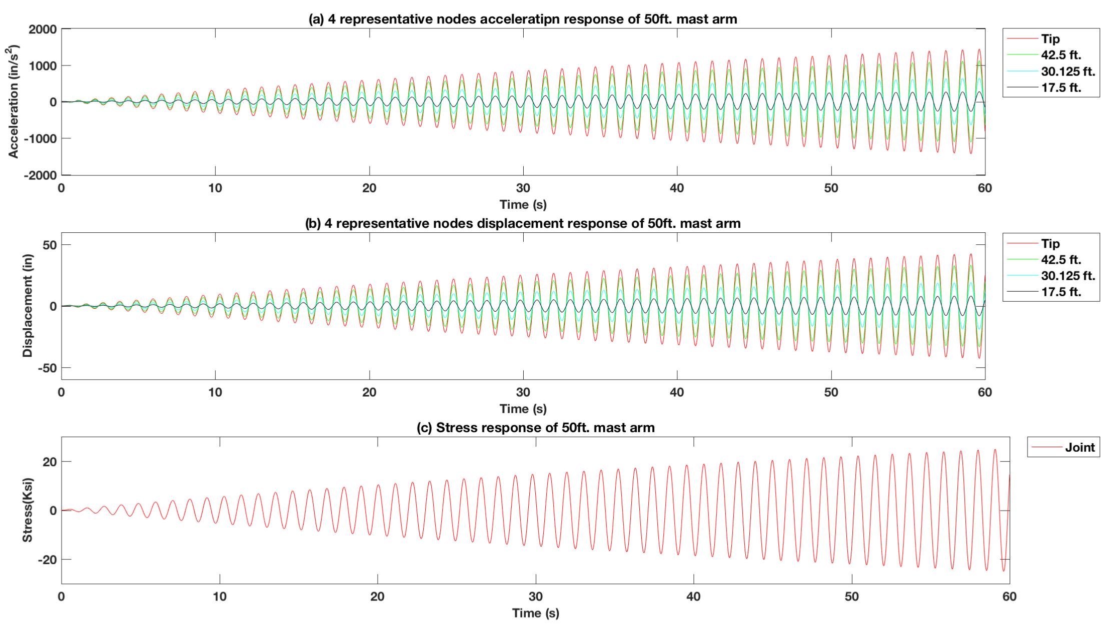

Figure 4-111 Force vibration response of excitation force at tip in $f_r = 1.0f_n$ of the 50 ft. mast arm signal pole structure model without TMD

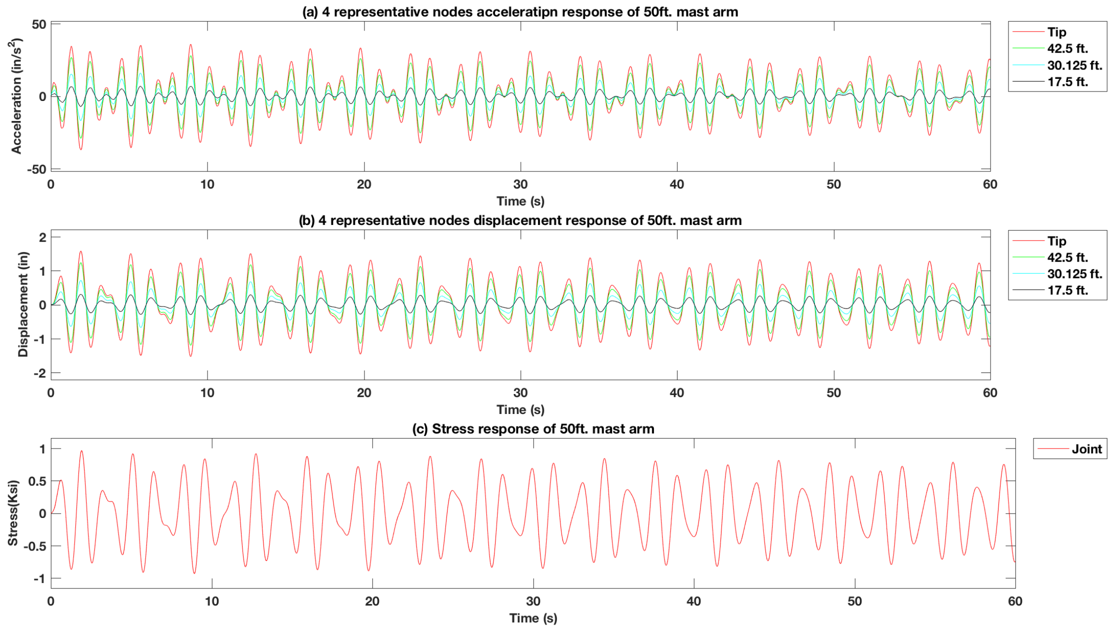

Figure 4-112 Force vibration response of excitation force at 3 signal head locations in $f_e = 0.7f_n$ of the 50 ft. arm signal support structure model without TMD

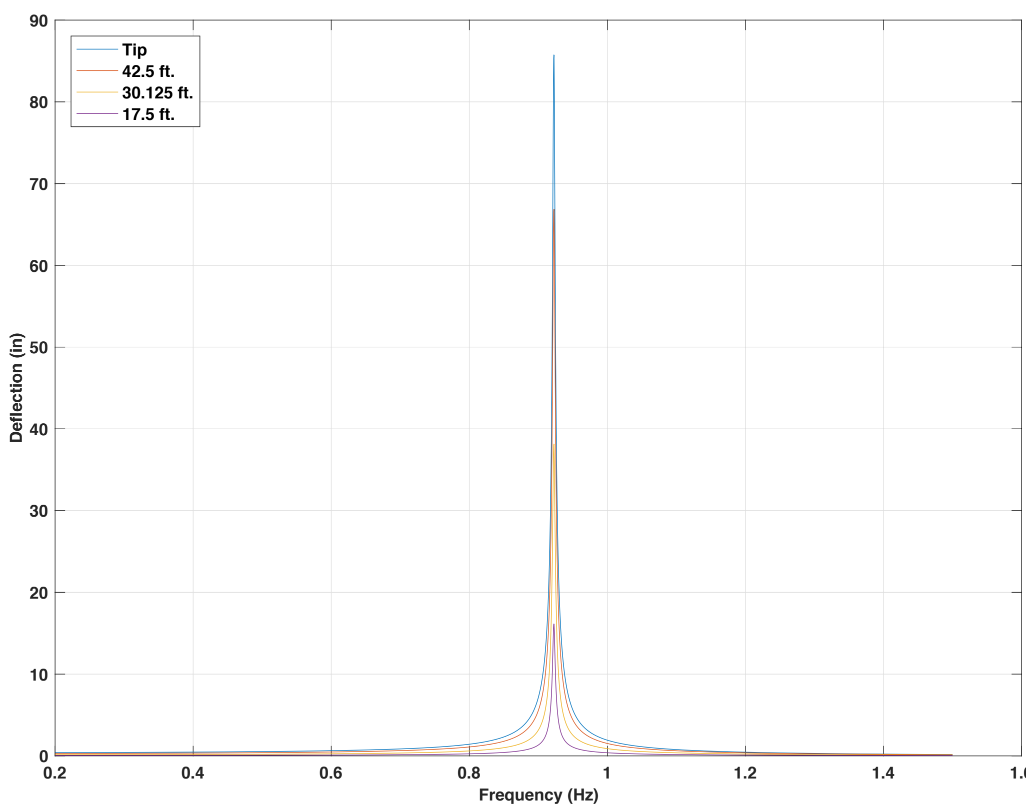

Figure 4-113 Harmonic response for excitation force on the mast arm tip of the 50 ft. arm signal support structure model without TMD

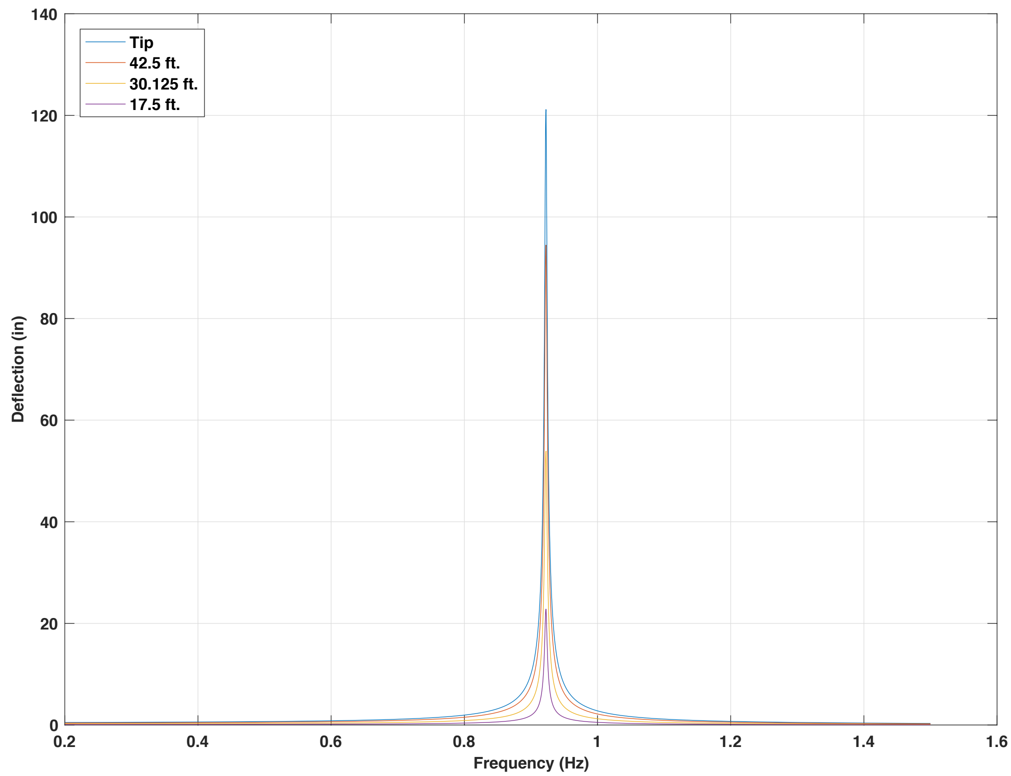

Figure 4-114 Harmonic response for excitation force on the mast arm signal heads locations of the 50 ft. arm signal support structure model without TMD

4.4.3 TMD Mass

In this comparison, also choose TMD masses of 15 lb. and 25 lb. Based on the initial model, calculate parameters for analyses:

Table 4-10 Preliminary model analysis for 50 ft. arm with 15lb. and 25lb. TMD

TMD mass	f_1 (Hz)	f_2 (Hz)	f_3 (Hz)	k	c	α	β
15 lb.	0.79	1.07	3.24	1.30	0.027	0.010	3.68E-4
25 lb.	0.76	1.11	3.24	2.17	0.045	0.010	3.68E-4

Although both the first and second mode shapes are shown as the first mode shape (ignore the position of TMD) for the signal support structures, and the contribution in deflection cannot determine the structure's peak value in harmonic analysis or force excitation, the frequency could be chosen between the first and second mode frequencies. In this study choose the second mode frequency as the free vibration excitation force frequency and initial frequency for force vibration excitation force.

Some of the representative results are shows below:

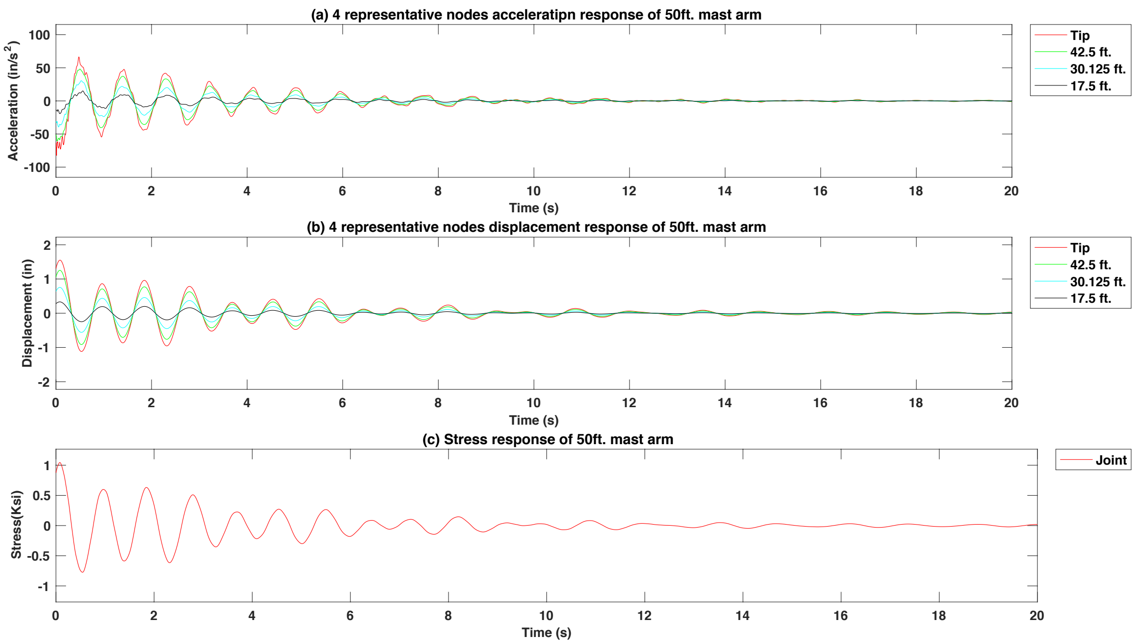

Figure 4-115 Free vibration response of the 50 ft. arm signal support structure model with 25lb. TMD in the same frequency of the structure

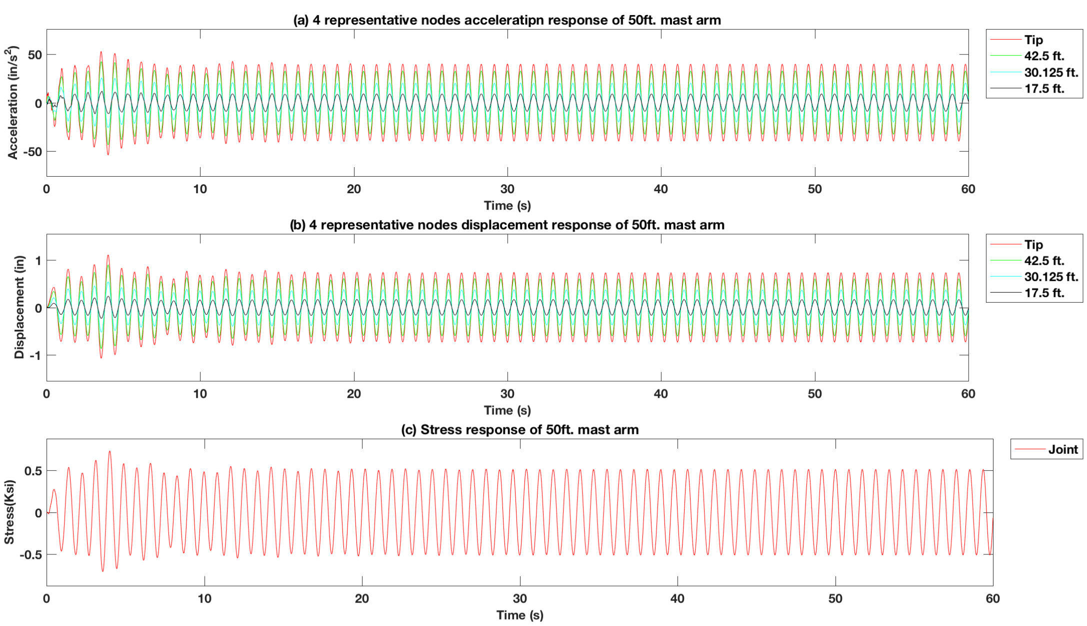

Figure 4-116 Force vibration response of excitation force at tip of the 50 ft. mast arm signal pole structure model with 15 lb. mass TMD using the $f_r = 1.1f_n$

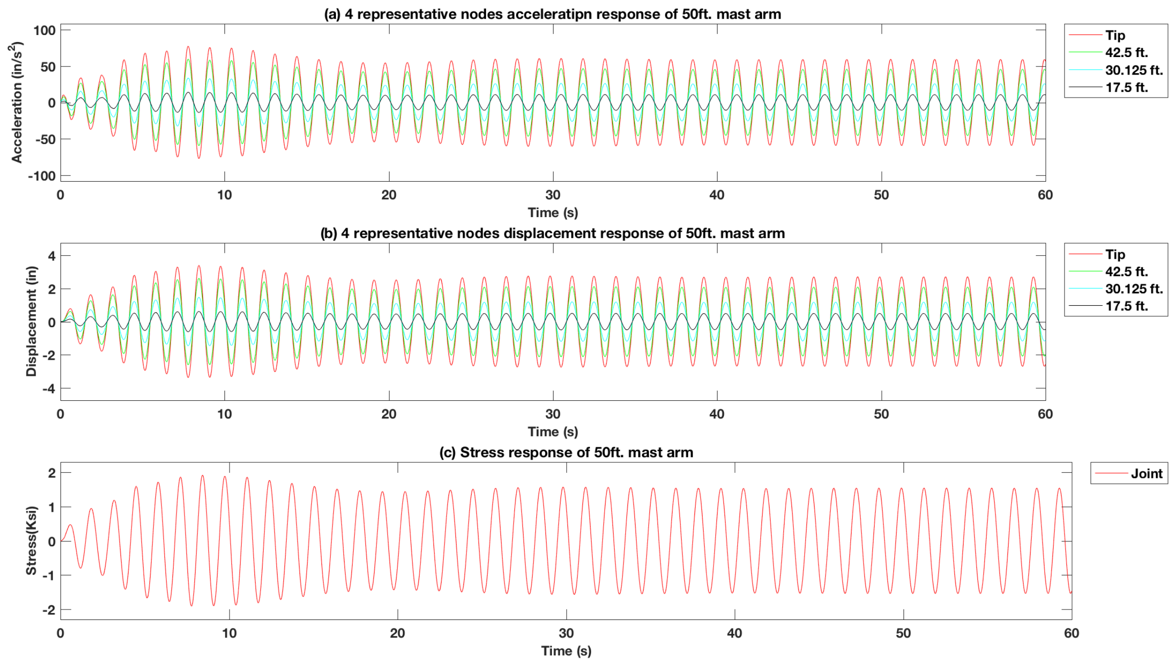

Figure 4-117 Force vibration response of excitation force at 3 signal heads location of the 50 ft. mast arm signal pole structure model with 15 lb. mass TMD using the $f_r = 0.7f_n$

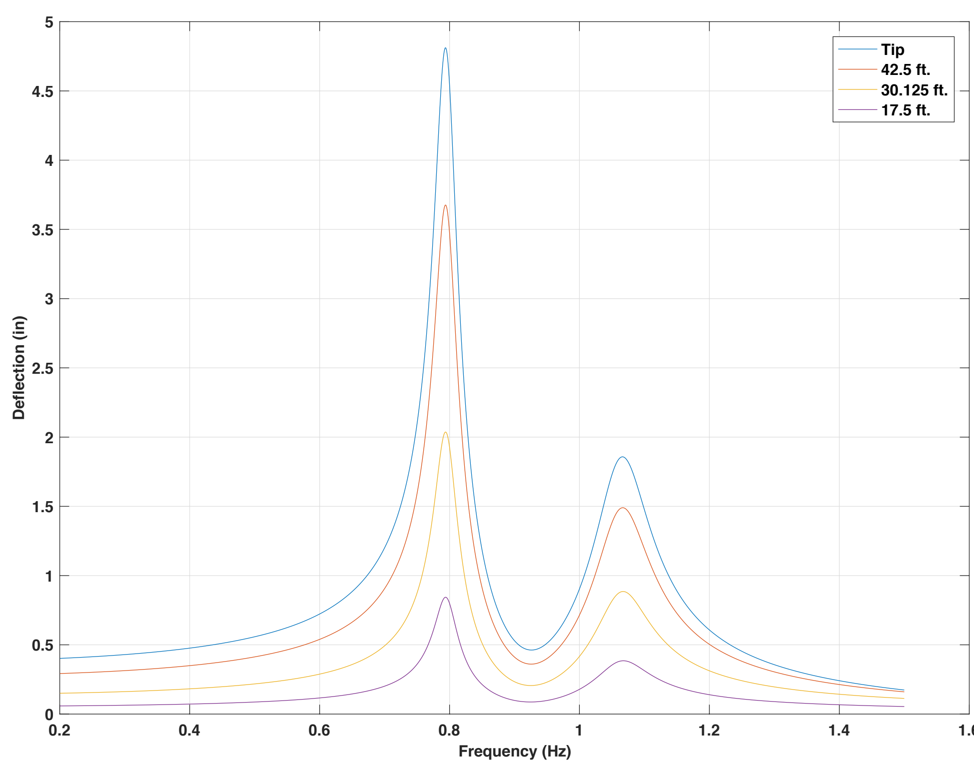

Figure 4-118 Frequency response for 50ft. mast arm with 15lb mass TMD, force on the tip

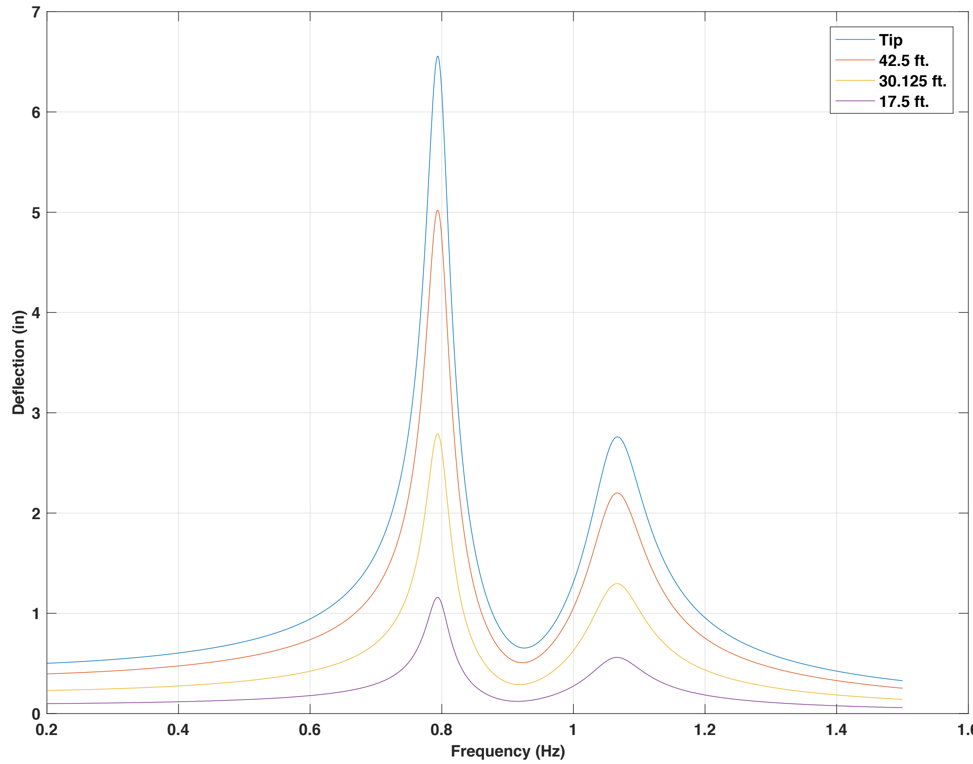

Figure 4-119 Frequency response for 50ft. mast arm with 15lb mass TMD, force on signal heads' location

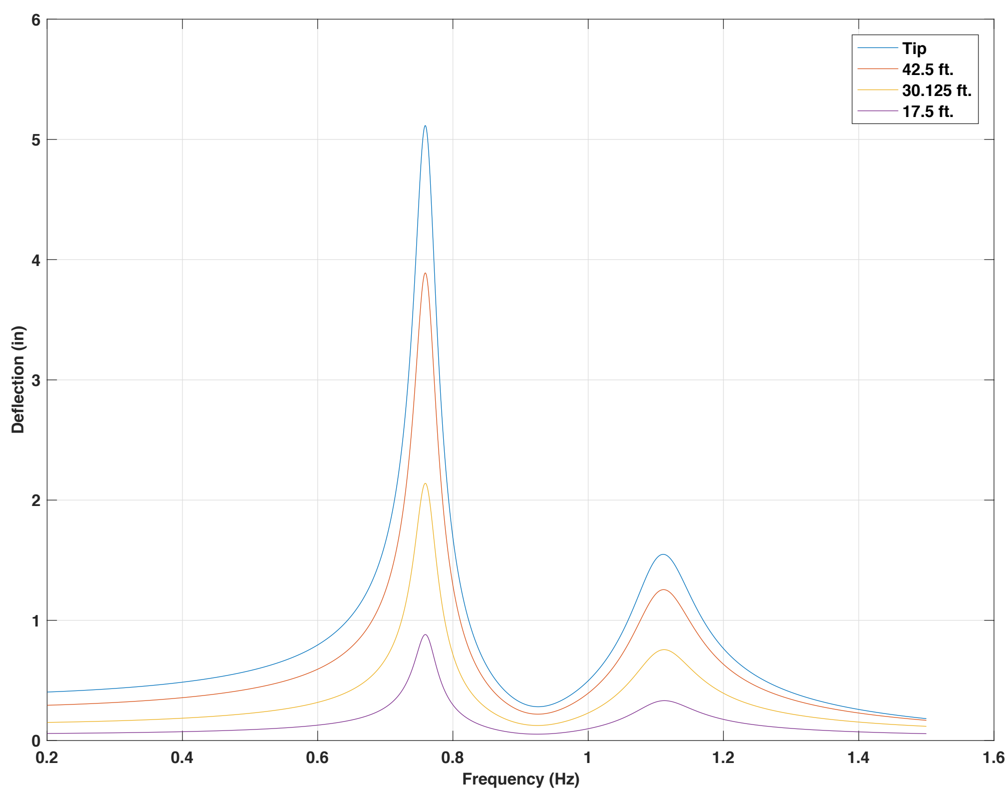

Figure 4-120 Frequency response for 50ft. mast arm with 25lb mass TMD, force on the tip

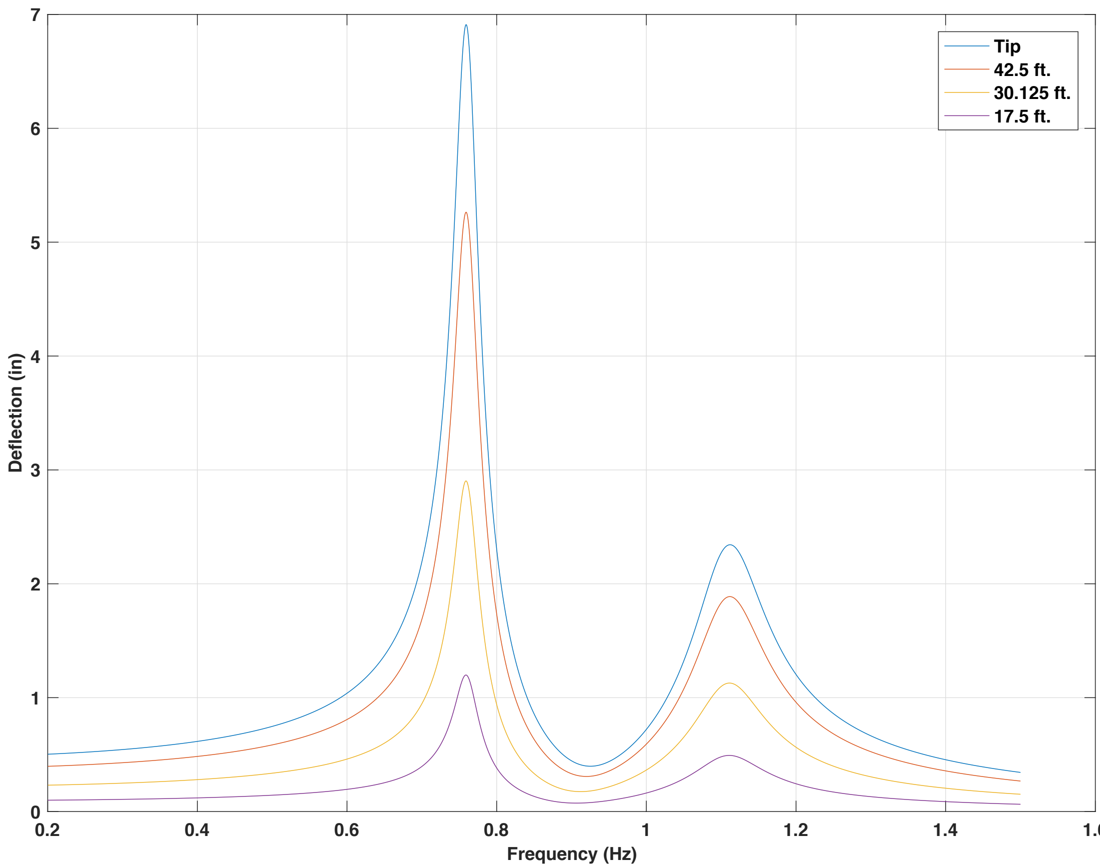

Figure 4-121 Frequency response for 50ft. mast arm with 25lb mass TMD, force on signal heads' location

4.4.4 TMD Frequencies

As analyzed for the previous model, i.e. 70 and 60 feet mast arm signal support structure models before, selecting the damper frequencies of 1.1 f, 0.9 f, 1.25 f, 0.75 f, 1.5 f, and 0.5 f, build the finite element model then do the modal analysis to get mode shapes and frequencies, and calculate corresponding stiffness and damping coefficient of the TMD, then corresponding Rayleigh damping matrix would be computed for the analysis input.

Table 4-11 Preliminary model analysis for 50-ft. arm with various TMD frequencies

TMD Frequency	f_1 (Hz)	f_2 (Hz)	f_3 (Hz)	k	c	α	β
1.1 f_n	0.82	1.13	3.24	1.58	0.297	0.011	3.667E-4
0.9 f_n	0.75	1.02	3.24	1.06	0.024	0.011	3.680E-4
1.25 f_n	0.84	1.25	3.23	2.04	0.034	0.011	3.663E-4
TMD Frequency	f_1 (Hz)	f_2 (Hz)	f_3 (Hz)	k	c	α	β
0.75 f_n	0.66	0.97	3.25	0.73	0.020	0.011	3.678E-4
1.5 f_n	0.86	1.46	3.23	2.93	0.041	0.011	3.653E-4
0.5 f_n	0.45	1.11	3.24	0.33	0.014	0.011	3.664E-4

Then do the same analysis as before, i.e. free vibration response, force vibration response and harmonic analysis. The representative results for each case are shown below:

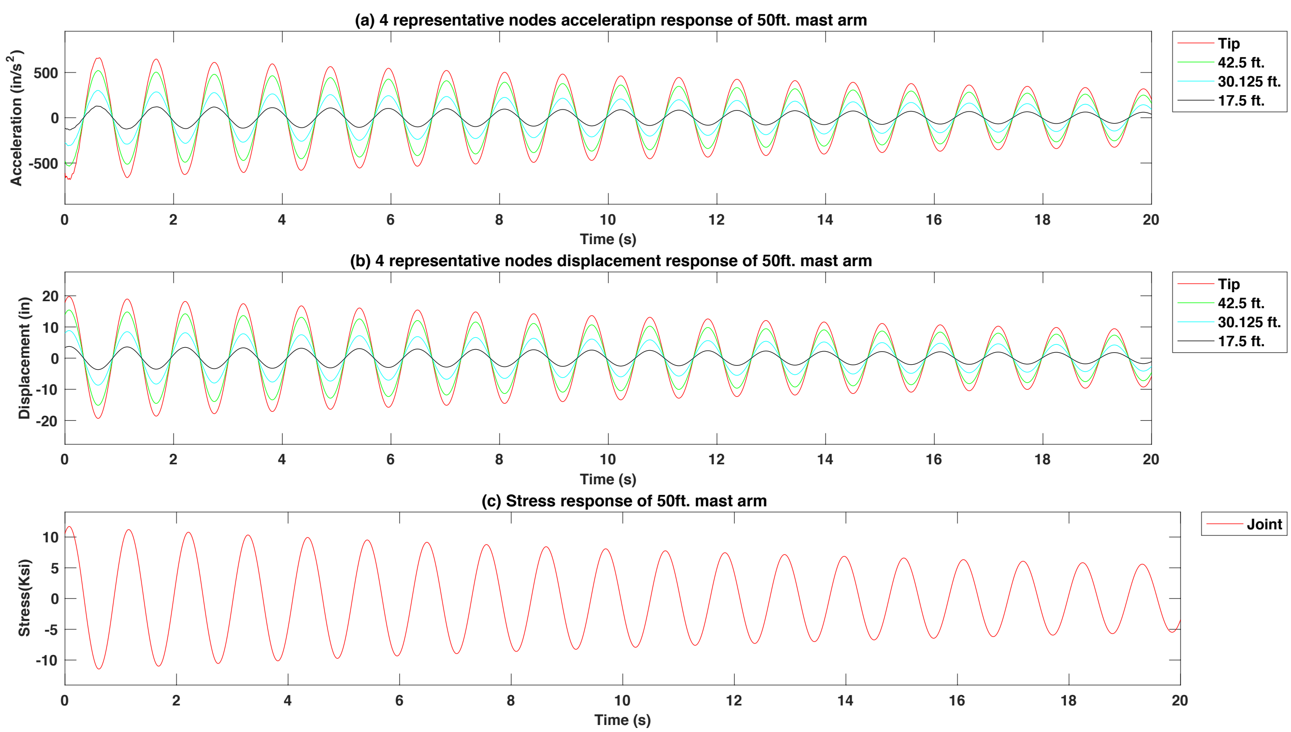

Figure 4-122 Free vibration response of excitation force at tip of the 50 ft. mast arm signal pole structure model with 15 lb. mass TMD using the $f_d = 0.5 f_n$

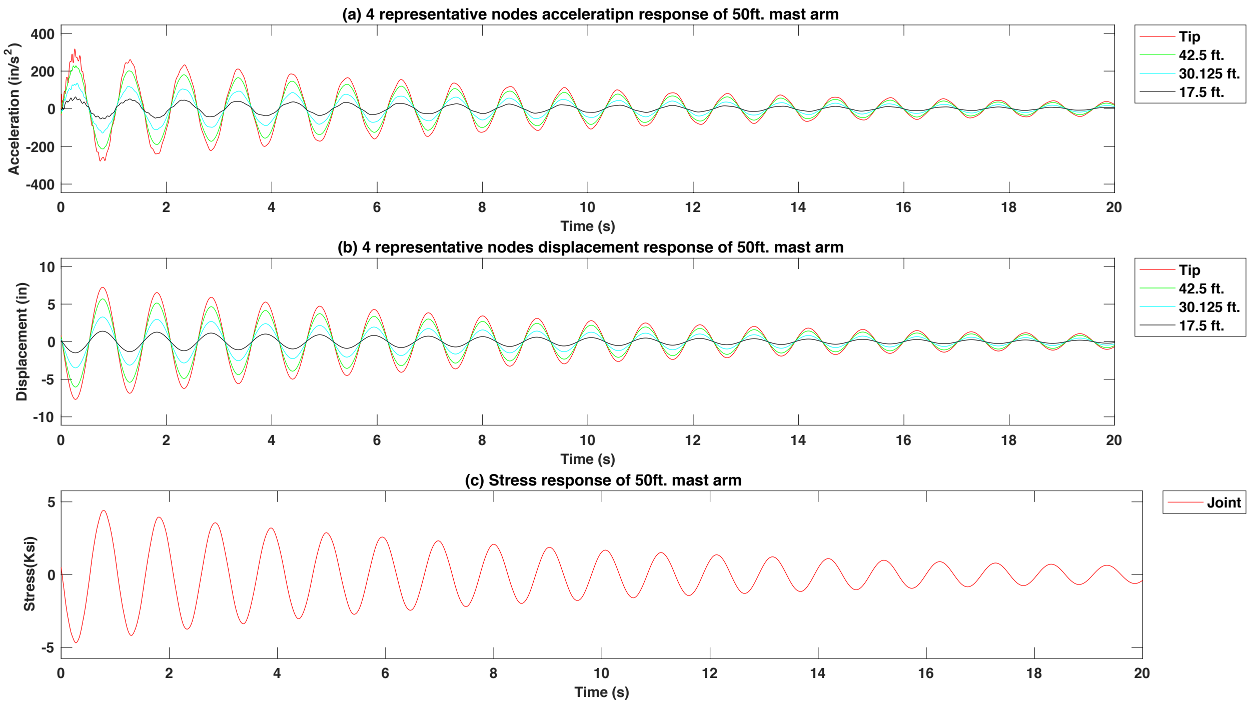

Figure 4-123 Free vibration response of excitation force at tip in natural frequency of the 50 ft. mast arm signal pole structure model with 15 lb. mass TMD using the $f_d = 0.75 f_n$

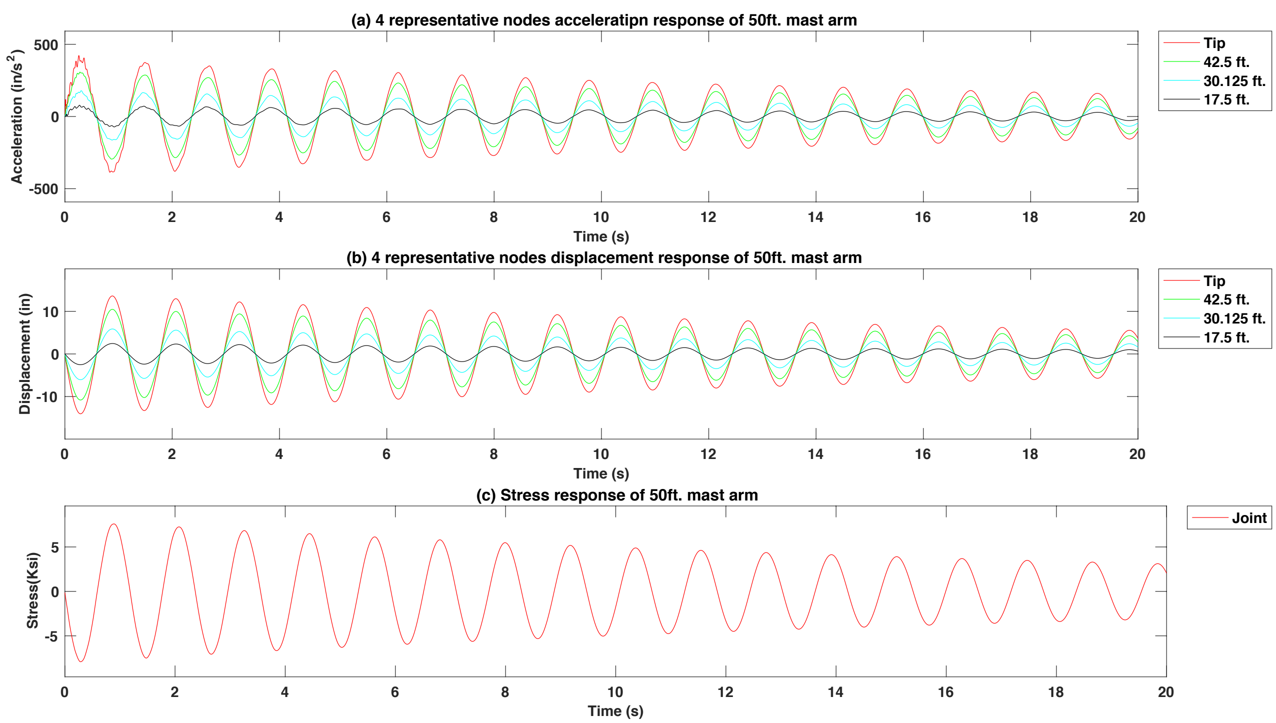

Figure 4-124 Free vibration response of excitation force at tip of the 50 ft. mast arm signal pole structure model with 15 lb. mass TMD using the $f_d = 1.25\ f_n$

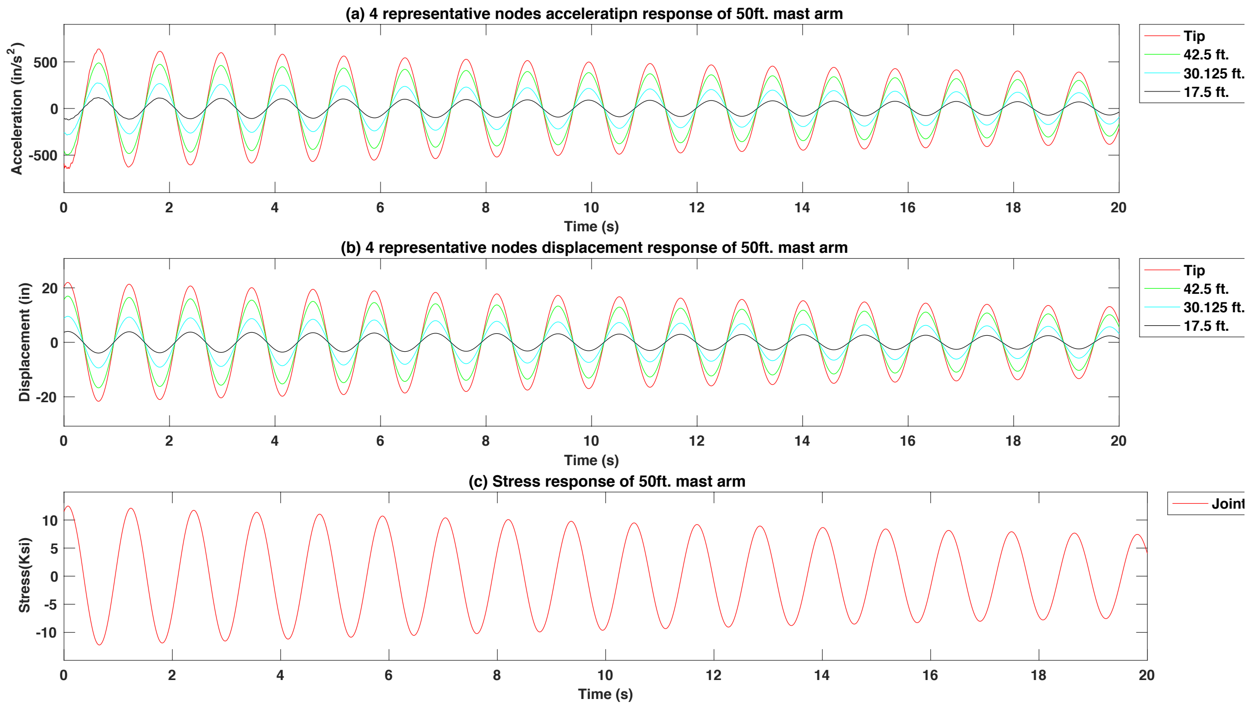

Figure 4-125 Free vibration response of excitation force at tip of the 50 ft. mast arm signal pole structure model with 15 lb. mass TMD using the $f_d = 1.5 f_n$

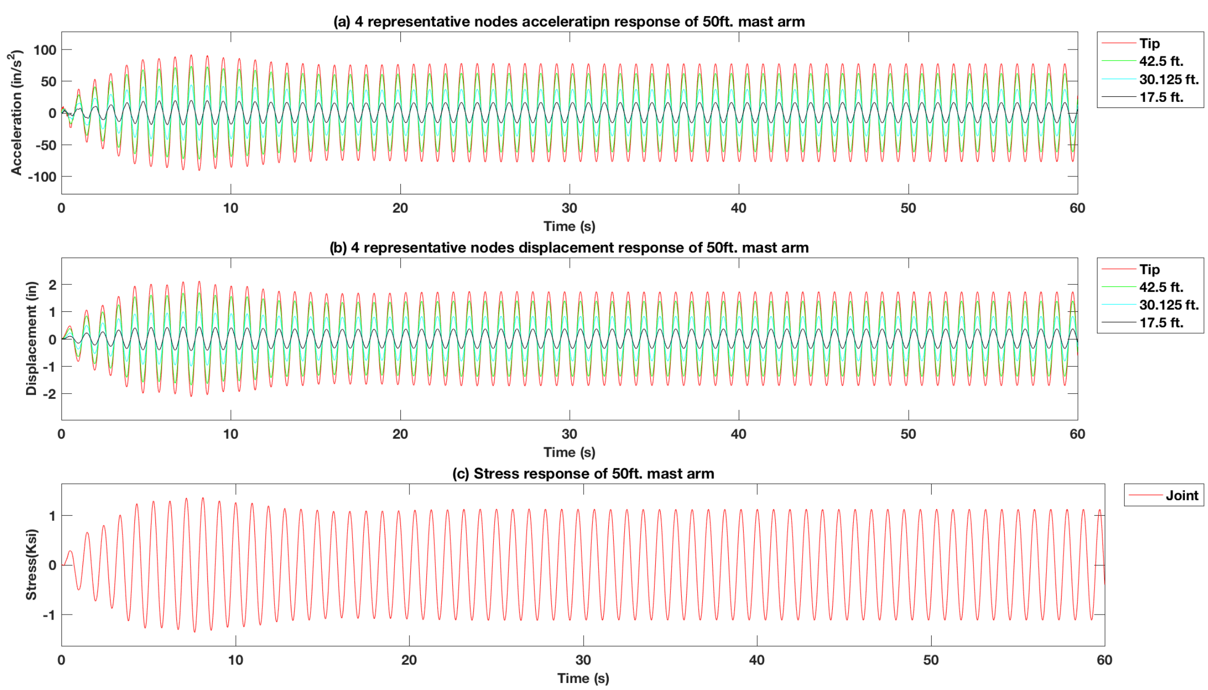

Figure 4-126 Force vibration response of excitation force at tip of the 50 ft. mast arm signal pole structure model with 15 lb. mass TMD using the $f_d = 0.9 f_n, f_f = 1.05 f_n$

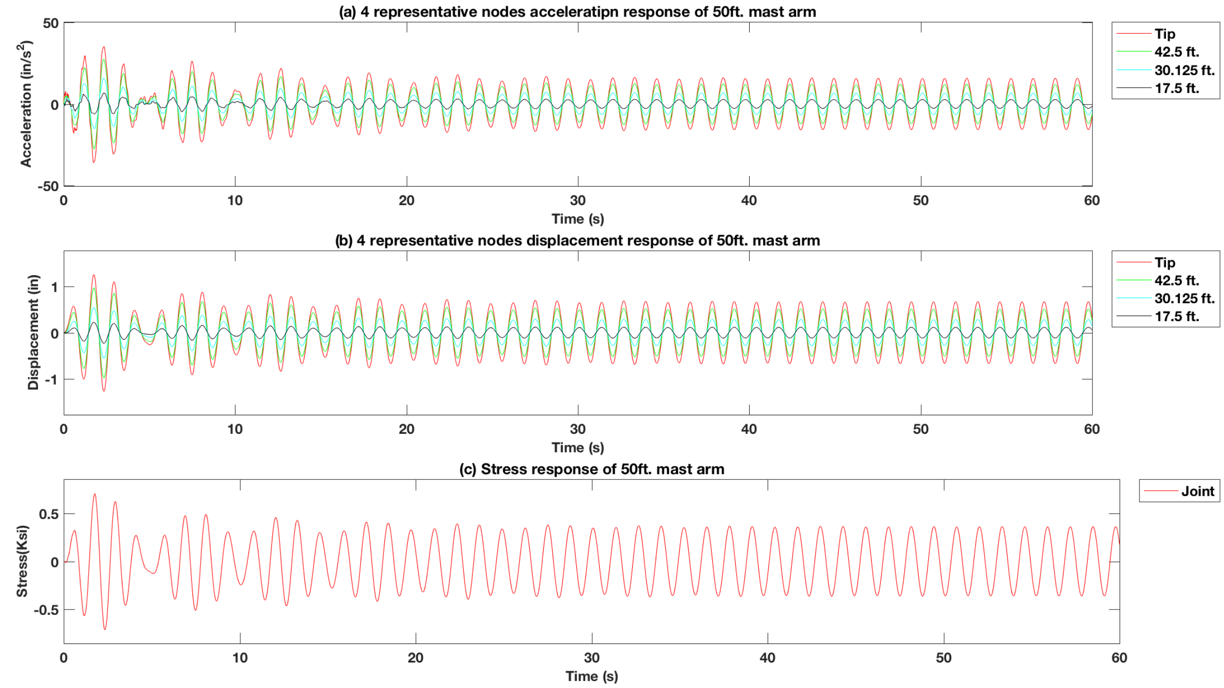

Figure 4-127 Force vibration response of excitation force at tip of the 50 ft. mast arm signal pole structure model with 15 lb. mass TMD using the $f_d = 0.75\, f_n$, $f_r = 0.8 f_n$

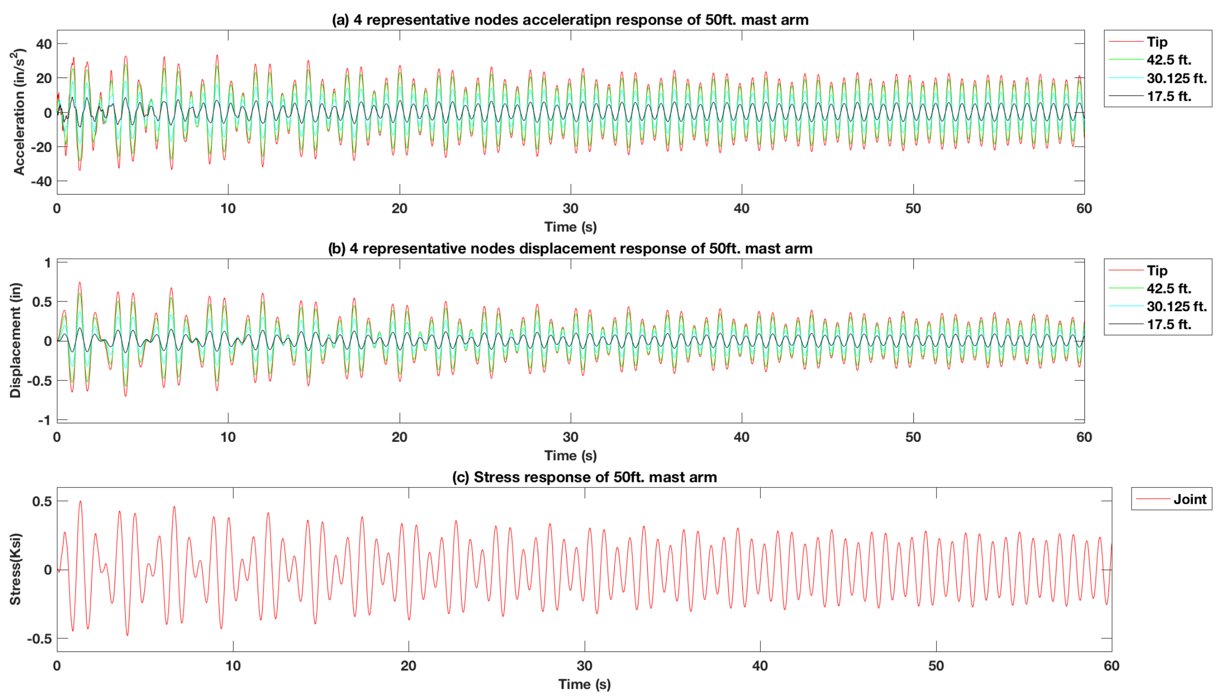

Figure 4-128 Force vibration response of excitation force at tip of the 50 ft. mast arm signal pole structure model with 15 *lb.* mass TMD using the $f_d = 0.5\, f_n$, $f_r = 1.4 f_n$

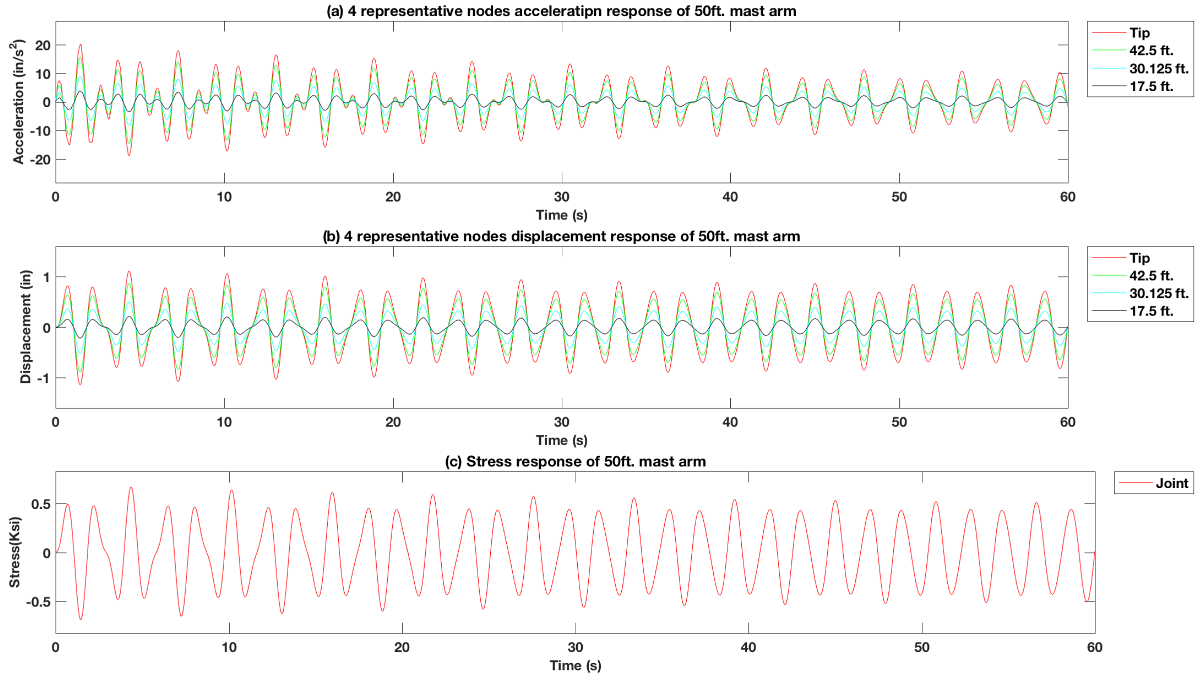

Figure 4-129 Force vibration response of excitation force at 3 signal heads location of the 50 ft. mast arm signal pole structure model with 15 lb. mass TMD using the $f_d = 1.5\, f_n$, $f_s = 0.6 f_n$

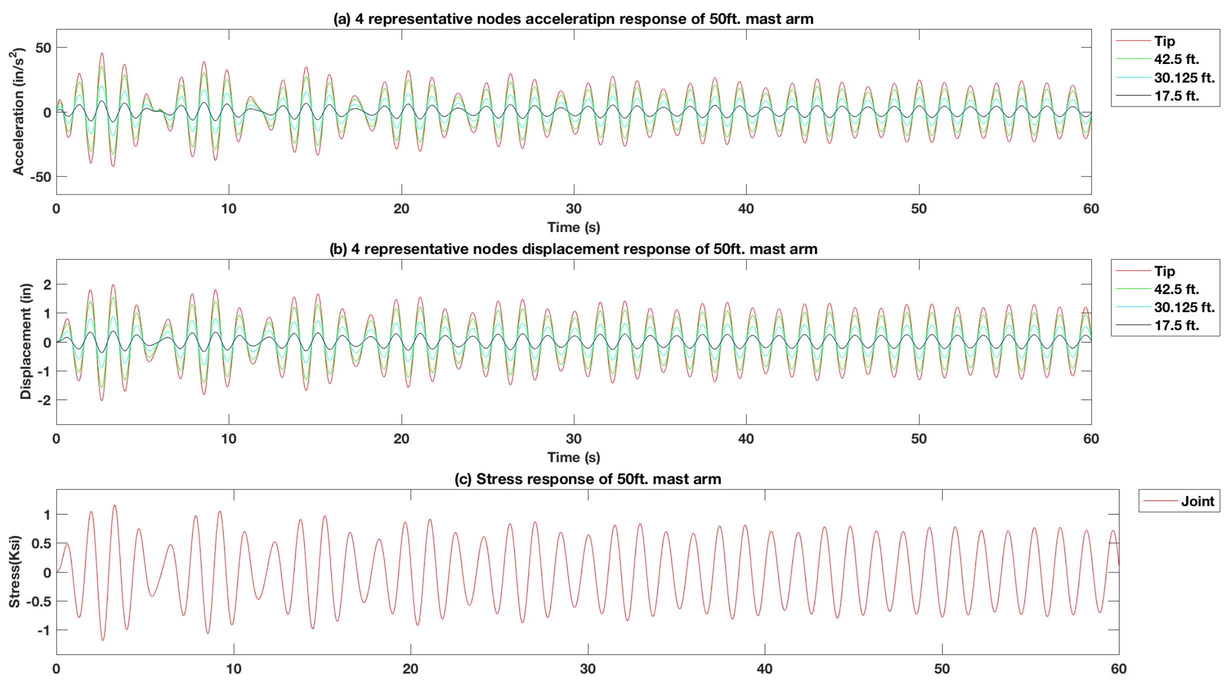

Figure 4-130 Force vibration response of excitation force at 3 signal heads location of the 50 ft. mast arm signal pole structure model with 15 lb. mass TMD using the $f_d = 1.25\, f_n$, $f_s = 0.8 f_n$

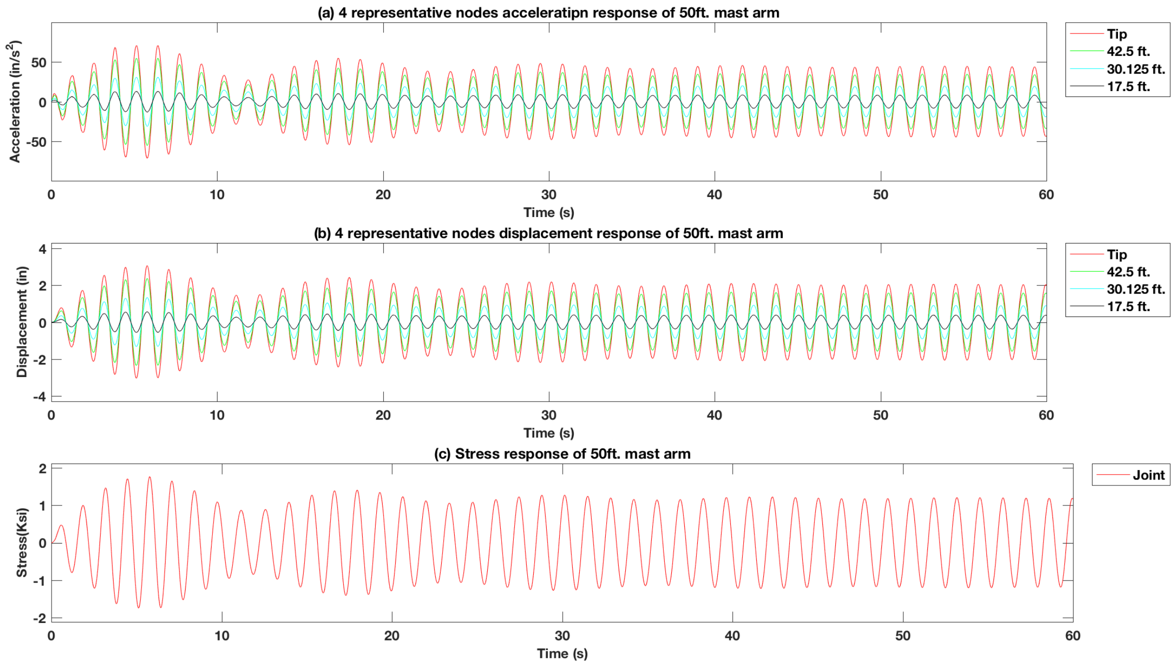

Figure 4-131 Force vibration response of excitation force at tip of the 50 ft. mast arm signal pole structure model with 15 lb. mass TMD using the $f_d = 1.1f_n, f_r = 0.9f_n$

For harmonic analysis, plot all frequency response curves:

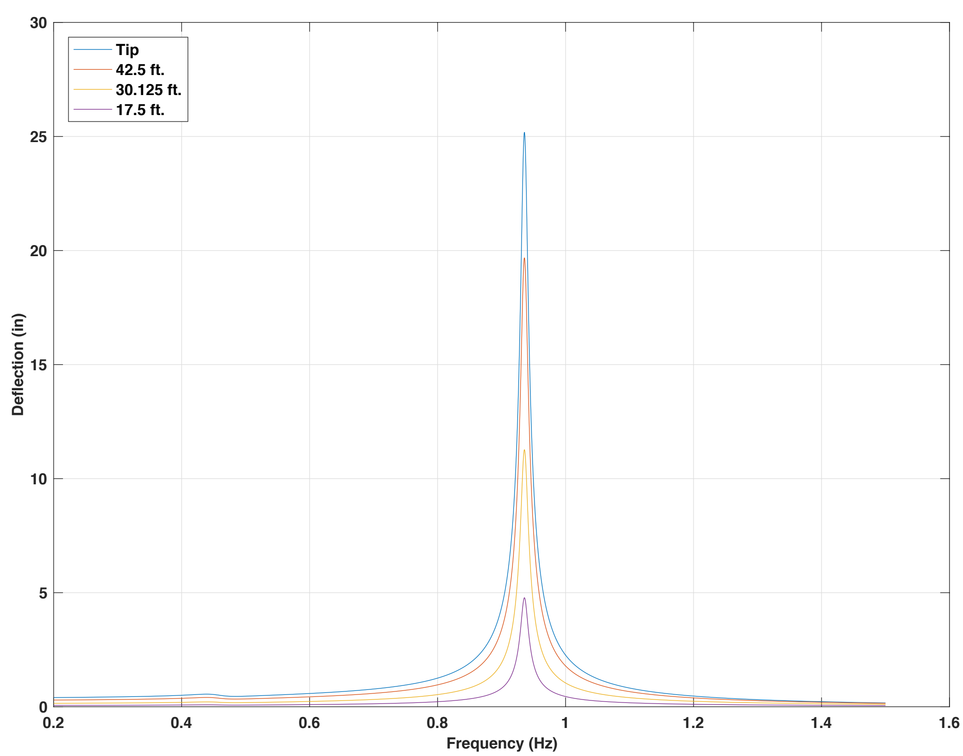

Figure 4-132 Frequency response for 50ft. mast arm with 15lb mass TMD, 5 lbf force on tip, $f_d = 0.5\, f_n$

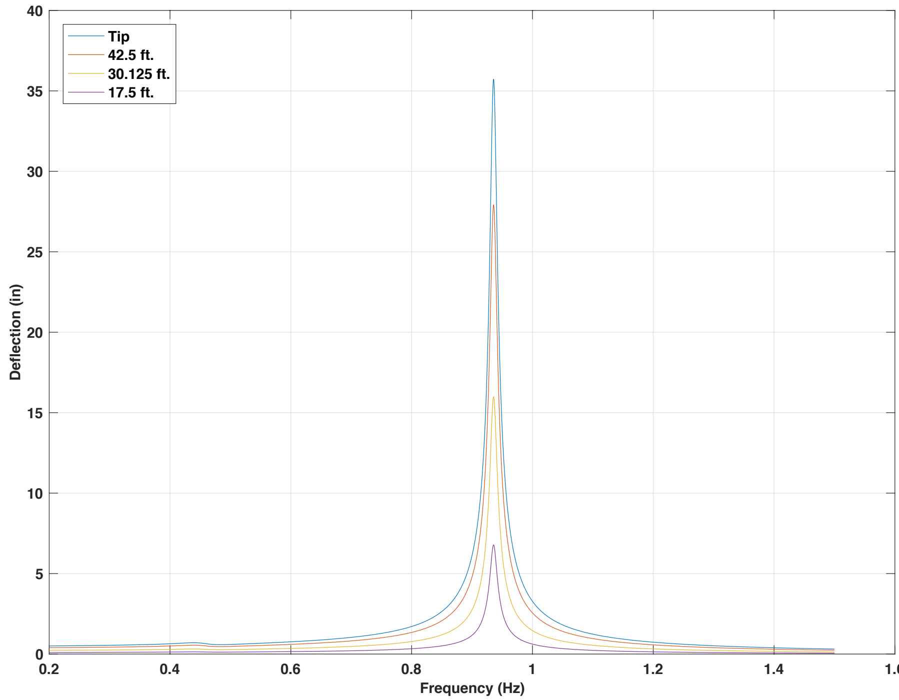

Figure 4-133 Frequency response for 50ft. mast arm with 15lb mass TMD, 5 lbf force on 3 signal heads location, $f_d = 0.5\, f_n$

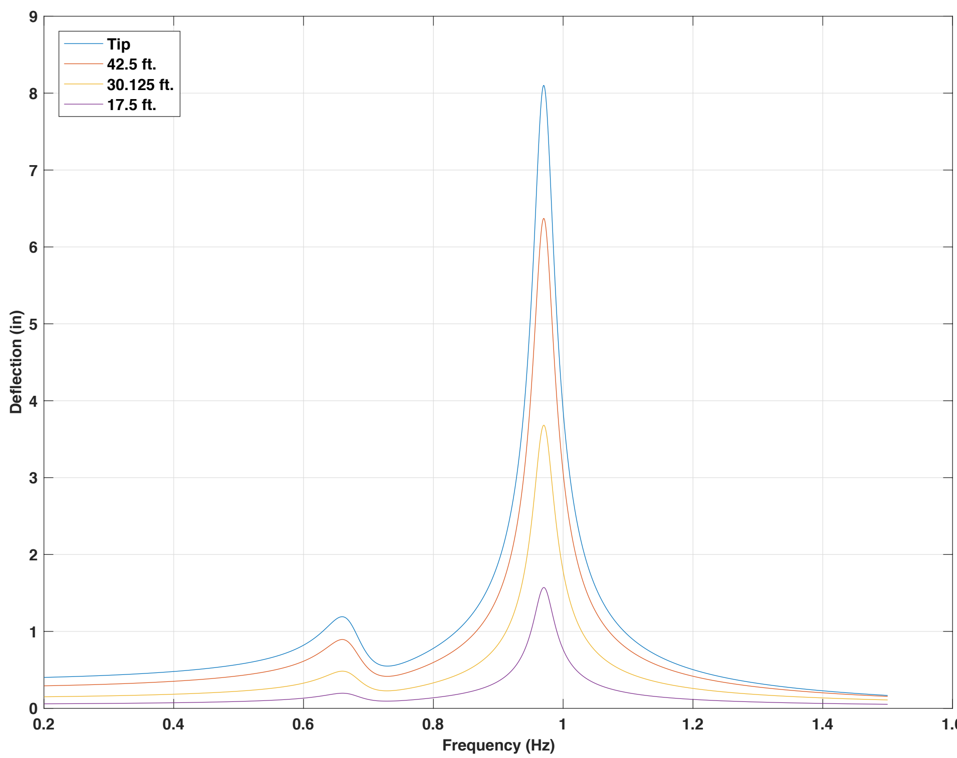

Figure 4-134 Frequency response for 50ft. mast arm with 15lb mass TMD, 5 lbf force on tip, $f_d = 0.75\, f_n$

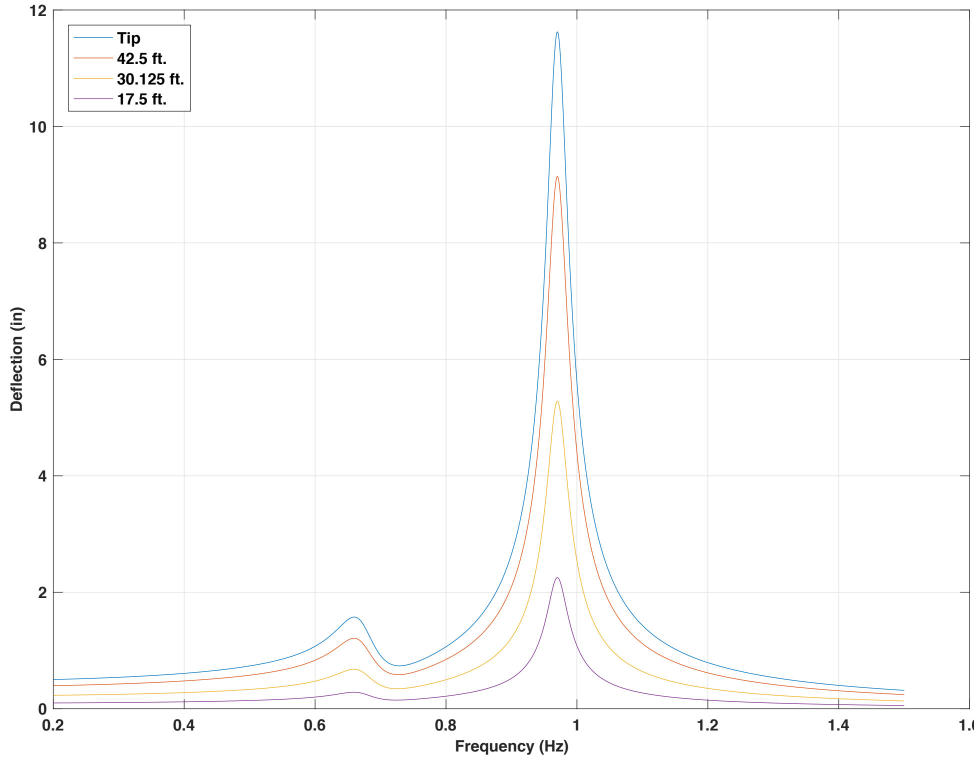

Figure 4-135 Frequency response for 50ft. mast arm with 15lb mass TMD, 5 lbf force on 3 signal heads location, $f_d = 0.75 f_n$

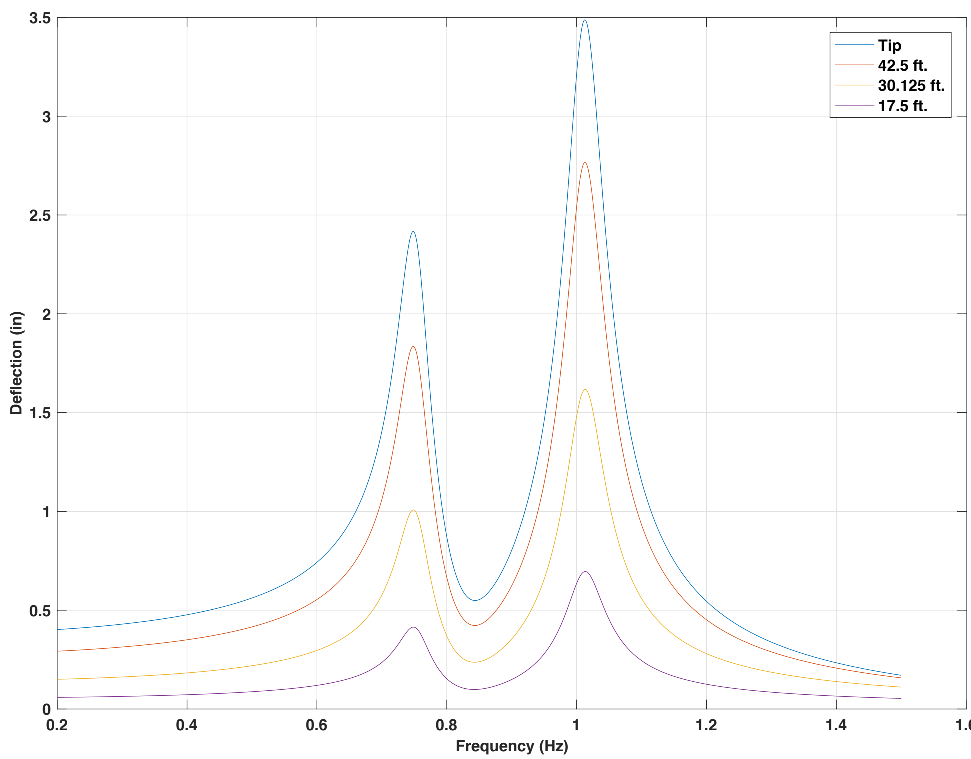

Figure 4-136 Frequency response for 50ft. mast arm with 15lb mass TMD, 5 lbf force on tip, $f_d = 0.9 f_n$

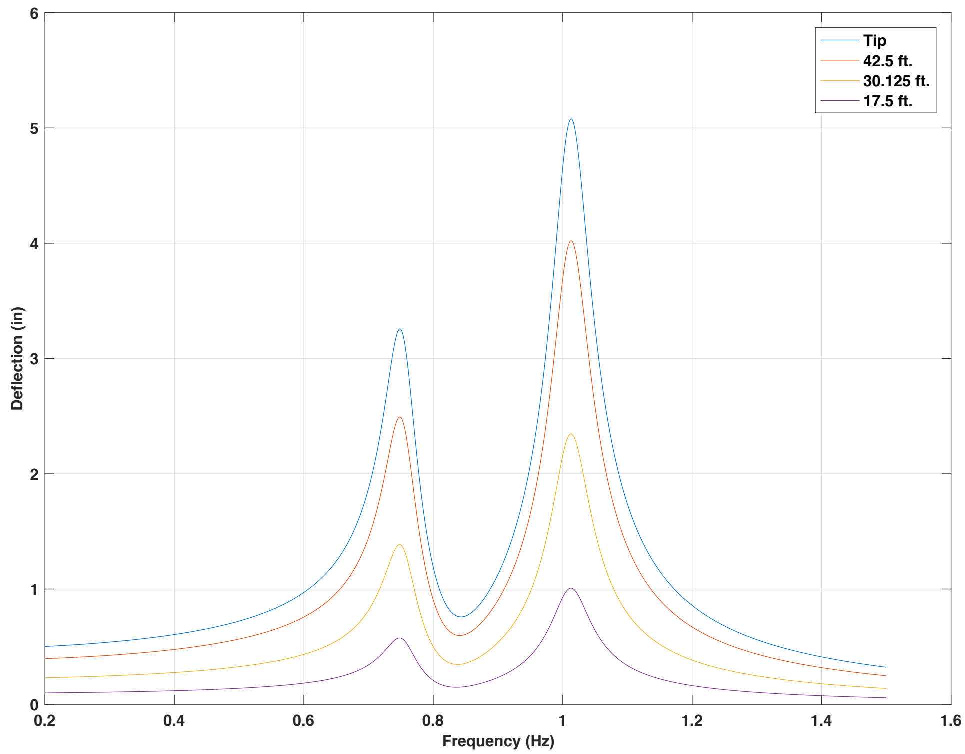

Figure 4-137 Frequency response for 50ft. mast arm with 15lb mass TMD, 5 lbf force on 3 signal heads location, $f_d = 0.9 f_n$

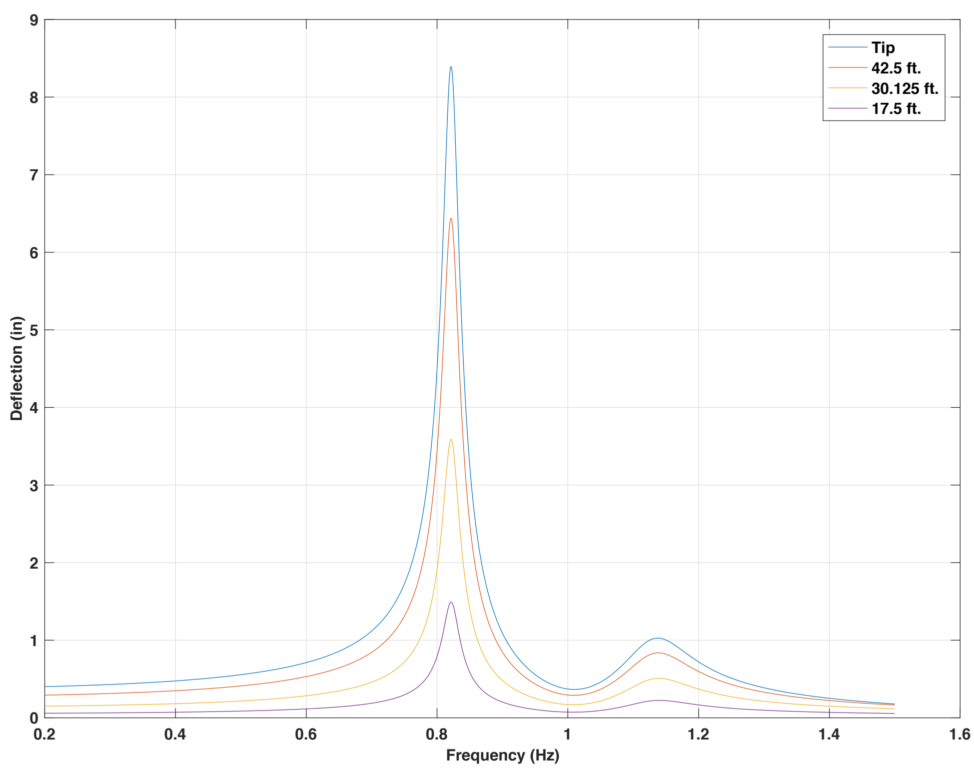

Figure 4-138 Frequency response for 50ft. mast arm with 15lb mass TMD, 5 lbf force on tip, $f_d = 1.1 f_n$

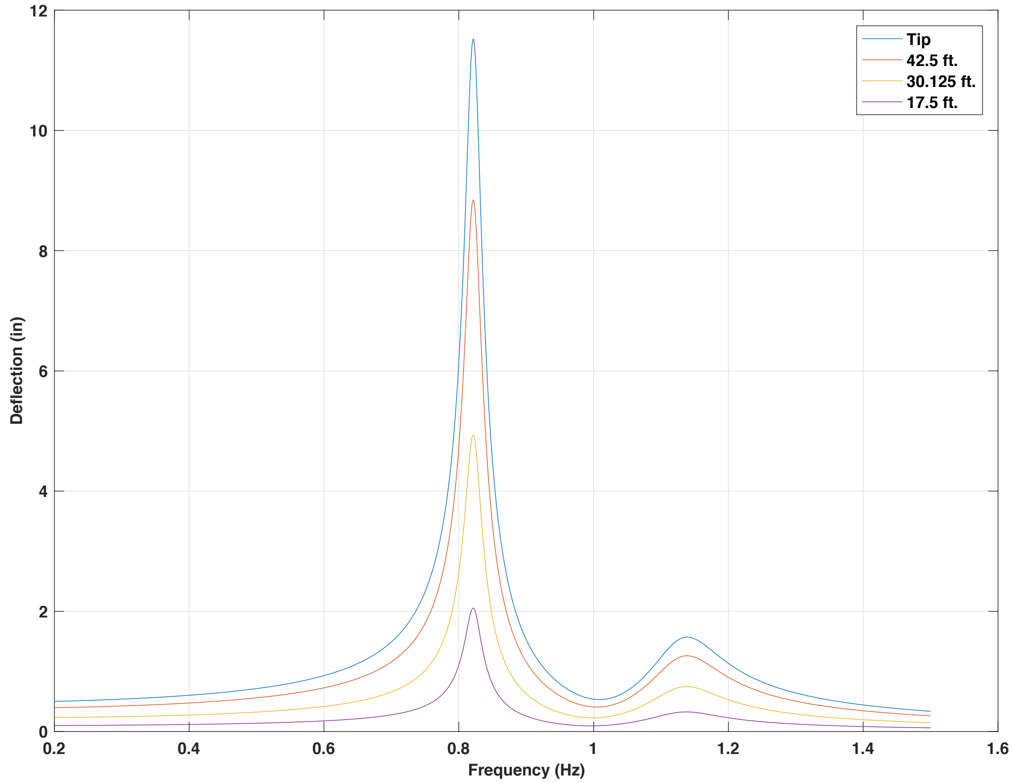

Figure 4-139 Frequency response for 50ft. mast arm with 15lb mass TMD, 5 lbf force on 3 signal heads location, $f_d = 1.1 f_n$

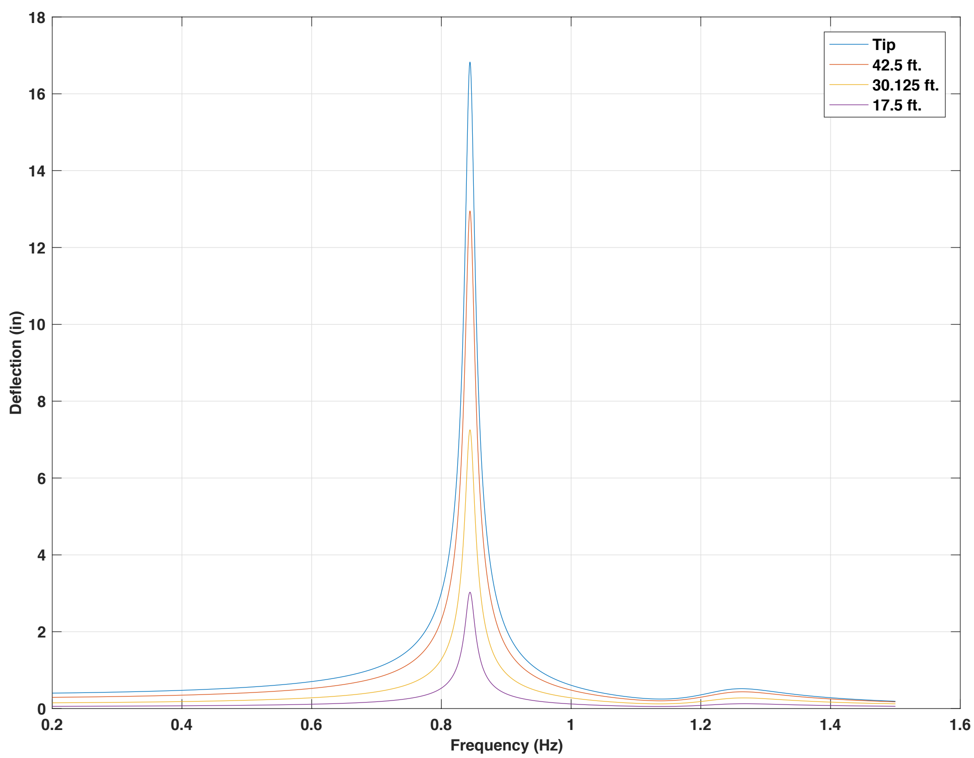

Figure 4-140 Frequency response for 50ft. mast arm with 15lb mass TMD, 5 lbf force on tip, $f_d = 1.25 f_n$

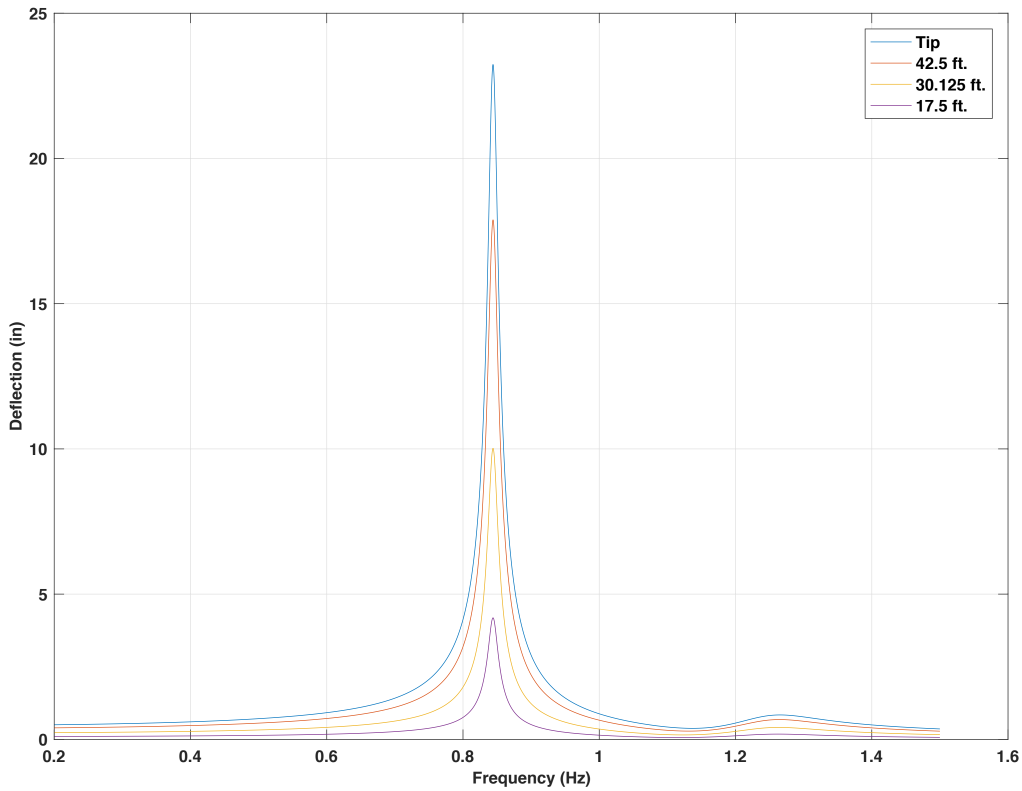

Figure 4-141 Frequency response for 50ft. mast arm with 15lb mass TMD, 5 lbf force on 3 signal heads location, $f_d = 1.25\, f_n$

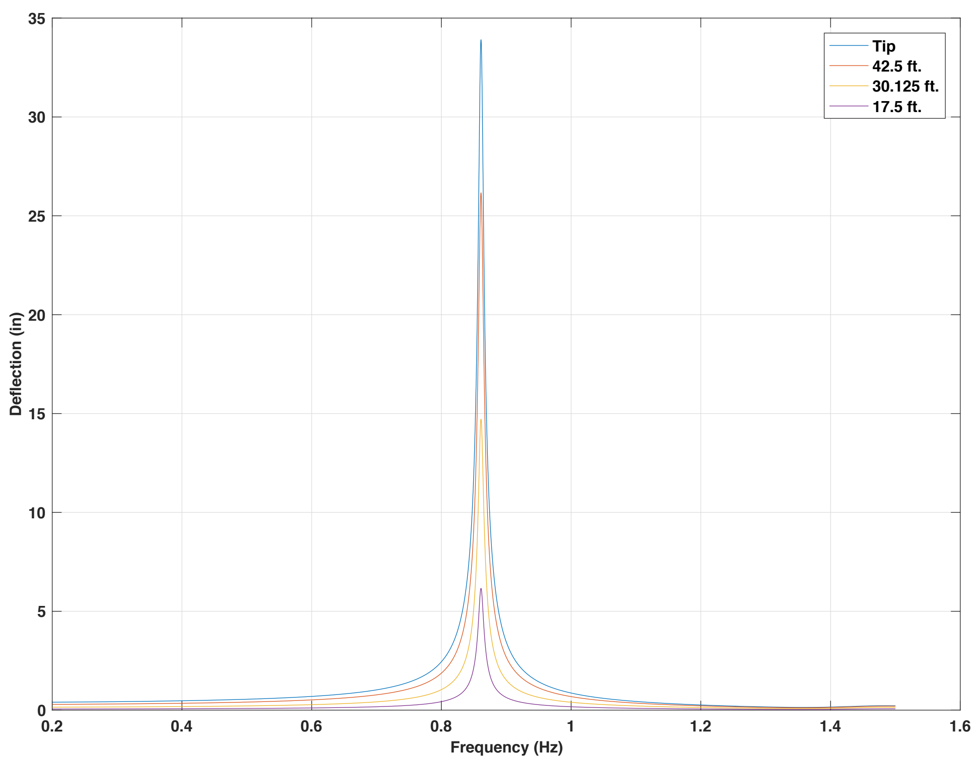

Figure 4-142 Frequency response for 50ft. mast arm with 15lb mass TMD, 5 lbf force on tip, $f_d = 1.5\, f_n$

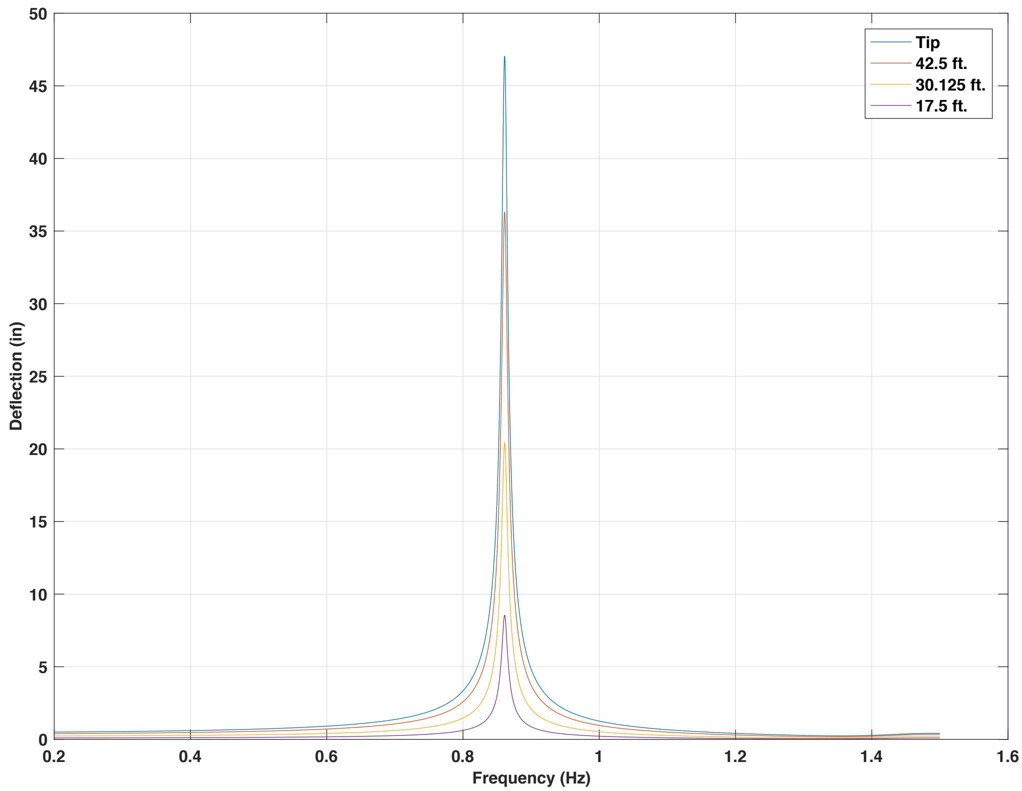

Figure 4-143 Frequency response for 50ft. mast arm with 15lb mass TMD, 5 lbf force on 3 signal heads location, $f_d = 1.5 f_n$

4.4.5 TMD Damping Ratio

As mentioned in previous section, this case will also use TMD in 1% of damping ratio with 25 lb. mass and it will be compared with 6% damping ratio with 25 lb. mass TMD, to simulate a Alcoa damper. The TMD will be at the tip of the mast arm unless specified. The pre-analysis calculation for the damper:

Table 4-12 Preliminary model analysis for 50 ft. arm with TMD in 1% damping ratio

TMD damping ratio	f_1 (Hz)	f_2 (Hz)	f_3 (Hz)	k	c	α	β
1%	0.76	1.11	3.24	2.17	0.0075	0.01	3.69E-04

And the representative plots of all the results are:

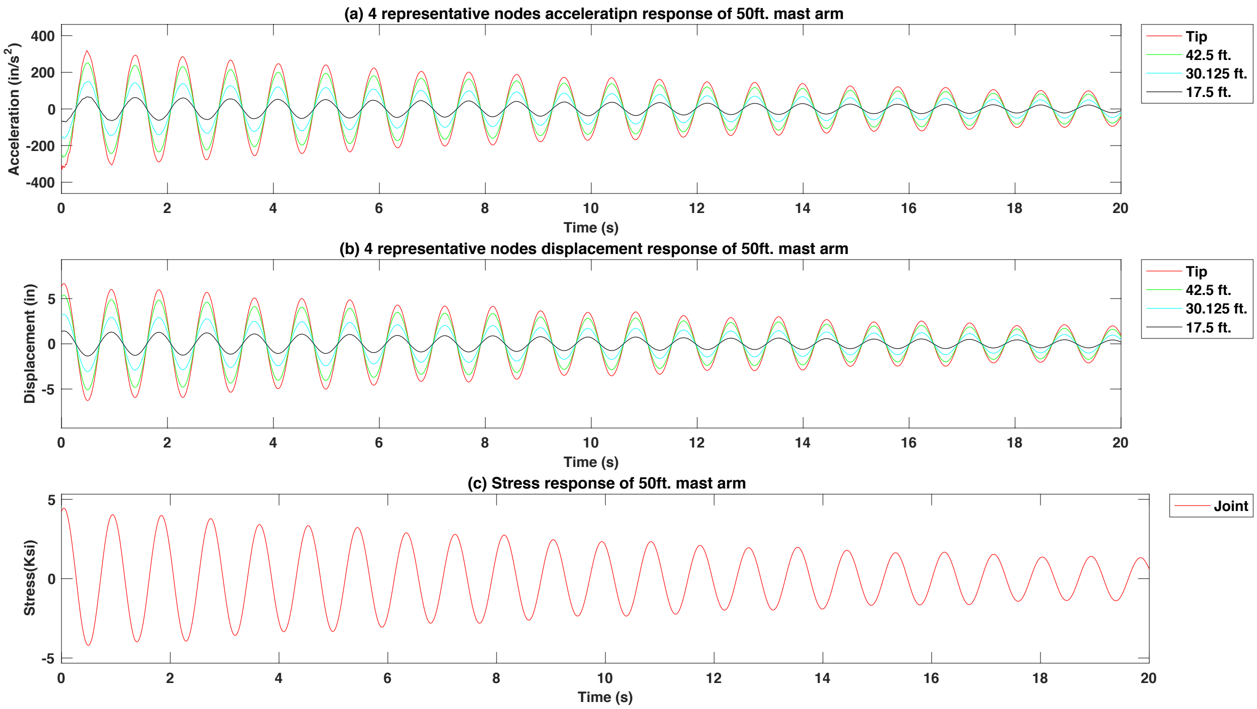

Figure 4-144 Free vibration response of excitation force at tip of the 50 ft. mast arm signal pole structure model with 25 lb. mass TMD using the $\xi = 1\%$

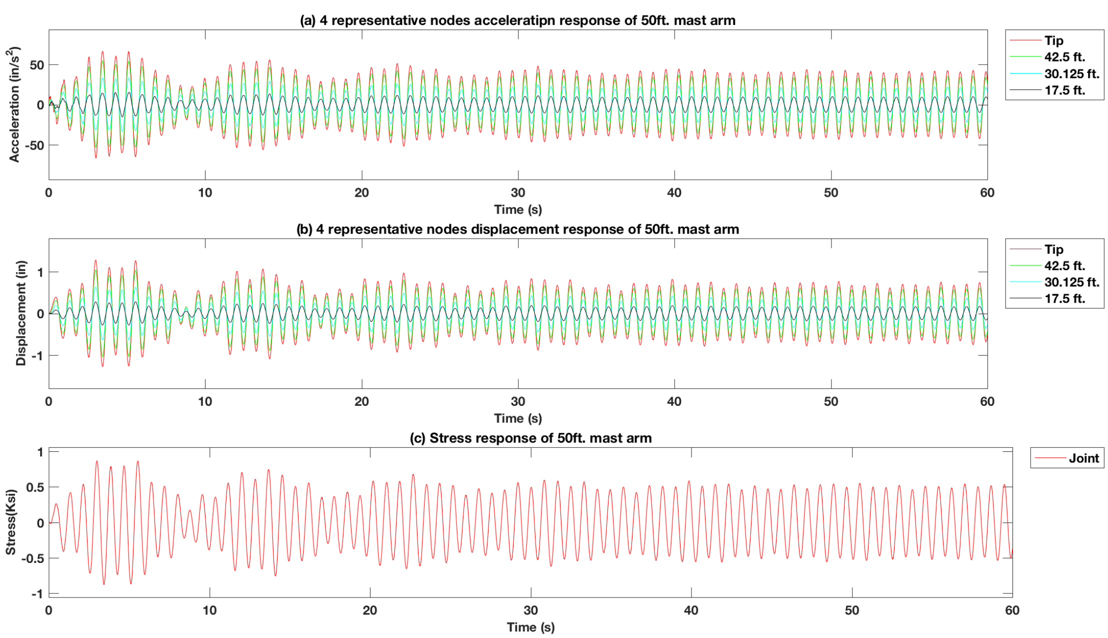

Figure 4-145 Force vibration response of excitation force at tip of the 50 ft. mast arm signal pole structure model with 25 lb. mass TMD using the $\xi = 1\%$, $f_d = 1.1 f_n$

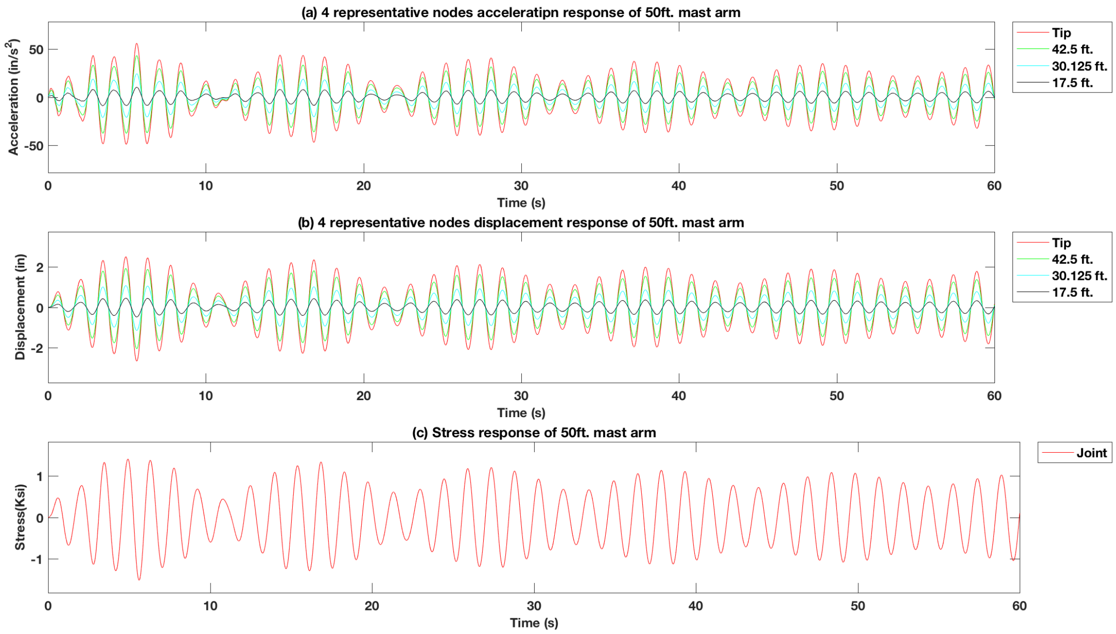

Figure 4-146 Force vibration response of excitation force at 3 signal heads position of the 50 ft. mast arm signal pole structure model with 25 lb. mass TMD using the $\zeta = 1\%$, $f_r = 0.6 f_n$

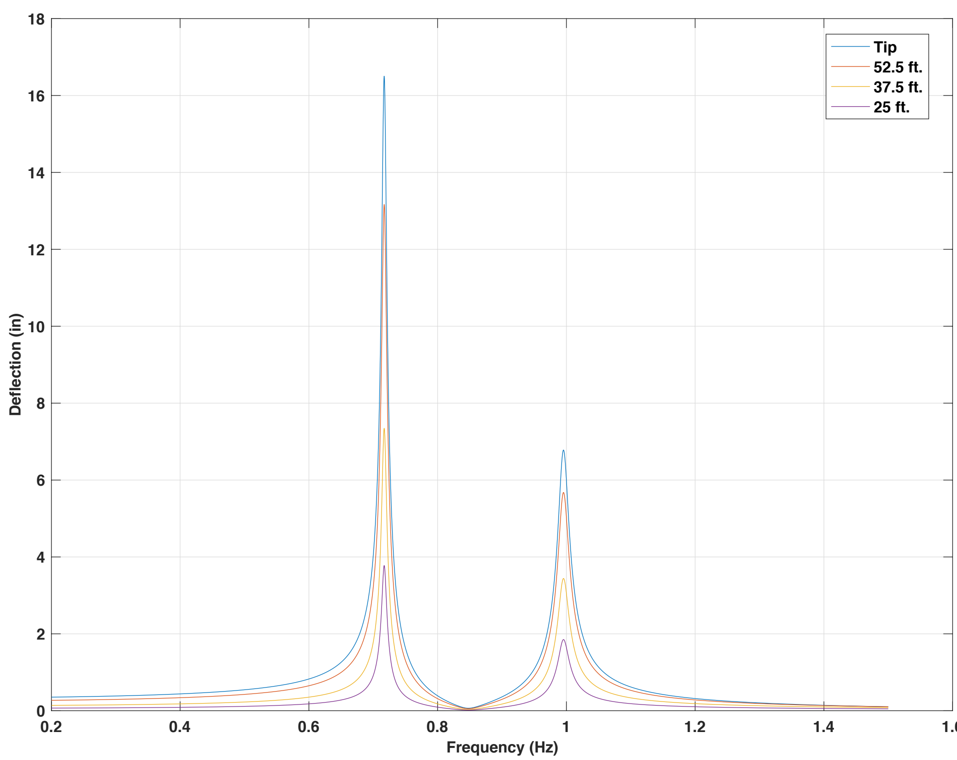

Figure 4-147 Frequency response for 50ft. mast arm with 25 lb. mass TMD using the $\zeta = 1\%$, 5 lbf force on tip of mast arm

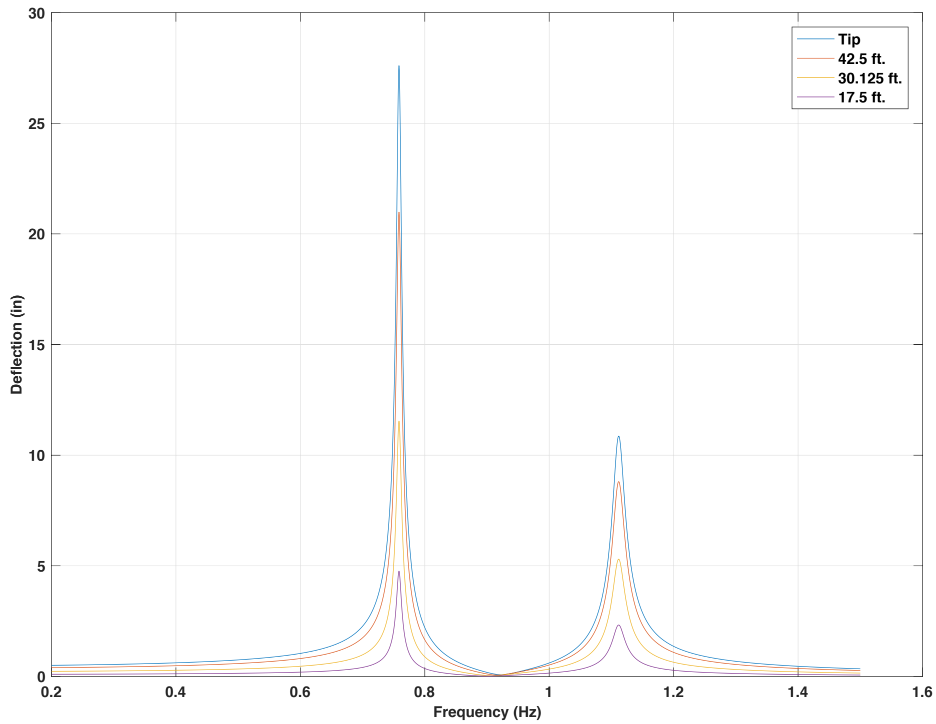

Figure 4-148 Frequency response for 50ft. mast arm with 25 lb. mass TMD using the $\xi = 1\%$, 5 lbf force on 3 signal head location

4.4.6 TMD Locations

Because the location of TMD could influence the structure's frequencies by changing the whole structure's stiffness matrix, location changes of TMD using 2.5*ft.*, 5*ft*. and 10*ft.* from mast arm tip with the same damper are applied in this case.

The Preliminary model analysis is:

Table 4-13 Preliminary model analysis for 50 ft. arm with TMD in different location

TMD Location (*ft.*)	f_1 (Hz)	f_2 (Hz)	f_3 (Hz)	k	c	α	β
2.5	0.80	1.06	3.23	1.30	0.027	0.010	3.687E-4
5	0.81	1.05	3.23	1.30	0.027	0.010	3.689E-4
10	0.83	1.03	3.23	1.30	0.027	0.010	3.689E-4

And the representative plots of the results are:

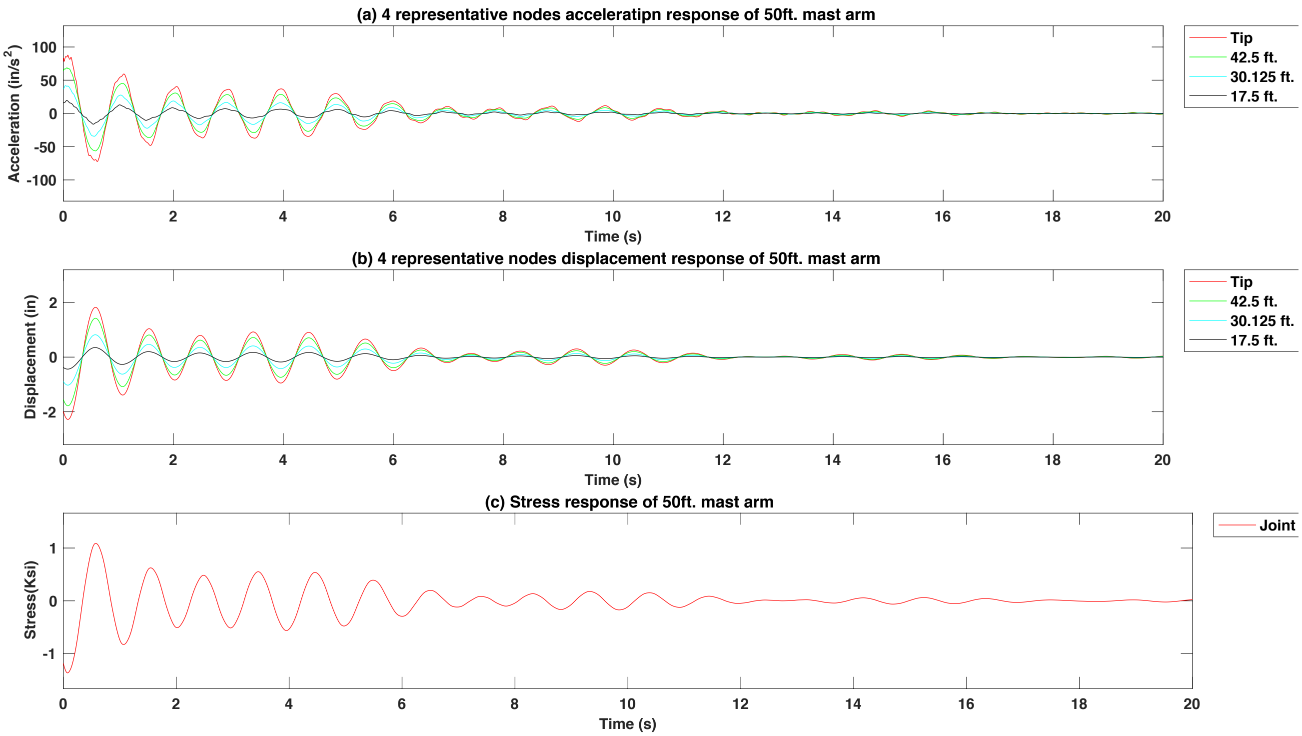

Figure 4-149 Free vibration response of excitation force at tip in the second mode frequency of the 50 ft. mast arm signal pole structure model with 15 lb. mass TMD at 10 ft from the tip

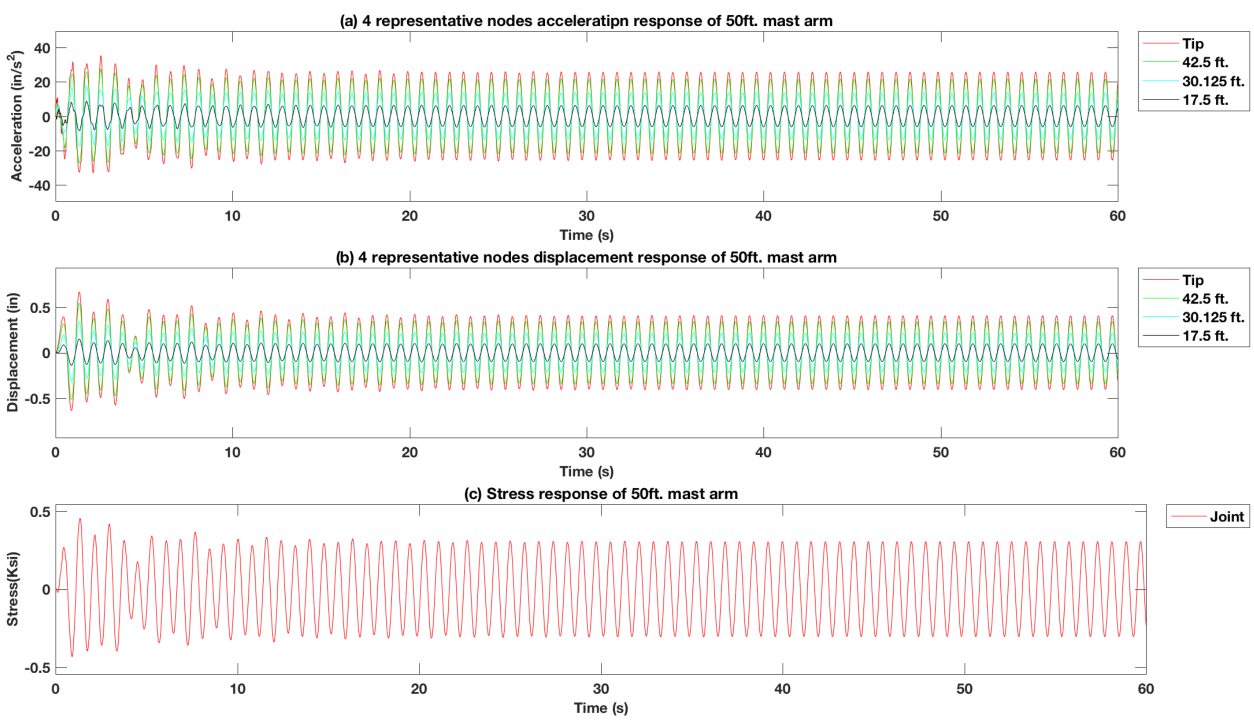

Figure 4-150 Force vibration response of excitation force at tip in the second mode frequency of the 50ft. mast arm signal pole structure model TMD at 2.5 ft from the tip $f_x = 1.2f_n$

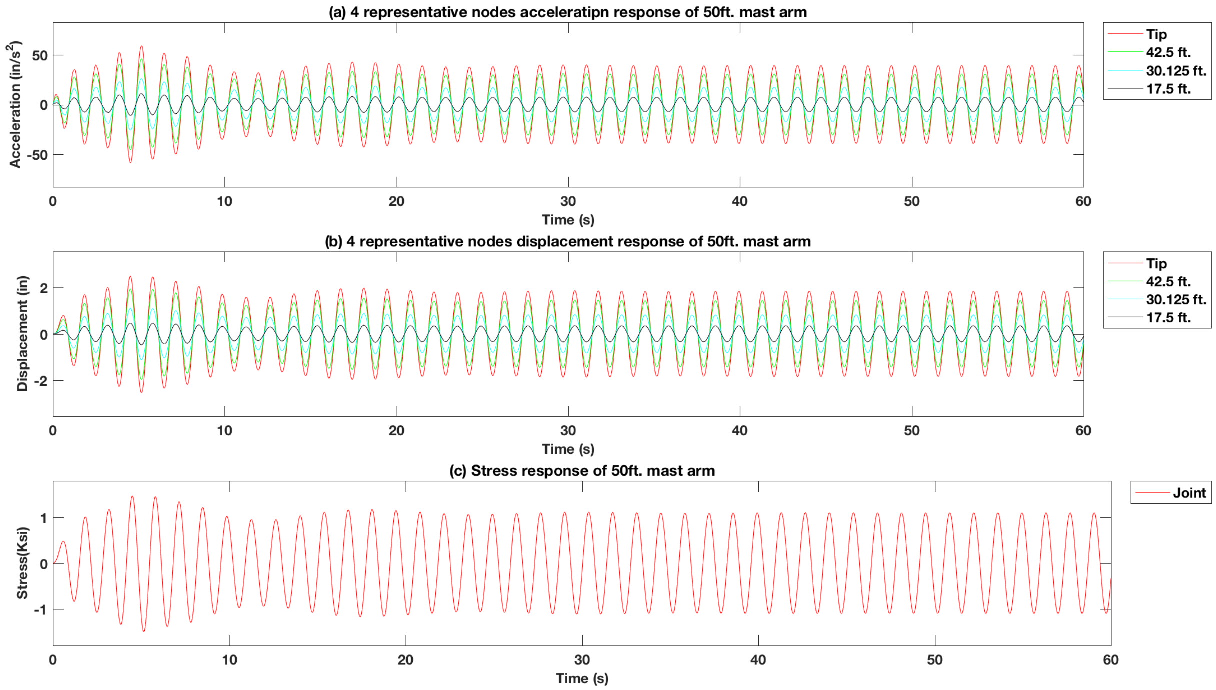

Figure 4-151 Force vibration response of excitation force at 3 signal heads position of the 50 ft. mast arm signal pole structure model TMD at 5 ft from the tip $f_r = 0.7 f_n$

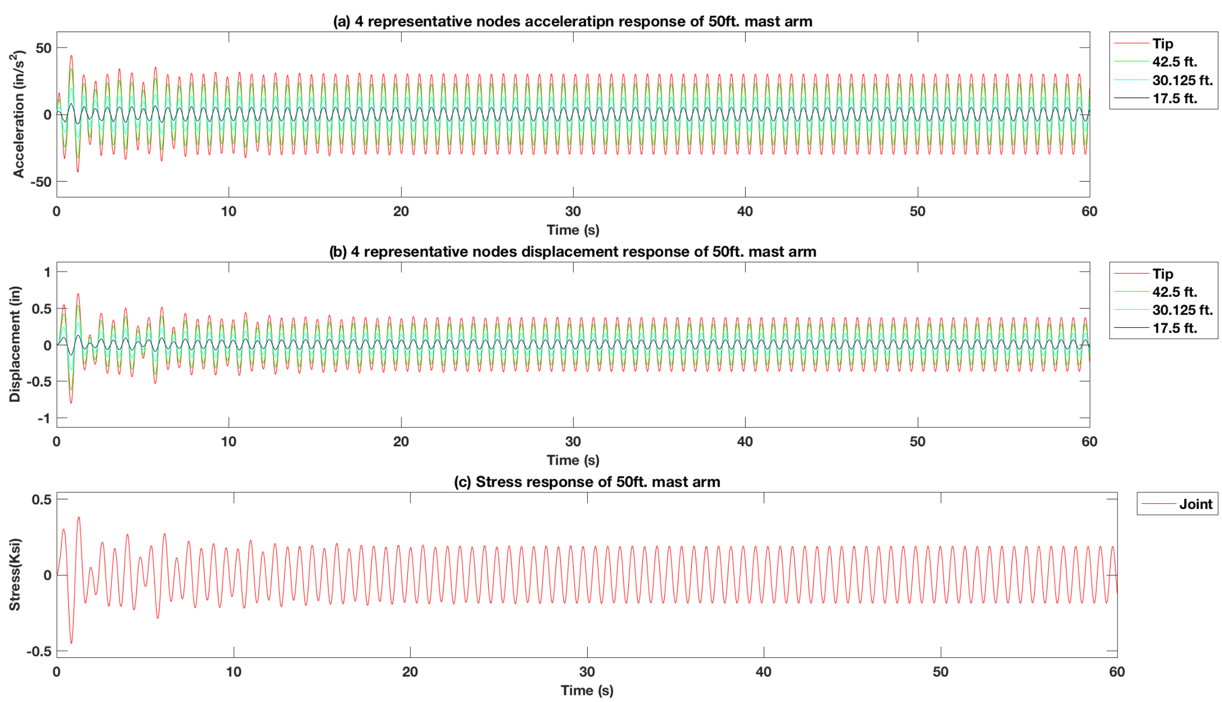

Figure 4-152 Force vibration response of excitation force at 3 signal heads position of the 50 ft. mast arm signal pole structure model TMD at 10 ft from the tip $f_r = 1.4 f_n$

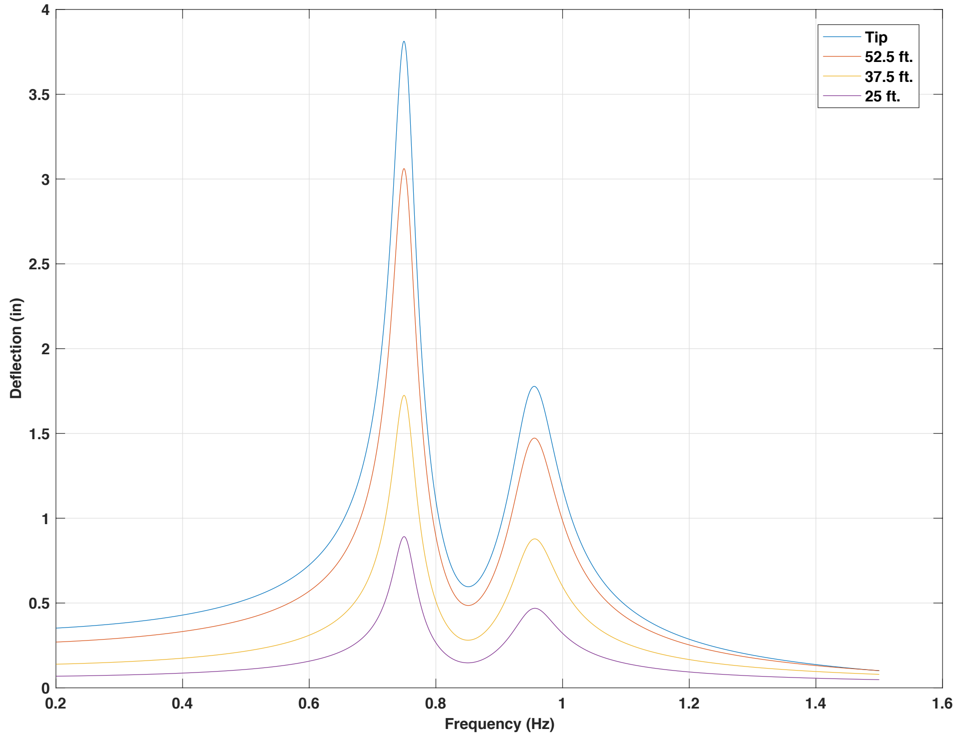

Figure 4-153 Frequency response for 50ft. mast arm with 15 lb. mass TMD at 1.5 ft from the tip, 5 lbf force on tip of mast arm, $f_d = 1.0f_n$

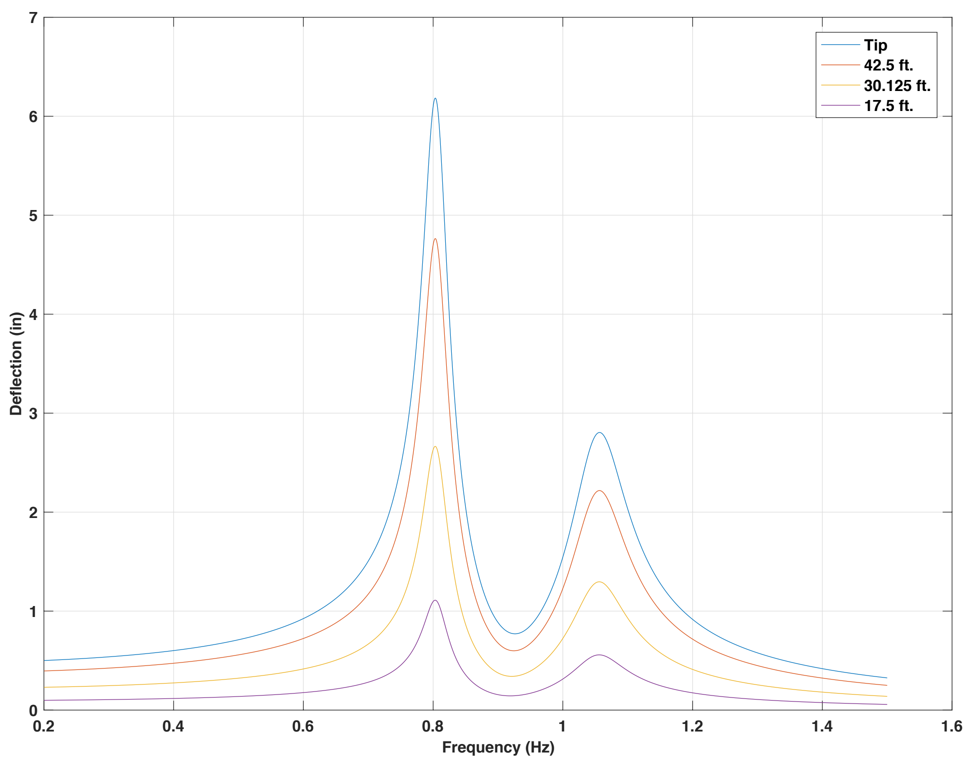

Figure 4-154 Frequency response for 50ft. mast arm with 15 lb. mass TMD at 1.5 ft from the tip, 5 lbf force on 3 signal head location, $f_d = 1.0f_n$

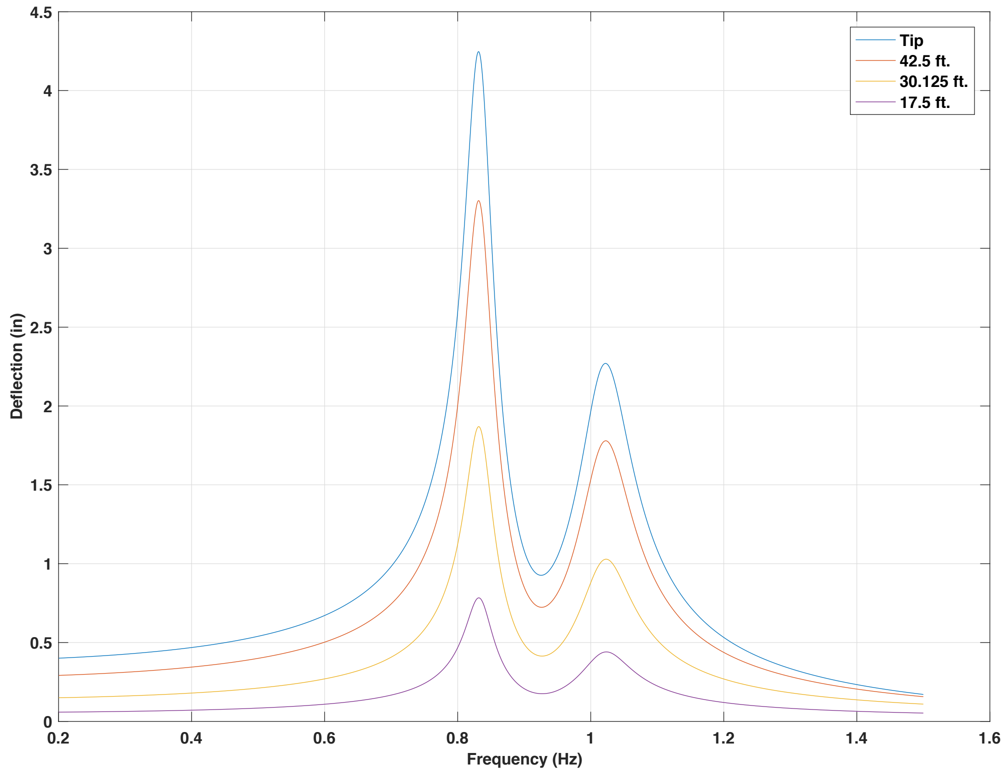

Figure 4-155 Frequency response for 50ft. mast arm with 15 lb. mass TMD at 5 ft from the tip $f_d = 1.0 f_n$, 5 lbf force on tip of mast arm

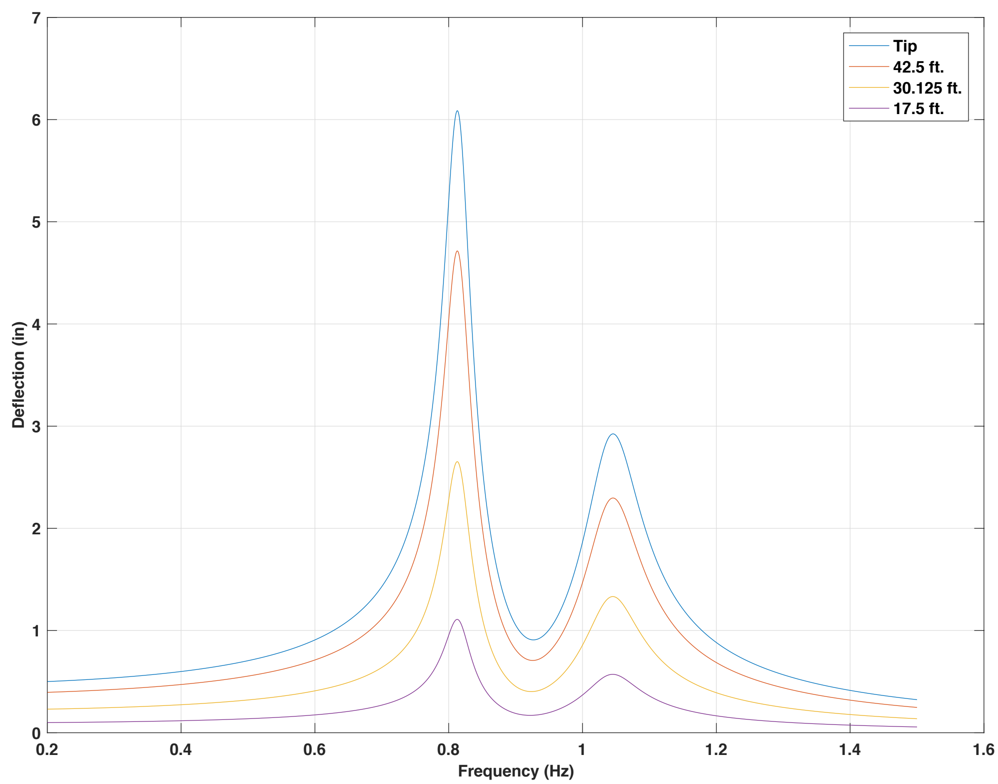

Figure 4-156 Frequency response for 50ft. mast arm with 15 lb. mass TMD at 5 ft from the tip, $f_d = 1.0 f_n$, 5 lbf force on 3 signal head location

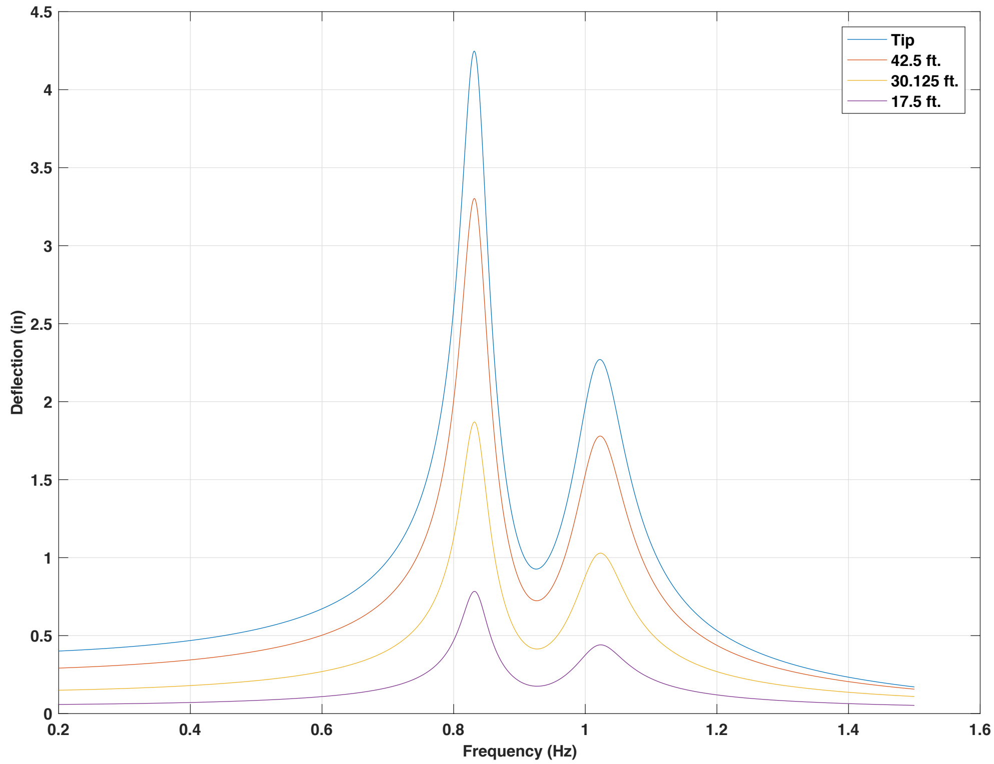

Figure 4-157 Frequency response for 50ft. mast arm with 15 lb. mass TMD at 10 ft from the tip $f_d = 1.0f_n$, 5 lbf force on tip of mast arm

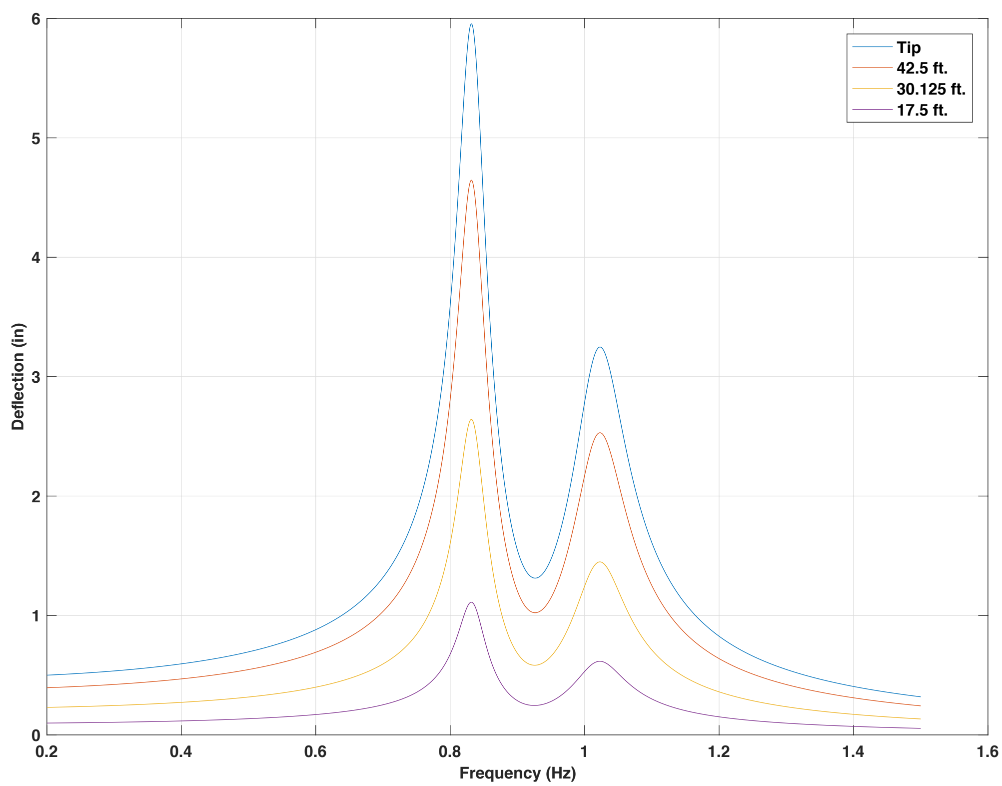

Figure 4-158 Frequency response for 50ft. mast arm with 15 lb. mass TMD at 10ft from the tip, $f_d = 1.0f_n$, 5 lbf force on 3 signal head location

4.5 Summary

After those analyses, some comparisons have been done like comparisons of the free vibration response and frequency response under different dampers but the same damping ratio as shows below. Also, other parameters include TMD masses, frequencies, locations, and the lengths of mast arm could be a variable to do the comparisons. In this summary, some representative results such as tip deflection response and frequency response under different TMD parameters of the 70 ft arm length model are plotted in the same figure shown

below:

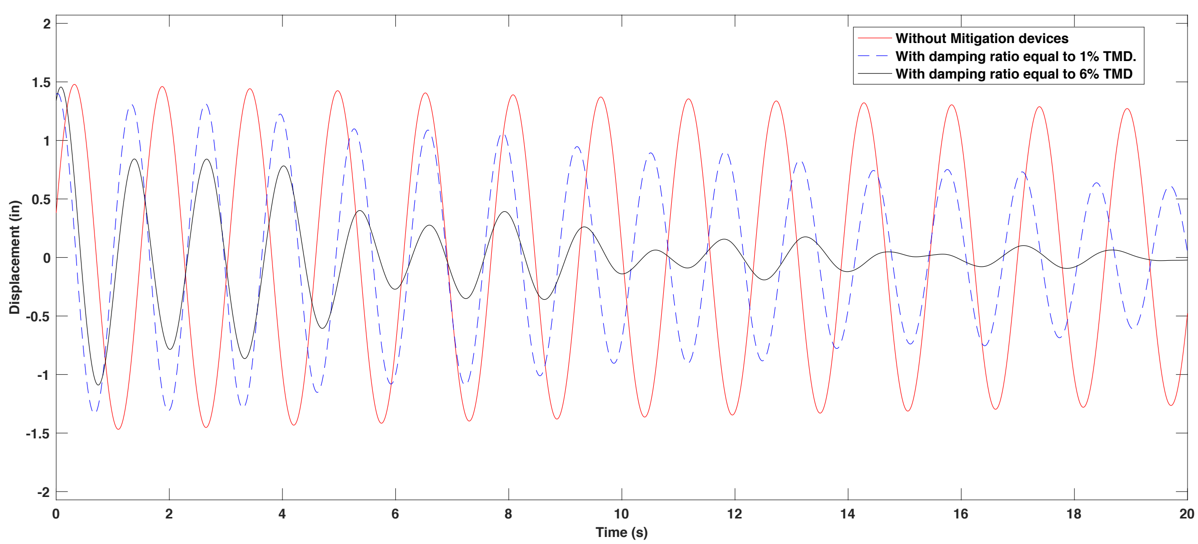

Figure 4-159 Comparison of free vibration response curve of 70 feet mast arm

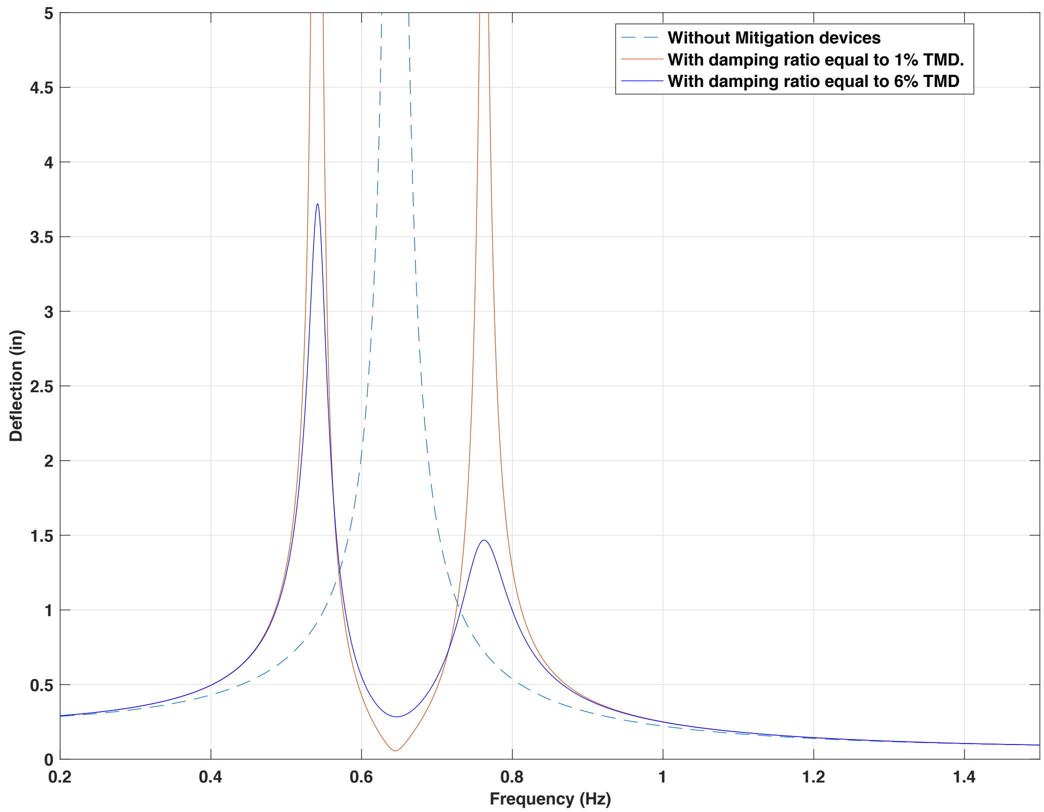

Figure 4-160 Comparison of frequency response curve of 70 feet mast arm

For the vibration mitigation devices, what we concerned most is their effectiveness. After doing these analyses, the equivalent damping ratio of each case could be calculated:

Table 4-14 Equivalent damping ratio calculation and comparison for 60 ft. mast arm model

TMD Properties				Damping ratio in the first mode frequency (%)	Damping ratio in the second mode frequency (%)	Peak Value (in.)	
Weight (lb)	Frequency (Hz)	Damping ratio	Location			Under First mode frequency	Under Second mode frequency
15	f_n	6%	Tip	2.337	3.693	4.15	1.82
25	f_n	6%	Tip	2.358	4.103	4.14	1.49
15	$0.9f_n$	6%	Tip	4.136	2.687	1.90	3.62
15	$0.75f_n$	6%	Tip	8.100	0.985	0.86	9.67
15	$0.5f_n$	6%	Tip	0.514	NA	26.92	NA
15	$1.1f_n$	6%	Tip	1.536	4.896	7.55	0.92

15	$1.25f_n$	6%	Tip	0.442	NA	16.11	0.44
15	$1.5f_n$	6%	Tip	0.435	NA	32.77	NA
TMD Properties				Damping ratio in the first mode frequency (%)	Damping ratio in the second mode frequency (%)	Peak Value (in.)	
Weight (lb)	Frequency (Hz)	Damping ratio	Location			Under First mode frequency	Under Second mode frequency
25	f_n	1%	Tip	0.558	0.839	16.5	6.78
15	f_n	6%	1.5*ft* from Tip	2.572	3.907	3.81	1.78
15	f_n	6%	5*ft* from Tip	2.594	3.876	3.75	1.88
15	f_n	6%	10*ft* from Tip	2.687	3.877	3.70	2.07

Cont. Table 4-14 Equivalent damping ratio calculation and comparison for 60 ft. mast arm model

Table 4-15 Equivalent damping ratio calculation and comparison for 50 ft. mast arm model

TMD Properties				Damping ratio in the first mode frequency (%)	Damping ratio in the second mode frequency (%)	Peak Value (in.)	
Weight (lb)	Frequency (Hz)	Damping ratio	Location			Under First mode frequency	Under Second mode frequency
15	f_n	*6%*	Tip	*2.32*	*3.93*	*4.812*	*1.858*
25	f_n	*6%*	Tip	*2.22*	*4.22*	*5.115*	*1.549*
15	$0.9 f_n$	*6%*	Tip	*3.74*	*2.97*	*2.417*	*3.487*
15	$0.75 f_n$	*6%*	Tip	*6.57*	*1.75*	*1.191*	*8.101*
15	$0.5 f_n$	*6%*	Tip	*0.65*	*NA*	*25.18*	*NA*
15	$1.1 f_n$	*6%*	Tip	*1.47*	*4.81*	*8.394*	*1.027*
15	$1.25 f_n$	*6%*	Tip	*0.95*	*5.77*	*16.63*	*0.517*
15	$1.5 f_n$	*6%*	Tip	*0.48*	*NA*	*33.91*	*NA*
25	f_n	*1%*	Tip	*0.53*	*0.90*	*20.43*	*7.183*
15	f_n	*6%*	*2.5ft from Tip*	*2.43*	*4.02*	*4.5*	*1.91*
15	f_n	*6%*	*5ft from Tip*	*2.47*	*3.92*	*4.393*	*2.013*
15	f_n	*6%*	*10ft from Tip*	*2.65*	*3.87*	*4.247*	*2.27*

Table 4-16 Equivalent damping ratio calculation and comparison for 70 ft. mast arm model

TMD Properties				Damping ratio in the first mode frequency (%)	Damping ratio in the second mode frequency (%)	Peak Value (in.)	
Weight (lb)	Frequency (Hz)	Damping ratio	Location			Under First mode frequency	Under Second mode frequency
15	f_n	*6%*	Tip	2.49	2.97	7.37	3.19
25	f_n	*6%*	Tip	2.30	4.09	8.013	2.727
15	$0.9\,f_n$	*6%*	Tip	4.00	2.77	3.702	6.485
15	$0.75\,f_n$	*6%*	Tip	8.30	1.42	1.693	17.03
15	$0.5\,f_n$	*6%*	Tip	0.56	NA	48.01	NA
15	$1.1\,f_n$	*6%*	Tip	1.54	4.88	14.2	1.71
15	$1.25\,f_n$	*6%*	Tip	0.84	5.91	29.58	0.825
15	$1.5\,f_n$	*6%*	Tip	0.45	NA	60.14	NA
25	f_n	*1%*	Tip	0.55	0.58	31.92	12.42
15	f_n	*6%*	*2.5ft from Tip*	*2.54*	*3.89*	*7.252*	*3.312*
15	f_n	*6%*	*5ft from Tip*	*2.35*	*3.85*	*7.146*	*3.45*
15	f_n	*6%*	*10ft from Tip*	*2.38*	*3.83*	*6.995*	*3.791*

Chapter 5: Experimental Validation

5.1 Backgrounds

A 50 ft. mast arm is provided by the Maryland State Highway Administration (MDSHA) and will be test in the Engineering lab, University of Maryland by Dr Chung C. Fu and Dr. Yunfeng Zhang. A free vibration test is done firstly by Dr. Zhang to verify the frequency and equivalent damping ratio of the structure.

5.2 Basic information and the procedure of the experiment

Geometry:

All the dimensions are the same as the Signal Pole Standard, and be measured as:

Table 5-1 Dimensions of the tested 50 ft mast arm

Measured	Outer Diameter 1 (mm)	Outer Diameter 2 (mm)	Thickness (mm)
30 *ft.* Segment	25.8	14.5	6.045
21.5 *ft.* Segment	16.2	8.5	4.724
Standard			
30 ft. Segment	25.4	14.7	6.35
21.5 ft. Segment	16.2	8.5	4.762

The three signals weights are 45lb, 45lb, and 70lb. in the location of 15 *ft*, 27 *ft*, and 45 *ft*. respectively.

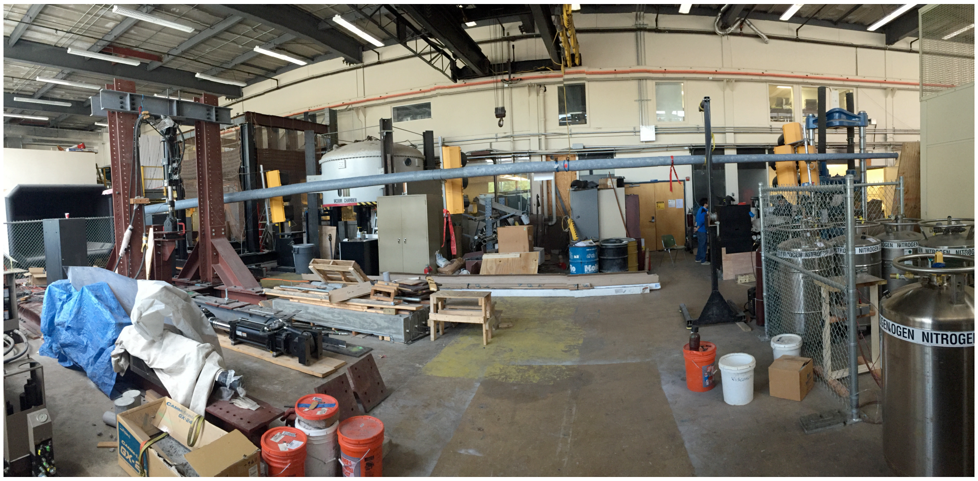

Figure 5-1 50 ft. mast arm for experimental use in the engineering lab

5.3 Results Validation

After install the mast arm and the signal heads, attach accelerometer on the mast arm and excite the mast arm tip with cyclic load for a short period and remove the load. Then the mast arm would begin the free vibration. The acceleration for all three dimensions would be recorded. Then plot the vibration response curve:

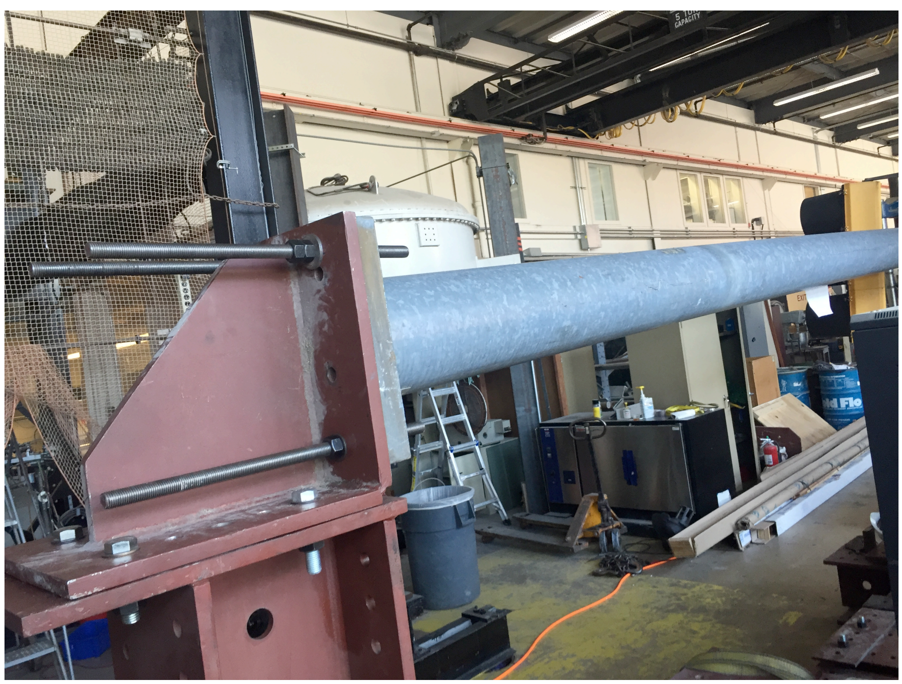

Figure 5-2 Boundary condition for the mast arm

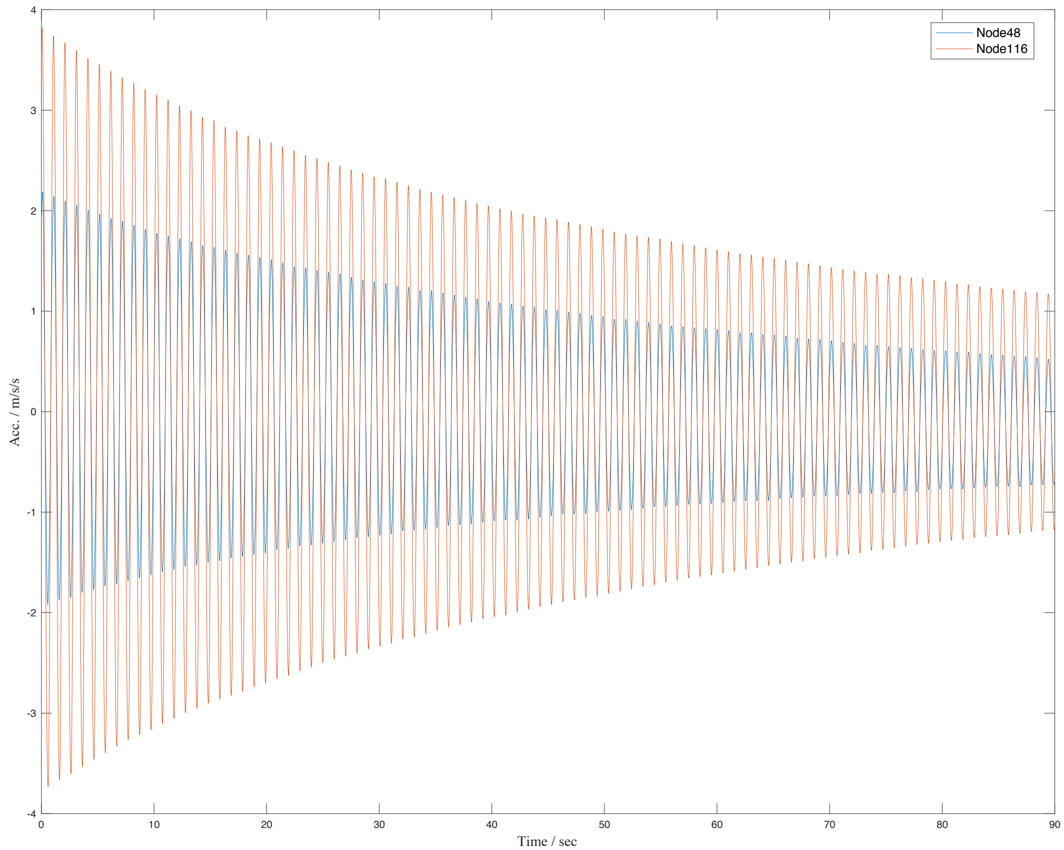

Figure 5-3 response curve for free vibration of 50 ft mast arm

The test result using professional grade accelerometer for mast arm free vibration test: The damping ratio is

$$\frac{\ln\left(\frac{3.007}{2.574}\right)}{2\times\pi\times 10} = 0.247\%.$$

The natural frequency of first mode is 0.982 Hz. Comparing with the results from the experiment, the initial calibration for structure's damping ratio and numerical analysis of the frequency are close to the experimental result. So the modified ANSYS model with the structure's equivalent damping ratio and signal heads (mass and locations) could be used for the future work.

Chapter 6: Conclusion, Discussion and Future work

6.1 Summaries and Conclusions

Tuned mass damper has been demonstrated to be an effective approach to vibration mitigation of mast arm signal pole structure based on the numerical analysis results presented in the previous chapters. From the parametric study results, the following research findings can be made for typical Maryland single mast arm signal pole structures:

[1] These three prototype single mast arm signal pole structures all exhibit high flexibility and low damping. In this situation, a TMD is shown to be useful for reducing the maximum deflection and stress range under dynamic load, especially for the harmonic load with a forcing frequency equal to the fundamental frequency of the signal pole structure. Although the response might increase slightly at other frequencies, the maximum response is still substantially reduced and would thus bring down the total counts of stress cycles exceeding a certain threshold level. If the code-specified deflection limit due to wind load has to be enforced, a TMD with proper design can be very effective in reducing the deflection and the stress in the fatigue hot spot area of mast arm-to-pole connection.

[2] The mass of the TMD is recommended to not exceed 5% of the total mass of the mast arm (Jerome J. Connor, 2002, with traffic signals installed), as evidenced by this parametric study results. The results of the TMD with 15lb and 25lb mass respectively indicate that a nonlinear relationship

exists between the vibration mitigation performances and the TMD mass. Also when the mass of the TMD increases, the first and the second mode frequencies would be further shifted away from the original fundamental frequency of the signal pole structure without TMD and the deflection due to gravity load would also increase.

[3] The fundamental frequency f_n of the single mast arm signal pole structure without TMD has to be first determined (e.g., through field test measurement). With a known fundamental frequency value, a TMD with its frequency ranging between $0.75f_n$ and $1.1f_n$ generally yield acceptable results. If the TMD frequency cannot meet with this condition, a relatively poor vibration mitigation result would occur.

[4] The viscous damping ratio of TMD is critical to its vibration mitigation performance. Compared with 1% viscous damping ratio, 6% damping ratio TMD shows a better performance from the finite element model analysis.

[5] For the TMD location considered in this study, these vibration mitigation effects appear to be comparable under same mast arm length and TMD parameters. Therefore, it is recommended to apply the TMD towards the inside of the mast arm to reduce the static deflection due to TMD weight.

6.2 Future work

The goal of this study is to find the optimal TMD parameter values and acceptable range of TMD parameters for vibration mitigation of typical Maryland single mast arm signal pole structures. Future research is needed to do experimental testing and extend the finite element analysis to include more sophisticated wind load such as transient vortex-induced wind loading. Additionally, achieving the favorable damping properties physically for the TMD in a cost effective way is deserved for a close look.

Bibliography

[1.] AASHTO LRFD Specification for Structural Supports for Highway Signs, Luminaires, and Traffic Signals, 2015

[2.] M. R. Kaczinski et al., NCHRP Report 412: Fatigue-Resistant Design of Cantilevered Signal, Sign and Light Supports, 1998

[3.] Richard Christenson, IDEA Project NCHRP-141 Final Report: Reducing Fatigue in Wind-Excited Traffic Signal Support Structures using Smart Damping Technologies, 2011

[4.] Richard Sause, NCHRP 10-70, Cost-Effective Connection Details for Highway Sign, Luminaire, and Traffic Signal Structures, 2011

[5.] R. J. Dexter et al. NCHRP REPORT 469: Fatigue-Resistant Design of Cantilevered Signal, Sign, and Light Support had found and summarized, 2002

[6.] Maryland Department of Transportation State Highway Administration Standards for Highways and Incidental Structures

[7.] Anil K. Chopra, Dynamics of Structures Theory and Applications to Earthquake Engineerng, 4th edition, 2011, ISBN-13: 978-0132858038

[8.] Jerome J. Connor, 2002, Introduction to Structural Motion Control 1st Edition, ISBN-13: 978-0130091383

[9.] ANSYS Mechanical APDL. ANSYS Academic Teaching Introductory. ANSYS, Inc. (2013).

[10.] Hector Cruzado (2007), Risk Assessment Model for Wind-Induced Fatigue Failure Of Cantilever Traffic Signal Structures, Ph.D. Dissertation, Texas Tech University, Lubbock, TX

[11.] Hamilton H.R, Riggs G.S and Puckett J.A (2000), Increased Damping In Cantilevered Traffic Signal Structures. Journal of Structural Engineering, April 2000.

[12.] Cook, R. A., Bloomquist D., Kalajian M. A., and Cannon V.A. (1998). Mechanical Damping Systems for Traffic Signal Mast Arms. Report No. WPI 0510775, Engineering and Industrial Experiment Station, University of Florida, Florida.

[13.] Cook. R. A., Bloomquist D., Richard D. and Kalajian M.A.(2001), Damping of Cantilevered Traffic Signal Structures ,Journal of Structural Engineering, December 2001.

[14.] Makita K.; Christenson R. E., Seto K. and Watanabe T. (2007). Optimal Design Strategy of Connected Control Method for Two Dynamically Similar Structures. Journal of Engineering Mechanics © Asce / December 2007

[15.] Davidson J.S., Fouad F.H., Abdalla R.S., Calvert B., Barton E and Warr R.A.(2004), Computer-Based Sign, Luminaires, and Traffic Signal Support Design Tools for State and County Engineers. FHWA/CA/OR- April 30, 2004.

[16.] Hamilton el al, Traffic signal structure damping, http://www.uwyo.edu/civil/research/kester/damping.html